Characterising the steroid metabolome in epithelial ovarian carcinoma

by

DAVID N. JEEVAN

A thesis submitted to the University of Birmingham for the degree of DOCTOR OF PHILOSOPHY

Institute of Metabolism and Systems Research
College of Medical and Dental Sciences
University of Birmingham
September 2022

Abstract

Epithelial ovarian cancer is an aggressive disease with a five-year survival rate of just 45% in the UK. The understanding of steroid hormone metabolism in epithelial ovarian cancer remains elusive. Steroid metabolites have not been fully characterised using mass spectrometry for benign and malignant ovarian masses.

I interrogated existing ovarian cancer genomic data to find changes in gene expression for steroidogenic enzymes and receptors and developed a biological study, using mass spectrometry for steroid analysis. I characterised steroid metabolism in epithelial ovarian cancer cell lines and fresh human ovarian tumours (benign, borderline and malignant). I demonstrated a time-course for androgen metabolism in Type 1 and 2 epithelial ovarian cancers cells and replicated this in *ex vivo* human ovarian tumours, observing several metabolic fluctuations in the newly synthesised steroid products. Unexpectedly, both the cell lines and tumours consistently showed downstream metabolism towards weaker androgens. I then conducted a multicentre prospective study investigating urinary steroid profiles in healthy women and women with benign and malignant ovarian tumours. In patients with Type 1 ovarian cancers, I identified five urinary steroid metabolites that differentiate them from Type 2 ovarian cancers, benign ovarian tumours, and healthy ovary. Surprisingly, these metabolites are derived in early classical steroidogenesis. Of interest, there were incremental increases in these five steroid metabolites with advancement from healthy ovary to benign mucinous tumour, to borderline mucinous ovarian tumour and to mucinous ovarian cancer.

In summary, I show that urinary steroid profiling can be utilised as a diagnostic tool for Type 1 ovarian cancers and provide evidence that steroid metabolism may be involved in the aetiology of mucinous ovarian cancer.

Acknowledgments

Firstly, I wish to acknowledge the agencies that have funded this work, Cancer Research UK, the Institute of Translational Medicine at University of Birmingham and Wellbeing of Women.

I would like to thank my esteemed and inspiring supervisors, Prof. Wiebke Arlt, Prof. Sudha Sundar and Dr Paul Foster. Thank you for your patience, your unwavering belief and for being great role models for aspiring academics. Prof Sundar, thank you for the best advice ever……. to get a dog! And without you, I would never have started this journey in research.

Thank you to all the wonderful people I have worked with at the IMSR, but specifically Dr Angela Taylor, Dr Lorna Gilligan, Dr Dean Larner, Fozia Shaheen, Hannah Ivison and Phil Guest who provided training and support. The efforts of the research nurses for patient recruitment were amazing, especially those at City Hospital, Birmingham, North Tees, and both Manchester University and Brighton and Sussex University Hospitals.

Thank you to my family especially my kind and patient wife, Alyssa, who moved to England to support my professional ambitions. Thank you to my in-laws, Tom and Claudia, who have provided welcome relief on our holidays and shown so much kindness. A special thanks to my dad, who has been praying for me throughout my medical career. Finally, I would like to dedicate this thesis to my mother, Leela, who gave so much love, but is sadly no longer with us.

My Lord God has navigated my path through this work and I pray he will use me to fulfil His plans.

Yet he did not waver through unbelief regarding the promise of God, but was strengthened in his faith and gave glory to God, being fully persuaded that God had power to do what he had promised. **Romans 4:20-21**

Table of Contents

List of Figures

List of Tables

List of Abbreviations

16a-OH-DHEA	16a-hydroxy-dehydroepiandrosterone
17aOHD	17a-hydroxylase deficiency
17HP	17a-hydroxypregnanolone
17OHP	17a-hydroxyprogesterone
17OHPreg	17a-hydroxypregnenolone
18-OH-THA	18-hydroxytetrahydro-11-dehydrocorticosterone
21OHD	21-hydroxylase deficiency
3a5a17HP	5a-17-hydroxypregnanolone
5aTHA	5a-tetrahydro-11-dehydrocorticosterone
5aTHB	5a-Tetrahydrocorticosterone
5aTHB	5a-tetrahydro-corticosterone
5aTHF	5a-tetrahydrocortisol
5PD	Pregnenediol
5PT	5-pregnene-3b,17a,20a-triol
ACA	Adrenal cortical adenoma
ACC	Adrenal cortical carcinoma
ACTH	Adrenocorticotrophin releasing hormone
AKR	Aldo-keto reductase

AKR1C3	17β-hydroxysteroid dehydrogenase type 5
An	Androsterone
BOT	Borderline ovarian tumour
CA125	Cancer antigen 125
CI	Confidence interval
CRH	Corticotrophin releasing hormone
CYP	Cytochrome P450
CYP11A1	Cholesterol side chain cleavage enzyme
CYP11B1	11β-hydroxylase
CYP11B2	Aldosterone synthase
CYP17A1	17a-hydroxylase
CYP19A1	P450 Aromatase
CYP21A2	21-hydroxylase
DHEA	Dehydroepiandrosterone
DHEAS	Dehydroepiandrosterone-sulfate
DHT	5α-dihydrotestosterone
E1	Estrone
E2	17β estradiol
E3	Estriol

EOC	Epithelial ovarian cancer
Et	Etiocholanolone
FTE	Fallopian tube epithelium
GC	Gas chromatography
GC-MS	Gas chromatography-mass spectrometry
hCG	Human chorionic gonadotropin
HGSOC	High grade serous ovarian cancer
HPA axis	Hypothalamic-pituitary-adrenal axis
HSD	Hydroxysteroid dehydrogenases
HSD11B1	11b-hydroxysteroid dehydrogenase type 1
HSD11B2	11b-hydroxysteroid dehydrogenase type 2
HSD17B	17β-hydroxysteroid dehydrogenase
HSD17B3	17β-hydroxysteroid dehydrogenase type 3
HSD3B1	3b-hydroxysteroid dehydrogenase type 1
HSD3B2	3b-hydroxysteroid dehydrogenase type 2
IQR	Interquartile range
IS	Internal standard
LC	Liquid chromatography
LC-MS/MS	Liquid chromatography tandem mass spectrometry

LGSOC	Low grade serous ovarian cancer
MS	Mass spectrometry
NADH	Nicotinamide adenine dinucleotide
NADPH	Nicotinamide adenine dinucleotide phosphate
PD	Pregnanediol
PD	Pregnanediol
POR	P450 oxidoreductase
PT	Pregnanetriol
PTONE	Pregnanetriolone
SIM	Selected ion monitoring
SRD5A2	5a-reductase type 2
SS	Stigmasterol
StAR	Steroidogenic acute regulatory protein
Std error	Standard error
STD/std	Standard deviation
STIC	Serous tubal intraepithelial carcinoma
STS	Steroid sulfatase
SULT2A1	Sulfotransferase
THA	Tetrahydro- 11-dehydrocorticosterone

THAldo	3α,5β- tetrahydroaldosterone
THB	Tetrahydrocorticosterone
THB	Tetrahydrocorticosterone
THDOC	Tetrahydro-11-deoxycorticosterone
THE	Tetrahydrocortisone
THF	Tetrahydrocortisol
THS	Tetrahydro-11-deoxycortisol

Chapter 1 General Introduction

1.1 Anatomy, physiology and histology of the normal ovary and Fallopian tube

1.1.1 Macroscopic anatomy of the ovary

The ovaries are paired organs that lie close to the uterus, and pelvic side walls. It has a convoluted and gyriform surface with increasing age In the adult, the normal ovary measures approximately 3 to 5 cm in the longest dimension and weighs between 5 to 8g but these vary depending on age and reproductive status. Each ovary is attached to the posterior surface of the broad ligament by a peritoneal fold (mesovarium), to the ipsilateral uterine cornu via the ovarian ligament, and to the lateral pelvic wall by the infundibulo-pelvic ligament (**Figure 1.1**)

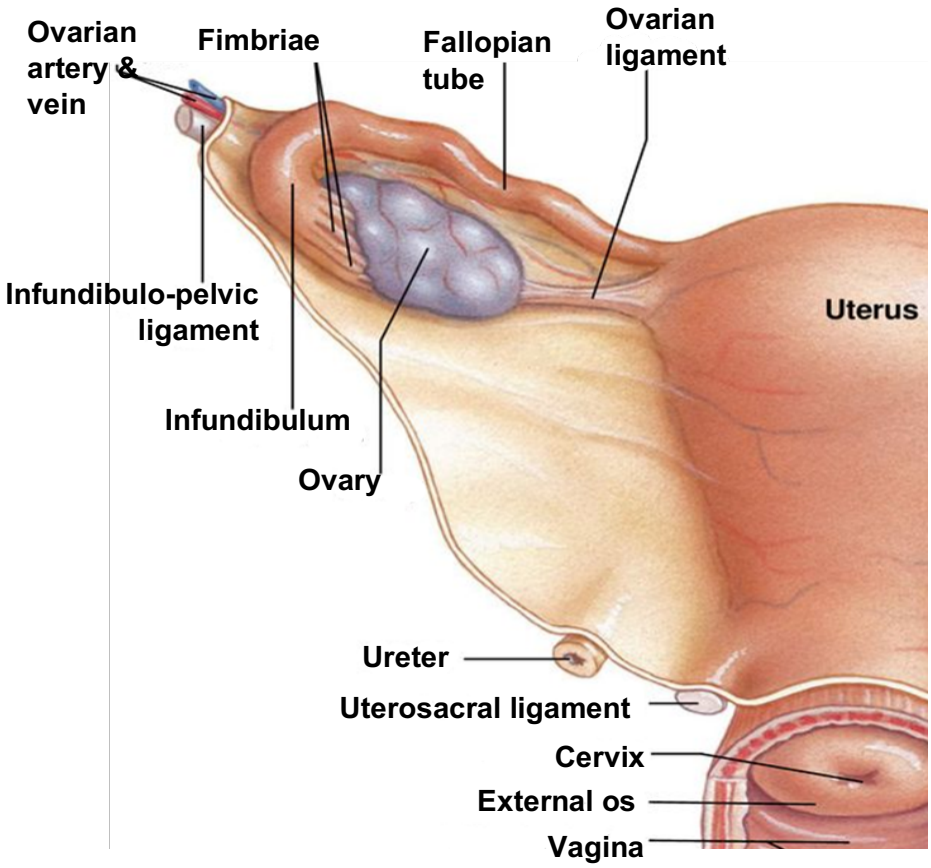

Fig. 1.1: Anatomy of the ovary (posterior view)

Adapted from Gynaecology 4th edition Shaw, Luesley & Monga 2010

1.1.2 Histology of the ovary

Beneath the outermost layer, the ovarian surface epithelium (OSE), the anatomy of the ovary consists of three main zones: the hilum, the central medulla and the cortex (**Figure 1.2).** The hilum is the point of attachment of the ovary to the mesovarium; it contains nerves, blood vessels and hilar cells and is composed of fibroconnective tissue. Hilar cells are the ovarian equivalent of Leydig cells found in the testis and are steroidogenically active with abundant amounts of eosinophilic cytoplasm, round nuclei, and occasional Reinke's crystalloids.

Ovarian stroma, composed of densely packed spindle cells resembling fibroblasts derived from mesenchymal cells is divided into two zones: the cortex and the medulla, although there is no definitive boundary. The central medullary area (derived from the mesonephric area) consists of loose connective tissue with blood vessels from the hilum branching through. Stromal interstitial cells respond to luteinizing hormone (LH) or human chorionic gonadotrophin (HCG) with androgen production. A variety of other cell types can be observed scattered throughout the stroma, including luteinized stromal cells, decidualized cells in pregnant women, endometrial stromal-type cells, smooth muscle cells, fat cells, and stromal Leydig cells (Weidner N., 2009). The cortex has an outer zone (tunica albuginea) and an inner zone which is the stroma, where the follicles are embedded. These primordial follicles consist of a primary oocyte surrounded by flattened granulosa cells .

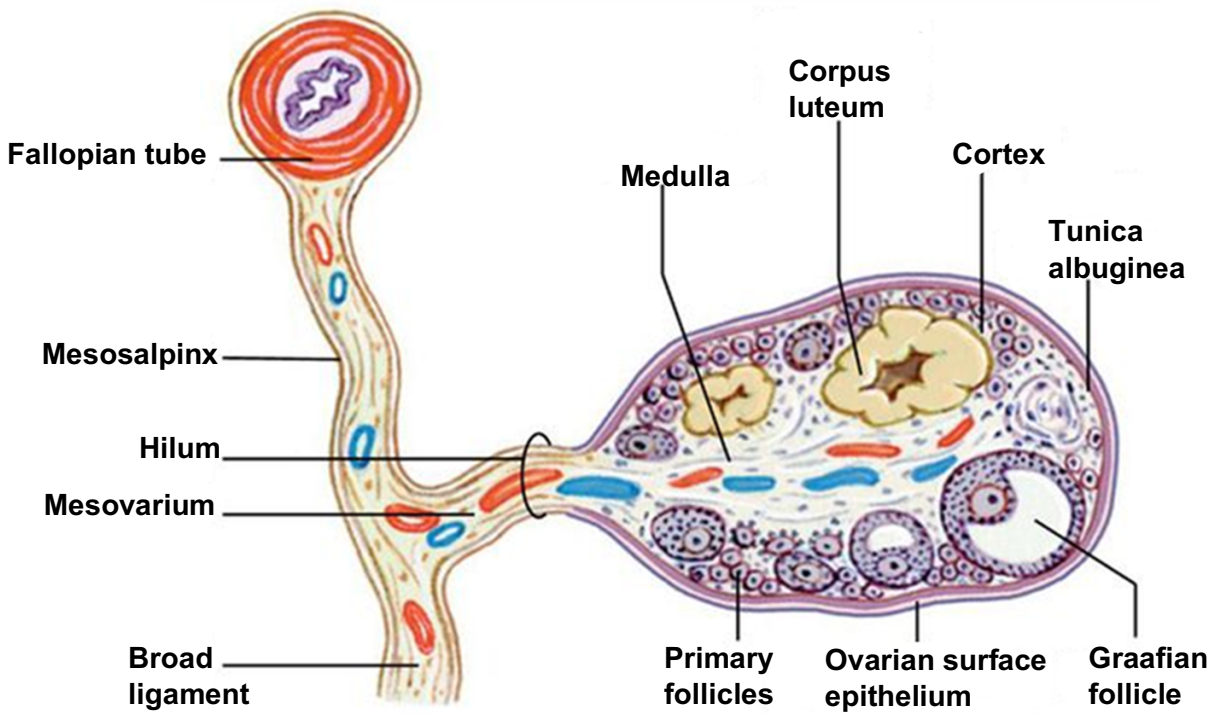

Fig. 1.2: Histological cross-section of the ovary

Adapted from Gynaecology 4th edition Shaw, Luesley & Monga 2010

1.1.3 Ovarian surface epithelium

Microscopically, the ovarian surface epithelium (OSE) is coelomic epithelium, a single layer of mesothelium, flattened as cuboid cells lying on a prominent basement membrane. Underneath it is very adherent to a thick collagenous layer, the tunica albuginea and then lies the stroma beneath. Anatomically, the OSE is the part of the pelvic peritoneum which overlies the ovary. It is thus a mesodermally derived mesothelium. In terms of physiologic functions, little is known beyond the fact that OSE seems to contribute to follicular rupture at ovulation by secreting proteases and subsequently proliferates to heal the ovulatory defect. However, it is important to note that OSE differs in multiple ways from extraovarian peritoneum, both structurally and

functionally (Auersperg et al., 2001). Whilst normal OSE has estrogen and progesterone receptors, it lacks cancer antigen 125 (CA-125), the ubiquitously used maker for ovarian malignancy. However, extraovarian peritoneum is CA-125 positive yet lacks these ovarian steroid receptors (Kabawat et al., 1983).

Extraovarian peritoneum does not have the tunica albuginea barrier and it is in direct contact with the structures beneath. As a result, in contrast to the extraovarian peritoneum, OSE has unusually limited access to metabolic exchanges with the stroma and circulation, as well as to growth factors and hormones; thus, it resides in a niche that keeps it in an isolated, quiescent state, which is ideal for a population of stem cells. In support of this concept, it was reported that OSE expresses several classical stem cell markers (Bowen et al., 2009). The concept of OSE as pluripotent stem cells is also in keeping with other stem cell-like characteristics that have been described (Szotek et al., 2008) and with the ability of OSE to differentiate to a fibroblastic or an epithelial phenotype, depending on microenvironmental conditions (Auersperg et al., 2001, Okamoto et al., 2009). Most malignant tumours arising from the extraovarian peritoneum are believed to be due to ovarian in origin but they can be *de novo* mesotheliomas, which differ profoundly in structure, function and clinical characteristics from OSE-derived ovarian carcinomas, indicating that they originate in fundamentally different progenitor cells (Auersperg, 2013).

1.1.4 Physiological function of the normal ovary

The physiologic responsibilities of the ovary are the periodic release of oocytes and the production of the steroid hormones (which is discussed in detail later). Both

activities are integrated in the continuous repetitive process of follicle maturation, ovulation, and corpus luteum formation and regression. The ovary is not a static endocrine organ. Its size and function expand and contract, depending on the intensity of stimulating tropic hormones. The ovary is regarded as a heterogeneous ever-changing tissue which cycles over weeks.

Ovarian follicle maturation

A female baby is born with a finite number of ovarian follicles which are quiescent till menarche. Maturity of these primordial follicles occurs for the purpose of reproduction. The granulosa cell layer first transitions from flattened to cuboid or columnar, forming the primary follicle. Next, the granulosa cell layer proliferates, forming a layer 3 to 5 cells thick (secondary or preantral follicle). The ovarian stroma surrounding the follicle differentiates into theca interna and theca externa cells. The thecal cells express receptors for insulin and LH and stimulation of these leads to high androgen production. Granulosa cells then secrete muco-polysaccharides, forming a single cavity in the follicle, with the oocyte peripherally located. Finally, granulosa cells surrounding the oocyte proliferate with follicle stimulating hormone (FSH) receptors (leading to estradiol and progesterone production) and also form the cumulus oophorus (graafian follicle) for ovulation (**Figure 1.2**). After ovulation, the follicle collapses and forms the corpus luteum. Grossly, corpora lutea are 1- to 2-cm rounded structures with serpiginous borders and a brown to yellow colour; cystic change is common. Microscopically, they are composed of luteinized granulosa cells with abundant pale cytoplasm, a round nucleus, and prominent nucleoli. If fertilization does not occur, the corpus luteum involutes, forming a corpus albicans. Corpus

albicans are essentially scars, composed of densely packed collagen fibres with occasional fibroblasts. Most are eventually resorbed and replaced by ovarian stroma. In menopause, the ovaries atrophy and typically have a cerebriform surface; remaining follicles become atretic and due to the lack of maturing follicles, ovulation ceases. The ovarian stroma in postmenopausal women can varying appearance from atrophy to hyperplasia.

1.1.5 Anatomy, physiology & histology of the normal Fallopian tube

The Fallopian tube is the site of early fertilisation and early embryonic development. Its role is a secretory organ and to pass the ovum from ovary to the uterine cavity (Patek, 1974). It is also the putative site of initiation of epithelial ovarian carcinogenesis (Crum et al., 2007, Kindelberger et al., 2007).

The normal Fallopian tube extends from the ipsilateral ovary to its terminus in the uterus and exists as a bilateral pair. They measure 9-11cm in length. At the ovarian end, the tube opens into the peritoneal cavity and is composed of finger like projections termed the fimbria (Soong et al., 2019)**.** It has a serosal outer surface, a middle smooth muscle wall and an inner lumen lined with Fallopian tube epithelial cells (**Figure 1.3)**. There are three types of fallopian tubal epithelial (FTE) cells that line the mucosa:

(i) Ciliated columnar cells (~25%) are most abundant in infundibulum and ampulla; estrogen increases production of cilia. They sweep the ovarian surface at ovulation to capture ovulated oocytes, and transport them towards the ampulla through ciliary motion and peristalsis.

(ii) Secretory cells (~60% are non-ciliated and produce tubular fluid. Progesterone increases their number while estrogen increases their height and secretory activity.

(iii) Intercalated cells (< 10%) are a morphological variant of the secretory cells.

The FTE cells contain nutrients for spermatozoa, oocytes and zygotes and produce tubal fluid. Major constituents are electrolytes and steroid hormones, largely from follicular fluid but also as transudate from the FTE.

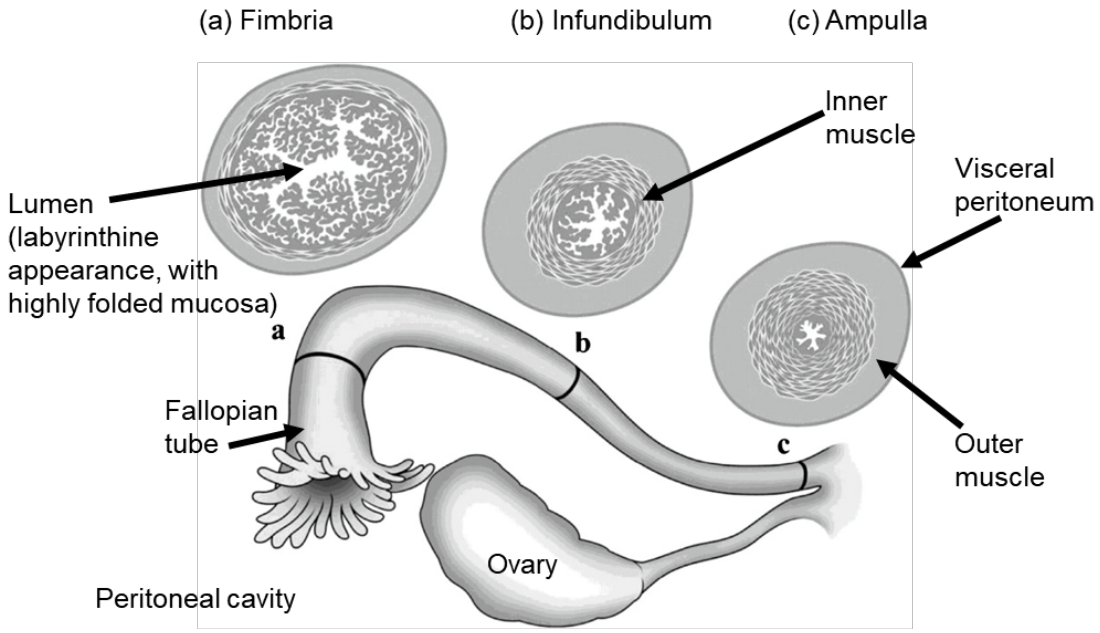

Fig. 1.3: Histological cross section of the Fallopian tube

The Fallopian tube has an outer serosa of flattened mesothelial cells of visceral peritoneum. Within it has a smooth muscle wall comprising of a longitudinal outer and an inner circular muscle. The innermost lining surrounding the lumen is the Fallopian tube epithelium; this is labyrinthine in appearance with highly folded longitudinal mucosa and this is the site of fertilisation. The mucosa has a richly vascularised lamina propria, a basement membrane and epithelial cells surrounded by stroma.

1.1.6 The role of the distal fallopian tube in epithelial ovarian cancer

Detailed pathologic examination of fallopian tube specimens over the past decade has led to a new understanding of "ovarian" high-grade serous carcinogenesis originating in the distal fallopian tube epithelium (FTE) (Crum et al., 2007) and this applies to the majority of epithelial ovarian cancers. However, a significant minority of around 30% of do not arise from FTE. In brief, the first step in the morphologic progression from normal FTE to high-grade serous carcinoma (HGSC) is the "p53 signature," characterized by foci of strong p53 immunopositivity and evidence of DNA damage in otherwise morphologically normal secretory FTE cells (Crum et al., 2007, Soong et al., 2019). This early precursor has low proliferative activity and is thought to develop from genotoxic injury to the secretory FTE of the distal fallopian tube, leading to unrepaired DNA damage, cell cycle arrest, and mutations in *TP53* (Crum et al., 2007, Folkins et al., 2008). The second step in this continuum is the development of a serous tubal intraepithelial carcinoma (STIC), characterized by multiple layers of morphologically atypical secretory FTE with a high proliferative index, and accumulation of mutant *TP53* (Crum et al., 2007, Chene et al., 2015). In the final step, highly aggressive subclones of STICs may locally expand (presenting as primary fallopian tube carcinoma) and exfoliate onto the closely associated ovarian surface/peritoneal cavity (presenting as primary ovarian/peritoneal carcinoma) (Tone, 2017, Crum et al., 2007).

1.2 Normal steroid biosynthesis in females

1.2.1 Commonly used terms

A steroid is derived from a common substrate (cholesterol) with the basic core structure typically composed of seventeen carbon atoms, bonded in a cyclopentanophenanthrene 4-ring structure. This comprises three six-carbon cyclohexane rings and one five-carbon cyclopentane ring. Biochemically altered through various enzymatic reactions, various functional groups are attached to this 4-ring backbone and by the oxidation state of the rings, which gives rise to steroid hormones (Carlson, 1989). A steroid hormone is a biologically active steroid that can bind to a receptor. The physiological categories of steroid hormones are androgens, estrogens, progestogens, mineralocorticoids and glucocorticoids. In females, the adrenal cortex, ovaries, and placenta are the primary sites of *de novo* steroidogenesis from cholesterol. Some of the resulting steroids can directly bind and activate steroid receptors in target cells of steroid action, whilst others require downstream activation but may be inactivated or diverted to other steroid pathways (Storbeck et al., 2019). A steroid precursor is a steroid that requires downstream metabolism to become a steroid hormone.

There are fewer steroid converting enzymes than there are steroid reactions so in most cases, steroid conversions are performed by the same enzyme in all tissues. Steroiodogenic enzymes synthesising the hormones are divided into two main groups, cytochrome P450 (CYP) enzymes catalysing oxidative reactions, which are mostly irreversible and the hydroxysteroid dehydrogenase (HSD) enzymes that catalyse the redox reactions, which are mostly reversible (Miller and Auchus, 2011).

The steroid hormone receptor family (estrogen receptor (ER), progesterone receptor (PR), androgen receptor (AR), mineralocorticoid receptor and glucocorticoid receptor is part of the larger superfamily of nuclear hormone receptors. The members of this superfamily function as ligand-gated transcription factors that modulate the expression of genes. Steroid binding induces receptor dimerization and conformational changes which allow translocation into the nucleus. Once inside the nucleus, the receptor dimer recognises and binds specific DNA sequences that in turn enhance or silence the transcription of specific target genes regulated by the receptor (Louie and Sevigny, 2017).

1.2.2 Principle of steroid metabolites and their excretion

Steroids are inherently lipophilic molecules. Metabolic conversions are therefore required to increase their water-solubility and enable efficient excretion via urine and bile. This metabolism is traditionally divided into two sequential stages, namely phase 1 and phase 2 reactions (Barnes, 1960). Phase 1 reactions alter the biological activity and at the same time add or reveal functional groups that function as targets for subsequent phase 2 reactions. Phase 2 reactions are conjugation reactions (sulfation and glucuronidation) that ultimately inactivate the compound and increase polarity and water solubility, thereby facilitating their excretion and concentration in the urine. The conjugated products are termed as steroid metabolites and are almost universally biologically inactive (Schiffer et al., 2019). Steroid metabolites should be considered as surrogates of distinct steroidogenic enzyme activities. Urinary excretion of steroid metabolites accounts for approximately 80% of all steroid excretion (van Kammen et

al., 1975) whilst excretion of unconjugated steroids is low, accounting for only 5–10% of the total urine steroid pool (Schiffer et al., 2019).

Advances in technology have allowed for the sensitive, specific, and simultaneous quantitative profiling of steroid precursors, steroid hormones and steroid metabolites, facilitating comprehensive characterization of the serum and urine steroid metabolomes. This allows the creation of steroid panels featuring multiple markers to identify diseases and it is gaining favour over quantification of single marker metabolites.

1.2.3 The classical steroidogenesis pathway

The pathways outlined in **Figure 1.4** are common to the adrenal glands and ovaries. In the first step, cholesterol is transported across the mitochondrial membrane by the steroid acute regulatory protein (StAR), where it is converted to pregnenolone by cholesterol side-chain cleavage enzyme (CYP11A1). Stimulation of this step is under pituitary hormone control; adrenocorticotropic hormone (ACTH) acting on the adrenal gland or luteinizing hormone acting on the ovary.

The glucocorticoid pathway involves conversion of pregnenolone to progesterone by 3β-hydroxysteroid dehydrogenase type II (HSD3B2), hydroxylation to 17-hydroxyprogesterone by 17α-hydroxylase (CYP17A1), further hydroxylation by 21-hydroxylase (CYP21A2) and, finally, 11β-hydroxylation by 11β-hydroxylase (CYP11B1) to form cortisol.

Alternatively, in the mineralocorticoid pathway, progesterone is first converted to deoxycorticosterone by CYP21A2, followed by three aldosterone synthase (CYP11B2) hydroxylation steps leading to the ultimate generation of aldosterone via the intermediate steroid precursors, corticosterone and 18-hydroxycorticosterone.

Finally, androgen synthesis requires consecutive 17α-hydroxylase and 17-20 lyase activities of the enzyme CYP17A1. CYP17A1 is located in the zona fasciculata and zona reticularis of the adrenal gland (Miller and Auchus, 2011, Suzuki et al., 2000) and in the ovaries it is located in the theca cells and in granulosa cells (Moon et al., 1978, Tsang et al., 1980). CYP17A1 utilises its dual enzymatic potential to successively hydroxylate pregnenolone to 17-hydroxypregnenolone and then convert the latter to dehydroepiandrosterone (DHEA). DHEA is predominantly secreted by the adrenal as dehydroepiandrosterone sulfate (DHEAS). DHEAS is generated by unconjugated DHEA being sulfated by DHEA sulfotransferase (SULT2A1) (Miller and Auchus, 2011). Steroid sulfatase (STS) reverses this step. DHEA and DHEAS are the most abundant steroid hormones in human circulation. Estrogens are formed from androgens (androstenedione and/or testosterone).

Steroid converting enzymes vary in their concentration in the tissues and thus the ratio of two enzymes will direct the pathway of steroid synthesis. In addition, some of these enzymes have a preferred steroid affinity. The affinity of HSD3B2 for pregnenolone is much lower than CYP17A1 (Miller and Auchus, 2011). Yet, CYP17A1 has a low affinity for 17-hydroxyprogesterone (Miller and Auchus, 2011, Auchus et al., 1998) limiting androstenedione synthesis. Therefore, androstenedione and testosterone are synthesised through HSD3B2 from DHEA.

HSD3B2 converts all its steroid substrates (pregnenolone, 17-hydroxypregnenolone, and DHEA) with the same efficiency (Lee et al., 1999) (Miller and Auchus, 2011). CYP17A1 function depends on the electron transferase P450 oxidoreductase (POR) (Pandey and Miller, 2005, Auchus et al., 1998) which is also required for the function of other CYP enzymes such as CYP21A2 and CYP19A1 (Miller and Auchus, 2011, Pandey and Miller, 2005).

1.2.4 Adrenal steroidogenesis

Adrenal steroidogenesis is a web of multi-step biosynthetic processes leading to the generation of mineralocorticoids (aldosterone from zona glomerulosa), glucocorticoids (cortisol from zona fasciculata) and androgen precursors (DHEA/androstenedione, from zona reticularis) from the common initial steroid precursor cholesterol. An outline of adrenal steroidogenesis is shown in **Figure 1.4**. The characteristics of adrenal steroidogenic enzymes are summarised in **Table 1.1**. Steroid synthesis in each zone of the adrenal cortex is regulated by distinct trophic hormones and negative feedback loops.

Zona glomerulosa. Mineralocorticoid synthesis occurs in in this zone within the context of the renin-angiotensin-aldosterone axis. It is absent of CYP17, preventing synthesis of any other steroid group. Renin is generated in the juxtaglomerular cells of the kidneys and mediates the cleavage of angiotensin I in the liver. Angiotensin I is converted to angiotensin II by the angiotensin-converting enzyme and binds to the angiotensin type II receptor in the adrenal cortex to stimulate aldosterone synthesis.

Aldosterone stimulates sodium reabsorption and potassium excretion in the renal tubules; the same electrolytes regulate renin production, closing the feedback loop.

Zona fasciculata. Glucocorticoid (e.g. cortisol) synthesis in this middle zone is activated by ACTH, which is released in response to the hypothalamic hormone, corticotropin-releasing hormone (CRH). Pulsatile pattern release of ACTH underpins the characteristic circadian rhythm of cortisol excretion by the adrenal glands. CYP11 is abundant in this area to catalyse glucocorticoid production. Circulating glucocorticoids exert negative feedback on the hypothalamus (CRH) and the pituitary (ACTH), completing the loop. Stressful stimuli (trauma, sepsis, surgery, psychological stress) can acutely potentiate ACTH excretion and, consequently, augment glucocorticoid synthesis.

Zona reticularis. The release of adrenal androgen precursors DHEA and androstenedione is also regulated by ACTH. These can be converted by peripheral tissues to active androgens and oestrogens.

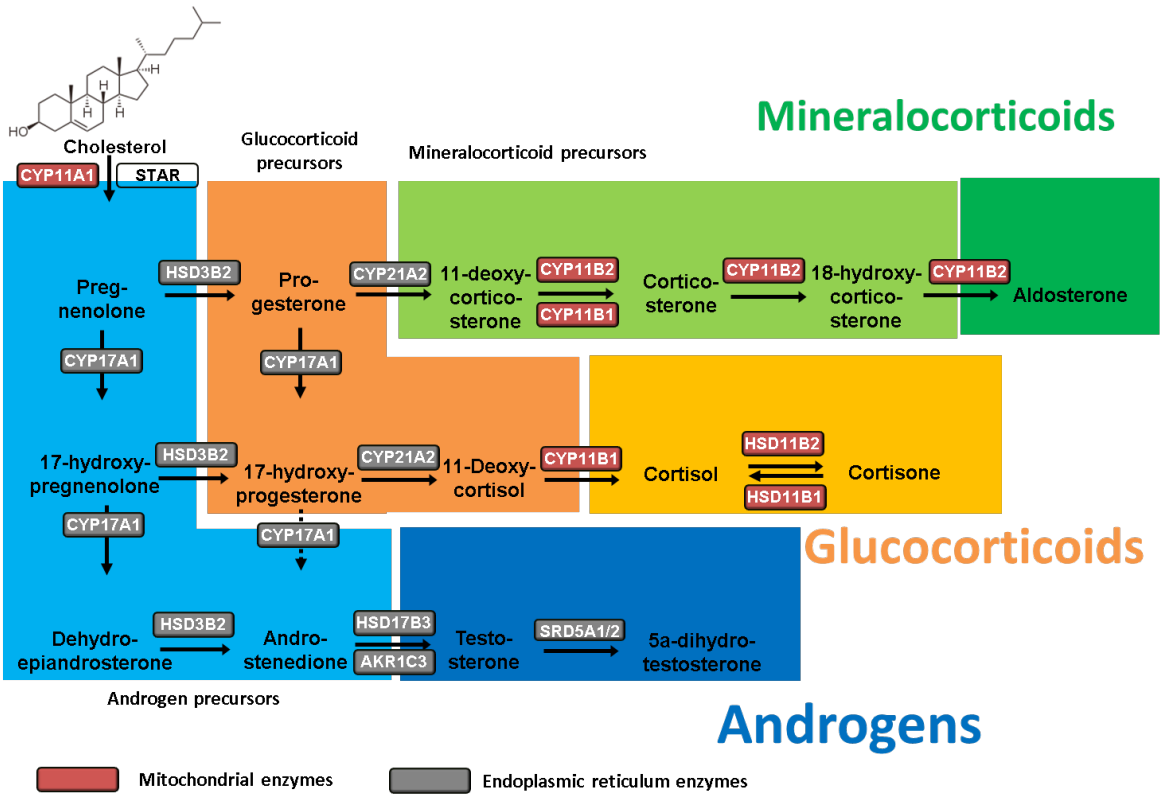

Fig. 1.4: An outline of steroidogenesis in the adrenal gland.

There are three biosynthetic pathways: the mineralocorticoid pathway, the glucocorticoid pathway and the androgen pathway. Each pathway involves steps mediated by endoplasmic reticulum (ER) enzymes and mitochondrial enzymes.

Steps in adrenal steroidogenesis

ACTH is implicated in the first stages of cholesterol handling by the adrenocortical cells: ACTH interaction with the melanocortin 2 receptor (MC2R) stimulates intracellular cyclic AMP (cAMP) formation, triggering the protein kinase A signalling pathway; this accelerates both ingress of cholesterol esters into adrenocortical cells and intracellular cleavage of esters to cholesterol (Feingold, 2000). The consequent steps of cholesterol metabolism are mediated by two broad categories of enzymes: a) cytochrome P450 enzymes and b) hydroxysteroid dehydrogenases.

Cytochrome P450 enzymes are subdivided into mitochondrial (type I) P450 enzymes (CYP11A1, CYP11B1, CYP11B2) and endoplasmic reticulum (type II) P450 enzymes (CYP17A1, CYP21A2 and aromatase, CYP19A1) (Miller and Auchus, 2011, Payne and Hales, 2004) (**Table 1.1**). All P450 enzymes catalyse monooxygenase reactions, inserting one atom of oxygen into organic substrates while the other oxygen atom is reduced to water; for this they require co-factor proteins which supply the essential electrons. Adrenodoxin/ adrenodoxin reductase is the protein couple donating electrons to all mitochondrial P450 enzymes, using reduced nicotinamide adenine dinucleotide (NADPH) as their cofactor. Endoplasmic reticulum-based P450 enzymes receive their essential electron flow from P450 oxidoreductase (POR).

Table 1.1 Enzymes involved in adrenal steroidogenesis

Gene	Enzyme	Protein	Tissue expression	Subcellular localization
CYP11A1	Cholesterol side-chain cleaving enzyme	CYP11A1	Adrenal cortex, ovary, testis, placenta	Mitochondria
CYP11B1	11β-hydroxylase	CYP11B1	Adrenal cortex (zona fasciculata/ reticularis)	Mitochondria
CYP11B2	Aldosterone synthase	CYP11B2	Adrenal cortex (zona glomerulosa)	Mitochondria
CYP17A1	17α-hydroxylase-17/20 lyase	CYP17A1	Adrenal cortex, ovary, testis	Endoplasmic reticulum
CYP21A2	21-hydroxylase	CYP21A2	Adrenal cortex	Endoplasmic reticulum
HSD3B2	3β-hydroxysteroid dehydrogenase type II	HSD3B2	Adrenal cortex, ovary	Endoplasmic reticulum
CYP19A1	Aromatase	CYP19A1	Adrenal cortex, ovary, testis, placenta, adipose tissue, bone	Endoplasmic reticulum

1.2.5 Ovarian steroidogenesis

Ovarian steroidogenesis commences with puberty when the onset of hypothalamic-pituitary-ovarian axis signalling leads to an increase in follicle stimulating hormone (FSH) and luteinizing hormone (LH) which act in concert to regulate steroidogenic activity (Herbison, 2016). Several second messengers are generated in response to these trophic hormones but the steroidogenic responses to them are mediated primarily through the generation of cAMP with activation of protein kinase A.

Steroidogenesis in the pre-menopausal ovary is a two-cell model involving the granulosa and theca cells, which surround the oocyte and form a follicle. The patterns of steroidogenesis vary during the menstrual cycle: 17β-estradiol (E2) is the principal product in the follicular phase, whereas progesterone is produced in the luteal phase. In addition, each cell type is differentially regulated by two pituitary hormones, FSH acting on granulosa cells and LH regulating both theca and granulosa cells (Shaw, 2010). Briefly, ovarian granulosa cells initiate steroidogenesis when stimulated by LH to express CYP11A1, via cAMP. CYP11A1 converts cholesterol to pregnenolone. Granulosa cells do not express CYP17A1. Pregnenolone and progesterone from granulosa cells diffuse into adjacent theca cells where there is abundant expression of CYP17A1 and HSD3B2 to produce the precursors of sex steroids (androstenedione, DHEAS). But theca cells do not express CYP19A1 so most androstenedione returns to the granulosa cells. FSH stimulates the granulosa cells, which contain abundant CYP19A1, to convert androstenedione to estrone (E1) and then to E2 via 17β-hydroxysteroid dehydrogenase type 1 (HSD17B1) **(Figure 1.5)**. Up to 95% of all E2 is from the preovulatory follicle and corpus luteum. In the luteal phase, HSD3B2 in the corpus luteum metabolizes pregnenolone to progesterone.

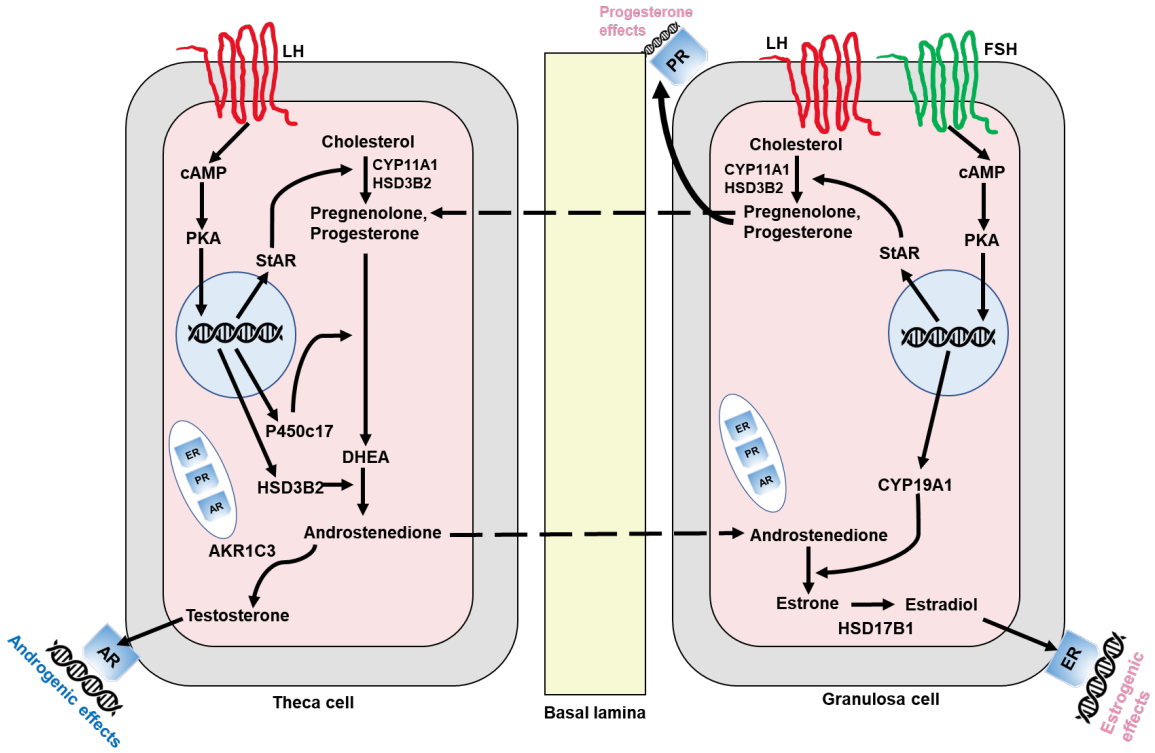

Fig. 1.5: The two cell–two gonadotrophin model for ovarian steroid biosynthesis

Protein kinase A (PKA), luteinizing hormone (LH), follicle stimulating hormone (FSH) – both gonadotrophins, androgen receptor (AR), progesterone receptor (PR), estrogen receptor (ER)

Small amounts of testosterone are directly secreted from the ovary, which is synthesised from androstenedione by 17β-hydroxysteroid dehydrogenase type 5 (AKR1C3) in theca cells and from the adrenal gland (30%). Most circulating testosterone is derived from conversion of DHEA (15%) and androstenedione (50%) in extraovarian tissues. While the ovary is capable of *de-novo* steroidogenesis, studies have shown that it also efficiently makes use of DHEA of adrenal origin to produce androgens and oestrogens (Arlt et al., 1999). Ovarian DHEA synthesis is very small in comparison to the adrenal (just 5% of adrenal secretion).

The presence of steroid 5α-reductase type 1 (SRD5A1), aldo-keto reductase 1C2 (AKR1C2), aldo-keto reductase 1C4 (AKR1C4) and 17β-hydroxysteroid

dehydrogenase type 6 (HSD17B6) has also been demonstrated for ovarian theca cells and some of those are required for the functioning of the backdoor pathway, which produces dihydrotestosterone (DHT) and it by-passes synthesis of DHEA, androstenedione and testosterone (Marti et al., 2017).

1.2.6 Androgen synthesis and signalling

Classical androgen synthesis

Androgens are responsible for secondary sex characteristics, external genitalia development and muscle growth. In women, androgens are synthesised in the adrenal glands and ovaries. Ovarian androgens are synthesised in thecal cells producing 50% total androstenedione and testosterone. LH surges cause fluctuations in androgen production by the ovary. Androgens stimulate target cells via the nuclear receptor, named androgen receptor (AR). The first androgen synthesized in this pathway is DHEA, which is converted from 17-hydroxyprogesterone by CYP17A1. DHEA is then converted to androstenedione by HSD3B2 (Miller and Auchus, 2011, Lasley et al., 2013). In the adrenal gland, the synthesis terminates with DHEA and androstenedione that are secreted into the circulation (Abraham, 1974). Androstenedione is converted into testosterone by AKR1C3, and subsequently metabolised into DHT by SRD5A1; both steps are performed in the ovarian theca cells (Abraham, 1974, Tsang et al., 1980) (**Figure 1.6**). However, DHEA and androstenedione are mostly aromatised to oestrogens (Miller and Auchus, 2011, Abraham, 1974).

Alternative pathway of androgen synthesis

There is an alternative synthesis of DHT through androsterone rather than testosterone (Auchus, 2004, Arlt, 2004, Wilson et al., 2003) (**Figure 1.6**). 17-hydroxyprogesterone is reduced by SRD5A1 to 5α-pregnan-17-ol-3,20-dione, that is then converted to 17-hydroxy-5α-pregnan-3α-ol-20one (17-OH-allopregnanolone) by AKR1C and to androsterone by CYP17A1 (Wilson et al., 2003). Androsterone can be converted to DHT either through androstanediol (Adiol or 3α–diol) or 5α-androstanedione (5α-dione). This pathway also functions in humans suffering from abnormalities in steroidogenesis (Miller and Auchus, 2011, Arlt, 2004). This same pathway has been shown to be activated in adult patients treated with abiraterone against prostate cancer (Attard et al., 2012). Their results also showed that this pathway might be active in the adrenal gland. Although this pathway is considered to be an alternative, it has been found that the metabolites of progesterone and 17-hydroxyprogesterone, allopregnanolone and 17-OH-allopregnanolone, respectively, are better CYP17A1 substrates than the “classic” steroids, namely, pregnenolone, progesterone and their 17α-hydroxylase forms (Gupta et al., 2003).

Moreover, 17-OH-allopregnanolone is the most efficient 17,20-lyase substrate (Gupta et al., 2003). This high affinity of CYP17A1 to the alternative androgens means that even under inhibition the residual enzymatic activity is enough to metabolise steroids downstream to CYP17A1 that can then be metabolised to DHT.

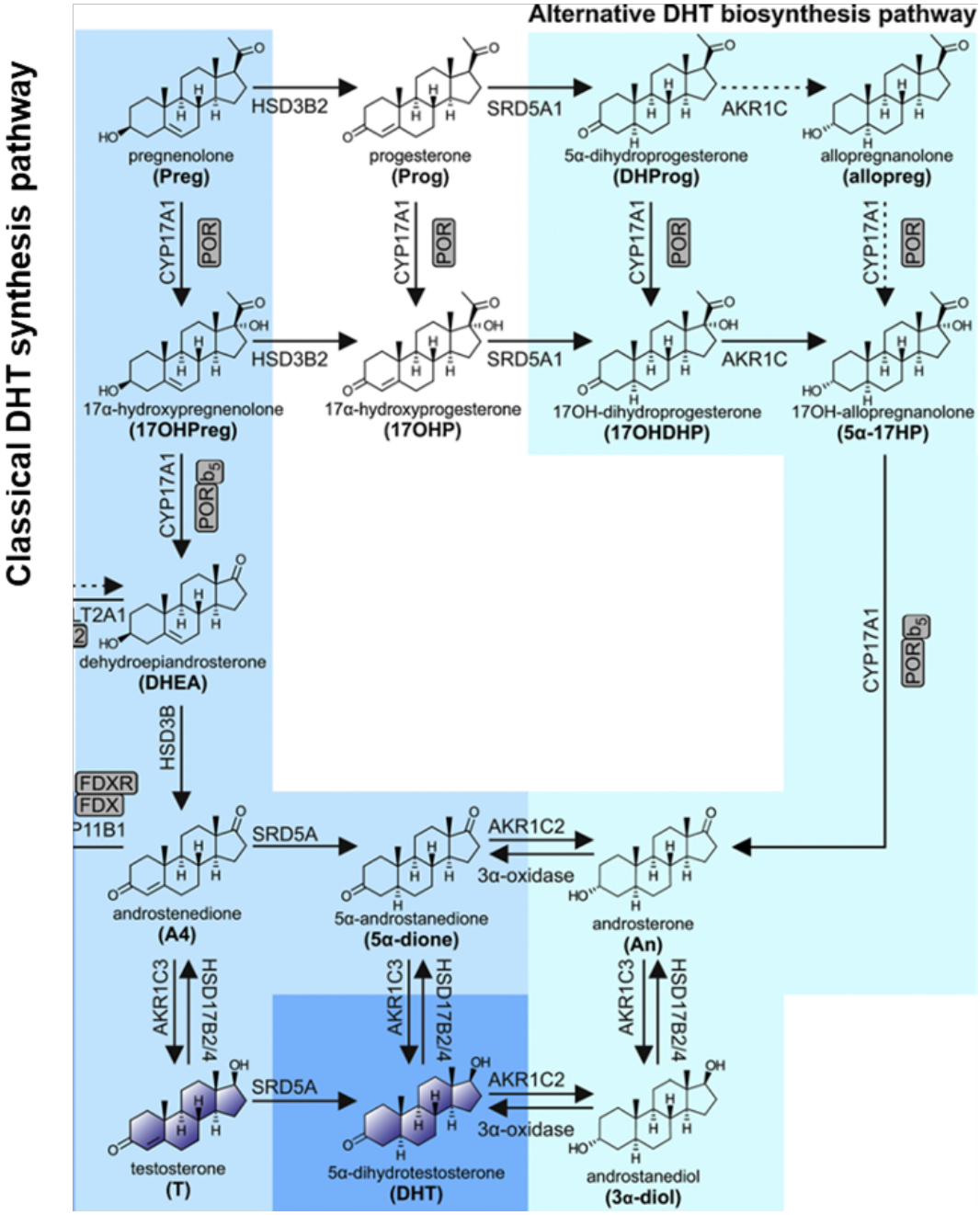

Fig. 1.6: Two pathways to active androgen synthesis

The classical DHT biosynthesis pathway and the alternative DHT biosynthesis pathway. Reproduced with permission. (Schiffer et al., 2019).

Androgen synthesis in pre-menopausal woman

Circulating estrogens and androgens are mostly bound to plasma albumin and sex hormone-binding globulin, leaving some 2-3% unbound to enter target tissues. Within the ovaries, the secretion rate of androgens is higher than that of estrogens. The two ovaries combined produce about 0.8-2.8 mg/day of androstenedione, 0.3-3.0 mg/day of dehydroepiandrosterone, and 0.06-0.10 mg/ day of testosterone compared with late-follicular (peak) 0.4-0.8 mg/day of oestradiol and 0.25-0.50 mg/day of estrone (Risch, 1998).

Androgen signalling

Androgens are largely considered as conducting their actions through the androgen receptor (AR). The AR has two pathways of transactivation: classical (ligand-dependent) and non-classical (ligand-independent).

Classical AR activation: AR belongs to the nuclear receptor superfamily. Androgens interact with AR to promote dissociation of AR from heat shock proteins and allowing AR to translocate into the nucleus and bind to specific DNA sequences known as androgen response elements (ARE) in conjunction with various AR co-factors. The co-factors bind to activated AR in a ligand-dependent manner to either enhance or repress its ability to transactivate the target gene; hence the AR complex can modulate gene transcription for various physiological and pathological functions.

Non-classical AR activation: Here, the androgen/AR complex signals without binding to DNA sequences. Instead, activation of second messenger pathways involves ERK/MAPK, mTOR activation via the PI3K-Akt pathway and involvement of the plasma

membrane components including G-protein coupled receptors and sex-hormone binding globulin receptor (SHBGR) which modulate intracellular Ca^{2+} concentrations and cAMP levels. They can also act via AR phosphorylation and/or AR-associated signalling proteins. These have been identified in several cell lines (Foradori et al., 2008). These effects occur within seconds. The difficulty of studying these non-DNA binding dependent actions *in vivo* is the lack of an appropriate animal model that can distinguish the receptor actions from each of the two pathways.

1.2.7 Postmenopausal ovarian steroid synthesis

The menopause results in the loss of ovarian follicles and accompanying granulosa cells so cyclical E2 and progesterone production by the follicles ceases. This typically occurs in the sixth decade of life. Despite a concomitant rise in FSH, the postmenopausal ovary does not respond. However, LH responsiveness is believed to persist in the ovarian hilum and stroma. There is evidence that the post-menopausal ovary does retain the capacity to produce androgens. Postmenopausal women make approximately 50% as much androgens as observed in men of the same age. Moreover, all androgens in women are made from circulating DHEA. About 80% of the serum DHEA in postmenopausal women is from adrenal origin while approximately 20% originates from the ovary (Labrie et al., 2017). Studies have demonstrated that the post-menopausal ovary (PMO) continues to possess gonadotrophin binding sites (Nakano et al., 1989) and is responsive to gonadotrophins (Dennefors et al., 1982) and that serum androgen levels decrease in post-menopausal women treated with GnRH agonists (Dowsett et al., 1988).

The adrenal gland produces predominantly DHEA and DHEAS which are converted to testosterone and DHT through peripheral metabolism. In contrast, the ovary synthesizes negligible amounts of DHEA and DHEAS and synthesises androstenedione, testosterone, and DHT. This is due to differences in steroidogenic enzyme expression in the two organs. In order for the post-menopausal ovary to continue to produce androgens, it must maintain the ability to express the enzymes necessary for androgen biosynthesis, and additionally, retain the ability to respond to gonadotrophins, specifically through activation of the LH/HCG receptor (LHCGR) by LH.

Studies utilising Northern blot analysis showed that the post-menopausal ovary possess the capacity to express the steroidogenic enzymes necessary for the initiation of ovarian steroidogenesis, but only ovaries from post-menopausal women with endometrial hyperplasia or cancer expressed all the enzymes necessary for androgen synthesis (Nagamani and Urban, 2003). Initially an analysis of ovarian steroidogenic enzymes by immunohistochemistry revealed complete absence of aromatase (CYP19A1) in all post-menopausal ovaries studied (Couzinet et al., 2001). In this same study, the enzymes essential for ovarian androgen synthesis were detected very weakly and were often found in scattered stromal cell populations, namely hilar cells.

Employment of sensitive methods of detection of ovarian steroidogenic enzyme detection have more recently been used. Real-time RT–PCR has detected StAR protein transcripts, CYP11A1 transcripts, HSD3B2 transcripts, but CYP17A1 transcripts were undetectable, suggesting the inability of the normal post-menopausal ovary to produce androgens (Jabara et al., 2003). Unfortunately, this study used

ovarian stromal cells in culture, resulting in the possibility of a phenotypic transformation from ovarian stroma *in vivo*.

A superior study was later performed to quantitatively and comprehensively determine the steroidogenic enzymes expressed in the human post-menopausal ovary (Havelock et al., 2006). RNA and protein obtained from post-menopausal ovaries were compared to samples of pre-menopausal ovarian stroma and inert myometrium (with no steroid converting enzymes as a control). Real-time RT–PCR was performed for *StAR*, *HSD3B1, HSD3B2, CYP17A1* and *CYP19A1.* Western blot analysis was performed for StAR, CYP11A1, CYP17A1,and HSD3B2. The post-menopausal and pre-menopausal ovarian stroma had a similar pattern of steroidogenic enzyme expression however *CYP19A1* and *HSD3B2* mRNA were greatly reduced in the post-menopausal ovary in comparison. HSD3B2 was not detectable in the postmenopausal ovary by Western blot analysis. This study supports the idea that the postmenopausal ovary retains some steroidogenic capacity (Havelock et al., 2006). Moreover, based on steroidogenic enzyme expression, the postmenopausal ovary has a unique pattern of steroidogenic enzyme expression that favours androgens derived from pregnenolone onwards rather than steroids derived from progesterone onwards in the classical steroidogenic pathway.

In a more invasive study, the postmenopausal ovary was shown to be hormonally active and contributing to the systemic pool of androgens. Serum from the ovarian veins of 13 postmenopausal women undergoing total abdominal hysterectomy and bilateral oophorectomy was analysed by radioimmunoassay and steroid hormone levels for androgens and estrogens were measured alongside peripheral blood collected preoperatively, intraoperatively, and postoperatively. The ovarian venous

samples had statistically higher concentrations for testosterone, androstenedione, DHEA, E1 and E2 compared to the peripheral samples. Postoperative levels of testosterone and E1 were statistically significantly lower than preoperative levels. Androstenedione, DHEA and estradiol levels were unchanged. (Fogle et al., 2007).

In conclusion, the normal postmenopausal ovary does perform steroid hormone synthesis, contributing significantly to the circulating pool of androgens and estrogens. Furthermore, this contribution appears to persist in women as long as 10 years after the menopause (Labrie et al., 2006).

The adrenopause

DHEA and its downstream converted product androstenedione are often referred to as 'adrenal androgens' but actually do not represent androgens as they lack capacity to bind to the androgen receptor (Arlt, 2004). There are no known DHEA specific receptors.

DHEA secretion exhibits a characteristic, age-associated pattern. At birth, circulating levels are high from synthesis in the immature fetal adrenal gland. At adrenarche (age 6-10 years) serum DHEAS concentration increases rapidly before peaking in the third decade of life and then steadily wanes to 10-20% of its maximum level by around 70 years of age. This phenomenon is described as the 'adrenopause' but cortisol secretion remains constant with age (Arlt, 2004). There is a clear sex difference too, with women having lower adult concentrations (Orentreich et al., 1984). The adrenopause is independent of the menopause.

1.2.8 Estrogen synthesis in normal post-menopausal ovary

Estrogen production drops significantly after the menopause. In a group of post-menopausal women, the serum from the ovarian vein had levels of estradiol and progesterone up to 90% lower than those of pre-menopausal women but the concentration of androgens (DHEA, androstenedione) were similar in pre-and post-menopausal women (Fogle et al., 2007).

In a separate study, oligonucleotide microarray analysis on post-menopausal ovaries and pre-menopausal ovarian stroma was performed to compare the gene expression profiles of each (Havelock et al., 2006). The steroidogenic gene expression pattern between the two groups was similar but in post-menopausal ovary there was reduced mRNA levels for all the steroidogenic enzymes and significantly less *CYP19* (aromatase*)* mRNA. A reduction in *CYP19* correlates with reduced estrogen production. The extra-gonadal sites such as the liver, brain, bone, adrenal glands and adipose tissue remain the primary sources of androgens and estrogens in the post-menopausal period.

1.2.10 Glucocorticoid and mineralocorticoids and the ovary

The ovary experiences regulation by glucocorticoids that exert agonist and antagonist influence on ovarian function. There are three ways this happens. The primary mechanism is indirect though altering levels of circulating gonadotrophins acting on the hypothalamus and pituitary gland. Stress leads to an increased glucocorticoid rise which suppresses gonadotrophin releasing hormone (GnRH) secretion in the

hypothalamus and lowers FSH and LH release from the pituitary gland. The second mechanism is also indirect and involves affecting the levels of metabolic hormones and growth factors such as insulin-like growth factor 1 (IGF-1). Lastly, glucocorticoids can directly modulate ovarian function through the presence of its receptor in ovarian cell types.

The ovary does not appear to produce glucocorticoids locally. HSD11B1 and HSD11B2 are responsible for the interconversion of cortisone to cortisol. Cortisone lacks biological activity; cortisol is the active steroid hormone. Both enzymes are found in several components of the ovary (oocytes, stroma and the ovarian surface epithelium). The presence of these receptors is not completely elucidated but one role is in ovulation. Ovulation is a natural inflammatory process when the ovarian surface is cyclically ruptured and repaired. Interleukin 1 (IL-1) and proinflammatory cytokines in the OSE induces HSD11B1 which responds to quell inflammatory tissue damage and reduce scarring of the tissue despite repetitive cyclical injury. The biological relevance of this HSD11B1 expression pattern in the ovary is unknown (Chapman et al., 2013).

The mineralocorticoid receptor expression is present on ovarian surface epithelium but CYP11B1, CYP11B2 and CYP21A2 protein expression is not seen in the ovary; these are conferred to the adrenal gland for production of mineralocorticoids and its precursors (Uhlén et al., 2015).

1.2.11 Embryological relationship between the ovary and adrenal gland

The two main steroid producing organs in the female are the adrenal glands and the

ovaries. The adrenal glands and the primitive gonads cortex share a common embryological origin: the urogenital ridge (**Figure 1.7**). At five weeks gestation, the urogenital ridge is formed by proliferation of coelomic epithelium (mesothelium) around the mesonephros which is the primordial structure for the urinary system and the gonadal ridge.

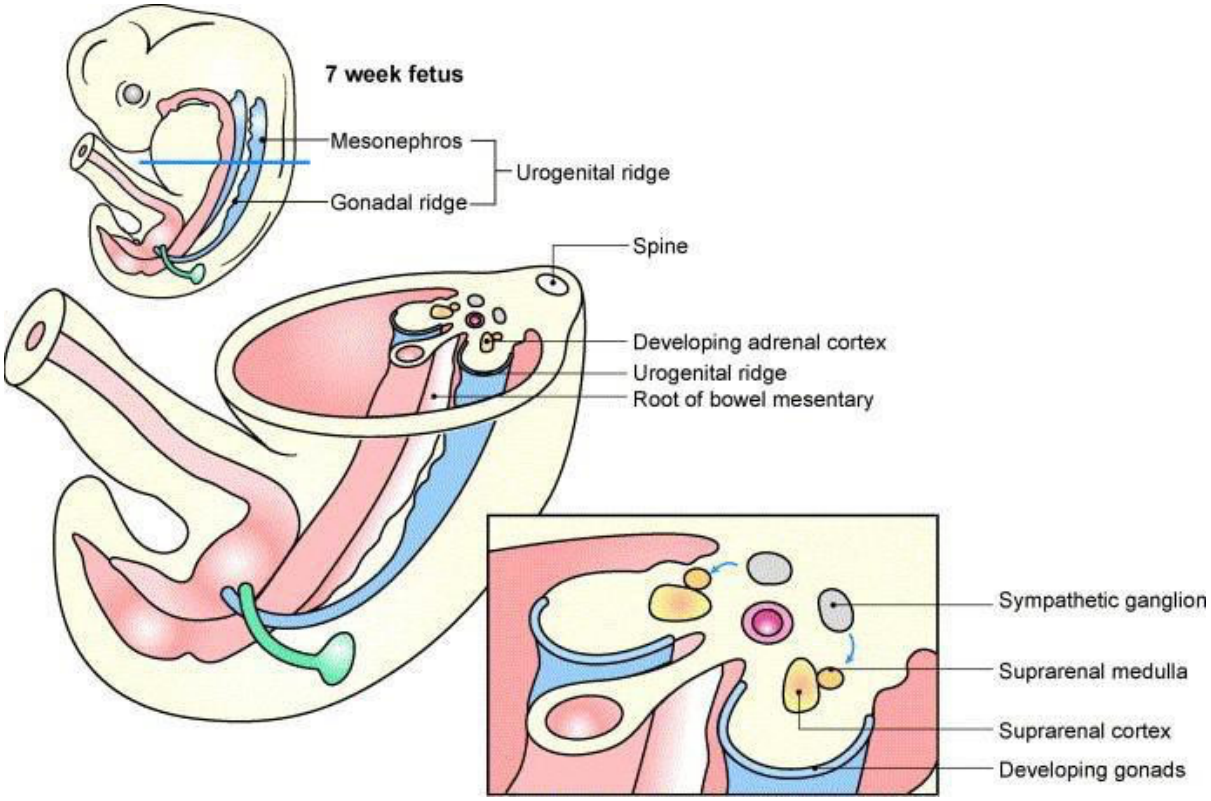

Fig 1.7: The urogenital ridge is the embryological origin of the adrenal glands and the ovaries

(Barwick et al., 2005)

The gonadal ridge develops laterally but continually to the mesonephros yielding the urogenital ridge and the adrenal glands and gonads (**Figure 1.8**).

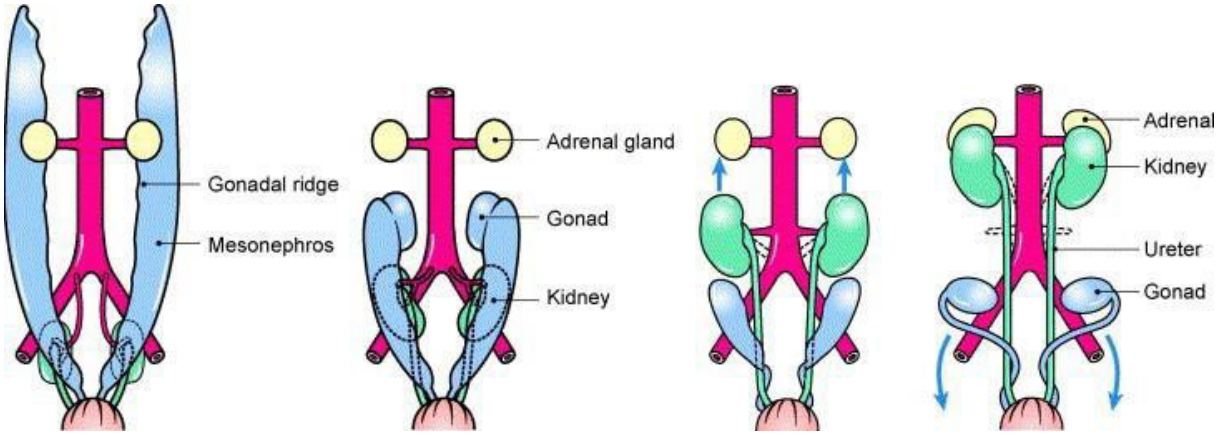

Fig. 1.8: Embryological development of the adrenal glands and ovaries
(Barwick et al., 2005)

The adrenal gland exists as a pair. They have two main parts; the outer cortex and the inner medulla. The adrenal cortex arises from the mesothelium of the urogenital ridge and the medulla arises from the neural crest tissue. By eight weeks, the cortex is separated from the rest of the mesothelium and is surrounded by connective tissue (mesenchyme). By the 9th week of gestation, the fetal adrenal cortex is functional and begins to synthesise cortisol and is under the control of adrenocorticotrophic hormone (ACTH). In the second and third trimesters, large amounts of dehydroepiandrosterone sulphate (DHEAS) is also produced which is catalysed by placental steroidogenic enzymes into androgens and estrogens. This contrasts with the ovary which commences steroidogenesis at puberty. The adrenal cortex differentiates into its three zones by 3 years of age (Barwick et al., 2005).

The genotype sex of the fetus is determined at conception and at the end of the 6th week of gestation, the gonad is morphologically indistinguishable as a testis or ovary and are termed non-differentiated. The mature ovary is composed of four main

components: surface epithelium, stroma, germ cells and sex cords. These components arise from distinct embryological origins (Shaw, 2010).

1.3 Epithelial ovarian neoplasms

1.3.1 Classification and histopathology of epithelial ovarian neoplasms

Primary tumours of the ovary are divided into three morphological categories that relate to the cell type and patterns of the tumour compared to the normal tissues present in the ovary. The categories are epithelial tumour (derived from the ovarian surface epithelium and adjacent stroma), germ cell tumours (originating from germ cells) and sex cord stromal type (originating from sex cord mesenchymal elements) (Chen et al., 2003). In this thesis, only epithelial tumours are discussed. The commonest epithelial ovarian tumours are shown in **Table 1.2**.

An epithelial tumour is classified as benign if there is an absence of both widespread epithelial cellular proliferation and invasive stromal behaviour.

An epithelial tumour is classed as borderline ovarian tumour (BOT) of low malignant potential or as atypically proliferating, if there is exuberant epithelial cellular proliferation but no invasive stromal behaviour.

An epithelial tumour is assigned malignant if there is invasive behaviour of the epithelial cells into the stroma. Almost 90% percent of all ovarian cancers in the Western world are derived from epithelial origin (Höhn et al., 2021).

Benign, BOT and malignant tumours can be solid or cystic or often mixed.

Epithelial ovarian tumours account for over 75% of all ovarian tumours. They are subclassified according to:

(i) epithelial cell subtype appearance (serous, mucinous, endometrioid, clear cell, transitional, squamous,

(ii) the relative amounts of epithelial and stromal components (when the stromal volume is larger than the cystic epithelial component, the suffix ‘fibroma’ is added)

(iii) the macroscopic appearance (solid, cystic, papillary).

Serous subtypes account for the majority of all ovarian tumours. Serous tumours are further subdivided into the following: serous cystadenoma, adenofibroma and cystadenofibroma (all benign), borderline serous ovarian tumour (SBOT) and serous adenocarcinoma (malignant) (Höhn et al., 2021).

Mucinous tumours are classified as mucinous cystadenoma and adenofibroma (both benign), borderline mucinous ovarian tumour (MBOT) and mucinous adenocarcinoma (malignant) (Höhn et al., 2021).

Highly malignant epithelial tumours lacking any specific differentiation are classified as undifferentiated. Epithelial tumours that are not designated as having a specific subtype commonly are recorded as adenocarcinomas not otherwise specified (NOS) (Höhn et al., 2021).

Table 1.2: Histological classification of common epithelial tumours of the ovary

Adapted from (Höhn et al., 2021)

SEROUS TUMORS
Benign
Serous cystadenoma
Serous adenofibroma
Serous surface papilloma
Borderline
Serous borderline tumor/atypical proliferative serous tumor
Serous borderline tumor—micropapillary variant/noninvasive low-grade serous carcinoma
Malignant
Low-grade serous carcinoma
High-grade serous carcinoma

MUCINOUS TUMORS
Benign
Mucinous cystadenoma
Mucinous adenofibroma
Borderline
Mucinous borderline tumor/atypical proliferative mucinous tumor
Malignant
Mucinous carcinoma

ENDOMETRIOID TUMORS
Benign
Endometriotic cyst
Endometrioid cystadenoma
Endometrioid adenofibroma
Borderline
Endometrioid borderline tumor/atypical proliferative endometrioid tumor
Malignant
Clear cell carcinoma

CLEAR CELL TUMORS
Benign
Clear cell cystadenoma
Clear cell adenofibroma
Borderline
Clear cell borderline tumor/atypical proliferative clear cell tumor
Malignant
Clear cell carcinoma

BRENNER TUMORS
Benign
Brenner tumor
Borderline
Borderline Brenner tumor/atypical proliferative Brenner tumor
Malignant
Malignant Brenner tumor

SEROMUCINOUS TUMORS
Benign
Seromucinous cystadenoma
Seromucinous adenofibroma
Borderline
Seromucinous borderline tumor/atypical proliferative seromucinous tumor
Malignant
Seromucinous carcinoma

MIXED EPITHELIAL AND MESENCHYMAL TUMOURS
Adenosarcoma
Carcinosarcoma

1.3.2 Subtypes of epithelial benign ovarian tumours

Epithelial benign tumours (also known as surface epithelial-stromal tumours) are believed to originate from the surface epithelium of the ovary. They are classified as benign because they lack exuberant cellular proliferation and invasive stromal behaviour. They account for approximately 60% of all ovarian tumours and occur primarily in women who are middle-aged or older and are rare in young adults, particularly before puberty. Surgical removal of all benign ovarian tumours is curative (Chen et al., 2003). Five major subtypes are included within this group: serous, mucinous, endometrioid, clear cell, and transitional cell (or Brenner type) (Scully R, 1999).

Benign Serous tumours

Benign serous epithelial-stromal tumours are formed by cells that resemble those of the internal lining of the Fallopian tube. Typically, these tumours are thin-walled cysts formed by a single chamber filled with a watery, straw-coloured fluid. The internal lining of the cyst is usually flat but may display a few coarse papillary projections. Benign

serous tumours account for approximately 25% of all benign ovarian neoplasms and nearly 65% of all ovarian serous tumours. Benign serous tumours most frequently occur between the fourth and fifth decades of life. In up to 20% of patients, benign serous tumours are bilateral (Chen et al., 2003).

Benign mucinous tumours

Mucinous tumours are epithelial ovarian tumours formed by cells that resemble either those of the endocervical epithelium or more frequently, those of the intestinal epithelium. Benign mucinous tumours are multiloculated cysts that are filled with opaque, thick, mucin material. They account for up to a quarter of all benign ovarian neoplasms and 75–85% of all mucinous ovarian tumours. Benign mucinous tumours most frequently occur between the third and fifth decades of life and rarely are bilateral (Chen et al., 2003, Morice et al., 2019).

Benign endometrioid tumours

Endometrioid tumours are epithelial ovarian tumours formed by cells that resemble those of the endometrium. They may be associated with the endometriosis and with hyperplasia or cancer of the endometrium. Benign endometrioid tumours occur infrequently and are predominantly cystic and unilateral (Chen et al., 2003).

Benign clear cell tumours

Clear cell tumours are epithelial ovarian tumours that are formed by clear, hobnail-like cells. Benign and borderline clear cell tumours are quite rare. Most clear cell ovarian tumours are malignant. All three (benign, borderline and malignant) can be predominantly solid or cystic with one or more polypoid masses protruding into the lumen (Chen et al., 2003).

Benign transitional cell (Brenner) tumours

Benign transitional cell ovarian tumours are known as Brenner tumours. They are formed by cells that resemble the urinary bladder lining (the transitional epithelium or urothelium). These tumours presumably are derived from surface ovarian epithelium that undergoes urothelium-like transformation (e.g., urothelial metaplasia). They may occur in association with similar tumours in the urinary bladder. They are solid and nodular, and most are unilateral. They often arise in association with endocervical-type mucinous and serous tumours, and they most frequently occur between the fifth and sixth decades of life. These tumours rarely occur. Most are very small, asymptomatic, incidentally discovered, and clinically irrelevant (Chen et al., 2003).

1.3.3 Subtypes of epithelial borderline ovarian tumours

Borderline ovarian tumours account for 10% of all epithelial ovarian tumours. Most are mucinous or serous and are confined to the ovary (Stage 1), hence leading to a better prognosis. They possess varying degrees of nuclear atypia, increased mitotic activity and multi-layered neoplastic cells but no stromal invasion. They behave clinically as benign tumours but some recur after surgical removal and some may see implants inside the peritoneal cavity (Chen et al., 2003).

Serous borderline ovarian tumours

Compared with benign serous ovarian tumours, serous borderline ovarian tumours (sBOT) have a flourish of finer papillary projections within the cyst cavity. Similar projections also may occur on the external surface of the tumour. Small tumourlets with similar features may be found elsewhere on the internal lining of the pelvic and abdominal cavities in up to 40% of patients. In most cases, these tumourlets do not progress, but they occasionally display invasive behaviour (Chen et al., 2003).

Borderline serous tumours account for 10–15% of all ovarian serous tumours and are typically diagnosed in the fifth decade of life. Up to one-third of these tumours are bilateral. Treatment is surgical removal. Reported 5-year survival rates are 70–95%. Recurrences may develop many years after the initial diagnosis, with intervals of 20–50 years reported. These recurrences usually are limited to the pelvic and abdominal cavities. It is estimated that 30–40% of patients with extraovarian spread die of progressive disease or other complications (Chen et al., 2003).

Low grade serous non-invasive tumours are considered serous borderline tumours. Unlike the other BOTs these are often bilateral and will have extraovarian implants in

30% of cases. After surgery, some serous BOTs will recur as invasive cancer, almost always as low-grade. Progression to high grade serous ovarian cancer (HGSOC) is rare (Kurman and Shih Ie, 2016).

Mucinous borderline ovarian tumours

Upon gross histological examination, borderline mucinous ovarian tumours (mBOT) are similar to benign mucinous ovarian tumours but may have solid regions and exhibit papillae projecting into the cyst chambers. They make up 10–14% of all ovarian mucinous tumours (Chen et al., 2003).

Borderline mucinous ovarian tumours most frequently occur between the fourth and sixth decades of life. About 40% of mBOTs of endocervical type are bilateral. In contrast, < 10% of borderline tumours of the intestinal type are bilateral (Morice et al., 2019). The endocervical type mBOTs may be associated with mucinous tumourlets or implants in the pelvic and abdominal cavities. Tumours of the intestinal type may be associated with pseudomyxoma peritonei, an accumulation within the pelvis and abdomen of large amounts of mucoid material (Kurman R, 2011). Most cases of pseudomyxoma peritonei originate in a primary appendix mucinous tumour with secondary involvement of the ovaries.

Treatment of borderline mucinous tumours is surgical removal and recurrence and metastatic disease are rare. Five-year survival rates are reported to be between 51% and 92%, depending on disease stage (Morice et al., 2019). However, mucinous BOTs appear to exhibit a higher propensity to develop into invasive ovarian carcinoma than other BOTs. The incidence of specific ovarian cancers following a diagnosis of a serous

or mucinous BOT was investigated in 4,281 women in Denmark between 1978 and 2021 (Hannibal et al., 2020). They calculated that women were 9 times more likely to develop a serous ovarian carcinoma if they had a previous serous BOT and women were 18 times more likely to develop a mucinous ovarian carcinoma following a previous mucinous BOT (**Table 1.3**).

Endometrioid borderline ovarian tumours

Borderline endometrioid tumours also are predominantly cystic and unilateral, but they often exhibit internal papillary projections. They represent one-fifth of all endometrioid ovarian neoplasms. Treatment of these tumours is surgical removal and the prognosis is excellent. Both benign and borderline endometrioid tumours are typically diagnosed in the sixth decade of life (Chen et al., 2003).

Clear cell borderline ovarian tumours

As stated before, borderline clear cell tumours are quite rare and most behave in a benign manner. The majority arise from benign endometrioid cysts (Chen et al., 2003)

Table 1.3: Incidence of ovarian cancer after diagnosis of a borderline ovarian tumour

Standardized incidence ratio (SIRs) of specific types of ovarian cancer in 2,058 women with a serous borderline ovarian tumour and 2,223 women with a mucinous borderline ovarian tumour in Denmark, 1978-2012. Standardized incidence ration (SIR); confidence interval (CI). The risk of developing a serous ovarian cancer from a serous borderline ovarian tumour was 9 times more likely compared to expected prevalence in the general population. For mucinous borderline ovarian tumours, women were 18 times more likely to develop a mucinous ovarian cancer than expected prevalence in the general population. Both shown in **bold**. Adapted from (Hannibal et al., 2020).

	Serous borderline ovarian tumours (n=2058)			**Mucinous borderline ovarian tumours (n=2223)**		
Ovarian cancer type	**Observed**	**Expected**	**SIR (95% CI)**	**Observed**	**Expected**	**SIR (95% CI)**
Serous	49	5.3	**9.2** (6.8-12.2)	<5	5+	0.6 (0.1-0.6)
Endometrioid	0	1.2	0.0 (0.0-3.1)	<5	<5	0.8 (0.0-4.4)
Clear Cell	<5	<5	2.3 (0.0-12.9)	0	0.5	0.0 (0.0-8.1)
Mucinous	<5	<5	1.2 (0.0-6.4)	17	0.9	**18.6** (10.8-29.8)
Other epithelial	11	2.1	5.1 (2.6-9.2)	7	2.2	3.3 (1.3-6.7)

Brenner borderline ovarian tumours

Brenner borderline ovarian tumours (borderline transitional cell ovarian tumours) characteristically contain solid and cystic areas, with papillary or polypoid projections

within the cyst lumen. These tumours are usually unilateral and most often occur between the sixth and seventh decades of life. They are believed to behave in a benign manner and rarely recur after surgical treatment (Chen et al., 2003).

1.3.4 Subtypes of epithelial ovarian cancer

Most malignant serous tumours are at least partially cystic. They may contain multiple cyst chambers, or loculations and solid areas. Most display an abundance of delicate papillae that project into the cyst cavities or outward from the external surface of the tumour.

High grade serous ovarian cancer (HGSOC) is the commonest ovarian cancer accounting for 70% of all cases and 90% of all serous ovarian cancers. It is heterogeneous in morphology but somatic tumour protein 53 (*TP53)* mutations are ubiquitous (>96%). It is classed as high grade due to marked nuclear atypia and a high mitotic index. Interestingly, whilst the number of somatic mutations per case in HGSOC is similar to most other solid malignant tumours, somatic mutations in mutated genes other than *TP53* occurred in no more than 5% of HGSOCs (The Cancer Genome Atlas Research Network, 2011). DNA copy number alterations are also part of the key characteristics. *CCNE1* amplification in HGSOCs, germline and somatic *BRCA*1/2 mutations and aberrations in homologous recombination DNA damage repair pathways are also implicated. TCGA gene expression analysis of over 300 HGSOCs identified four molecular subtypes: immunoreactive, differentiated, proliferative and mesenchymal. They all had distinct clinical outcomes; immunoreactive appeared to favour survival best.

The suspected pathway for carcinogenesis in this group is initiation by disruption of DNA repair, followed by chromosomal instability, copy number change and segregation into one of the four molecular subtypes (Höhn et al., 2021, Kurman and Shih Ie, 2016, Chen et al., 2003). The pathogenesis of ovarian cancer is attributed to a precursor lesion in the fallopian tube, designated STIC (described earlier). STIC lesions were first found in women having risk reduction salpingo-oopherectomy for *BRCA* germline mutation but they did not have a corresponding lesion on the ovary. STIC lesions also possess *TP53* mutation which is found in the concomitant ovary with high grade serous carcinoma . In mouse models, inactivation of *BRCA*, *TP53* and *PTEN* lead to the development of STIC lesions and HGSOC (Sherman-Baust, 2014). Both hysterectomy and oopherectomy alone have been shown not to prevent ovarian cancer; thus, ovarian cancer is of tubal origin. A precursor for STIC has yet to be identified (Kurman and Shih Ie, 2016).

Low grade serous ovarian cancer

LGSOCs characterised by mild or moderate nuclear atypia and a limited mitotic index. They are invasive and evolve from atypical serous tumours/ serous BOTs in a stepwise fashion characterised by mutations in *KRAS*, *BRAF* and *ERBB2* oncogenes. These activate the MAP kinase signal transduction pathway. Pure serous cystadenomas do not harbour these mutations. The precursor lesion for serous BOTs is considered to be a hyperplastic lesion in the fallopian tube (papillary tubal hyperplasia). The MAP kinase pathway plays a critical role in the transmission of growth signals into the nucleus and ultimately switches on neoplastic transformation. LGSOCs account for

10% of all serous ovarian carcinomas. Treatment for both grades include surgical removal and chemotherapy. Most tumours are widely disseminated at the time of diagnosis (Kurman and Shih Ie, 2016).

Carcinosarcoma

Carcinosarcomas are also attributed to arise from STIC lesions. They make up 1-3% of all ovarian cancers. They contain epithelial and mesenchymal components. Both the carcinomatous and sarcomatous components of the tumours have *TP53* mutation and occasionally germline *BRCA2* mutation (Kurman and Shih Ie, 2016).

Mucinous ovarian carcinomas

Compared with mBOTs, malignant mucinous ovarian tumours may contain more papillary projections within the cyst cavities, larger solid areas with necrosis and haemorrhage and stromal invasion. They are classically multilocular, thin walled cysts with mucinous fluid and are large 15-25cm in diameter. Between 6% and 20% of malignant mucinous tumours are bilateral. On average, diagnosis occurs in the sixth decade of life but around a quarter of women diagnosed with mucinous ovarian cancer are <44 years at presentation compared with 7% in high grade serous ovarian cancer (Morice et al., 2019).

Primary mucinous ovarian cancers account for up to 3% of all epithelial ovarian cancers, so they are very rare. (Seidman et al., 2004, Heinzelmann-Schwarz et al., 2006). The differential diagnosis is a primary mucinous bowel cancer which has

metastasised to the ovary and this is common. To distinguish from the two diagnoses, a raft of immunohistochemistry testing is required and it is a very challenging decision for histopathologists. Mucinous carcinomas display considerable heterogeneity, with components of mucinous cystadenoma mixed with borderline ovarian tumour features and obvious carcinoma hallmarks (**Figure 1.9)**. The *KRAS* mutation is found in all three components supporting their clonal relation and providing strong evidence that mucinous cystadenomas are the precursor lesions. The cell of origin for mucinous ovarian cancer remains unknown. As stated before, they lack ER and PR expression. *TP53* and *HER2* mutations are observed in the carcinomatous component of these tumours (Heinzelmann-Schwarz et al., 2006, Morice et al., 2019).

A recent genomic study analysed the data for over 250 mucinous ovarian cases (22 benign, 39 MBT and 195 MOC). They outlined a model for progression from benign mucinous tumours to mucinous BOTs to localized low-grade mucinous ovarian cancer and progressively through to high-grade and/or metastatic mucinous ovarian cancer. Benign tumors were shown to initiate with either a *KRAS* or *CDKN2A* event. Mucinous BOTs were significantly more likely to have both events and with additional copy number alterations. The study showed grade 1 mucinous ovarian cancers have yet more copy number alterations and are more likely to have a *TP53* mutation. In the majority of grade 3 mucinous ovarian cancers (20 out of 23), they had associated benign and/or borderline components and further increased copy number alterations (Cheasley et al., 2019). With Mucinous BOTs suggested as precursors to high-grade mucinous ovarian cancer, this contrasts with high-grade serous ovarian carcinoma that hardly ever derive from borderline or low-grade disease which corroborates the Danish study data (Hannibal et al., 2020) (**Table 1.3**).

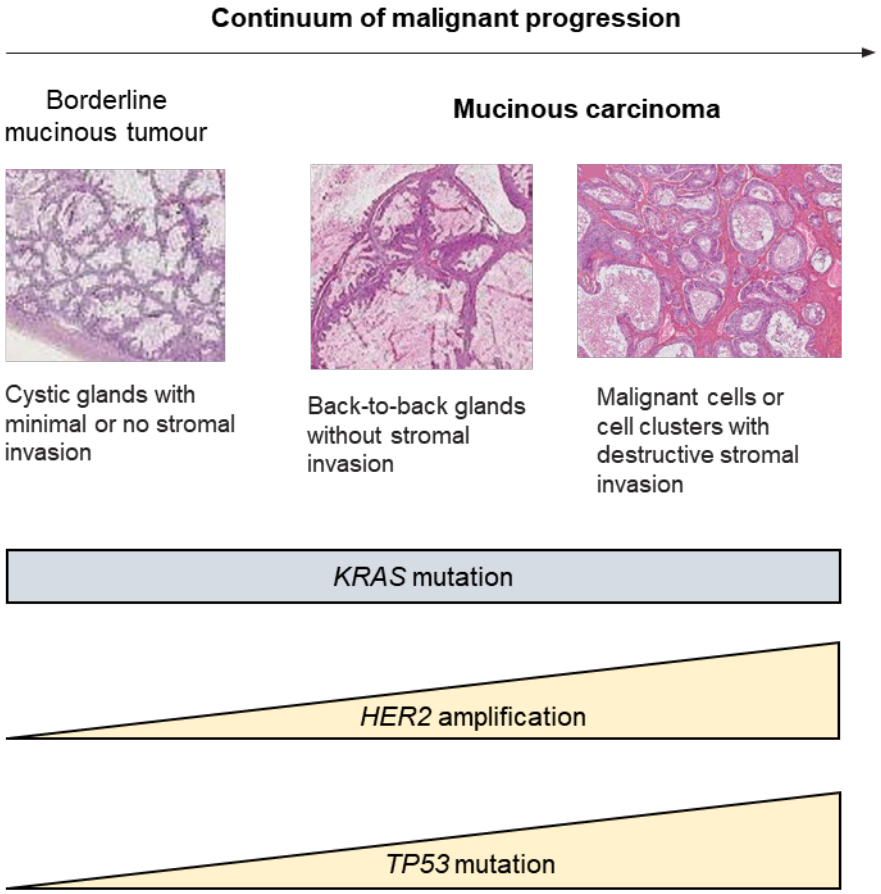

Fig. 1.9 Stages in the progression of mucinous ovarian tumours.

Mucinous ovarian tumors develop on a continuum from benign epithelium to preinvasive (borderline) carcinoma to mucinous carcinoma. KRAS mutations are an early event, whereas other oncogenic alterations (HER2 amplifications or TP53 mutations) may be acquired later in the course of malignant transformation (adapted from (Morice et al., 2019)

Up to 80% of mucinous ovarian cancers are diagnosed at Stage I; one reason for this is that they present as very large tumours that generate symptoms while the disease is localised. When diagnosed and treated at Stage I, the prognosis is excellent (five-year survival is >90%) but when the disease has metastasised to the peritoneal cavity, overall survival is 12-33 months. Surgery is the main treatment for mucinous ovarian cancers because they are almost always insensitive to chemotherapy.

Five-year survival rates are 83% for patients with Stage I tumours, 55% for patients with Stage II tumours, 21% for patients with Stage III tumours, and 9% for patients with Stage IV tumours (Morice et al., 2019). Under the model of progression, additional genetic events have been observed to drive invasion with increasing tumour grade, stage and metastasis.

Primary peritoneal cancer

Serous or mucinous tumours identical to those occurring in the ovary may arise in multiple locations within the pelvic and abdominal cavities. They sometimes coincide with ovarian tumours of identical type. When they do so, it may be difficult to establish whether the extraovarian sites represent implants originating from the ovarian tumour or *de novo* malignancies. However, in clinical practice, *de novo* primary peritoneal cancer is very rare (Chen et al., 2003).

Endometrioid and clear cell carcinoma

Malignant endometrioid ovarian tumours may be cystic or predominantly solid. They are the second most common malignant epithelial ovarian cancer and account for approximately 80% of all ovarian endometrioid tumours and 10–15% of all ovarian carcinomas. On average, diagnosis occurs in the sixth decade of life.

Approximately 13–28% of these tumours are bilateral. Most malignant endometrioid tumours are confined to the ovaries and adjacent pelvic structures; 20–25% are associated with endometrial carcinoma, which is commonly regarded as an

independent primary tumour. Studies suggest that 15% of patients with endometrioid ovarian carcinomas possess a synchronous endometrial carcinoma in the uterine corpus. These cancers are often cystic, unilocular and have a rough internal surface that is polypoid with solid areas which distinguishes it from serous cancer.

Malignant ovarian endometrioid carcinomas are considered to have a better prognosis than either mucinous or serous carcinomas. The reported 5-year survival rates are 78% for patients with Stage I tumours, 63% for patients with Stage II tumours, 24% for patients with Stage III tumours, and 6% for patients with Stage IV tumours (Chen et al., 2003).

Clear cell carcinomas

Clear cell carcinomas are the least common of the malignant epithelial ovarian cancers (<4%). Almost 90% of case only involve a single ovary. They possess a clear 'hob-nail' cells appearance on the epithelium. Benign and borderline clear cell tumours are quite rare. They can be predominantly solid or cystic with one or more polypoid masses protruding into the lumen. On average, diagnosis occurs in the fifth decade of life.

Two-thirds of all women with malignant clear cell tumours have never given birth, and 50–70% have endometriosis. One-fourth of all clear cell tumours arise in the lining of benign endometrioid cysts and 60% are Stage I tumours at diagnosis.

Survival rates for clear cell carcinomas are poorer than for other epithelial ovarian carcinomas. The reported 5-year survival rates are 69% for patients with Stage I tumours, 55% for patients with Stage II tumours, 14% for patients with Stage III tumours and 4% for patients with Stage IV tumours (Chen et al., 2003).

Both endometrioid carcinoma and clear cell carcinoma of the ovary are associated with corresponding borderline ovarian tumours and both the BOTs and carcinomas are associated with endometriosis (up to 42% of cases) and confirmed by molecular genetics. Inactivation of *ARID1A* (tumour suppressor gene) was detected in 50% of clear cell carcinomas and 30% of endometrioid ovarian cancers. The mutation and loss of expression in *ARID1A* is seen in the carcinomas and adjacent endometrioma epithelium but the distal areas of the endometrioma epithelium do not display the same aberrations. *PTEN* somatic mutations are also implicated in both these carcinomas and are seen in endometriomas. ER and PR expression is frequent and have *p53* wildtype status (Kurman and Shih Ie, 2016).

Seromucinous carcinoma

The evidence is compelling that these tumours are derived from endometriosis since a third of cases are associated with endometriosis and this is similar to the frequency found in endometrioid and clear cell carcinomas. Seromucinous tumours typically express ER and PR, which closely resembles the immunoprofiles seen in endometrioid and clear cell carcinomas too. For this reason, these three ovarian carcinomas which appear to be derived from endometriosis are referred as endometriosis related tumours (Chen et al., 2003).

Transitional cell ovarian carcinomas and Malignant Brenner Tumours

Malignant transitional cell tumours also contain solid areas and cystic areas with internal papillary or polypoid projections, often on one ovary. They are referred to as

transitional cell carcinomas when they lack benign transitional cells. They are described as malignant Brenner tumours when benign transitional areas are identified.

Whereas most (70–100%) transitional cell carcinomas present at an advanced stage, only 10–20% of malignant Brenner tumours do so. Malignant Brenner tumours have excellent prognosis when they are confined to the ovary, and, stage-for-stage, they may have better prognosis than transitional cell carcinomas; however, it has been reported that metastatic transitional cell carcinomas respond much better to chemotherapy than do any other type of surface epithelial-stromal tumours (Chen et al., 2003).

1.3.5 Type 1 and Type 2 epithelial ovarian cancers

A dualistic model is now established for epithelial ovarian cancers: Type 1 and Type 2. The understanding of epithelial ovarian cancers currently is that it is a family of related but distinct tumours with substantial differences in molecular features, clinic-pathological characteristics and behaviour (**Table 1.4**).

Type 1 carcinomas have been divided into three subtypes: a) endometriosis-related (endometrioid, clear cell and seromucinous) b) fallopian tube related (low grade serous carcinoma) and c) germ cell related (mucinous tumours).

The precursor lesions for Type 1 carcinomas are benign (e.g., endometriosis, papillary tubal hyperplasia) which implant on the ovary and progress stepwise to adenomas and atypical proliferative tumours before undergoing malignant transformation.

In contrast Type 2 tumours are at their inception established carcinomas, arising in the fimbria (STIC lesions), and implanting on the ovary and other sites in the abdomino-pelvic cavity. Many Type 2 tumours appear to derive from tubal epithelium.

This difference in the precursor lesions is thought to explain why Type 1 carcinomas remain confined to the ovary for long periods, with an indolent course whereas Type 2 carcinomas spread rapidly and are highly aggressive at their onset (Kurman and Shih Ie, 2016).

Table 1.4: Molecular features and clinical behaviour of Type 1 and Type 2 ovarian cancer

Feature	**Type 1**	**Type 2**
Stage	Frequently early stage	Almost always advanced
Tumour grade	Low	High
Proliferation activity	Typically low	Always high
Ascites	Rare	Common
Chemosensitivity	Fair	Good
Early detection	Possible	Challenging
Overall clinical outcome	Good	Poor
Precursor	Borderline ovarian tumour	Serous tubal intraepithelial carcinoma lesion
Chromosomal instability	Low	High
TP53 mutation	Infrequent	Ubiquitous

Clinical behavioural differences between Type 1 and Type 2 ovarian cancers

Type 1 tumours are often diagnosed at Stage 1 and are almost always low grade (except for clear cell carcinoma). Removal of the affected ovary is generally curative. However, metastatic Type 1 tumours are largely chemo-resistant, possibly because of

slow proliferation or an intrinsic mechanism and are associated with a poor prognosis. They are however genetically stable and targeted therapies, such as kinase inhibitors can be beneficial. They account for 10% of deaths from ovarian cancer. They present as large cystic masses that can be detected manually on pelvic examination and transvaginal ultrasound.

Type 2 tumours conversely account for 90% of deaths from ovarian cancer. They are rarely found at Stage 1 and are initially sensitive to chemotherapy due to high proliferation and defects in DNA repair capability but then resistance emerges. The earliest precursor lesion of Type 2 tumours are STICs. The minute size of these is below the level of detection of current methods. To make an impact on reducing mortality rates, the focus needs to be on detecting Type 2 tumours earlier and identifying novel therapies for metastatic Type 1 cancers (Kurman and Shih Ie, 2016).

1.4 Epithelial ovarian cancer in clinical practice

1.4.1 Epidemiology of epithelial ovarian cancer

Worldwide, ovarian cancer is the seventh most commonly occurring cancer in women and the eighth most common cause of death from cancer (Bhatla and Denny, 2018). Whilst breast cancer is the most common cancer in women, 85% of women diagnosed survive five years or more but ovarian cancer is lethal; just 42% of women diagnosed with ovarian cancer in England survive their disease for 5 years or more.

In the UK, epithelial ovarian cancer (EOC) is the sixth most common cancer among women and accounts for 4% of all new cases of cancer in females. It carries the highest

mortality of all the gynaecological cancers and accounts for 6% of all female cancer deaths in the UK. There are around 7,500 new ovarian cancer cases in the UK every year . The crude incidence rate is 24 new cases per 100,000 women in the UK but this is predicted to rise to 32 per 100,000 by 2035 (NCIN, http://www.ncin.org.uk/).

EOC typically occurs in postmenopausal women, with incidence highest in women 75-79 years. The risk that a woman will be diagnosed with the disease is 1 in 50 in their lifetime (CRUK 2016-18 data, https://www.cancerresearchuk.org).

Regrettably, improvements in imaging and CA125 serum measurement have not changed a statistic that over 70% of newly diagnosed cases will feature disease outside of the pelvis (FIGO Stage III/IV). Furthermore, 1 in 4 patients present as an emergency with EOC. In 1 in 5 patients for all disease stages they will not receive any anti-cancer treatment in England. This rises to 1 in 4 patients for stage II-IV disease (NCIN, http://www.ncin.org.uk/).

1.4.2 Clinical presentation

Classic symptoms associated with ovarian cancer, particularly at new onset and occurring more than 12 times per month, are persistent abdominal distension, abdominal or pelvic pain, early satiety and/or loss of appetite and increased urinary urgency and/or frequency. A few case–control studies investigating symptoms in women with ovarian cancer and comparing them to symptoms in women without ovarian cancer demonstrate that patients with ovarian cancer are symptomatic for a variable period before diagnosis and this challenges the perception of ovarian cancer as the "silent killer" (https://www.nice.org.uk/guidance/cg122).

1.4.3 Diagnosis of ovarian cancer

In the UK, recommendations for diagnosis and referral are based on National Institute for Health and Clinical Excellence (NICE) guidelines on the Recognition and Initial Management of Ovarian Cancer (www.nice.org.uk/guidance/cg122).

In primary care, women are advised to report symptoms. GPs are advised to be prompted by the symptoms (especially in women over 50 years) to measure CA125 and if this is 35IU/ml or greater, a pelvic and abdominal ultrasound scan should be arranged. If the ultrasound scan suggests ovarian cancer, the patient is referred to secondary care. If clinical examination suggests ascites and/or a mass, the patient should be referred immediately to secondary care.

In secondary care, the Risk of Malignancy Index 1 (RMI 1) is recommended and if the RMI 1 score is greater than 250, specialist multidisciplinary team review at Gynaecological Cancer Centre is required.

If the ultrasound scan, serum CA125 and clinical status suggest ovarian cancer, a CT scan of the thorax, abdomen and pelvis is necessary to establish the extent of the disease. A tissue diagnosis is required to confirm ovarian cancer before considering chemotherapy.

The prospective Canadian Diagnosing Ovarian Cancer Early (DOVE) study investigated whether symptom triggered testing would increase the rate of early-stage diagnosis of ovarian cancer (Gilbert et al., 2012). The analysis of 1455 women demonstrated that DOVE patients presented with reduced tumour burden than the general population of patients, significantly lower serum CA125 levels and attained significantly higher complete tumour resection rates (due to the lower tumour burden)

even though no stage shift *per se* was noted. The investigating team concluded that because the development of most (high grade serous) ovarian cancers is thought to be extra-ovarian, early diagnosis programmes should ideally aim to identify low-volume disease, rather than early-stage disease and that diagnostic approaches should be modified accordingly.

1.4.4 Screening and prevention

There is currently no role for organized screening programmes in women considered at low risk of development of ovarian cancer; and the role of ovarian cancer screening in women at high risk of ovarian cancer is yet to be established.

The UK Collaborative Trial of Ovarian Cancer Screening (Jacobs et al., 2016) and The American Prostate, Lung, Colorectal and Ovarian (PLCO) Cancer Screening Randomised Controlled Trial (Gohagan et al., 2000) both did not show a reduction in mortality from ovarian cancer.

1.4.5 Risk stratification

High-risk populations (lifetime risk greater than 10%) for ovarian cancer are identified by family history and limited genetic testing. Currently there is no evidence to support a mortality benefit from screening in low-risk populations and this is not advised (Jacobs et al., 2016).

Non-genetic risk factors include early menarche, late menopause, nulliparity, current or recent hormone replacement therapy use, endometriosis, talc use, black tea

consumption and obesity (body mass index >40). Genetic risk factors associated with developing ovarian cancer include personal or family mutations to mismatch repair genes (Lynch Syndrome) or *BRCA* genes and a first degree relative with ovarian cancer (**Table 1.5**). Around 40% of women who inherit the harmful *BRCA1* mutation and 17% of women who inherit *BRCA*2 mutation will develop ovarian cancer by age 80 years (Kuchenbaecker et al., 2017).

Table 1.5: Summary of mutations in high penetrance genes & conferred risk of developing ovarian cancer

Gene mutation	Increase in risk of developing ovarian cancer (till age 80 years)	Reference
*BRCA*1	39-44%	(Kuchenbaecker et al., 2017)
*BRCA*2	17%	
MLH1 & MSH2 (Lynch Syndrome)	10-15%	(Bonadona et al., 2011)
RAD51C, RAD51D	11-12%	(Loveday et al., 2012)
BRIP1	5.8%	(Ramus et al., 2015)
PALB2	5%	

Risk reduction strategies and protective factors

Known protective factors include use of the combined oral contraceptive pill, pregnancy, breast feeding and tubal ligation or salpingectomy. Hysterectomy alone

appears to have no benefit in protection from ovarian cancer; in a population-based health record linkage study of 837,942 Australian women there was no evidence of protective benefit from hysterectomy (Dixon-Suen et al., 2019). This is likely because the tubes are often left behind when the ovaries are conserved during benign hysterectomy. A hysterectomy with unilateral salpingo-oophorectomy appears protective with similar effect estimates as seen in women who have undergone unilateral salpingectomy or bilateral salpingectomy. Tubal ligation appears to be protective which is in keeping with the tubal origins of ovarian cancer (**Table 1.6**).

Table 1.6: Protective surgery and medication for ovarian cancer

Protective factor	OR	95% CI	Reference/year
Hysterectomy with unilateral salpingo-oopherectomy	0.65	045-0.94	(Rice et al., 2013)
Unilateral salpingectomy	0.71	0.56-0.91	(Madsen et al., 2015)
Bilateral salpingectomy	0.35	0.17-0.73	
Tubal ligation	0.87	0.78-0.98	
Combined hormonal contraception ever-use (and greater than10 years)	0.73 (0.43)	0.66-0.81 (0.37-0.51)	(Havrilesky et al., 2013)

Prospective multicentre cohort studies have demonstrated that risk-reducing bilateral salpingo-oophorectomy (RRBSO) is associated with a lower risk of EOC, first diagnosis of breast cancer, all-cause mortality, breast cancer–specific mortality, and

ovarian cancer–specific mortality in *BRCA*1- and *BRCA*2-mutation carriers (Heemskerk-Gerritsen et al., 2015, Domchek et al., 2010). The risk of primary peritoneal cancers is not influenced by RRBSO. The role of RRBSO for primary surgical prevention has expanded to include not just BRCA1/BRCA2 carriers but also women at intermediate risk (≥4–5% lifetime-risk of EOC). RRBSO surgery reduces EOC risk by 80–96% (Domchek et al., 2010, Heemskerk-Gerritsen et al., 2015). There are ongoing studies evaluating the role of opportunistic salpingectomy in the prevention of ovarian cancer in low-risk women.

1.4.6 Alternative methods of detecting ovarian cancer

RMI 1 is the current risk scoring method for detecting ovarian cancer. The RMI 1 tool combines 3 pre-surgical features (measured serum CA125 levels, ultrasound imaging [U] and menopausal status [M]) to create an index score: RMI I score = U×M×CA125 (NICE, https://www.nice.org.uk/guidance/dg31/chapter/4-Evidence). With a cut-off score at 250, the sensitivity for ovarian malignancies including BOTs is 72.5% and the specificity is 88.7% (Yamamoto et al., 2009). Other models for guiding decision for women with suspected ovarian cancer (e.g., ADNEX) offer increased sensitivity relative to RMI 1 but at a cost of lower specificity (Westwood et al., 2018). New blood biomarkers for epithelial ovarian cancer have been demonstrated but none of these have become established in practice (**Table 1.7**) (Holcakova et al., 2021).

Table 1.7: Proposed candidate biomarkers for ovarian cancer

Transthyretin, Ca15.3, CaA72.4
TP53
Glycodelin, mesothelin, MMP7
CYFRA21-1 VTCN1

A newly marketed test is CancerSEEK; a blood panel analysis of circulating free tumour DNA searching for combined mutations (including *TP53*) and 8 circulating protein biomarkers, including CA125. The initial case-control study recruited clinically diagnosed patients and 812 controls from an asymptomatic population. Sensitivity was 98% with 79% specificity for invasive epithelial ovarian cancer (Cohen et al., 2018). Similar approaches to detect tumour DNA using mutation profiling have been reported in novel lower genital tract specimens such as vaginal and endocervical liquid cytology samples, tampons, and uterine lavage (Holcakova et al., 2021).

1.4.7 Prognosis and management

Whilst the dualistic model of Type 1 and Type 2 illustrates very different clinical-pathogenic behaviour, the vast majority of patients are diagnosed with high grade serous ovarian cancer which is diagnosed at advanced stage. The survival rate for ovarian cancer is strongly related to the stage of disease at the time of diagnosis. Women diagnosed with early-stage disease have a better 5-year survival rate than those diagnosed with late-stage disease (**Table 1.8**). Early-stage ovarian cancer may

be an unexpected post-operative histological finding in cases that have been managed as a benign condition. Further surgery may then be required for completed staging.

For patients with primary advanced ovarian cancer, the British Gynaecological Cancer Society (BGCS) recommend neoadjuvant chemotherapy followed by interval debulking surgery with the aim of achieving complete cytoreduction (Fotopoulou et al., 2017). There is a role for primary debulking surgery and adjuvant chemotherapy, if complete surgical cytoreduction as a primary therapy is considered achievable.

Current management of ovarian cancer is radical surgery and chemotherapy which are directed at established cancer but not at the mechanisms by which cells are neoplastic. Curative treatment remains elusive and understanding the molecular pathogenesis of ovarian cancer to create new approaches are needed. One approach is to focus on earlier detection.

Table 1.8: TNM and FIGO Classification for Epithelial Ovarian Carcinoma with associated 5-year survival figures by disease stage for England for 2013-2017.

5-year survival data is from patients diagnosed from 2013-2017 and reported by Office for National Statistics, Cancer survival by stage at diagnosis in England is reported for 2019.

TNM	FIGO Stage	Description	5-year Survival (England)
T0		No evidence of primary tumour	
T1	**1**	Tumour limited to the ovaries	**95%**
T1a	**1a**	Tumour limited to one ovary; capsule intact, no tumour on ovarian surface; no malignant cells in ascites or peritoneal washings	
T1b	**1b**	Tumour involves one or both ovaries, no tumour on ovarian surface; no malignant cells in ascites or peritoneal washings	
T1c	**1c**	Tumour involves one or both ovaries with any of the following: capsule ruptured, tumour on ovarian surface, malignant cells in ascites or peritoneal washings	
T2	**2**	Tumour involves one or both ovaries with pelvic extension	**70%**
T2a	**2a**	Extension and/or implants on uterus and/or tube(s). no malignant cells in ascites or peritoneal washings	
T2b	**2b**	Extension to other pelvic tissues; no malignant cells in ascites or peritoneal washings	
T2c	**2c**	Pelvic extension (2a or 2b) with malignant cells in ascites or peritoneal washings	
T3	**3**	Tumour involves one or both ovaries with microscopically confirmed peritoneal metastasis outside the pelvis and/or regional lymph node metastasis	**25%**
T3a	**3a**	Microscopic peritoneal metastasis beyond pelvis	
T3b	**3b**	Macroscopic peritoneal metastasis beyond pelvis 2 cm or less in greatest dimension	
T3c +/-N1	**3c**	Peritoneal metastasis beyond pelvis more than 2 cm in greatest dimension and/or regional lymph node metastasis	
M1	**4**	Distant metastasis (excludes peritoneal metastasis)	**15%**

1.5 Current understanding of steroid hormone behaviour in epithelial ovarian cancer

1.5.1 The association of non-sex steroid hormones in epithelial ovarian cancer

Glucocorticoids

In vitro studies have shown glucocorticoids to promote ovarian cancer tumour cell survival, metastasis and drug resistance (Chen et al., 2021). Activation of the glucocorticoid receptors can upregulate the expression of anti-apoptotic genes (*SGK1* and *MKP1/DUSP1*) in ovarian tumours (Melhem et al., 2009). Furthermore, dexamethasone induces upregulation of *ROR1* (receptor tyrosine kinase-like orphan receptor) expression in ovarian cancer. *ROR1* is important for cell growth, migration and invasion and its increased expression correlates with reduced overall survival in ovarian cancer patients. (Karvonen et al., 2020).

NR3C1 encodes the glucocorticoid receptor (GR). GR can function both as a transcription factor that binds to glucocorticoid response elements in the promotors of glucocorticoid responsive genes to activate their transcription, and it regulates other transcription factors. It is present in the cytoplasm but upon ligand binding it transfers to the nucleus as a dimer. Inflammatory responses, cellular proliferation and differentiation in target tissues transcend from activation of the receptor. Mutations in this gene are typically associated with glucocorticoid resistance.

Using RNA sequencing (RNAseq) and clinical data from 188 serous ovarian cancer TCGA cases, *NR3C1* expression above the median correlated with worse overall survival (p=0.015, Hazard ratio = 1.67, 95% CI 1.10-2.53). Median overall survival was

3.0 years in *NR3C1* high expression cases compared with 3.71 years in low *NR3C1* expression cases (Veneris et al., 2017). GR protein expression was evaluated by immunohistochemistry using tissue microarrays of tumours from 481 epithelial ovarian cancer patients which included 12 patients with borderline ovarian tumours (Veneris et al., 2017). High expression of GR was defined as intensity 2+ or 3+ in 1> of tumours cells). GR varied according to histological subtype. Highest prevalence of GR expression was observed in the serous cancers (48%) and lowest prevalence was in endometrioid cancers (2/32, 6%). Clear cell and mucinous cancers had high GR expression in 11 out of 42 (26.2%) and 2 out of 17 (11.8%) cases respectively. Carcinosarcomas had the largest proportion of cases with high expression with 4 out of 7 cases (57.1%). When borderline ovarian tumours were analysed, few exhibited high GR expression (2/12, 16.7%). Incidentally, no GR staining was observed in the ovarian epithelium of a separate 4 cases of benign tumours.

In early-stage tumours treated by surgery, approximately 30% of tumours had high GR protein expression; however advanced stage tumours treated with neoadjuvant chemotherapy before delayed debulking surgery had an increased rate of 62.3% high GR expression compared with 41.9% in unmatched primary debulking surgery cases ($p=0.006$). However, the authors did not clarify if steroids were given as anti-emetics with neoadjuvant chemotherapy to that cohort of patients.

High GR protein expression correlated positively with advanced stage at diagnosis (early vs advanced, $p=0.037$) and median progression free survival (PFS) was significantly decreased in cases with high GR expression (20.4 months) compared to those with low GR expression (36 months) ($p<0.001$) after multivariate analysis.

Overall survival was not associated with GR expression status in this study (Veneris et al., 2017).

Mineralocorticoids

There is no current evidence to demonstrate a role or association for mineralocorticoids in ovarian tumorigenesis or disease progression.

1.5.2 Evidence to implicate estrogen and progestogen involvement in epithelial ovarian cancer

Epithelial ovarian cancer tissue and its associated draining ovarian vein have been shown to contain several folds greater (>100-fold) estrogen and progesterone than in peripheral venous serum. Surprisingly, lower concentrations of E2 (but not progesterone) were found in ovarian cancer tissue and peripheral serum with Stage III/IV disease rather than Stage I/II. (Lindgren et al., 2002). These data suggest that an ovarian tumour might be an estrogen source fuelling early carcinogenesis. In addition, ER, has been shown to be significantly increased in expression in the stroma of epithelial ovarian cancers, particularly Type 1. This suggests the ovarian stroma is stimulated locally by sex-steroid hormones such as estrogens that may initiate neoplastic growth (Blanco et al., 2017).

If estrogens are promoting ovarian carcinogenesis, then it may be performed either by receptor-dependent or receptor-independent mechanisms (**Figure 1.10**). **In the**

receptor dependent mechanism, estrogen binds to the nuclear receptors, ERα and ERβ, leading to the transcriptional activation of estrogen-responsive genes that are the signalling system for cell differentiation and division. Among these genes are proto-oncogenes such as *c-fos*, *c-myc*, *HER2/neu* and growth factors. Alternatively, estrogens can bind to membrane bound G-protein coupled estrogen receptors (GPER) to activate the secondary messenger systems; thus, GPER confers rapid non-genomic effects of estrogens (Mungenast and Thalhammer, 2014).

The transcriptional effects of estrogens on target genes are mediated by activation of ERα and ERβ. The normal ovary expresses predominantly ERβ but the ERα:ERβ ratio seems to change in favour of ERα in the progression from normal ovary to primary EOC and then to metastatic disease (Schüler-Toprak et al., 2018, Chan et al., 2017). ERα induces transcription of several genes that stimulate cell proliferation which is associated with increased risk of mutations that when accumulated in cells, lead to malignant transformation. High expression of ERα is associated with a poor prognosis in EOC. However, ERβ is associated with improved overall survival; it has been shown to nullify cell proliferation effects of ERα in ovarian cancer cells (Schüler-Toprak et al., 2018). However**,** there is no clear understanding of the mechanisms of pathogenesis related to ERα and ERβ in EOC.

In the receptor independent mechanism, formation of reactive metabolites (4-hydroxyestrogens) can occur by hydroxylation of estrogens by cytochrome P450 enzymes (CYP1A1, CYP1A2 and CYP1B1), expressed locally in epithelial ovarian cancer tissues. 4-hydroxyestrogens are then oxidized to quinone intermediates that react with the purine bases of the DNA in cells. This results in genotoxic DNA adducts

which have carcinogenic effects (Cavalieri and Rogan, 2011). In addition, free radicals are generated by the redox cycle of 4-hydroxyestrogens back to quinone derivatives and these species can accumulate and cause DNA mutations in various genes that lead to neoplastic transformation of the cells (Yager, 2015). *CYP1A1* and *CYP1B1* have both been observed to be expressed at a higher level in epithelial ovarian cancer ovaries compared to normal ovary (Downie et al., 2005).

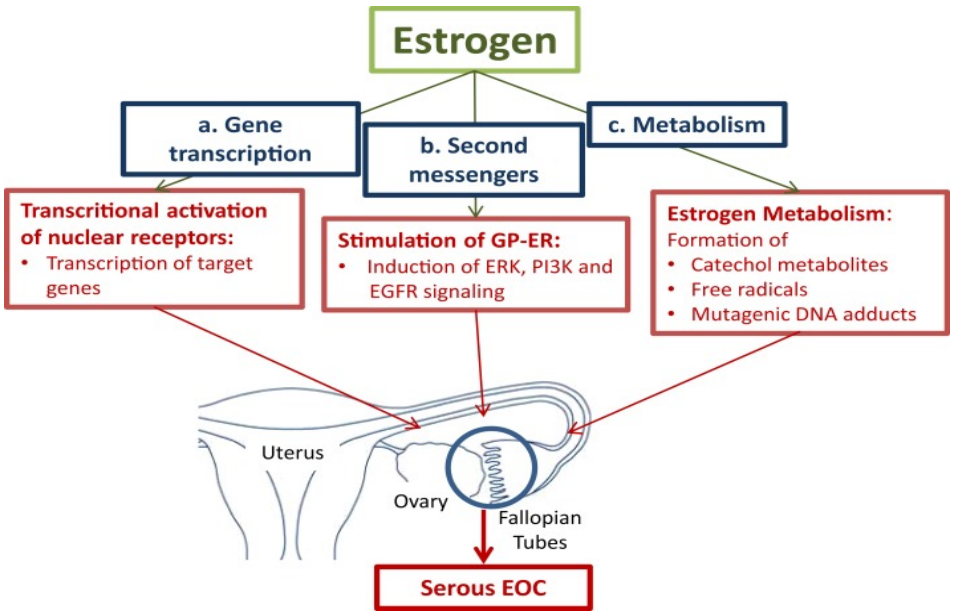

Fig. 1.10: Pathways for estrogen to convert tumour promoting effects in cells in the Fallopian tubes and ovaries.Published with permission. (Mungenast and Thalhammer, 2014)

(a.) Activation of the nuclear estrogen receptor-α (ER-α) leads to the transcriptional activation of estrogen-responsive genes, which stimulate cell proliferation.

(b.) Binding to membrane-bound G-protein-coupled estrogen receptor (GPER) activates second messenger systems. In cancer cells, estrogen induces extracellular-signal regulated kinase (ERK), phosphoinositide 3-kinase (PI3K), and epidermal growth factor receptor (EGFR) leading to enhanced cell proliferation.

(c.) The formation of reactive metabolites leads to the generation of mutagenic DNA adducts. Free radicals from the metabolic activation of estrogens will cause mutations. Accumulation of mutations will lead to neoplastic transformation of proliferating cells.

ER and PR receptors as prognostic biomarkers for ovarian cancer survival

The results of a tissue microarray-based analysis of PR and ER expression in 2933 women with invasive epithelial ovarian cancer for 12 international sites was reported in the Ovarian Tumor Tissue Analysis consortium study (Sieh et al., 2013). It showed that ER and PR positive expression status was highest in low grade serous ovarian cancer but it had no association with improved survival with this subtype or any of the Type 1 ovarian cancers. However, the low numbers of each of these could have prevented identification of real associations.

In HGSOC, only PR expression (but not ER) was independently associated with improved overall survival. PR expression associated with improved overall survival for HGSOC is consistent with previous studies. PR activation induces apoptosis in ovarian cancer cells which may contribute to improved survival. PR is transactivated by ERβ and PR expression might be a biomarker of improved prognosis because it indicates a functionally intact ER pathway and tumour behaviour that is less aggressive (Sieh et al., 2013).

BRCA mutations and the risk of epithelial ovarian cancer

High estrogen concentrations may be the contributing risk in 5-15% of patients with ovarian cancer attributed to germline *BRCA1* and *BRCA2* gene mutations (Ramus and Gayther, 2009). Carriers of these mutations are exposed to higher titres of E2, which may trigger breast and ovarian cancers (Widschwendter et al., 2013) and hence in women who possess these mutations, the subsequent removal of both ovaries and Fallopian tubes have their risk reduced for these cancers (Manchanda et al., 2011).

1.5.3 Evidence to implicate androgen involvement in epithelial ovarian cancer

Epidemiological and *in vitro* data postulate androgens are involved in epithelial ovarian cancer but the role and mechanisms by which this is mediated is unclear. The knowledge on steroidogenic synthesis and endocrine activity *in vitro* in ovarian cancer cells is limited due to older methods of radioimmunoassay but the consensus is that the production of androgens by the ovaries is vastly greater than that of all other steroid hormone groups.

Ovarian surface epithelium is androgen responsive

The normal ovarian surface epithelium has been demonstrated to be an androgen responsive tissue. Eight primary cultures of human OSE were treated with mibolerone (synthetic androgen) causing stimulation of increased DNA synthesis and an increase in proliferation of cells and a decrease in cell death (Edmondson et al., 2002). Similarly malignant OSE cell lines and normal OSE primary cultures showed androgen stimulated increase in cell growth which was reversible by flutamide (anti-androgen) (Syed et al., 2001). AR expression in primary ovarian cancer cultures derived from ascitic fluid has been demonstrated, and, after treatment with DHT, cell division increased in 6 out of 11 primary cultures (Elattar et al., 2012).

In animal studies, mice had OVCAR3 cells (HGSOC cell line) subcutaneously implanted and were then treated with DHT +/- enzalutamide, an anti-androgen. They confirmed that DHT increased tumour volume and that this was reduced with

enzalutamide. AR protein expression was confirmed in the OVCAR3 cell line using Western blotting (Park et al., 2016). These findings would suggest AR is involved in ovarian cancer progression but there are contrary opinions to this.

Androgen receptor expression in epithelial ovarian cancer

Reports on AR expression in epithelial ovarian cancer vary. Here, I summarise these findings. AR expression has tended to be more prevalent in serous than in non-serous tumours. AR expression was detected in 91% of epithelial ovarian cancers by biochemical receptor assay (Kühnel et al., 1987) and between 43.5 to 86% by immunohistochemistry in four separate studies (Chadha et al., 1993) (Cardillo et al., 1998) (Lee et al., 2005) (Sheach et al., 2009b). In a tissue microarray with 322 samples of primary ovarian carcinoma, AR was expressed in 43.7% of samples but most highly in serous ovarian carcinomas (47.5%) (Lee et al., 2005). AR expression scores by immunohistochemistry showed no correlation with FIGO stage, residual disease or CA125 levels, but AR expression was again detected specifically in serous ovarian cancers (Sheach et al., 2009b). Furthermore, studies have shown the AR+ve serous cancer subtype promotes cancer development through the regulation of the cell cycle by androgen stimulation (de Toledo et al., 2014).

The association of AR expression level and their importance in ovarian cancer progression remains to be determined. Two studies show no association between AR immunohistochemistry scores and FIGO stage in malignant ovarian tumour (Sheach et al., 2009b, de Toledo et al., 2014) whilst a third study states that AR levels are significantly reduced in serous ovarian carcinomas compared with benign or borderline

disease but are not altered by cancer stage or metastatic progression (Butler et al., 2013). At present, the evidence suggests that over-expression of AR is not a feature in epithelial ovarian cancer.

Postulated roles for androgens stimulating progression in epithelial ovarian cancer

The precise functions of androgens within ovarian epithelial cells are not completely elucidated. Whilst the hypothesis of over-expression of AR in epithelial ovarian cancer has been abandoned, the presence of AR and AR signalling in tumours may still be involved in tumour development and progression though promoting proliferation and cell migration and invasion, observed in some studies.

OSEC2 (normal ovarian surface epithelial cell line) and OVCAR3 (HGSOC cell line) were shown to express AR on Western blot analysis (Sheach et al., 2009b). In response to androgen treatment, OVCAR3 responded with an increase in cell proliferation and RT-PCR detected a significant upregulation of 121 genes including oncogenic GTPases *Rab25* and *Rab35*. *Rab 35* was identified as the most differentially expressed gene upon androgen stimulation and the protein was observed in 95% of samples by immunohistochemical evaluation; and its expression correlated with AR levels (Sheach et al., 2009b).

Rab25 and Rab35 belong to the Rab protein family and have pivotal roles in cancer pathophysiology. Rab25 governs cellular signalling pathways activation, allowing it to control a diverse range of cellular functions, including cell proliferation, cell motility and

cell death. Aberrant expression of Rab25 is linked to cancer development. Elevated expression of Rab25 correlates with poor prognosis and aggressiveness of ovarian, breast and other cancers (Wang et al., 2017). Rab35 is involved in cell-surface receptors recycling (endocytosis) (Kouranti et al., 2006) and may play a role in the modulation of p53 by regulating the p53-related protein kinase (PRPK) giving it oncogenic potential (Abe et al., 2006).

As discussed before, in the classical pathway, AR combines with co-factors that may promote tumorigenesis. ARA70 is a reported AR-associated co-activator that enhances the trans-activational potential of AR up to 10-fold. ARA70 transcripts were negative in normal OSE but was found to be highly expressed in 17 out of 20 ovarian carcinomas of various histological subtypes. Because expression of ARA70 could significantly magnify or alter the androgenic response pattern in ovarian cancer cells, this may explain why AR over-expression is not a feature of the disease (Shaw et al., 2001).

The epidermal growth factor receptor (EGFR) is over-expressed in up to 98% of EOC and the activation of signalling cascades is associated with cell proliferation, migration, invasion, and angiogenesis with resistance to apoptosis. AR is known to stimulate the synthesis of EGFR by autocrine and paracrine pathways and in 60 serous ovarian cancers, Western Blot analysis demonstrated a positive correlation between EGFR and AR (Gui and Shen, 2012).

Activation of AR on SKOV3 cells (HGSOC cell line) by DHT showed modulation of Interleukin 6 and 8 (IL-6, IL-8). These are pro-inflammatory cytokines that are among the most abundant in ovarian cancer ascites (40- 500-fold higher than serum). IL-6 is

secreted by ovarian cancer cells and has been demonstrated to be involved in autocrine growth of ovarian cancer cells by activation of AR gene promotor regions. IL-6 signalling is associated with regulating tumour cell proliferation, invasion and angiogenesis (Lane et al., 2011). Meanwhile IL-8 has been reported to promote tumour growth *in vivo* (Shahzad et al., 2018). DHT was shown to enhance IL-6 and IL-8 secretion and significantly promoted SKOV3 cell proliferation (Wang et al., 2007).

Postulated roles of androgens in epithelial ovarian cancer, independent of AR

There is evidence that androgens can encourage aberrant cell proliferation independent of AR activation. Disruption to intra-cellular signalling of transformation growth factor beta 1 (TGF-ß1) has been associated with carcinogenesis and several human diseases. TGF-ß1 is a cytokine and potent cell growth inhibitor that regulates the proliferation and differentiation of cells, embryonic development, cell migration and apoptosis.

Typically, in the healthy ovary, ovarian surface epithelial cells are growth inhibited by TGF-ß1. Furthermore, primary epithelial ovarian cancer cells isolated from ascitic fluid and have also been shown to growth inhibited by TGF-ß1 (Hurteau et al., 1994) (Havrilesky et al., 1995). However, in several ovarian cancer cell lines (HEY, OVCAR3, SKOV3) low dose DHT down-regulated mRNA expression for the TGF-ß1 receptors. Therefore, androgens were hypothesised to promote ovarian cancer progression by decreasing expression of TGF-ß1 receptors on tumour cells and thus reducing the action of TGF-ß1. The study then demonstrated *in vitro* that some ovarian cancer cell lines later did not regain their sensitivity to TGF-ß1 when the androgen was counter-treated with hydroxy-flutamide (androgen antagonist) (Evangelou et al., 2000).

Furthermore, in a separate study of primary cultured cells from healthy ovary and primary ovarian cancer, TGF-ß1 limited cell proliferation and then addition of DHT reversed it (Evangelou et al., 2003). In a more recent separate study, these findings were reconfirmed where human epithelial ovarian cancer tissues were observed to have decreased TGF-ß1 receptors and in ovarian cancer cell lines, DHT decreased expression of the receptor (Kohan-Ivani et al., 2016). Hence in conclusion, androgens can disrupt the TGF-ß1 signalling pathway and potentially cause ovarian tumour development as previously described (Blobe et al., 2000) (**Figure 1.11**).

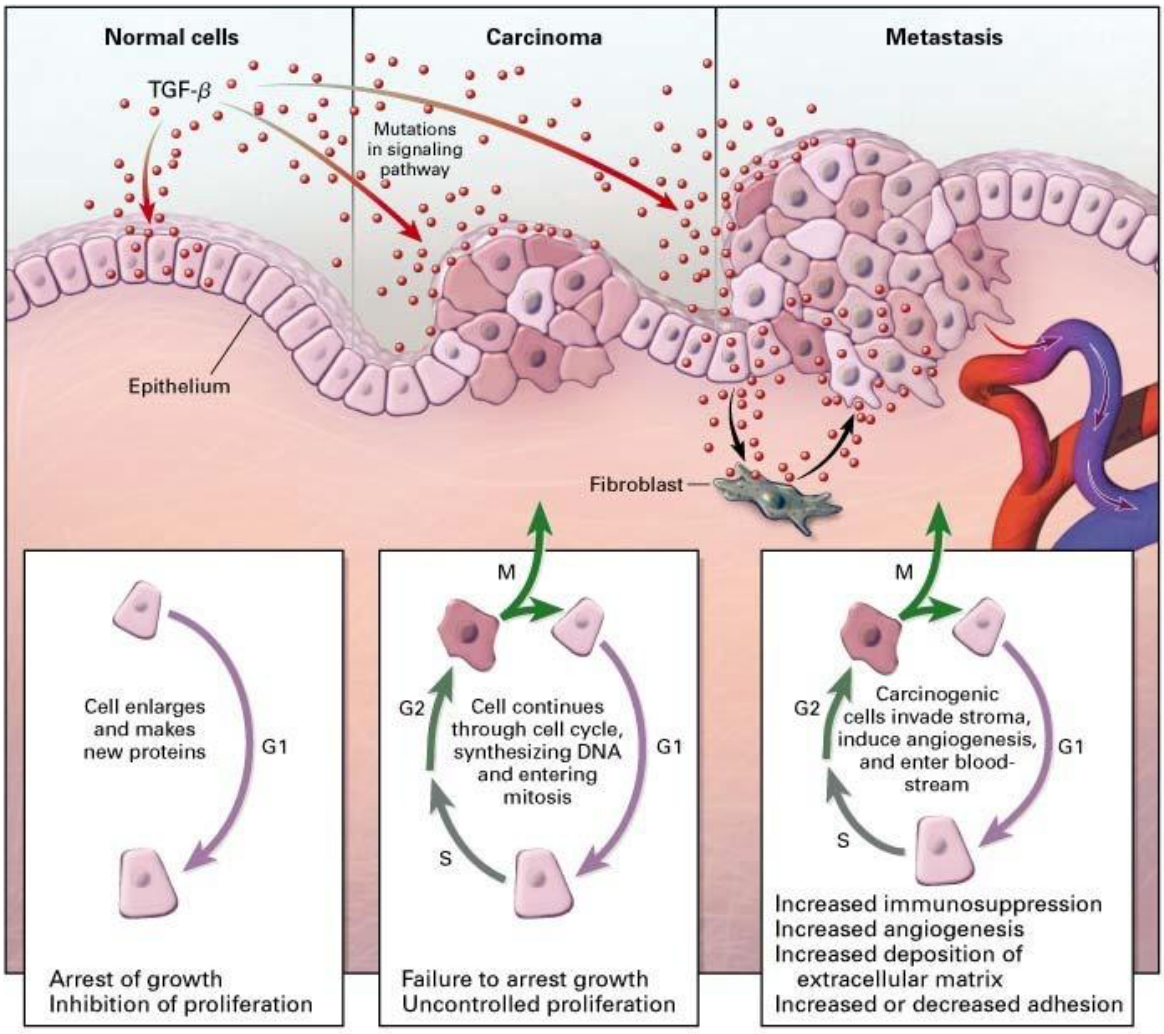

Fig. 1.11: Role of transforming growth factor β (TGF-β) in cancer development

Published with author's permission (Blobe et al., 2000).

In normal epithelial cells, TGF-β, acting through its signalling pathway, arrests the cell cycle at the G1 stage to inhibit proliferation, induce differentiation, or promote apoptosis.

During the transformation of a cell into a cancer cell, various components of the TGF-β signalling pathway are mutated, making the cell resistant to the effects of TGF-β.

These TGF-β–resistant cancer cells, which proliferate in an unregulated manner, as well as the surrounding stromal cells (fibroblasts), then increase their production of TGF-β. This TGF-β, by acting on the surrounding stromal cells, immune cells, and endothelial and smooth-muscle cells, causes immunosuppression and angiogenesis and increases the invasiveness of the tumour.

1.5.4 The androgen metabolome in ovarian cancer

In 1964, the presence of luteinized stromal cells immediately adjacent to primary and metastatic ovarian tumours was described along with oxidative enzyme activity and these were labelled as enzymatically active stromal cells. It was postulated that these active stromal cells stimulated proliferation of neoplastic epithelium by local synthesis of steroid hormones (Scully and Cohen, 1964).

EOC is most commonly found in post-menopausal women and the postmenopausal ovary remains relatively androgenic, as evidenced by 15-fold higher testosterone concentrations in the ovarian vein compared with peripheral vein serum (Fogle et al., 2007). Hence the historical hypothesis of the 1960s would now be amended to androgens are locally synthesised to stimulate proliferation of neoplastic epithelium in the ovary.

In EOC, androgens appear to be differentially associated with ovarian cancer subtypes. In a pooled analysis of 7 nested case-control studies from the Ovarian Cancer Cohort Consortium (OC3), the association between pre-diagnosis circulating androgens (testosterone, free testosterone, androstenedione, DHEAS and SHBG) and development of epithelial ovarian cancer was investigated. This was a very large study featuring a population of 1331 EOC patients with 3017 matched controls. Multivariable conditional logistic regression was used to assess risk associations in pooled individual data. Testosterone was positively associated with all EOC subtypes but other endogenous androgens and SHBG were not associated with overall risk. Higher concentrations of testosterone and androstenedione associated with an increased risk in endometrioid and mucinous ovarian cancers but not serous or clear cell cancers. An

inverse association was observed between androstenedione and high-grade serous tumours (Ose et al., 2017). The higher concentrations of testosterone and androstenedione were particularly significantly increased with risk of developing mucinous ovarian cancers. This suggests that Type 1 ovarian cancers may have a very active androgen synthesis pathway in comparison to the serous tumours.

In a immunohistochemical analysis of ovarian tumour stroma (benign, BOT and malignant), four steroid enzymes (CYP17, CYP19, AKR1C3 and HSD17B1) were studied to validate Scully and Cohen's hypothesis (Blanco et al., 2017). The four proteins were assessed in three locations: on the OSE, in the central stroma and in the stroma adjacent to the OSE. CYP17 converts progesterone to androstenedione and pregnenolone to DHEA, which is integral for the biosynthesis of androgens, was the most significantly expressed enzyme in the adjacent stroma to the OSE of the various tumour subtypes, particularly in endometrioid and mucinous tumours. The second most expressed enzyme was AKR1C3 (converts androstenedione to testosterone) also in the stroma adjacent to the OSE. In HGSOC, increased CYP17 correlated with increased AR expression in the adjacent stroma to the OSE but decreased AR in the OSE. AKR1C3 was also consistently very immunoreactive in the adjacent stroma to the OSE for all the tumour subtypes and increased AKR1C3 correlated strongly with increased AR in the adjacent stroma to the OSE. This suggest that androgens, whilst being a source for estrogens, may be acting in an autocrine fashion in the stroma of the tumour. Furthermore, expression of these four proteins was significantly higher in mucinous and endometrioid ovarian tumours ($p<0.01$) compared to serous ovarian tumours; hence these findings are strongly suggestive of androgens being produced in an autocrine mechanism in Type 1 ovarian cancers (Blanco et al., 2017).

1.5.5 Hormonal therapy for epithelial ovarian carcinoma

Although most ovarian cancers express ER, PR and AR, their receptor status is not routinely tested to dictate primary chemotherapy. However, for recurrences or end-stage disease these tests may be performed to guide the use of hormonal therapy when other chemotherapy agents have been exhausted. They are also used as a maintenance therapy after first line chemotherapy treatment (Li et al., 2021). No routine anti-glucocorticoid or anti-mineralocorticoid drugs are used in ovarian cancer care.

Anti-estrogen therapy

Pre-clinical models have demonstrated that ovarian cancer cells that express high levels of ER are stimulated by estrogens and inhibited by anti-estrogens, establishing a rational for hormonal therapy. ER positivity is highest in EOC subtypes HGSOC, LGSOC, endometrioid OC (81, 88 and 77% respectively) and these tumour types do exhibit response to tamoxifen and aromatase inhibitors in clinical studies. However, ER positivity is only around 20% in clear cell and mucinous carcinomas (Li et al., 2021) and the response is expectedly poorer.

Androgen targeted therapy

The number of anti-androgens tested so far in EOC is limited. AR is expressed in up to 90% of cases of EOC. Co-activators such as ARA70, AIBI1 and p44 are reported to influence AR activity in EOC. AR has been shown to influence EGFR and TGF-β1

signalling pathways that affect tumour growth, described earlier. Abiraterone, a CYP17 inhibitor that irreversibly inhibits androgen biosynthesis was evaluated in a Phase II study of 42 patients with recurrent serous ovarian cancer and AR+ve >10% on tumour staining. However, only 1 patient with low grade serous ovarian cancer achieved a sustained clinical benefit (Banerjee et al., 2020). In pre-clinical studies, enzalutamide, an AR inhibitor was shown to significantly reduce growth of EOC xenografts (Park et al., 2016) and this finding has led to a Phase II study exploring this treatment approach. Phase II studies of cyproterone acetate and flutamide have reported response rates of 4-7% (Thompson et al., 1991) (Tumolo et al., 1994) (Vassilomanolakis et al., 1997). A study of goserelin (GnRh agonist) and bicalutamide (anti-androgen) reported a progression free survival of 11 months (Levine et al., 2007).

Progestogen therapy

There are some studies utilizing progestogens as hormonal therapy, but they have featured very few numbers of patients, with a lack of biomarkers to predict the response and often they did not report the hormone receptor expression levels in ovarian cancer tissue. One study has investigated the combination of medroxyprogesterone acetate with primary adjuvant chemotherapy for advanced EOC and showed both progression free survival and overall survival were longer compared to controls (Niwa et al., 2008).

1.6 The utility of mass spectrometry in epithelial ovarian cancer

1.6.1 Mass spectrometry in steroid analysis

One of the concerns about implicating steroids, steroid metabolites and steroid hormones in the epithelial ovarian cancer is the legitimacy of the methods used for steroid analysis. In the past, immunoassays were widely adopted as the method of choice for steroid analysis in clinical chemistry laboratories because of its simplicity, low cost and the lack of availability of tests for less common analytes. However, the immunoassay method is now considered sub-optimal for steroid analysis due to problems such as cross reactivity with similar analytes, and standardisation issues between laboratories (Taylor et al., 2015). Another problem is accurate quantification of low concentration of steroids in post-menopausal women.

Mass spectrometry techniques are superior to immunoassays regarding specificity and its ability to measure large panels of steroids in a single sample. This has prompted the editors of Journal of Clinical Endocrinology and Metabolism to recommended to avoid using immunoassays and instead use mass spectrometry for the measurement of sex steroids (Handelsman and Wartofsky, 2013).

1.6.2 Gas chromatography-mass spectrometry

Gas chromatograph- mass spectrometry (GC-MS) has been routinely employed for analysis of urinary steroid metabolite profiles in patients with suspected inborn steroidogenic disorders. It is highly valued for diagnosing rare disorders with high diagnostic sensitivity and specificity and it is considered the gold standard tool in

clinical steroid investigations (Shackleton, 1986, Krone et al., 2010). A detailed explanation of this technique is discussed in **Chapter 2**. Briefly, GC-MS permits the highest potential of all methods for separation of multiple steroids in a liquid analyte. A sample is vaporised and the gaseous steroids travel through a heated column and arrive at the mass spectrometer at different times. Each steroid compound elutes from the column at a different time based on its boiling point and polarity. The time of elution is referred to as a compound's retention time and this enables identification of the compound, by comparing it to a table of retention times for all known compounds. The method for steroid profiling by GC-MS has been developed over 40 years ago (Shackleton and Snodgrass, 1974). However, this method remains cumbersome, expensive and time consuming. Sample preparation requires enzymatic deconjugation of intact steroid conjugates and is not applicable to high-throughput assays (Storbeck et al., 2018) (Marcos and Pozo, 2015).

1.6.3 Tandem liquid chromatography-mass spectrometry

In contrast to GC-MS, tandem liquid chromatography mass spectrometry (LC-MS/MS) permits rapid specific and sensitive high-throughput analysis of several liquid analytes and is appropriate for samples which contain compounds that cannot withstand the high temperatures during gas chromatographic separation. Sample preparation is less complex than GC-MS. It requires small sample volumes and has shorter analysis times. It is the gold standard for measurement of individual steroids and steroid panels but it is limited in defining novel steroid metabolomes. This technique is discussed in further detail in **Chapter 2**.

1.6.4 Androgen precursors and metabolites

The post-menopausal ovary and epithelial ovarian cancers are active in biosynthesis of steroids but the pattern of synthesis and metabolism is not yet characterised. The evidence discussed in this chapter indicates that ovarian tumours produce androgens but their metabolic fate is unknown.

There are many steroid precursors and metabolites along the steroid biosynthetic pathways but they are not routinely measured in clinical biochemistry. Identification and quantifying these metabolites provide a truly comprehensive steroid profiling tool because the detection of minute changes in steroidogenesis illuminates all the intermediate steps that are likely to be perturbed in the setting of epithelial ovarian cancer. For example, DHEA can be converted to androstenedione (A4) by peripheral HSD3B2, with androstenedione then in the role of steroid precursor for the synthesis of testosterone by AKR1C3. Thus, DHEA is metabolised to androstenedione and testosterone. Subsequently the steroid hormone, testosterone, can be metabolised to the more potent, DHT by SRD5A1, amplifying the androgen signal.

Androstenedione can also be converted to another steroid precursor, 5α-androstanedione (5a-dione) prior to conversion to DHT by AKR1C3, hence bypassing testosterone. Furthermore, androstenedione can be converted to inert androgen metabolites, androsterone (An) and etiocholanolone (Et) for urinary excretion (**Figure 1.12**). GC-MS and LC-MS/MS can reliably measure these steroid precursors, steroid hormones and metabolites.

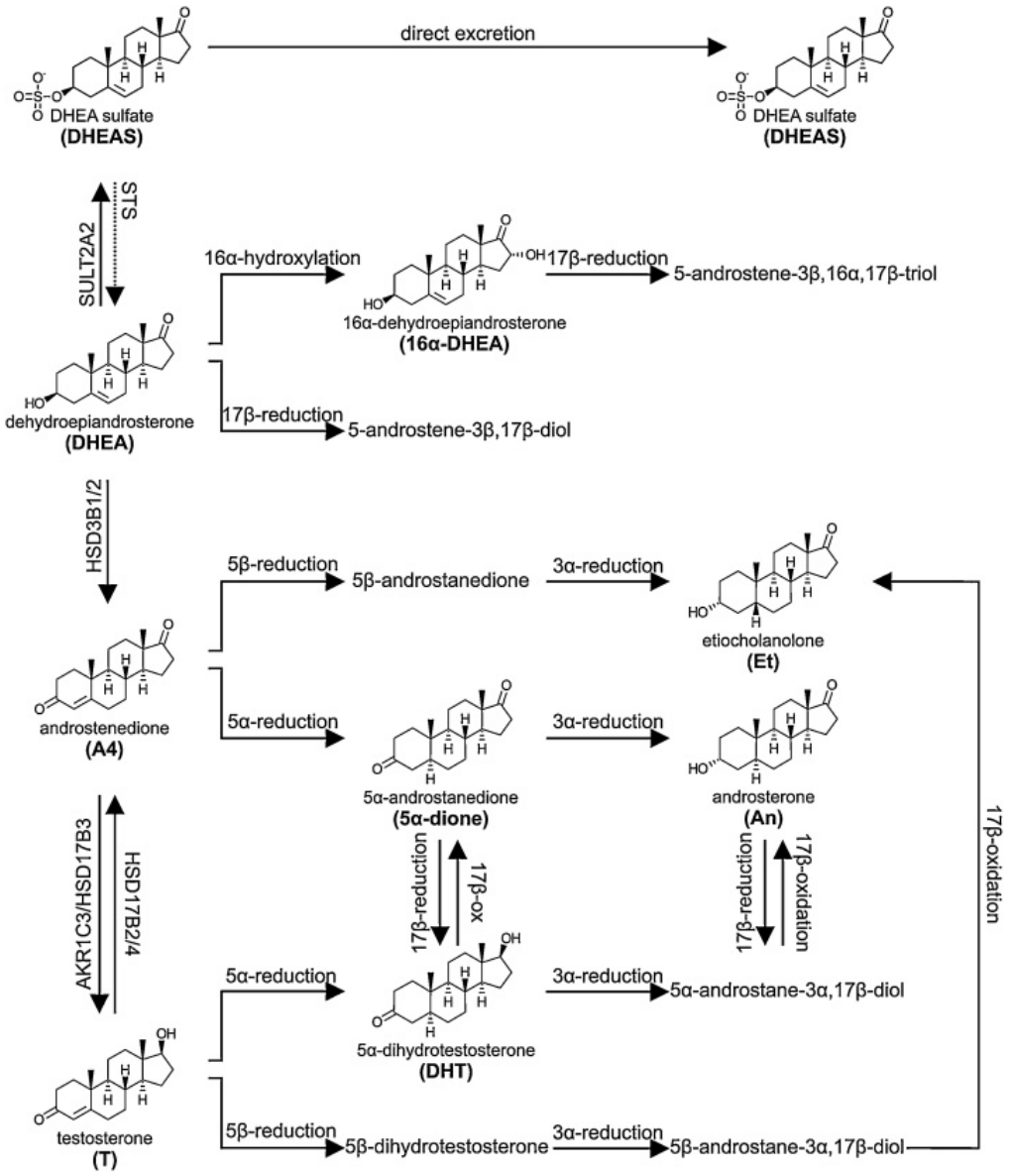

Fig. 1.12: Schematic overview of the metabolism of androgen precursors to active androgens and urinary metabolites.

The major serum androgen precursors are positioned on the left. The primary urinary androgen metabolites on the right are androsterone (An) and etiocholanolone (Et). The metabolism of each steroid is shown from left to right and the urine products are shown. DHT and testosterone are active steroid hormones (active androgens). (Schiffer et al., 2019)

1.6.5 Quantitative analysis of estrogens and progestogens

Quantitatively, estrogens circulate at significantly lower levels than androgens and exist at <100pmol/L and further decline in post-menopausal women. Estrone (E1), estrone sulfate (E1S), 17b-estradiol (E2) are the primary estrogens in circulation. Most estrogens bind to SHBG and are conjugated when excreted. Estriol (E3) for instance, is rapidly excreted in urine and so serum levels are almost undetectable. Peripheral tissues expressing CYP19A1 produce estrogen but this peripheral estrogen production often functions in a paracrine and intracrine manner and as such circulating concentrations are not reflective of concentrations achieved locally (Simpson et al., 2000) (Labrie, 2015). Immunoassay methods are poor for quantifying estrogens mainly due to cross-reactivity with isomers of estrogens and this imprecision is amplified when the analyte is in very low concentrations. At present, there is no universal methods for estrogen analysis. Methods for GC-MS and LC-MS/MS for estrogen metabolite analysis have been described in the literature but none are validated and routinely used. The limitation at present is the lower limit of quantification and the estrogenic isomers and stereoisomers which are confounders.

Progesterone is the only true natural progestogen but other precursors in this family are pregnenolone, 17a-hydroxyprogesterone and 17a-hydroxypregnenolone (Schiffer et al., 2019). These are metabolised by the liver and the major urinary metabolites are 5-pregnenediol (5-PD), pregnanediol (PD), 5-pregnenetriol (5-PT) pregnanetriol (PT) and 17a-hydroxypregnanolone (17-HP). All of these can be reliably measured by both GC-MS and LC-MS/MS.

1.6.6 Mass spectrometry steroid analysis in epithelial ovarian cancer

The ovary and the adrenal gland are related embryologically and are both competent of steroidogenesis. Urine steroid profiling by gas chromatography-mass spectrometry (GC-MS) in conjunction with sophisticated machine learning analysis (steroid metabolomics) has recently been introduced as a sensitive and specific biomarker tool for the original diagnosis of primary ACCs in a large retrospective study (Arlt et al., 2011). Most adrenocortical cancers (ACC) are biochemically active but tend to present with a steroidogenic pattern characterized by abundance of steroid precursor metabolites which can be used to diagnose the disease.

However, studies on steroid hormone profiling in women with epithelial ovarian cancer are extremely limited. In one study, radioimmunoassay was employed to analyse serum samples to examine the utility of oestradiol, progesterone and 17-hydroxyprogesterone with CA125 as tumour markers in post-menopausal women with ovarian cancer (O'Brien et al., 1994). An inverse relationship between CA125 and both progestogens was identified but the study had 44 patients and it pre-dates the classification of Type 1 and type 2 tumours.

In a single study utilising targeted GC-MS, the concentration of 23 urinary steroids (androgens, progestogens and corticoid metabolites) in 15 postmenopausal women with epithelial ovarian cancer and ten aged-matched healthy women was analysed. The study observed that pregnanediol (PD), was found to be significantly higher in the patients compared with controls. The metabolites of cortisol and corticosterone metabolites were also significantly higher (Bufa et al., 2008). The changes in the levels of these steroid metabolites identify the important role of considering non-sex steroid hormones may be implicated in EOC.

1.6.7 The role of untargeted metabolomics beyond steroids in epithelial ovarian cancer

In the last decade, mass spectrometry has been slowly employed to unravel the complex interplay of the global metabolome of ovarian cancer. At present metabolomic studies have identified a variety of metabolomic signatures specific to ovarian cancer and they can be grouped into three principal classes: lipids, amino acids and metabolites derived from the glycolysis and the Krebs cycle. Metabolic fingerprints have been described but their translation to clinical application has been limited due to a lack of independent, large validation studies (Saorin et al., 2020). None of these metabolic fingerprints have reported steroid metabolites or steroid precursors in their findings.

1.7 Summary, hypothesis and aims

The ovary and adrenal gland are competent at steroidogenesis, with both organs arising from the urogenital ridge during human fetal development (Barwick et al., 2005). There are studies that demonstrated the influence of androgens on the proliferation of epithelial ovarian cancer cells and how they can influence tumour progression directly and independently of the androgen receptor (Edmondson et al., 2002, Evangelou et al., 2000, Kohan-Ivani et al., 2016). Very early studies have shown the venous blood of ovarian cancers producing higher concentrations of sex steroids than control post-menopausal ovaries (Fogle et al., 2007, Lindgren et al., 2002, Heinonen, 1991). Altered steroid hormone receptor expression in EOC compared to normal ovary has also been demonstrated (Blanco et al., 2017, Veneris et al., 2017, The Cancer Genome Atlas Research Network, 2011, Butler et al., 2013, Sheach et al., 2009b, Chan et al., 2017, Schüler-Toprak et al., 2018). However, the characteristic behaviour of epithelial ovarian cancer for steroid synthesis and steroid metabolism remains unknown.

In the past, attempts to observe steroid metabolism with immunoassay technology, have been limited by cross-reactivity and sensitivity issues. Most studies predominantly used ovarian cancer cell lines rather than patient specimens. The ability of mass spectrometry to follow steroid metabolism accurately in cell and tissue media and serum and urine samples from patients is a huge leap in methodology.

Mass spectrometry-based comprehensive profiling of the 24-h urine steroid metabolome for adrenal cancer has been established. Adrenal cancer can be characterized by an accumulation of a panel of steroid precursors and it generates a

characteristic “malignant steroid fingerprint”, which can differentiate benign from malignant adrenal tumours with 90% sensitivity and 90% specificity (Arlt et al., 2011). Hence EOC patients may also exhibit a steroid profile for diagnostic utility. Currently, there are very few published studies examining steroid profiling for EOC and all lack clinical and histopathological data which limits their relevance to improving diagnostic and therapeutic advancement (Bufa et al., 2008, Cuzick et al., 1983).

My main hypothesis is that steroid metabolism in epithelial ovarian cancer is distinct for this disease and by characterising the steroid metabolic behaviour, there is potential to identify novel diagnostic tools and therapeutic targets.

My main aim is to examine the steroid metabolome in epithelial ovarian cancer in comparison to benign ovarian tumours and healthy ovary for mechanistic insight and biomarker discovery. I will undertake integrated experiments *in vitro*, *ex vivo* and *in vivo* to identify these steroid metabolites and observe their fluctuations. Finally, I aim to provide proof-of-concept for urine steroid profiling as a novel detection tool for epithelial ovarian cancer. The specific hypotheses and study aims are described below.

1.7.1 Steroidogenic activity and androgen metabolism occurs in ovarian cancer cell lines

To test my hypothesis that androgen metabolism occurs in ovarian cancer cell lines, I will interrogate The Cancer Genome Atlas (TCGA) data on epithelial ovarian cancer and Genotype-Tissue Expression (GTEx) data for normal ovary for mRNA expression of steroidogenic enzymes and compare for fluctuations that would support

steroidogenic changes in the disease. I will then choose representative epithelial ovarian cancer cell lines and analyse their mRNA expression of selected steroid synthesising enzymes and compares these to the GTEx and TCGA datasets. Finally, I will investigate *in vitro* steroidogenic activity in the representative epithelial ovarian cancer cell lines by treating them with steroid precursors and observing downstream steroid synthesis and metabolism using mass spectrometry.

1.7.2 Steroidogenic activity and androgen metabolism occurs in human ovarian tumours

To test my hypothesis that androgen metabolism occurs in human ovarian tumours I will obtain *ex-vivo* representative ovarian tumour specimens and normal ovary and investigate their mRNA expression of selected steroid synthesising enzymes and compare these with the representative ovarian cancer cell lines. I will then investigate the *ex vivo* steroidogenic activity in these tumours by treating them with steroid precursors and observing downstream steroid synthesis and metabolism using mass spectrometry and compare it with the results from the ovarian cancer cell lines.

1.7.3 Urine steroid profiling can be used to detect epithelial ovarian cancer

To test my hypothesis that urine steroid profiling by mass spectrometry can detect epithelial ovarian cancer I will perform urinary steroid analysis on 24h urine collections from untreated patients with epithelial ovarian cancer, benign ovarian tumour and normal ovary cohorts and compare the differences. I will also compare the urinary steroid profiles to the steroids and metabolites synthesised by ovarian cancer cell lines and *ex vivo* ovarian tumours.

Chapter 2 General methods

2.1 Bioinformatics (in silico) analysis of RNA-sequencing cancer databases

Publicly available tissue transcript datasets for ovarian cancers can be interrogated to ascertain potential interaction between transcript levels and clinical characteristics.

Validated genes involved in the classical steroidogenic pathway were selected and corresponding data was accessed from The Cancer Genome Atlas (TGCA) for Ovarian Serous Cystadenocarcinoma (TCGA-OV, Nature 2011) and the Genome Tissue Expression (GTEx) project. RNA sequencing data (RNA-seq) from 426 patients with high grade serous ovarian carcinoma was accessed from cBioPortal, a TCGA genome data analysis portal (https://www.cbioportal.org/) (filename gdac.broadinstitute.org_OV.Merge_rnaseqv2__illuminahiseq_rnaseqv2__unc_edu__Level_3__RSEM_genes_normalized__data.Level_3.2016012800.0.0.tar).

Normalised mRNA expression data was downloaded for log2 transformation. Clinical data for staging, age and 5-year survival were extracted simultaneously for the purpose of identifying if any of the genes were independent predictors. Control data for the serous ovarian cancer patients are not available from TCGA. As a comparator, data on 88 female healthy controls with normal ovaries was downloaded from a GTEx portal (file name phs001034.v1.p1 created on 14 January 2017. (Access link ftp://ftp.ncbi.nlm.nih.gov/dbgap/studies/phs001034/phs001034.v1.p1)

Data was recorded in TPM units (transcripts per million) from both databases. All tumour specimens were collected before systemic therapy. All data was transformed using the formula $\log_2$[TPM+1]. GEPIA software (Gene Expression Profiling Interactive Analysis) was utilised to unify the datasets. Briefly, GEPIA uses recomputed raw RNAseq data before processing through a uniform pipeline (**Figure 2.1**).

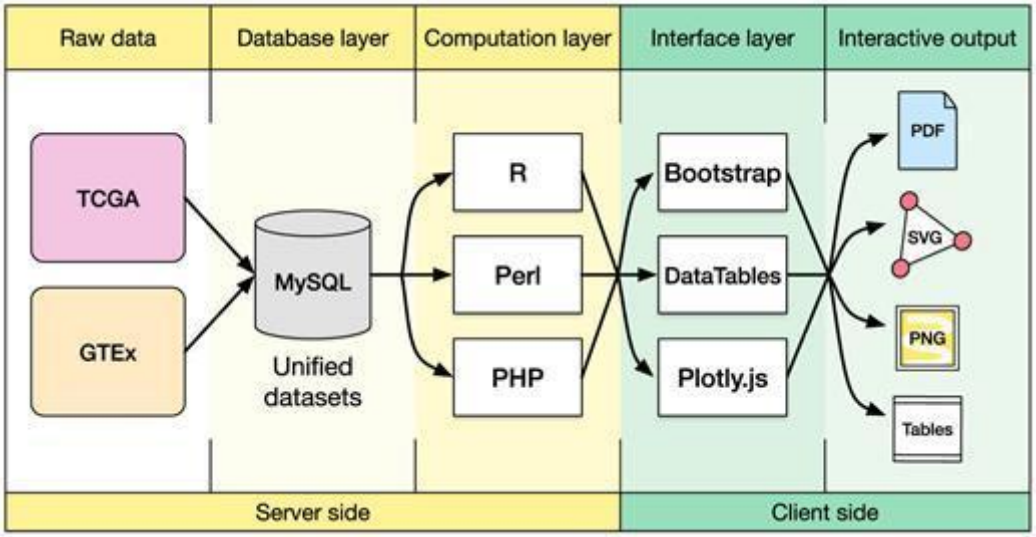

Fig. 2.1 : GEPIA software: Flow diagram for dataset processing of TCGA and GTEx RNAseq data for comparison analysis

Adapted from (Tang et al., 2017)

Normalised $\log_2$ TCGA data and GTEx data was then used for differential analysis by one-way ANOVA, using disease state (Tumour or Normal) as the variable for calculating differential expression. GEPIA software was used for this as well. Log_2 fold change cut-off ($\log_2$FC) was set at 1.0. The p-value for significance was set at 0.01. The $\log_2$FC is defined as [median (Tumour) – median (Normal)]. Genes with higher $\log_2$FC values and lower p-values than the pre-set thresholds were considered as significant differentially expressed genes.

The prognosis of each group for each gene of interest was examined using Kaplan-Meier survival analysis. Expression for each gene of interest was compared as a prognostic indicator with a high expression cut off set at >75% of the data values and low expression at <25% for the data. The log-rank test was used to compare the two

groups by testing the null hypothesis that there was no difference in survival between high and low expression for each gene of interest with significance set at $p<0.05$.

The Oncomine database (http://www.oncomine.org) was also employed to determine candidate genes involved in Type 1 epithelial ovarian cancers (further details described in Chapter 3).

2.2 Description of ovarian cancer cell lines and cell line validation

For the *in vitro* tumour models used in this study, four human epithelial ovarian cancer cell lines were selected: OVCAR5, CAOV3, IGROV1 and NIH-OVCAR3 (OVCAR3). Molecular profiling and systematic genomic comparison based on copy number changes, mutations and mRNA expression profiles have been used to rank which cell lines are most suitable for models of ovarian cancer and this informed the decision on procurement of the cell lines (Domcke et al., 2013). High grade serous ovarian cancer is the most common subtype and hence three representative cell lines were chosen (OVCAR5, CAOV3 and OVCAR3). IGROV1 was selected as a representative of endometroid/clear cell type. There are very few cellular models for mucinous and low grade serous ovarian carcinoma and they possess little certainty in their molecular profiling to validate their use as a competent model; hence these were excluded from this study.

OVCAR5 and CAOV3 ovarian cancer cells were provided as gifts by Dr Paul Foster (University of Birmingham, England). IGROV1 ovarian cancer cells was also provided

as a gift by Dr Jason Yap (University of Birmingham, England). OVCAR3 was purchased from American Type Culture Collection (ATCC).

OVCAR3 cell line was established in 1982 from the malignant ascites of a 60-year-old Caucasian patient with advanced high grade serous ovarian carcinoma. It expresses the androgen, estrogen and progesterone receptors (Hamilton et al., 1983).

OVCAR5 was established from the ascitic fluid of a 67-year-old patient with advanced ovarian adenocarcinoma without prior chemotherapy. It is widely used for drug screening and molecular target identification. Both OVCAR5 and OVCAR3 have been shown to rapidly form large intraperitoneal tumours and aggressive metastases *in vivo* xenograft studies female athymic mice; this is a model of HGSOC which reliably generates tumours and/or ascites (Mitra et al., 2015). OVCAR3 has the tumour protein 53 (*TP53)* mutation status and *CCNE1* amplification and is ranked high against likely serous ovarian cancer based on copy number profile. OVCAR5 is wild-type for *TP53*. does not possess *TP53* status.

CAOV3 is a serous adenocarcinoma cell line from a 54-year-old ovarian cancer patient (Buick et al., 1985). It is a widely cited cell line. It carries the *TP53* mutation and it is ranked as likely high grade serous ovarian cancer based on copy number profiles.

IGROV1 cell line was derived from a 47-year-old woman suffering from a stage III ovarian cancer (Benard et al., 1985). The histological diagnosis was confirmed as mixed endometrioid and clear cell carcinoma. It has multiple mutations including *TP53, BRCA1* and *BRCA2, PI3KCA, PTEN and ARID1A.*

2.3 Propagation of cell lines

Frozen pellets for CAOV3 and OVCAR5 cells were thawed and added to 5ml of Dulbecco's Modified Eagle's Medium (DMEM) (Gibco, Thermo Fisher). The samples were then centrifuged at 1,200rpm for 5 minutes at room temperature. The media was then aspirated to leave the cell pellet and resuspended in 12ml DMEM and incubated at 37°C with 5% CO_2 using Dulbecco's Modified Eagle's and 10% fetal bovine serum and 1% penicillin-streptomycin. Cells were grown in 75cm^3 cell culture flask (T75, Corning) and split to new flasks when they reached 80% confluence. Splitting involved washing the cells with Phosphate-Buffered Saline (PBS, Sigma) followed by addition of 2ml trypsin (Gibco, Thermo Fisher) and incubation at 37°C for 5 minutes. Trypsin was inactivated by addition of an equal amount cell media. The cells were centrifuged at 1,000 rpm for 5 minutes. Pelleted cells were re-suspended in 15ml of plain media and the cell density was estimated by microscopy and then finally the cells were transferred to a new T75 flask using a 1:3-1:5 ratio.

OVCAR3 and IGROV-1 were recovered similarly from cryopreservation but were incubated in Roswell Park Memorial Institute 1640 (RPMI-1640, Sigma) medium with 20% fetal bovine serum, 1% penicillin-streptomycin and 0.01mg/ml bovine insulin.

All experiments for CAOV3, IGROV-1 and OVCAR5 were performed using passage numbers 24-30. Experiments with OVCAR3 were performed using passage numbers 18-24.

Authentication for the three donated cell lines were confirmed through Short Tandem Repeat (STR) genetic analysis performed by Northgene (Newcastle, UK) followed by comparison against the profile located on the ATCC database. STRs are microsatellite

DNA areas consisting of 2-13 nucleotides repeated in a row. Analysis identifies the number of repeats for each STR; the combination of multiple STRs generates a profile which is unique for each cell line.

2.4 Gene expression in cell lines

2.4.1 RNA extraction

RNA extraction was performed using the RNeasy mini kit (Qiagen) according to the manufacturer's instructions. The kit uses a silica-based membrane and a high salt buffer system for purification of RNA molecules.

Cells were grown as a monolayer in a 75cm^3 flask to 80% confluence. The cells were washed twice with PBS and then 1ml QIAzol was then pipetted directly on to the cells for 5 minutes at room temperature. The adherent cells were detached with a rubber cell scraper. The cell lysate was transferred into a 2ml microcentrifuge tube and left at room temperature for 5 minutes to promote disassociation of nucleoprotein complexes. Chloroform (140µL) was added to the lysate and shaken vigorously for 15s and then left at room temperature for 3 minutes. The tube was centrifuged for 15min at 12,000 x g at 4°C to separate the RNA from the organic material. The upper aqueous phase containing the RNA was transferred to a new collection tube and 525µl ethanol was added and mixed by pipetting up and down. From this mix, 700µl of the sample was pipetted into a RNeasy Mini Spin Column in a 2ml collection tube. This was centrifuged at 8000 x g for 15s at room temperature. The flow through into the collection tube was discarded. This step was repeated for the remainder of the sample.

A series of purification steps to eliminate the ethanol were performed. Buffer wash (700µL, Buffer RWT, Qiagen) was added to the RNeasy Mini spin column. Then 500µl of a second buffer wash (Buffer RPE, Qiagen) was added to the column and it was centrifuged at 10,000 x g for 15s. An additional 500µL Buffer RPE was added to the column and centrifuged at 10,000 x g for 2 minutes. The flow through was discarded after each centrifugation.

The spin column was then transferred to a new 1.5ml Eppendorf tube and 30µL RNase-free water was directly pipetted on to the column's membrane. It was centrifuged at 10,000 x g for 1 minute to elute all the RNA into the tube. RNA concentration was determined by spectrophotometry (Labtech Nanodrop Spectrophotometer ND-1000), by pipetting 1µL of each RNA sample. Only samples with a 260/280nm absorbance ratio of approximately 2.0 and a 260/230 nm ratio of 2.0-2.2 were considered of satisfactory RNA purity. Lower ratios indicate the presence of protein, phenol or contaminants.

2.4.2 Reverse transcription

Reverse transcription to generate complementary DNA (cDNA) was performed using a High-Capacity cDNA Reverse Transcription Kit (Applied Biosystems), following the manufacturer's instructions. 1000ng of RNA (volume 10µL) was added to 10uL of reaction mix. The reaction mix consisted of 1µL reverse transcriptase, 4.2µL nuclease free water, 0.8µL dNTPs, 2µL reverse transcriptase buffer and 2µL random primers. The total reaction volume was 20µL. The reaction volumes were incubated at 25°C for 10 minutes, then 37°C for 120 minutes followed by denaturing of the reverse

transcriptase at 85°C for 5 minutes to terminate. All handling of RNA and cDNA samples was performed on ice to limit nucleic acid degradation. 30µL of nuclease free water was then added to the cDNA to create a final volume of 50µL. This was stored at -20°C until required.

2.4.3 Real-time PCR

Gene expression was quantified by real-time polymerase chain reaction (qPCR), using Taqman Gene Expression Assays. With real-time PCR, the DNA template of interest is subjected to consecutive cycles of replication by use of sequence-specific primers, with synchronous measurement of the end of product at the end of each cycle by fluorescence. The higher the concentration of the specific sequence (template) in the original sample, the earlier the cycle of fluorescence first becomes detectable. Serial measurements of template fluorescence during the exponential replication phase allow reliable estimation of DNA concentration in the original sample.

Each replication cycle consists of 3 steps:

Denaturation: heat is applied (95°C) to melt double stranded DNA to single stranded DNA

Annealing: the primers hybridize with their complementary sequences within the single strands of DNA. The temperature is lower than the melting temperature of the primers.

Extension: DNA polymerase extends the primers, leading to replication of the gene of interest. The temperature required is 60-72^{o}C. The annealing and extension stages were combined to a 1-minute incubation at 60°C per cycle.

With TaqMan technology, fluorescence emission is accomplished using specially designed probes. Each probe is complementary to a sequence within the gene of interest (GoI), where it promptly binds during annealing, downstream of the primer. The 5' end of the probe has an attached 'reporter' fluorescent dye, while the 3' end has a 'quencher' dye of different wavelength, which quenches the reporter fluorescence. During replication cycles, DNA polymerase cleaves the probes that are attached to the DNA template releasing the reporter, whose fluorescence can now be emitted. The earliest cycle in which emitted fluorescence exceeds the threshold of 'significant' detection is termed Ct. It is inversely related to the original template concentration in the sample of interest. Low Ct values indicate high expression of the gene of interest. Gene expression is normalised to a reference gene; a gene which is ubiquitously expressed in all human tissues.

All reactions were carried out at a total volume of 10µL, comprising:

1µL of cDNA	5µL 2x Taqman Universal PCR master mix (Thermo Fisher)
3.5µL nuclease-free water	0.5µL probe-primer of gene of interest

The reaction volumes were pipetted into a 96 well plate (Applied Biosystems). Reactions were run in a 7500 ABI qPCR analyser. The incubation was 50°C for 2 minutes, 95°C for 10 minutes, followed by 40 cycles of 95°C incubation for 15s (denaturation) then 60°C for 1 minute (annealing-extension). Three reference genes were included (*HPRT1, ACTB, GUSB*) and the best performing gene for expression was *ACTB* (beta actin). All reactions were normalised against the reference gene

ACTB (beta actin). Data were expressed as the cycle number at which logarithmic PCR plots cross a calculated threshold line (Ct value) and used to determine ΔCt values [ΔCt= (Ct of target gene) – (Ct of reference gene)]. To compare gene expression between a sample of interest and a control sample, ΔΔCT values were used, defined as ΔΔCt values = ΔCt(Sample) = ΔCt (control). Results were also expressed as fold change in gene expression to control, derived using the equation, fold change = $2^{-\Delta CT}$

2.5 *In vitro* steroid profiling by liquid chromatography-tandem mass spectrometry

The steroidogenic activity of the ovarian cancer cell lines was characterised by comprehensive steroid profiling of the cell media by liquid chromatography tandem mass spectrometry (LC-MS/MS). LC-MS/MS is a powerful analytical tool which combines the ability of liquid chromatography to separate substances in a sample according to their chemical properties with the capacity of mass spectrometry for separation according to molecular mass. With high performance liquid chromatography (HPLC), the sample is carried through a column by a liquid (mobile phase). The column is equipped with a lining ('stationary phase') which binds the various molecules within the sample (analytes) with a strength that depends on the molecule polarity. The polarity of the mobile phase then increases progressively, leading to sequential elution of the analyte detachment at different times (retention times) according to their polarity (Taylor et al., 2015). Having been separated according to their polarity, analytes enter the mass spectrometry analysers. In LC-MS/MS, two sequential MS analysers are employed to enhance overall specificity. Entering the first MS analyser, sample analytes are ionised and travel through a quadrupole at times that are determined by their mass-to-charge ratio. In the second analyser, molecules undergo fragmentation

into smaller particles in a special collision cell; generated ionised fragments are then selected according to their mass-to-charge ratio with a second quadrupole. This results in highly specific detection, as the various analytes beget unique fragmented ions, leaving their very specific analytical fingerprint.

Modern mass spectrometry-based techniques (either LC-MS/MS or gas chromatography-mass spectrometry, GC-MS) have been established as the most sensitive and specific method of steroid hormone analysis, outperforming the traditional immunoassays with their significant analytical lacunae reactivity between similar analytes, low sensitivity and poor inter-lab standardisation (Taylor et al., 2015). LC-MS/MS has a distinct advantage over GC-MS as a high-throughput analytical method with shorter sample preparation and reduced staff costs, thus making it more cost-effective to run in laboratories.

To explore steroidogenesis in these *in vitro* cell models, the four ovarian cancer cell lines were incubated in 6-well plates (Corning) with 2 ml of the relevant media supplemented with 1% penicillin-streptomycin but excluding foetal bovine serum. Serum-free media was used as serum itself contains steroids which may confound results. For each experiment, the cell lines were treated with a single steroid at 100 nmol/L concentration and then incubated at 37^{o}C, 5%CO_2. Experiments were repeated at five time points (2h, 4h. 8h, 12h and 24h) and were performed in triplicate. At the end of each time point, the cell media was then transferred to silanized tubes and stored at -20^{o}C.

To extract steroid hormones from cell media, the cell media was thawed and 20 µl of serum steroid internal standard solution was transferred to each tube and vortexed briefly, followed by addition of 3 ml Methyl tertbutyl ether (MTBE, Sigma) and further vortexed. After 30 minutes to allow the liquids to settle, the top layer (liquid phase) was transferred to a 96-well plate using Pasteur pipettes. MTBE was evaporated to dryness at 55^{o}C. At the point of running the plate, the samples were reconstituted in 125 µl of 50:50 H_2O/methanol and centrifuged at 1,200 rpm.

Steroid metabolite identification and quantification was performed by LC-MS/MS, with reference to a linear calibration series (**Table 2.1**) and appropriate internal standards (Acquity^{TM} Ultra Performance Liquid Chromatographer, Xevo TQ Mass Spectrometer) as described previously (Jühlen et al., 2015, Haring et al., 2013).

Table 2.1 Sample calibration series for cell media steroid measurement

Calibration number	Added volume of serum steroid stock / internal standards (µl)	Added volume of cell media (µl)	Concentration (ng/ml)
C0	0	1000	0
C1	0.5	999.5	0.5
C2	1	999	1
C3	5	995	5
C4	10	990	10
C5	25	975	25
C6	50	950	50
C7	100	900	100
C8	250	750	250
C9	500	500	500

2.6 Cell Proliferation Assay

Cellular proliferation was assessed after culturing all four epithelial ovarian cancer cell lines and treating them with a single steroid at different concentrations and then using a BrdU colorimetric kit (Cat no. 11647229001, Roche) as per the manufacturer's instructions. BrdU 5-bromo-2'deoxyuridine incorporates into the newly synthesized DNA of replicating cells (during the S phase of the cell cycle), substituting for thymidine during DNA replication (Hawker, 2003). Following a DNA denaturing step, incorporated BrdU can be detected by anti-bromodeoxyuridine peroxidase antibodies (anti-BrdU-POD). The resulting immune complexes can then be enhanced for fluorescence using tetramethyl-benzidine (TMB). The fluorescence emitted by a given well is therefore proportional to the total amount of DNA, which in its turn is proportional to cell number before denaturing.

Cells were split using trypsin as described earlier. All four cell lines were seeded in separate 96 well plates (Corning) overnight (5 x 10^3 cells per well) in 100µL serum-free media for 24 hours to starve them (and promote cell proliferation when treated). Then the wells were rinsed twice with 200uL PBS and 100µL control or treatment media was added for a further 24h as per the following plan.

A	Cells + 100uL plain media only (background control)	Control
B	Cells + 100uL media with FBS	Control
C	Cells + 100uL media with charcoal stripped FBS	Control
D	Cells + 100uL media with charcoal stripped FBS + 1uM steroid	Steroid treated

E	Cells + 100uL media with charcoal stripped FBS + 100nM steroid	Steroid treated
F	Cells + 100uL media with charcoal stripped FBS + 10nM steroid	Steroid treated
G	Cells + 100uL media with charcoal stripped FBS	Control
H		Blank

Treatment media consisted of a single steroid and concentration in phenol red free RPMI or DMEM with 10% charcoal stripped FBS (steroid free FBS) and 5% penicillin-streptomycin.

To study the effects of steroid hormones *in vitro* without the confounding effects of hormones present in FBS, growth factors and cytokines need to be removed by charcoal stripping of serum. Dextran-coated charcoal was placed in the fridge overnight. An equal amount to that of the FBS to be stripped was centrifuged at 500 x g for 10 minutes to pellet the charcoal. The supernatant was then decanted and the same volume of FBS was added and vortexed to mix thoroughly. The mix was then incubated for 12 h at 4 °C to create charcoal stripped FBS. The control group used phenol red free RPMI or DMEM with 10% FBS and 5% penicillin-streptomycin only. Five biological replicates (wells) were used in each experiment. Four concentration strengths of 1 nmol/L, 10 nmol/L, 100 nmol/l and 1 µmol/L for four individual steroids (DHT, testosterone, androstenedione, 5-adione) were used per experiment. Cells were incubated with the steroids for 24 hours before performing the BrdU assay.

BrdU assay

Media was aspirated from the 96-well plate before rinsing it with PBS. Then 10 µL BrdU labelling solution was added to each well and the plate was incubated at 37°C for 2h. The BrdU pyrimidine analogue replaces thymidine in the DNA of proliferating cells.

The wells were then emptied of media and 200 µL FixDenat™ was added to each well to denature the DNA and left to stand at room temperature for 30 minutes. The denaturing agent was then removed and 100 µL Anti-BrdU-POD antibody solution was added to each well and again left to stand at room temperature for 90minutes. The monoclonal antibody binds to BrdU incorporated in newly synthesised cellular DNA and the immune complexes are detected in a subsequent substrate reaction.

The antibody solution was then removed and the wells were washed with PBS three times. Tetramethyl-benzidine (100 µL) was added to each well until colour visualisation occurred. After 10 minutes, the plates were run in a Wallac Victor 1420 multilabel spectrophotometer to measure absorbance of the samples at 405 nm (1.0s).

Blank wells were also used to measure the background fluorescence and then deducted from all absorbance values. The absorbance levels for each treatment were calculated as a proliferative index.

2.7 Patient recruitment and sample collection

2.7.1 Study registration and patient recruitment

REC ref 18/NE/001: Investigation into new biomarkers for diagnosing and treating ovarian cancer

For elements of the proposed study, pre-operative 24-hour urine collections, serum and ovarian tumour tissue from patients were required **(Table 2.2).**

Table 2.2 Schedule of sample collection from recruited patients

Time point	Sample collected
Pre-operative appointment	9.0 ml serum
Day of surgery	24h urine collection performed within last 48h
	Ovarian tumour biopsy

To recruit patients from the NHS for this project-based research, Ethics approval was sought and granted from the Health Research Authority under REC ref 18/NE/0011 'Investigation into new biomarkers for diagnosing and treating ovarian cancer'. It was registered as a multi-centre observational study recruiting healthy women and women with suspected or confirmed ovarian cancer. Eligible recruits were identified from twelve individual Gynaecology cancer units and centres across NHS England. Between January 2018 and March 2020, 233 women were consented and recruited to donate samples.

Inclusion criteria were :

1. Women with a suspected benign ovarian tumour / borderline ovarian tumour / ovarian cancer undergoing primary surgery
2. Women with a confirmed histological biopsy diagnosis of primary ovarian cancer or borderline ovarian tumour ovarian cancer but not begun treatment
3. Women with a possible benign or borderline adnexal mass about to undergo surgery
4. Healthy women with morphological normal ovaries, undergoing oopherectomy as part of hysterectomy for benign pathologies

Exclusion criteria focussed on patients who had started chemotherapy or were using steroid/hormone-based treatments:

1. Using hormonal contraception / implant in last 3 months
2. Used HRT on GnRH analogues in last 3 months
3. Used steroid treatment in last 3 months including inhalers
4. Commenced chemotherapy
5. Undergoing delayed debulking surgery

Further healthy control samples were also available. Urine samples that had been stored at -20°C from 33 healthy female volunteers (University of Birmingham ethics approval ERN_17_0494) were also included in the study.

2.7.2 Twenty-four-hour urine collections

24-hour urine collections from participants with suspected ovarian cancer were performed at home (a sterile collecting bottle was provided with instructions) and then brought by the patient to the hospital on the day of surgery (within 48h). The total volume was recorded and then aliquots were taken, centrifuged at 1,500 rpm to remove debris and then transferred to 5 ml sterile screw cap cryovials and stored at -20°C for GC-MS analysis in batches. Samples were transferred on dry ice to University of Birmingham.

2.7.3 Serum sample collection

Recruited patients attending their pre-operative investigations were requested to give an extra sample of blood. 9ml blood was collected in a Greiner Z-serum clot activator tube (Model code: 455092). The sample was then allowed to clot for 1 hour on ice, before being centrifuged at 2800 x *g* for 15 minutes at 4°C. The serum was then transferred into aliquots of 500 µL in sterile 2 ml screw cap tubes and stored at -80°C. Samples were transferred on dry ice to University of Birmingham for analysis. These samples were kept with an intention to perform LC-MS/MS and untargeted metabolomics on them in a future study.

2.7.4 Ovarian tumour tissue samples

Research and Development (R&D) at Sandwell & West Birmingham NHS Trust (SWBH) granted permission to obtain ovarian tumour tissue from study participants

under REC 18/NE/001. Fresh tumour pieces were taken directly from the whole ovarian specimen at surgery, washed with room temperature PBS (Sigma) and transferred in RPMI (Gibco) at room temperature to the University within 3 hours. In the tissue culture hoods, specimens were cut into small cubes (1 cm^3). Areas of necrosis and haemorrhage were discarded. The cut tissues were then transferred to 5 ml screw cap cryovials and filled with RNAlater (Thermo Fisher) and placed in the fridge for 24h before being transferred to a -80°C freezer. These samples were kept with an intention for RNA-seq analysis at a later date. The remaining fresh tissue were used for steroid tissue incubation experiments.

2.7.5 Clinical data collection

A clinical record form (CRF) was completed with each participant's specimen. Study teams at each recruitment site were asked to record the following patient data: age, BMI, CA125 value at diagnosis, the times and date of urine collection, final histology and any history of previous hormone replacement therapy. *BRCA* mutation status and RMI score (risk of malignancy index) data was also requested, if known.

Not all recruits provided samples due to challenges with logistics but a total 333 specimens were obtained. No matched samples for urine, serum and tumour tissue were obtained but matching samples for serum and urine, and, matching tumour and urine, and matching tumour tissue and serum were obtained (**Table 2.3**).

Table 2.3 Breakdown of specimens obtained from recruits

Specimen type	**n**
24h urine collection	194
Serum	122
Ovarian tumour and metastatic tissues	17

Matching samples	**n**
24h Urine and serum	41
24h Urine and tissue	5
Serum and tissue	17
24h Urine, serum and tissue	0

2.8 Ovarian tumour tissue steroid profiling by liquid chromatography tandem mass-spectrometry

Ovarian tumour tissue was prepared into small pieces weighing approximately 90-100 mg (wet weight). Tissue was placed in 10 ml centrifuge tubes (Corning) with 5 ml phenol-red free RPMI, 5% charcoal stripped serum, 1% penicillin-streptomycin and steroid treatment (100 nmol/L).

Four individual steroid treatments were used in each experiment (5-adione, androstenedione, testosterone and DHT). Each experiment was performed at three

time points, 12h, 24h and 36h with controls. All experiments had three replicates. Controls were composed of the media and steroid treatment without tissue. All the tubes were then placed in a hybridization incubator (Techne HB-1D), pre-warmed to 37°C, that rotated the tubes in a clockwise motion. Tubes were then removed from the hybridiser at each elapsed time point and vortexed briefly for 30 seconds. The tissue was removed and the remaining supernatant was aspirated into silanized tubes and stored at -20°C till ready for steroid extraction by LC-MS/MS (**Figure 2.2**).

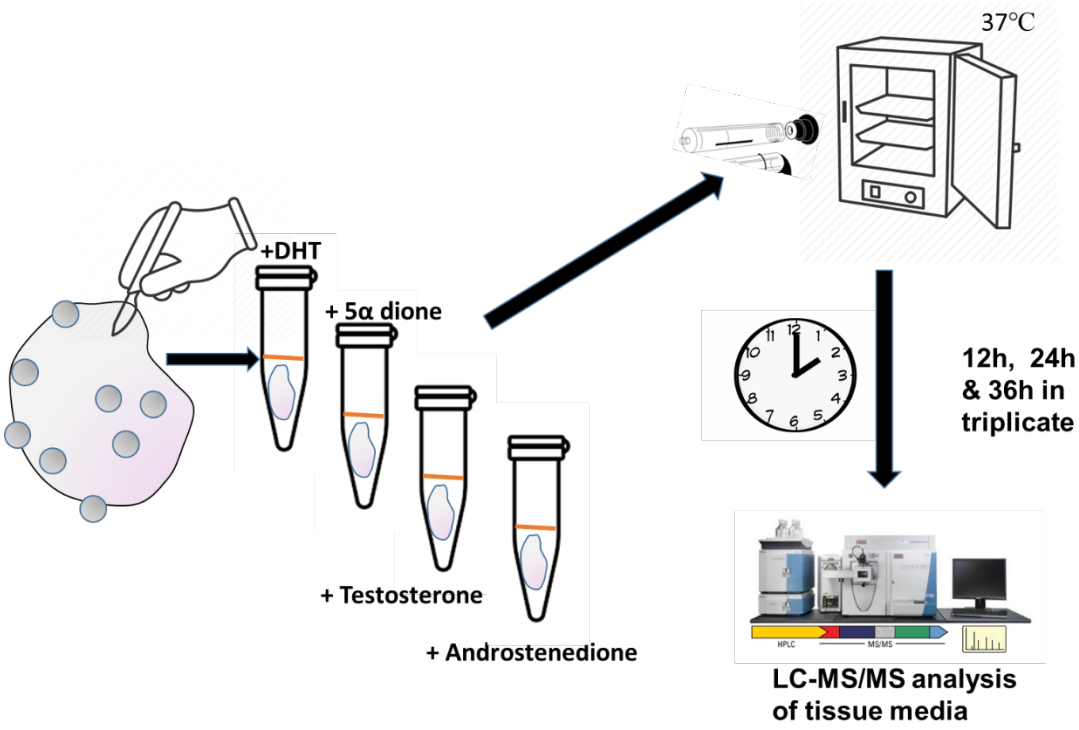

Fig. 2.2: Ovarian tumour tissue incubation with four separate steroids with supernatant analysis by liquid chromatography tandem mass-spectrometry (LC-MS/MS) to evaluate tumour steroid metabolism

To extract steroid hormones from the tissue media, the tissue media was thawed and 20 µl of serum steroid internal standard solution was transferred to each tube and vortexed briefly, followed by addition of 3 ml Methyl tertbutyl ether (MTBE), (Sigma)

and further vortexing. After 30 minutes to allow the liquids to settle, the top layer (liquid phase) was transferred to a 96-well plate using Pasteur pipettes. MTBE was evaporated to dryness at 55^{o}C under N2 flow/stream. At the point of running the plate, the samples were reconstituted in 125 µl of 50:50 H2O/methanol and centrifuged at 1,200 rpm.

Steroid metabolite identification and quantification was performed by LC-MS/MS, with reference to a linear calibration series (**Table 2.1**) and appropriate internal standards (AcquityTM Ultra Performance Liquid Chromatographer, Xevo TQ Mass Spectrometer) as described previously (Haring et al., 2013, Jühlen et al., 2015). The final data was then normalised to the wet weight.

2.9 Urine steroid metabolite profiling by gas chromatography mass spectrometry

Urinary steroid metabolite excretion from 24-hour urine samples was analysed by gas chromatography mass spectrometry (GC-MS) using a commonly described technique (Shackleton, 1986, Shackleton and Snodgrass, 1974). The first separation stage (gas chromatography) involves evaporation of purified and chemically processed (derivatised) steroid samples which run in a gaseous form, through a column (stationary phase) at different speeds according to their affinity to the column. At the end of the column, steroids reach the mass spectrometer, where they are bombarded with electrons and fragmented into molecule-specific ionised particles in a special

collision cell. The resulting fragments are then selected according to their mass-to-charge ratio through acceleration within a quadrupole (Arlt et al., 2011, Taylor et al., 2015).

Deconjugation: First, steroids were extracted from urine with a SepPak column (Waters, USA): 1 ml of urine sample was loaded after washing the columns with 4 ml methanol and 4 ml of ddH_2O. Then, the loaded column was washed with 4 ml ddH_2O and the steroids were eluted in 4 ml methanol into a clean silanized tube. After evaporation (heat block at 55°C under N_2), sulfate and glucuronide groups were enzymatically removed from conjugated steroids by incubating for 3 hours at 55°C in the hydrolysis buffer (3 ml 0.1M acetate buffer [pH 4.8-5.0] + 10 mg ascorbate +200 units Helix pomatia (sulfatase/glucuronidase); (all Sigma-Aldrich, UK). The cooled sample was then loaded again on a SepPak column and eluted into a clean glass tube with 4 ml methanol.

Derivatization: After evaporation under N_2, three drops of 2% methoxyamine-pyridine was added; the tube was vortexed vigorously and incubated at 55°C for one hour. After further evaporation under N_2, 75 µl of N- trimethylsilylimidazole (Sigma-Aldrich, UK) was added, vortexed and incubated at 120°C overnight. Then, the samples underwent liquid-liquid extraction by adding 2 ml cyclohexane and 2 ml ddH_2O (vortexing after each step). After centrifugation (1,000 x *g* for 5 minutes), the bottom later layer was removed into waste. Then, another 2 ml dH_2O were added, vortexed, centrifuged and removed. Finally, the top layer containing the extract in cyclohexane was concentrated by evaporation under N_2 and reconstituting in 400 µl of cyclohexane and transferred to injection vials.

The samples were then injected into an Agilent 5975 GC mass spectrometer. Targeted

quantification of the steroid metabolites (selective ion monitoring, SIM) was then performed using Chemstation software (Agilent) which has been calibrated and fully optimized by the Steroid Metabolism Analysis Core team at IMSR, University of Birmingham. Androgens, mineralocorticoid and glucocorticoid metabolite excretions were calculated, adjusting for total 24h urine volume.

2.10 Statistical analysis

Statistical analysis and schematic depiction of data was completed using GraphPad Prism Software. Data are represented as mean ± standard error (mean ± SEM) values, unless otherwise stated. Data that are not normally distributed are presented as median ± interquartile range (IQR). Two-group comparisons were made using Student's paired t-test for normally distributed data. Non-parametric data was analysed by Kruskal Wallis test to compare control, benign ovarian tumours, borderline ovarian tumours and ovarian cancer groups; for significance values of $p<0.05$. Multiple comparisons were performed by one-way ANOVA followed by post-hoc multiple comparison testing (Dunn's test).

Chapter 3 Androgen metabolism in epithelial ovarian cancer cell lines

3.1 Introduction

There is evidence to support progression of epithelial ovarian cancer by androgens through direct stimulation of the androgen receptor (AR) and independent of AR. The synthesis of androstenedione and testosterone by epithelial ovarian cancers in post-menopausal women has been demonstrated by ovarian vein sampling (Heinonen, 1991).

AR expression is observed in the surface epithelium of normal ovary and in ovarian cancer but at present, there is a lack of evidence to confirm that it is a consistent feature of epithelial ovarian cancer growth (de Toledo et al., 2014, Sheach et al., 2009a, Lee et al., 2005, Butler et al., 2013). AR has not been shown to be prognostic for high grade serous ovarian cancer but androgens may still be implicated in ovarian tumorigenesis and progression through AR-independent pathways.

In one study comparing four malignant OSE cell lines and four normal OSE cultures the androgens, DHT and testosterone, stimulated increase in cell growth which was reversible by flutamide, an anti-androgen (Syed et al., 2001). Progesterone was also shown to stimulate growth. However, DHT and testosterone treatments had differing effects on the rate of cellular proliferation with DHT being more potent. Some of the malignant cell lines were reported to have differential activities of SRD5A1 which may have explained the distinct cellular responses (Lau et al., 1999).

In another study AR expression in 11 primary ovarian cancer cultures derived from ascitic fluid was observed and after treatment with DHT, cell division increased in 6 out of 11 primary cultures (Elattar et al., 2012).

However, androgens are capable of downstream effects independent of AR which can dysregulate normal proliferation. Typically, in the healthy ovary, ovarian surface epithelial cells are growth inhibited by TGF-ß1 but low dose DHT down regulates mRNA expression for the TGF-ß1 receptors in several ovarian cancer cell lines. Furthermore, some ovarian cancer cell lines treated with androgens remained insensitive to TGF-ß1 after counter-treatment with an androgen antagonist (hydroxy-flutamide) (Evangelou et al., 2000, Kohan-Ivani et al., 2016). TGF-β1 inhibits proliferation and induces apoptosis in various cell types including ovarian cancers and an abundance of loss-of-function mutations in the TGF-beta receptor are considered a pathway to ovarian tumorigenesis (Blobe et al., 2000). Furthermore, DHT and testosterone may be metabolised to other steroids that may result in alternative effects.

Whilst previous reported efforts focus on understanding how potent androgens such as DHT may contribute to ovarian cancer development and progression, there have been two investigations into identifying if pre-cursor androgens, such as 5α-androstanedione (5α-dione), androsterone (An), androst-5-ene-3β,17β-diol (3a-diol / Adiol) or their androgen metabolites are involved. Previously there has been a case-control study observing pre-diagnostic serum concentrations of 12 androgens against the risk of developing ovarian cancer for 579 women in the Women's Health Initiative Observation Study (Langer et al., 2003). These women had serum samples taken between 1996-1998 and the mean time from serum collection to diagnosis was 6.9 years (standard deviation 3.8 years). LC-MS/MS was performed retrospectively on these samples (n=410 control, n=102 serous cancers, n=67 non-serous). The analysis found there were no associations between androgen and androgen metabolite and

overall cancer risk or any associations with the risk of developing serous ovarian cancer. However, androsterone glucronide, an androgen metabolite, was associated with an increased risk of developing Type 1 ovarian cancer (p=0.01) (Trabert et al., 2019). In a similar study higher concentrations of serum testosterone and androstenedione (samples collected >2 years before diagnosis) were also associated with an increased risk in endometrioid (n=166) and mucinous ovarian cancers (n=193) (OR log2=1.33 [1.03–1.72]) but not serous (n=667) or clear cell (n=61) subtypes. However, some samples were analysed by radioimmunoassay (Ose et al., 2017).

By considering the potential role of all androgens observed in epithelial ovarian cancer and acknowledging the superiority of mass spectrometry for steroid detection, **this chapter aimed to identify steroidogenic pathways and steroids and their metabolites that may be potential biomarkers or therapeutic targets.**

My initial aims were to generate results that would potentially identify important potential steroidogenic pathways in epithelial ovarian cancer for biological studies. To inform the decision on suitable experiments, I aimed to compare gene expression between epithelial ovarian cancer and normal ovary from publicly available datasets and generate a list of steroidogenic targets for biological investigation for potential biomarkers. Once the datasets had been analysed, representative epithelial ovarian cancer cell lines would be chosen to perform the biological studies. In addition to this, I would perform quantitative real-time PCR (RT- qPCR) on these cell lines and observe gene expression for the same steroidogenic targets identified in the larger datasets, searching for correlation and to illuminate the potential pathway for androgen

metabolism. Then I would observe androgen metabolism in these cell lines using steroid treatments to activate those pathways and observe the fluctuations in downstream androgen metabolites using mass spectrometry. Cellular proliferation would then be assessed in the presence of these detected androgens. These results would direct if there are androgens that could be potential diagnostic biomarkers.

3.2 Methods

3.2.1 Gene expression analysis: interrogation of public datasets for steroidogenic dysregulation in epithelial ovarian cancer

From the vast human steroid synthetic pathways summarised in **Figure 3.1**, several validated genes of interest (GoI) for enzymes and receptors were selected to determine if their gene expression differed between epithelial ovarian cancer and normal ovary. The results of this analysis would help direct which steroid metabolic components to study.

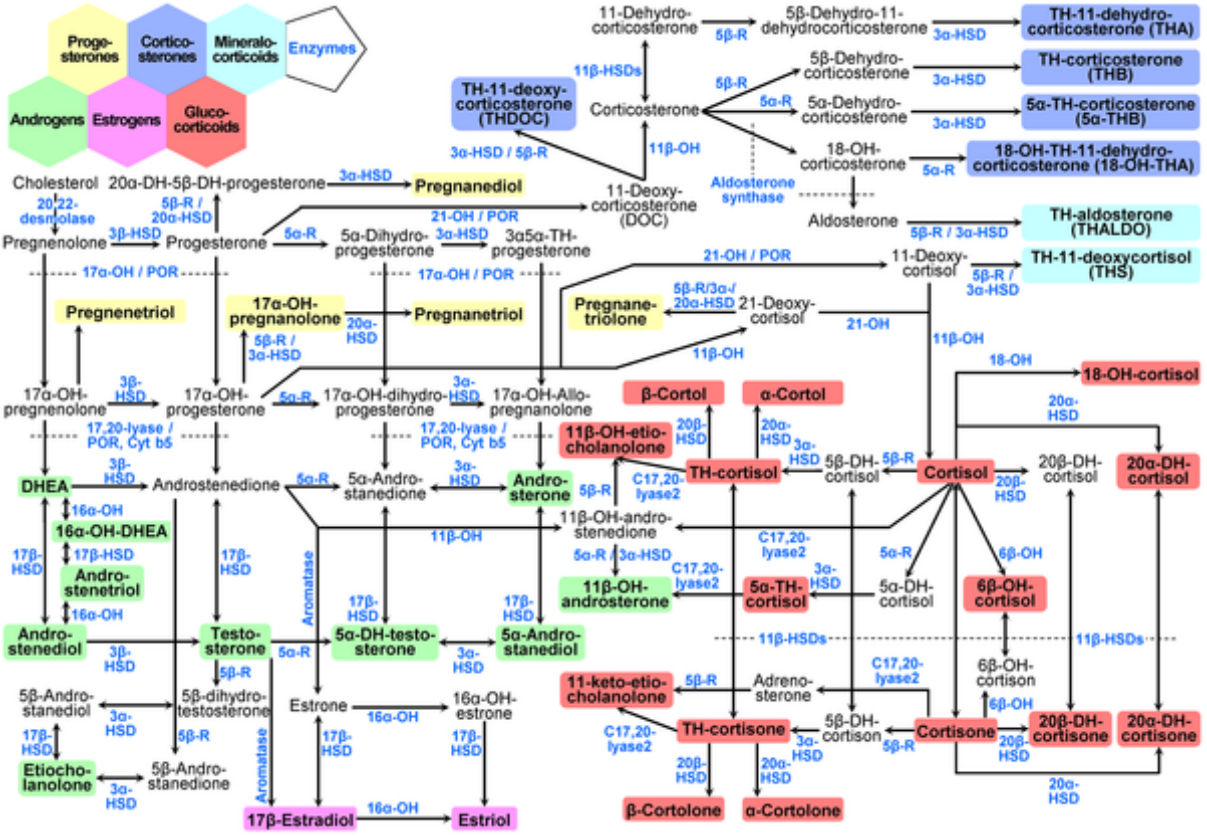

Fig. 3.1: Pathways of human steroid hormone biosynthesis

Adapted from (Ackermann et al., 2019). Steroid biosynthesis is complex and incorporates multiple enzymes (blue) to perform conversions. All these pathways and their components were interrogated in public datasets for gene expression for normal ovary and serous ovarian cancer.

High grade serous ovarian cancer is the commonest presentation of the disease and TCGA has the most cited and comprehensive gene expression dataset that is available publicly. GTEx contains gene expression data for normal ovary which is also frequently cited in genomic comparison studies for ovarian disease. Data from TCGA (n=426 serous ovarian carcinoma) and GTEx (n=88 normal ovary) were downloaded and analysed. GEPIA software (Gene Expression Profiling Interactive Analysis) was employed to unify the datasets and normalise the data (described in **Chapter 2**) (Tang et al., 2017). Of the 88 control patients, 36 patients were pre-menopausal and 52 patients were postmenopausal. Then using the same application, differential analysis

for all genes of interest was performed using a one-way ANOVA. A post-test was not possible without the original raw data. The variable for calculating the differential expression was the disease state (Tumour or Normal). The list of genes interrogated and the results are shown in **Figure 3.2.** The (log2FC) fold cut off =1 and p-value cut off = 0.01. Genes with higher log2FC values and lower p values than pre-set thresholds were considered differentially expressed genes.

Since Type 1 ovarian cancers such as mucinous and endometroid and clear cell cancers occur less frequently than serous ovarian cancer, there were no large public repositories with mRNA expression data compatible with the GEPIA platform. There is no TCGA data either for Type 1 ovarian cancer. Hence an alternative database and platform was used to obtain gene expression data: the OncoMine database (https://www.fishersci.co.uk/shop/products/oncomine-research-premium-edition-license-4/p-7076126) .OncoMine is a public online database consisting of previously published and publicly available microarray data (Rhodes et al., 2007). Again, the chosen genes of interest were investigated for expression in Type 1 ovarian cancers. As the number of samples for Type 1 ovarian cancers in Oncomine's available datasets were small, a meta-analysis between datasets was performed comparing Type 1 cancers with normal ovary to search for changes in expression. The same process was then repeated for serous ovarian cancers and all epithelial ovarian cancers in its database to seek any further findings.

The analysis of mRNA expression fold change was filtered by selecting "ovarian carcinoma vs normal analysis" on the application. The standard normalisation and parameters provided on the OncoMine application were p-value <0.05, fold change > 1. A p-value cut-off of <0.01 was not available on OncoMine. Due to tissue or sample

heterogeneity among each independent experiment and the different technological detection platforms, the identification of significantly expressed genes is inconsistent in different studies. However, OncoMine provides a meta-analysis tool for gene expression which is a validated integration analysis tool with an unbiased approach (Sims et al., 2008).

3.2.2 Real-time qPCR of genes of interest involved in steroid metabolism

To confirm if the steroidogenic genes identified in the public datasets were truly differentially expressed in epithelial ovarian cancer, I chose representative ovarian cancer cell lines to determine if they also had a similar gene expression profile and to decide on their suitability for further biological study.

Messenger RNA (mRNA) for real-time qPCR was obtained from four ovarian cancer cell lines using a QIAGEN micro RNAeasy kit; method described in **Chapter 2**. The selected gene targets are listed in **Table 3.2** and were based on the steroidogenic targets identified in gene expression data from the public repositories. Taqman gene primers (Thermo Fisher Scientific) for these targets were obtained as shown below.

Assay ID	Taqman Gene Primer
Hs00971645_g1	Human SRD5A1 primer
Hs00970004_m1	Human HSD17B3 primer
Hs00366267_m1	Human AKR1C3 primer
Hs01046816_m1	Human AKR1C2
Hs01100353_m1	Human HSD17B4 primer
Hs00171172_m1	Human AR primer

Hs01556702_m1	Human PGR primer
Hs00605123_m1	Human HSD3B2 primer
Hs00366258_m1	Human HSD17B6 primer
Hs01124136_m1	Human CYP17A1 primer
Hs00903411_m1	Human CYP19A1 primer
Hs01060665_g1	Human ACTB primer
Hs02800695_m1	Human HPRT1 primer
Hs00939627_m1	Human GUSB primer

A suitable human ovarian surface epithelium (OSE) cell line was not able to be sourced, however, pooled cDNA from 5 women with normal ovarian tissue was available (Invitrogen™ Gene Pool™ Product Code 10594383) and was used as the control for normal ovary gene expression. Three reference genes were selected: *ACTB*, *HPRT1* and *GUSB* and the best performing reference gene for expression was *ACTB*, which was used in the calculations for double delta Ct analysis (Schmittgen and Livak, 2008).

The four chosen ovarian cancer cell lines selected for the biological studies were CAOV3, IGROV1, OVCAR5 and OVCAR3 (described in **Chapter 2**). RNAseq expression data from The Cancer Cell Line Encyclopaedia (CCLE) (https://portals.broadinstitute.org/ccle/about) was downloaded for several potential cell lines. The genes expressed in analysis of the public repositories were cross referenced for expression in the RNAseq data for each prospective cell line. Expression of the androgen receptor, *AR*, was considered not to be required in all the cell lines because *AR* expression in primary ovarian cancer samples has been reported to be present in 43.7% of primary ovarian cancer samples (Lee et al., 2005).

Ovarian cancer cell lines are considered more representative when they are selected after genomic comparison between the cancer cell lines and ovarian cancer tissue samples. One frequently cited publication, documented the ranking of cell lines based on reported copy-number changes, mutations and mRNA expression profiles that most closely resembling ovarian cancer and this was used to inform the decision on the final choices (Domcke et al., 2013). All the cell lines were grown in the recommended media and passaged according to the distributors' instructions. The four cell lines used were genetically authenticated as per American National Standards Institute ASN-0002-2011. No cell lines for benign ovarian tumour and borderline ovarian tumours were able to be sourced. IGROV1 was used to represent Type 1 ovarian cancers, the others are all representative of high serous ovarian carcinoma (Type 2). The expression of the genes in these 4 ovarian cancer cell lines were first compared with the gene expression data from the public datasets using a Student's unpaired t-test for statistical analysis. Then I considered how the differentially expressed genes may influence androgen metabolism in ovarian cancer cells.

3.2.3 Steroid metabolism observed in ovarian cancer cell lines over 24h

Once the putative genes involved in androgen metabolism in epithelial ovarian cancer were selected and potential pathways identified, I tested the four cell lines with steroids that may activate the pathway. The four cell lines were grown in its recommended media with foetal bovine serum (FBS) in 75cm^3 flasks (Corning) as described in **Chapter 2**. Then for each of the lines, cells were loaded on to 6 well plates at a concentration of 300,000 cells/ well in 1 ml media without FBS (serum free media) and

incubated at 37 ºC. The cells were left in the wells overnight. Next day, the media was aspirated from each well and replaced with fresh 2 ml serum free media. The steroid treatment was added directly to the cells and mixed by gentle plate rocking. The selected steroids were, 17-hydroxy-progesterone, DHEA, androstenedione, 5α-dione, testosterone and DHT. I considered these five treatments as most likely to activate the androgen metabolism pathway identified from gene expression analysis. 100 nmol/L was selected as the most likely concentration to demonstrate metabolic changes and has been used in steroid assays on ovarian cancer cell lines in past literature (Kohan-Ivani et al., 2016, Lebbe et al., 2017). To generate a time course depicting downstream steroid metabolism following each steroid treatment, each experiment was performed with five different time intervals (2h, 4h, 8h, 12h and 24h) to allow observation of multiple steps in downstream androgen metabolism.

At the end of each specific timepoint, the plates were removed and placed on ice. The supernatant from each well was transferred frozen to individual silanized glass vials, labelled and stored at -20ºC. The steroid content of the cell culture supernatant was analysed by LC-MS/MS as described in **Chapter 2**. Three independent triplicate experiments were performed for each steroid treatment, with each of the cell lines, for each time interval. LC-MS/MS was performed to determine the steroid concentrations of DHT, testosterone, androstenedione, 5α-dione, 3-adiol and androsterone as described in **Chapter 2**. The mass spectrometry platform in the laboratory had been validated in the detection of androgen metabolites. The results used for analysis were from experiments within 3 cell passages.

The Bicinchoninic Acid (BCA) method was used for the quantitative determination of total protein concentration from each well (Pierce Microplate BCA Protein Assay Kit,

Thermo Fisher Scientific). Briefly the reduction of Cu^{2+} to Cu^{+} in proteins can be detected by a reagent containing bicinchoninic acid and the purple-coloured reaction of the product can be detected by a selective spectrophotometer that is almost linear with increasing protein concentrations over a broad working range (20–2000 µg/mL). The spectrophotometer was set at 570nm absorbance and the calibration series was used to plot a standard curve to determine the protein concentration for each unknown sample and these values were used to normalise the steroid concentrations. The normalised steroid concentrations were tabulated to derive the mean and standard deviation values. These were then plotted to graphically display the metabolism of each androgen steroid treatment over 24 hours and the products synthesised and their concentrations.

3.2.4 Cellular proliferation of ovarian cancer cell lines in presence of steroids

Increased cell proliferation is required for tumorigenesis in ovarian cancer and hence I chose to investigate if my selected steroids also influenced cell proliferation. DHT is cited as being able to significantly increase ovarian cancer cell proliferation (Syed et al., 2001) however there is lack of clarity other androgens and steroids are capable of this.

Quantification of cellular proliferation in response to treatment with 17-hydroxy-progesterone, androstenedione, 5α-dione, DHT and testosterone was determined using a colorimetric immunoassay (Cell Proliferation Elisa, BrdU, Roche) based on the measurement of 5-bromo-2'deoxyuridine (BrdU) incorporation during DNA synthesis. The method is described in **Chapter 2**. For this experiment, charcoal stripped fetal

bovine serum (FBS) was used with each steroid treatment. FBS contains several steroids, but charcoal stripping removes these but retains the other growth factors that cells require (described in **Chapter 2**). Experiments were performed in triplicate for each steroid treatment and cell line. A student's paired t-test was used for statistical analysis. The mean and SD values were obtained and plotted graphically.

3.3 Results

3.3.1 Gene expression analysis: interrogation of public datasets for steroidogenic dysregulation in epithelial ovarian cancer

Data for multiple gene targets involved in steroidogenesis were downloaded and compared between TCGA serous ovarian carcinoma gene expression dataset with the GTEx dataset for normal ovary (**Figure 3.2**). After unifying these two separate datasets and normalising it, GEPIA identified only 3 significant genes in serous ovarian cancer, *SRD5A1, ESR1, SULT2B1,* that had an increased expression with a log2 fold change >1 ($p<0.01$). None of these genes were related to a specific pathway. However, GEPIA identified 17 significant genes in serous ovarian cancer with *decreased* expression with a log2 fold change >1 ($p<0.01$) between normal ovary and ovarian serous carcinoma (**Figure 3.3**). This included groups of genes for receptors (PGR, ERβ and AR). Then there was a group of genes focussing on the early pathway in steroidogenesis: *STAR* and *CYP11A1* which are responsible for conversion of cholesterol to pregnenolone. *STAR* had a log2 fold change difference of -8.2 and *CYP11A1* had a fold change difference of -4.6 which were the biggest differences

seen. The genes for enzymes involved in androgen metabolism that were down regulated were *AKR1C3*, *HSD17B7, HSD17B6 and CYP17A1*. *CYP19A1* also had reduced expression in serous ovarian cancer, Genes involved in glucocorticoid synthesis were also down regulated and these were *HSD11B*1, *AKR1C1* and *CYP21A2*. Also, *NR5A1*, which encodes for steroidogenic factor 1 (SF1) had decreased expression. SF1 is an orphan nuclear receptor and a transcription factor that regulates genes in steroidogenesis and gonadal development.

Receptors

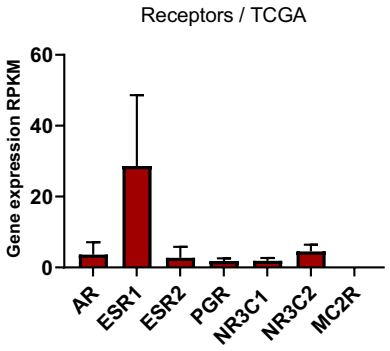

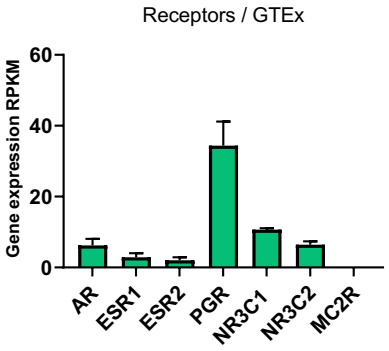

CYP

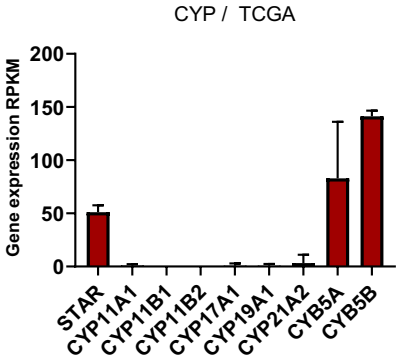

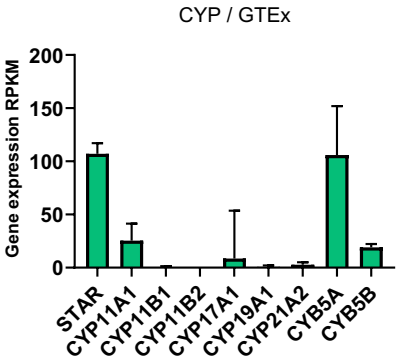

HSD3B
HSD11B

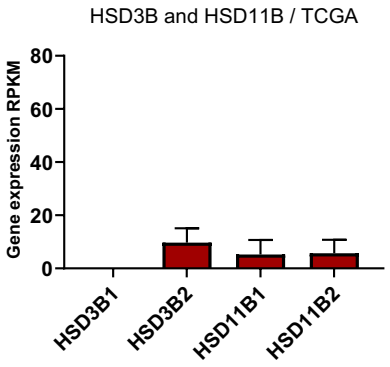

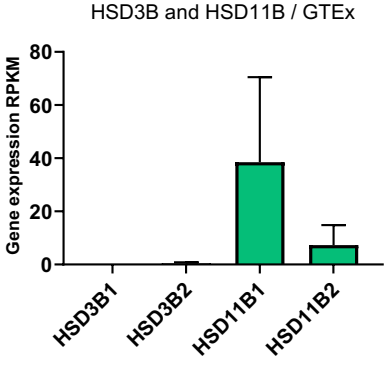

HSD17B

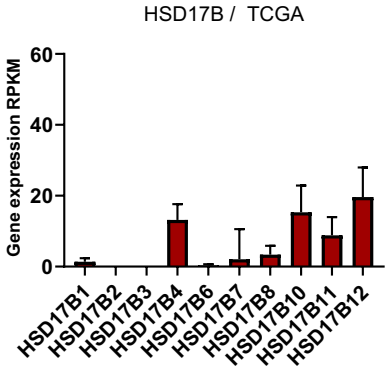

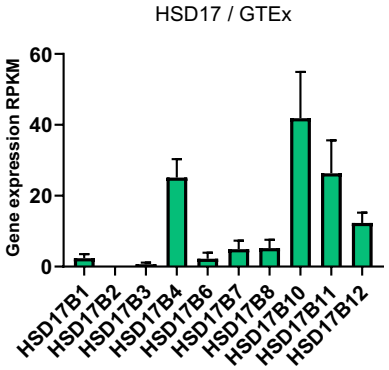

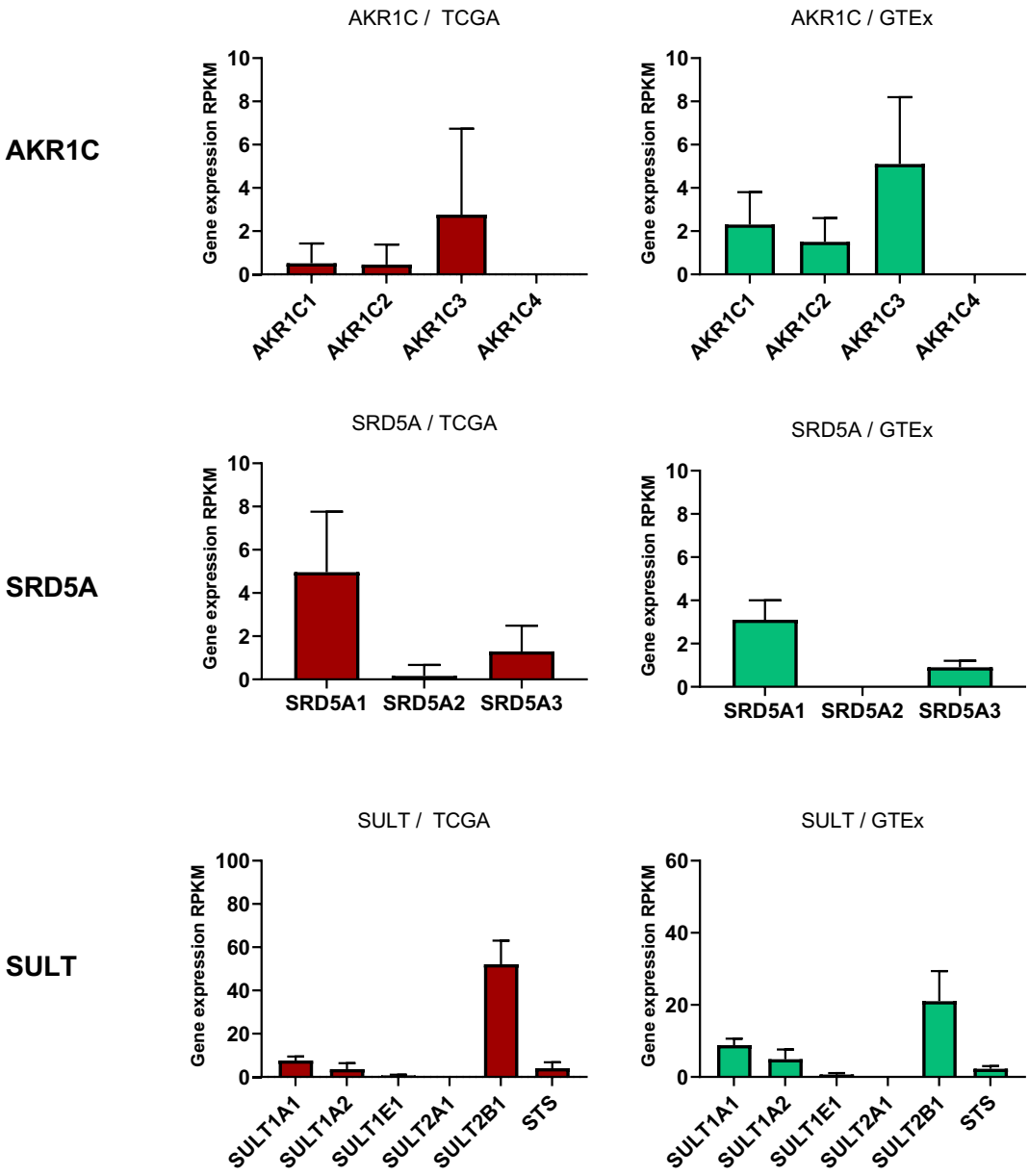

Fig 3.2: RNA-seq data for multiple gene targets involved in steroid synthesis and metabolism.

RNA-seq data were obtained for multiple genes involved in steroid metabolism. The graphs show the selected genes' expression values (RPKM) from two separate sources of data: serous ovarian cancer TCGA (n=426) in red and normal ovary (GTEx, n=88) in green. Related components involved in steroid metabolism are separated into groups. **SULT** : sulfotransferases that permit activation of a steroid by removal or donation of a sulphate group**. SRD5A** : 5a-steroid dehydrogenases performing 5a-reduction on the steroids to convert them. **CYP** enzymes (Cytochrome P450) perform synthesis or catabolism of steroids into active and inactive metabolites. **Receptors**: these include androgen receptor, progesterone receptor, estrogen receptors alpha and beta and the mineralocorticoid and glucocorticoid receptors. **HSD** (hydroxysteroid dehydrogenases) perform biosynthesis and metabolism of several steroids. These datasets were then unified, normalised and then compared using Gene Expression Profiling Interactive Analysis (GEPIA).

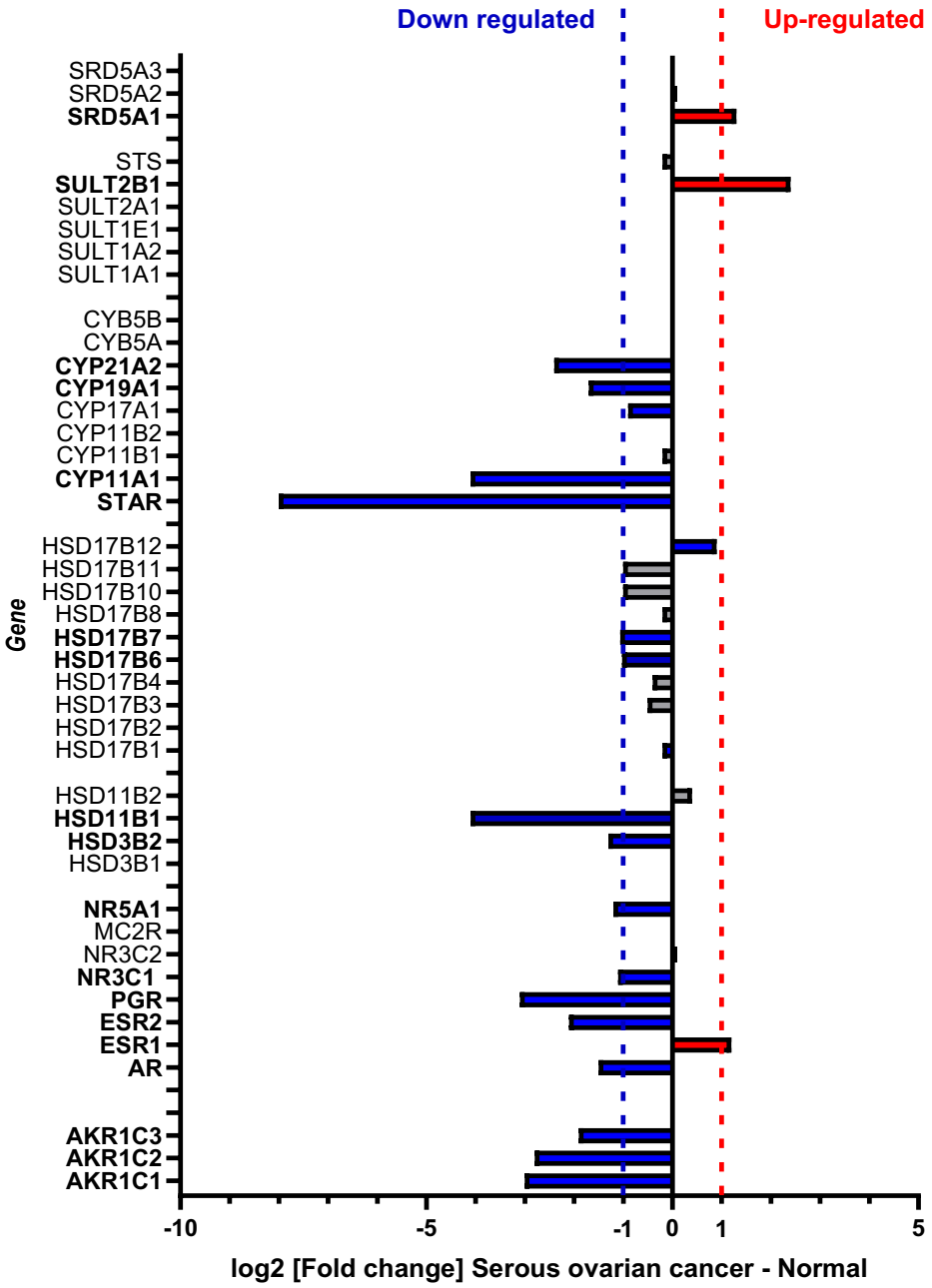

Fig. 3.3: Difference in gene expression for selected steroidogenic targets between serous ovarian cancer (n=426) and normal ovary (n=88)

Gene Expression Profiling Interactive Analysis (GEPIA) was used to determine expression of genes from the two groups and then compare for fold change differences. Fold change (log2 FC) for each gene is displayed between the two groups. The significant fold cut off was set at -1 or +1 (broken lines), p-value cut off = 0.01; these genes are in bold on y-axis. The overall trend displayed downregulation of several genes (blue bars) involved in steroid metabolism for serous ovarian cancer compared to normal ovary. Only three genes (red bars) were identified with significantly increased expression: *SRD5A1, ESR1 SULT2B1* in serous ovarian cancer.

All the genes with fold change difference >1 in the comparison between TCGA and GTEx data were investigated for influence on survival. OncoLnc (www.oncoLnc.org) performs a log-rank test using TCGA ovarian serous adenocarcinoma data. The log-rank test was used to test the null hypothesis that there is no difference between women with serous ovarian cancer with high expression of the gene of interest and low expression of the gene of interest in the probability of death at any timepoint. High expression was set at >75% of median expression and low expression was set at <25% of the median expression value. None of the genes identified were shown to influence survival using the log-rank method.

Oncomine had limited numbers of complete gene expression profiles for many of the less common ovarian cancers. The data used for this analysis were sourced from two studies (Hendrix et al., 2006, Lu et al., 2004). From these two studies, Oncomine possessed data for 20 clear cell ovarian carcinomas and these were compared against 9 normal ovaries (menopausal status unknown). From the selected panel of steroid metabolism related targets, Oncomine identified only *AKR1C3* was significantly over-expressed in clear cell adenocarcinoma (log2 FC [1.1] p=0.044) when compared to normal ovary but no genes were down-regulated significantly. No significant differences were seen in the comparison of the targets between endometrioid ovarian cancers (n=60) and normal ovary (n=9). In a comparison for all mucinous ovarian cancer (n=22) against normal ovary (n=9), the significantly differential expressed genes were *HSD17B*4 (log2 FC [1.74] p=0.044), *AKR1C3* (log2 FC [1.22] p<0.01). No genes were identified as under-expressed in this comparison either. In a comparison for all serous ovarian cancers with data on Oncomine (n=153): the significantly up-regulated genes were *HSD17B7* (p=0.017), *HSD17B3* (p=0.048) and *SRD5A1*

(p=0.028). Whilst the upregulation of *SRD5A1* correlates with the comparison between TCGA serous ovarian cancer and GTEx datasets, *HSD17B3* and *HSD17B7* were not identified as over-expressed in the TCGA serous ovarian cancer data (**Table 3.1**). Survival analysis using the log-rank method on this application did not suggest any of these genes were prognostic.

Table 3.1: Summary of upregulated gene expression implicated in steroid metabolism for Type 1 and 2 epithelial ovarian cancers compared to normal ovary.

Significant genes were identified by GEPIA [1] and Oncomine [2] platforms (p-values stated). All genes had a fold change>1 compared to normal ovary. Oncomine possessed data for n=9, normal ovaries compared with GEPIA n=88.

Here, serous ovarian cancer has 5 genes with over-expression implicated in steroid synthesis, metabolism and action. 2 genes were identified for mucinous ovarian cancers, 1 gene was identified for clear cell cancers and none for endometrioid ovarian cancer.

Type 2	**Type 1**		
Serous ovarian cancer (n =416) [1]	Endometrioid ovarian cancer (n=60) [2]	Clear cell ovarian cancer (n=20) [2]	Mucinous ovarian cancer (n=22) [2]
ESR ***P=0.007***			
SULT2B1 ***P=0.008***			
SRD5A1 ***P=0.009 (n=416)*** ***& P=0.028 (n=153)*** [2]			
		AKR1C3 ***P=0.044***	***AKR1C3*** ***P=0.008***
HSD17B3 [2] ***P=0.048***			
			HSD17B4 ***P=0.042***
HSD17B7 [2] ***P=0.017***			

Interpretation of the gene expression data

The results of the identified genes summarised in **Figure 3.3** and **Table 3.1** were considered in the context of known pathways for steroid metabolism that involves the genes identified (**Figure 3.4**). As the focus of the study leaned towards androgens based on the literature search and in serous ovarian cancer (as this is the most common form of the disease) I filtered the list to create a specific panel of genes from the genomic analysis that were most likely to demonstrate steroid metabolic changes. **Hence, the genomic analysis supported investigating the following enzymes and metabolic steps: SRD5A1, AKR1C2, AKR1C3, HSD3B2, HSD17B3 and HSD17B4.** SRD5A1 is a steroid 5a-reductase that converts androstenedione to 5α-androstanedione (5α-dione) and converts testosterone to DHT. AKR1C2 is an aldo-keto reductase that converts 5α-dione to androsterone and converts DHT to 3a-diol. AKR1C3 is another aldo-keto reductase that performs conversion of androstenedione to testosterone and conversion of 5α-dione to DHT. The 17-beta-hydroxysteroid dehydrogenases (HSD17B) are a large family involved in the dehydrogenation of steroids. HSD17B3 converts androsterone to 3a-diol mimicking AKR1C3. HSD17B4 converts DHT to 5α-dione and converts testosterone to androstenedione; therefore, it reverses the effects of AKR1C3. HSD3B2 also converts pregnenolone to progesterone and initially it was thought that studying this enzyme was considered unlikely to derive new insights. However, it converts DHEA to androstenedione, so it was retained for *in vitro* investigation. CYP17A1 was also included even though it did not feature as a significantly altered expressed gene but it performs conversion of progesterone to 17-hydroxyprogesterone which CYP17A1 then converts again to androstenedione, which is an androgen of interest. The roles of the receptors were considered and AR and PR

were chosen to be investigated through cell proliferation studies. Gene expression analysis thus provided an initial rationale to examine androgen metabolism in representative epithelial ovarian cancer cell lines. These genes encode for enzymes in steroid synthesis; therefore, the next step was to characterise their behaviour and activity in the cell context.

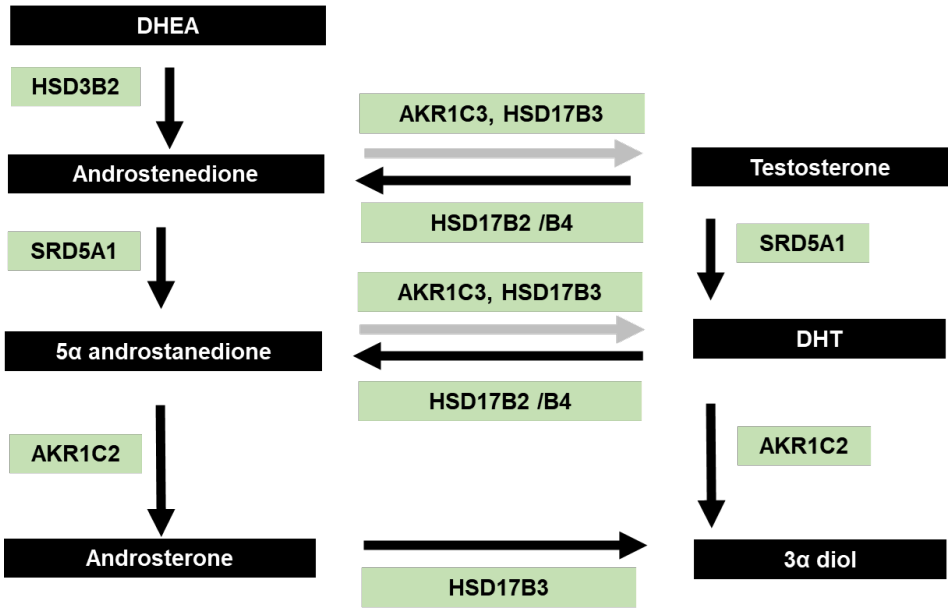

Fig. 3.4: Pathway of androgen synthesis and metabolism
(Enzymes, green and androgens, black)

Reasons for the remaining genes not being investigated in the cell context varied. CYP19A1 converts testosterone to estradiol but our mass spectrometry platform was not validated at the time to detect estrogens adequately. Similarly, HSD17B7 performs conversion of estrone to estradiol which cannot be detected accurately. AKR1C1 converts progesterone to the inactive form 20-α-hydroxprogesterone and this step was unlikely to provoke changes in steroid metabolism. STAR and CYP11A1 perform conversion of cholesterol to pregnenolone as the initial step in steroid synthesis and

since both were significantly downregulated, it was perceived that inclusion of these targets would not offer new insights into steroid metabolism. HSD11B1 converts cortisone to cortisol but since CYP11B1 and CYP21A2 are required to create cortisol and both are not expressed in normal ovary or malignant ovaries, these were excluded from *in vitro* investigation. Similarly, SULT2B1 converts DHEA to the inactive form DHEA-sulphate and this was not considered to be an avenue to investigate.

Since estrogens cannot be detected reliably using LC-MS/MS, the estrogen receptors were omitted from this study and SF1(NR5A1) was determined as an outlier receptor that would require alternative experiments and the literature does not support SF-1 having a significant role in epithelial ovarian cancer. Following the decision on the metabolic steps to be investigated *in vitro*, the choice of steroid treatments was, 17-hydroxy-progesterone (a glucocorticoid precursor), DHEA and androstenedione (androgen pre-cursors) and testosterone and DHT (androgens).

3.3.2 Real-time qPCR of genes of interest involved in steroid metabolism

Four cell lines were chosen (described in Chapter 2) and prior to the steroid metabolism studies, the relevant genes identified from the data analysis were analysed in these cells by RT-qPCR. This was to ensure that the chosen cell lines were appropriate. The gene targets were: *AKR1C2, AKR1C3, HSD3B2, HSD17B3, HSD17B4, HS17B6, CYP17A1, CYP19A1, SRD5A1, PGR* and *AR*. Three reference genes were selected (*ACTB, HPRT1* and *GUSB*). Pooled total RNA from normal ovaries was obtained and used as the control for comparison. The best expressed

reference gene across the four cell lines and the control was *ACTB*. The results are shown in **Figure 3.5.**

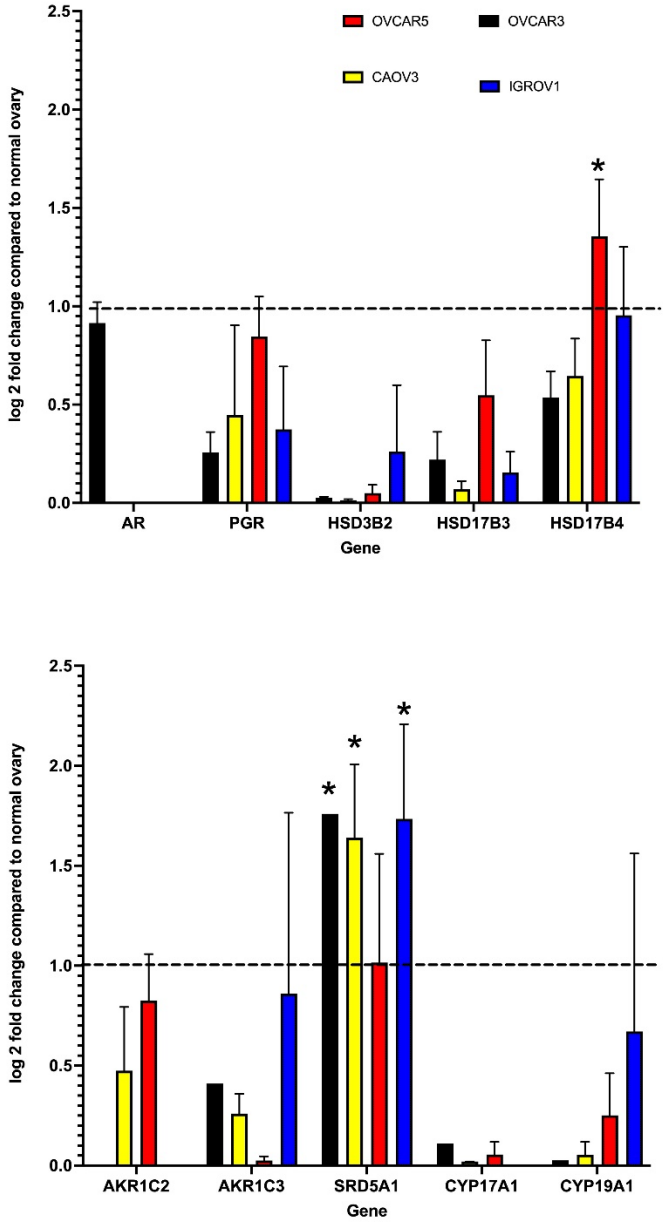

Fig. 3.5: Changes in expression of selected genes implicated in androgen metabolism for four epithelial ovarian cancer cell lines compared to normal ovary.

Log2 fold changes are displayed. Pooled total RNA from 5 normal ovaries was used as the comparison (not shown). *SRD5A1 had significantly increased expression (fold change >1, broken line) in three out of four cancer cell lines compared to normal ovary.*

* *indicates p<0.05 for upregulated genes only.*

Increased *SRD5A1* expression with a fold change >1 ($p<0.05$) was observed in 3 out of 4 of the cancer cell lines which was largely consistent with the TCGA dataset for this gene. However, of the relevant identified genes initially determined as downregulated in TCGA, *HSD17B4* was identified as having an increased log2 fold change of 1.1 ($p=0.047$) compared to normal ovary in OVCAR5 and in the other cell lines the average increased log2 fold change was 0.7. However, *HSD17B3* and *AKRC13* were identified as under expressed in TCGA dataset and this was also observed in the four cancer cell lines.

3.3.3 Steroid metabolism observed in ovarian cancer cell lines over 24h

Steroidogenic activity was observed in the four epithelial ovarian cancer cell lines and the data was depicted as time courses for reduction of starting steroid treatment and simultaneous synthesis of downstream steroids.

Addition of 100 nmol/L DHEA and 17-hydroxyprogesterone to all the cell lines did not stimulate any steroid synthesis. The initial concentration of these steroids remained static at all timepoints (data not shown).

Addition of 100 nmol/L androstenedione, however, resulted in metabolic activity across all four cell lines. Androstenedione concentrations in the supernatant decreased steadily at each timepoint, suggesting continuous downstream conversion. In OVCAR3, OVCAR5 and IGROV1 there was up to a 32% fall in androstenedione (at 24h) whilst in CAOV3 there was a 70% reduction in the available steroid **(Figure 3.6)**. Simultaneously, the concentration of 5α-androstanedione (5α-dione) increased at each timepoint with a correlated decrease in androstenedione in all four cell lines. 5α-

dione production was highest at 24h in CAOV3 (33 nmol/L), with the remaining cell lines producing approximately 20 nmol/L at 24h. Activation of androstenedione to testosterone was minimal in the four cell lines. OVCAR5, CAOV3, IGROV1 produced up to 2 nmol/L of testosterone after 24h and up to 10 nmol/L in OVCAR3. No further downstream conversions were observed.

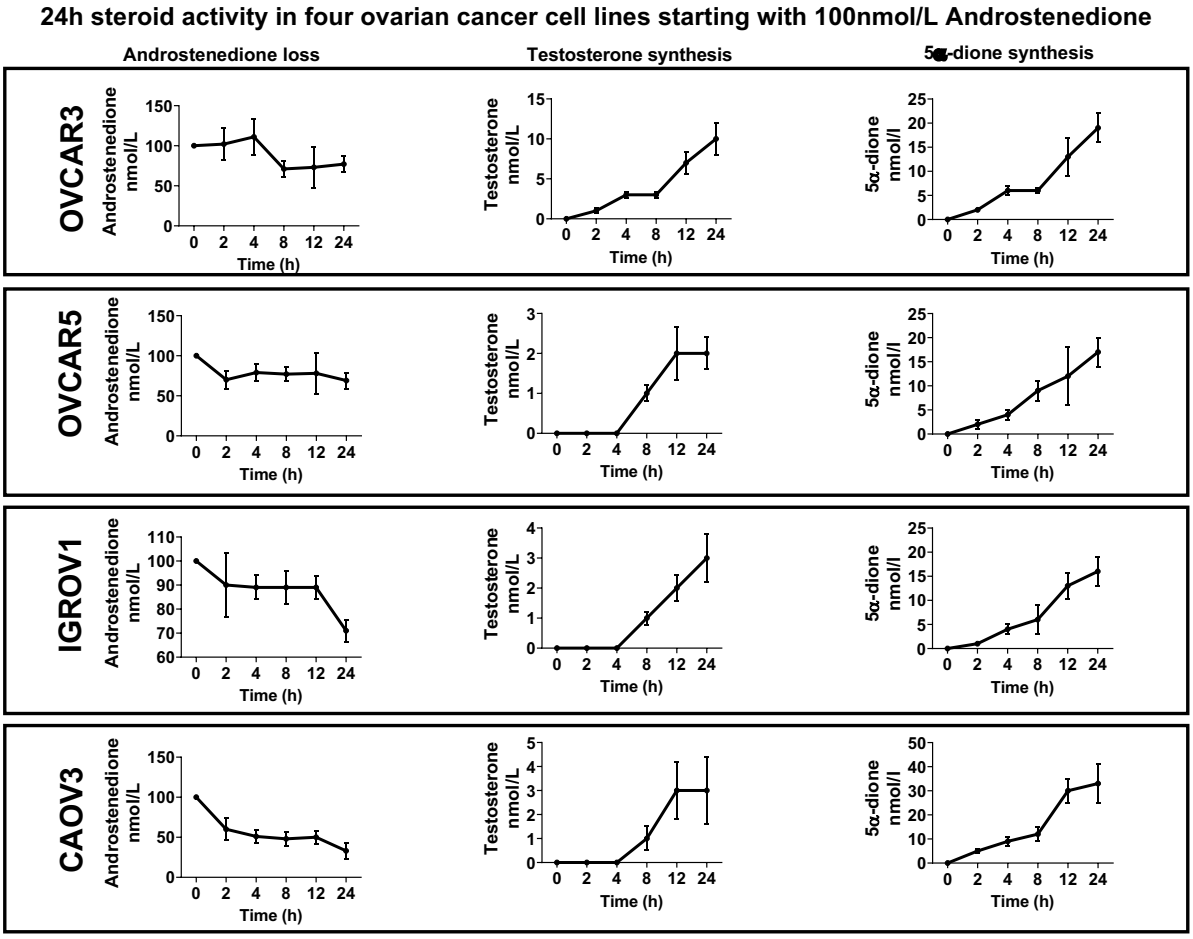

Fig. 3.6: Steroid activity in four ovarian cancer cell lines treated with 100 nmol/L androstenedione over 24h.

All experiments performed in triplicate in serum-free media. Steroid analysis of the cell media at each timepoint was performed by LC-MS/MS. Mean + SD values are plotted. Here, the loss of androstenedione (left panel) is observed alongside simultaneous steroid synthesis of testosterone and 5a-dione.

Addition of 100 nmol/L testosterone to four ovarian cancer cell lines exhibited metabolic activity (**Figure 3.7**). The testosterone concentration decreased steadily over time. The initial concentration of testosterone decreased by nearly 90% in IGROV1 at 24h, whilst in CAOV3, OVCAR5 and OVCAR3, levels fell by 45%, 28% and 31% respectively. In this experiment, production of androstenedione was observed simultaneously with the metabolism of testosterone in all four-cancer cell lines. The highest production of androstenedione was observed in IGROV1 with 32 nmol/ at 24h. In OVCAR5, CAOV3, OVCAR3, androstenedione production at 24h was 15 nmol/L, 4 nmol/L and 3.5 nmol/L respectively. The decrease in testosterone in the supernatant was simultaneous with production of 5α-dione in all four cell lines; by 24 hours, in IGROV1 5α-dione concentration rose to 11 nmol/L, in CAOV3 it rose to 6 nmol/L and in OVCAR5 it rose to 4 nmol/L. 5α-dione was not observed in OVCAR3 after testosterone addition.

Metabolism of testosterone to DHT was observed in OVCAR3 with almost 8 nmol/L after 24 hours and a peak of 4 nmol/L after 12h in OVCAR5. No appearance of DHT was seen in IGROV1 or CAOV3 after addition of testosterone.

Addition of 100 nmol/L DHT did not lead to any downstream steroid synthesis in the four cell lines. In OVCAR3, which expresses *AR*, the concentration of DHT decreased to 20 nmol/L (±4 nmol/L) after 24 hours but the starting concentration remained static in the other three cell lines (results not shown).

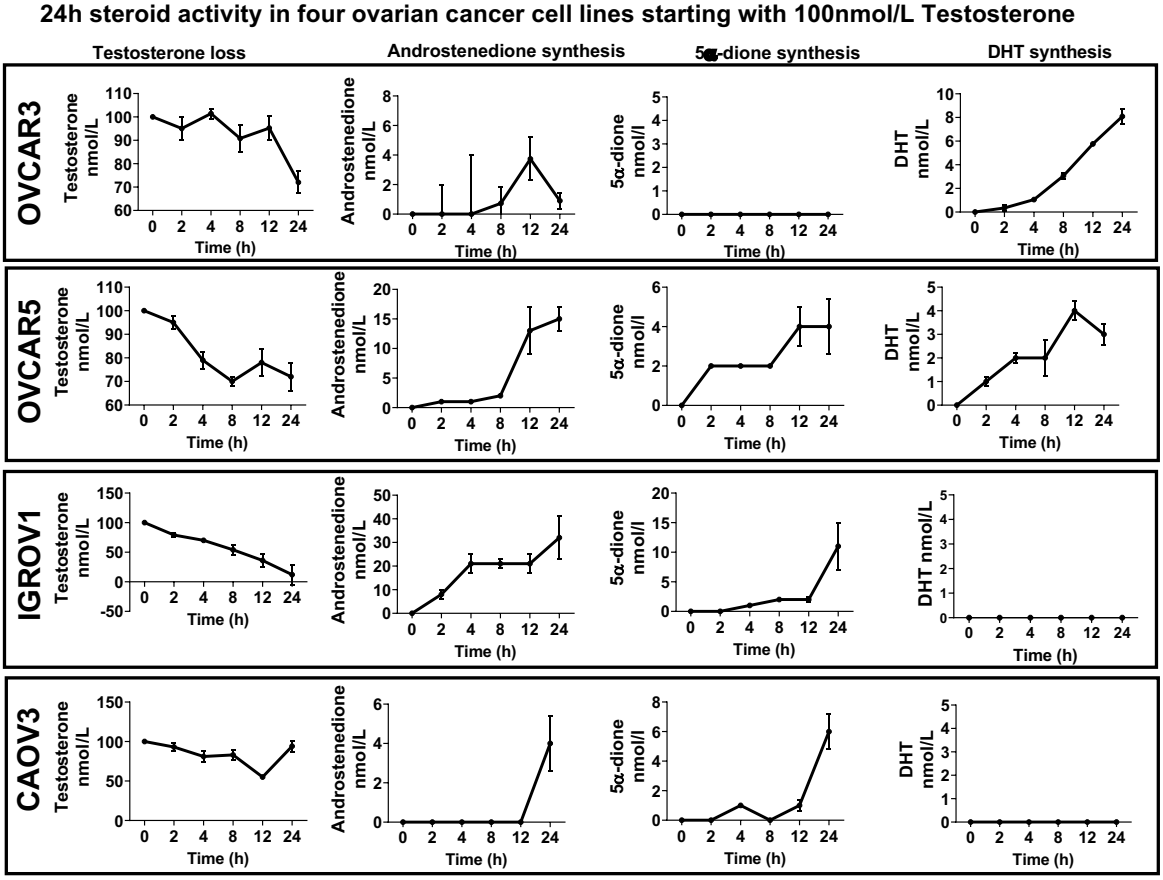

Fig. 3.7: Steroid activity in four ovarian cancer cell lines treated with 100 nmol/L testosterone over 24h.

All experiments performed in triplicate in serum-free media. Steroid analysis of the cell media at each timepoint was performed by LC-MS/MS. Mean + SD values are plotted. Here, the loss of testosterone (left panel) is observed alongside simultaneous steroid synthesis of androstenedione, 5a-dione and DHT.

Addition of 100 nmol/L 5α-dione to the four selected cell lines did result in production of DHT (approximately <2 nmol/L). However, androsterone synthesis was observed in OVCAR5 and CAOV3 with increasing concentration at each timepoint and simultaneous decrease in 5a-dione. In OVCAR5, the concentration of androsterone at 24 hours was 60 nmol/L with a simultaneous fall in 5α-dione to 40 nmol/L. In CAOV3, there was 7 nmol/L androsterone after 24 hours treatment with 5-adione but in the

remaining two cell lines, very negligible amounts of androsterone were synthesised with minimal decrease in 5α-dione **(Figure 3.8).** The presence of the androgen metabolite, 3a-diol, was not confirmed in any of the *in vitro* experiments, as the amounts produced were below the lower limit of quantification on the LC-MS/MS platform.

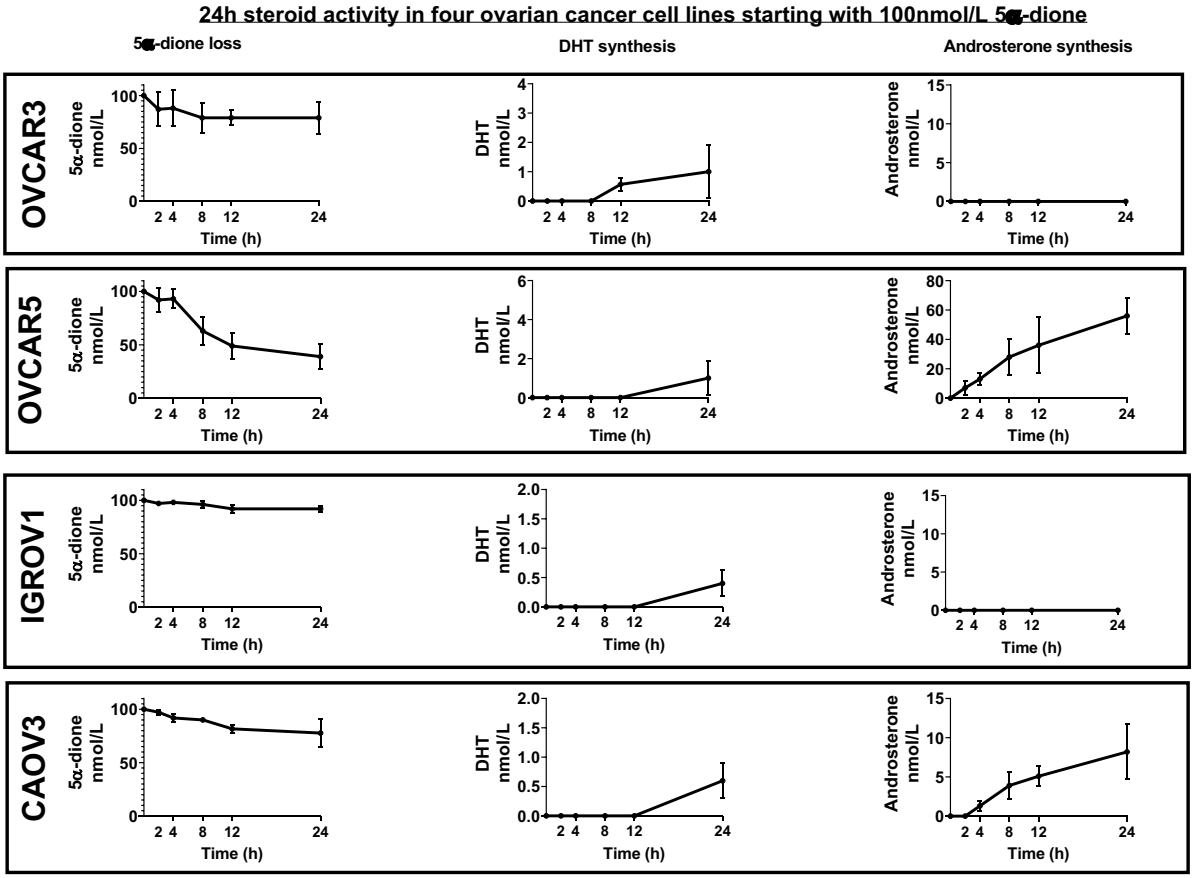

Fig. 3.8: Steroid activity in four ovarian cancer cell lines treated with 100nmol/L 5α-dione over 24h.

All experiments performed triplicate in serum-free media. Steroid analysis of the cell media at each timepoint was performed by LC-MS/MS. Mean + SD values are plotted. Here, the loss of 5a-dione (left panel) is observed alongside simultaneous steroid synthesis of DHT and androsterone.

3.3.4 Cellular proliferation of ovarian cancer cell lines in presence of steroids

The four selected ovarian cancer cell lines displayed androgen metabolism and therefore it was of interest to see whether these androgens impacted cell proliferation compared to controls.

High concentration of DHT(>100 nmol/L) was confirmed to stimulate significant cell proliferation in OVCAR3, which does express *AR* (**Figure 3.9**). However, the three other cell lines did not express *AR* and whilst they did not demonstrate cell proliferation that reached significance DHT treatment, there was a trend of increasing proliferation which may represent AR-independent stimulation. The addition of 17-hydroxyprogesterone, androstenedione, androsterone and testosterone to all four cell lines did not stimulate cell proliferation that reached significance nor were any obvious trends observed. 5α-dione was the commonest downstream steroid synthesised in the time course experiments but it also did not significantly affect cell proliferation. However, IGROV1, the Type 1 ovarian cancer cell line did demonstrate a trend of increasing cell proliferation in the presence of 5α-dione that was not observed in the other cell lines. As discussed before, androgens have been postulated to have a role in tumour development independent of AR signalling.

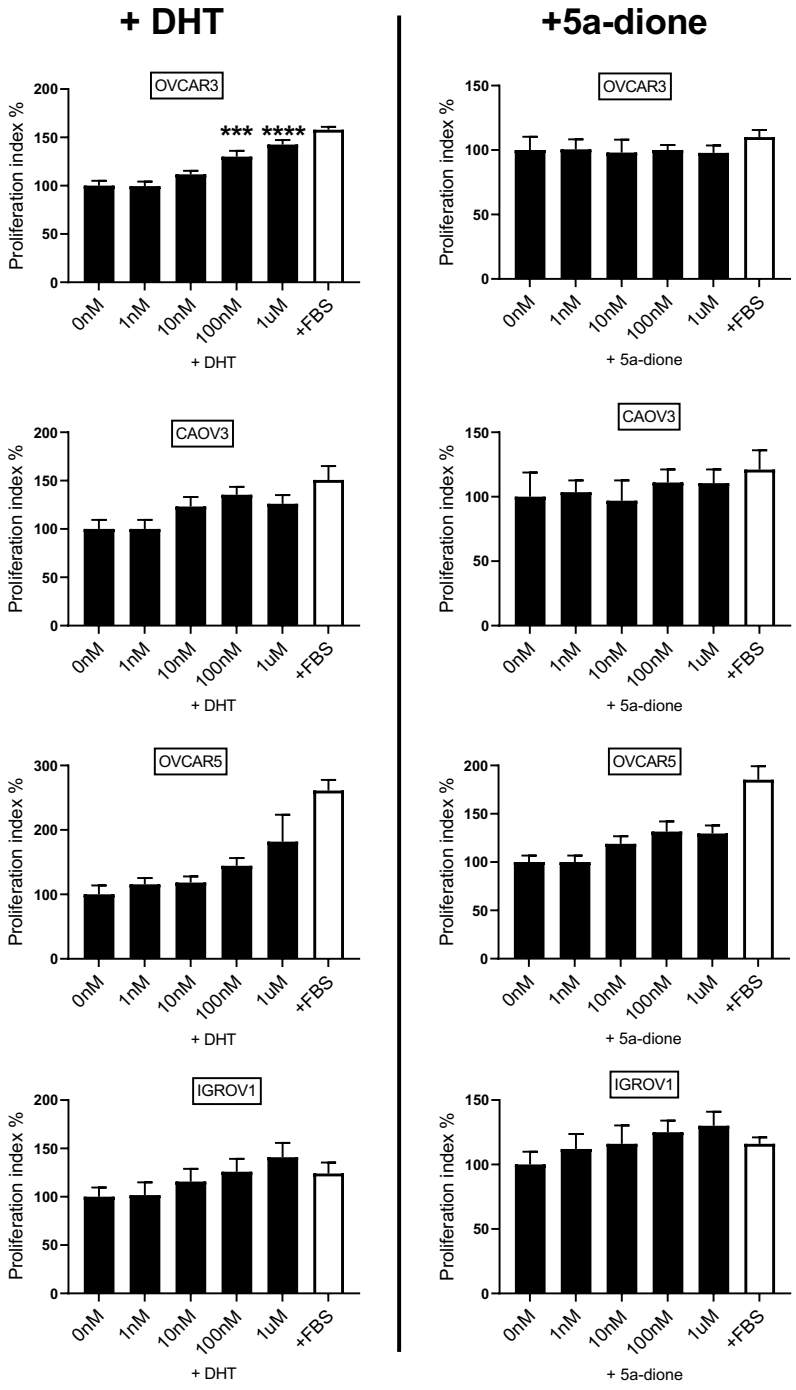

Fig. 3.9: Cell proliferation assays in ovarian cancer cells with DHT & 5α-dione.

Four ovarian cancer cell lines were stimulated for 24h with DHT and 5α-dione and charcoal stripped serum before analysis using a BrdU colorimetric assay (n=3). Non stripped fetal bovine serum (FBS) in relevant media was used as a positive control (white box) for comparison. A significant increase in cell proliferation was only observed in OVCAR3 (androgen receptor positive), with stimulation with DHT at 100nM (p-value < 0.001) and 1μM (p<0.0001) when compared to 0nM. Data represents mean ± SD.

3.3 Discussion

Here I show for the first time the androgen synthesis and metabolism pathways in epithelial ovarian cancer cell lines noting the fluctuations followed over 24h period demonstrating successive conversion steps in the pathway. These downstream steroids appear to converge in a pool of weaker androgens, 5α-dione, androstenedione and androsterone, which is unexpected as previous research would suggest the ovaries preferentially promote synthesis of potent androgens and then estrogens. The genes that encode for the enzymes that stimulate this activity are present in these cell lines although it is uncertain if they may be overall down-regulated from normal healthy ovary. This is because the TCGA dataset for ovarian serous carcinoma for the genes of interest in this study were largely downregulated whilst this was not seen in the chosen cell lines. The two most frequent steroid metabolism steps seen in the cell line time course experiments were performed by SRD5A1 (androstenedione to 5α-dione) and HSD17B4 (testosterone to androstenedione). Increased cellular proliferation was confirmed to be associated with treatment with DHT in ovarian cancer cell lines (OVCAR3) with *AR* expression which has already been documented. However, the other androgens and androgen pre-cursors did not replicate this behaviour. An interesting observation was the Type 1 ovarian cancer cell line, IGROV1, demonstrated more frequent steroid synthetic steps along with higher concentrations of products compared to the Type 2 ovarian cancer cell lines. A summary of the androgen metabolism cascade identified in these ovarian cancer cell line experiments is shown in **Figure 3.10.**

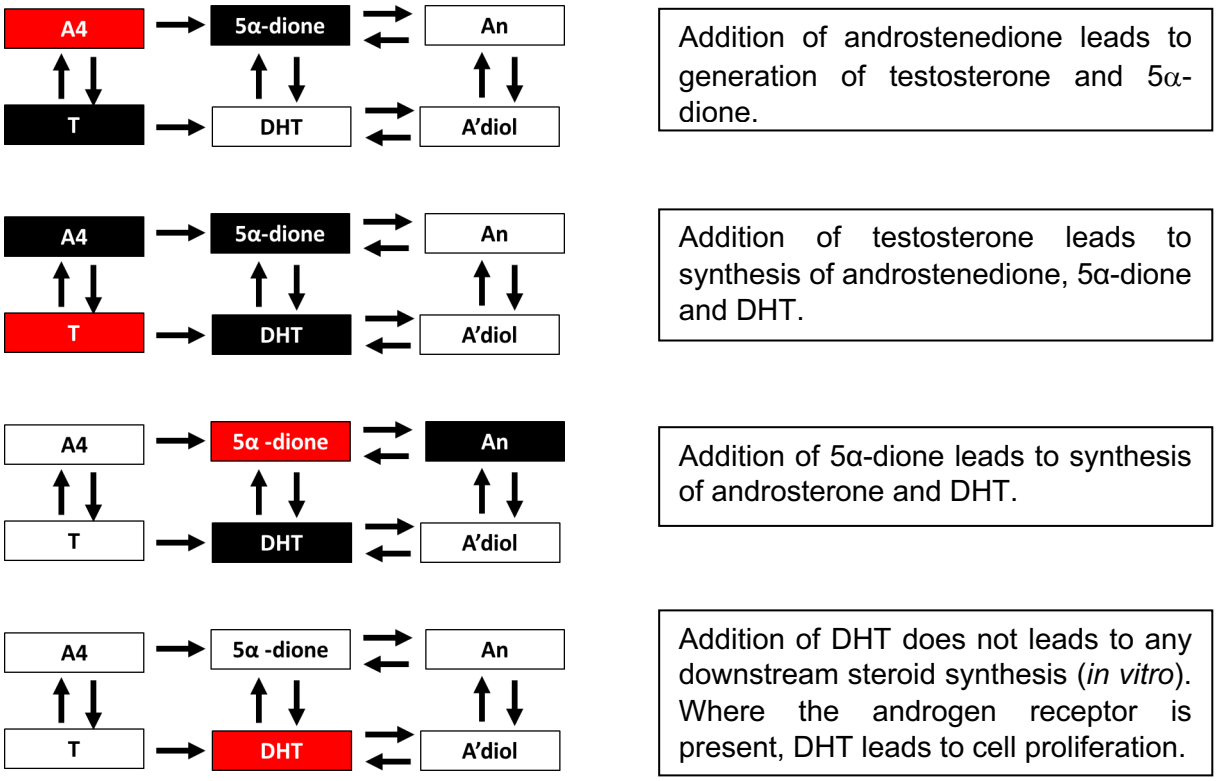

Fig. 3.10: Summary of the observed steroidogenic pathways in four epithelial ovarian cancer cell lines

Four cell lines: IGROV1, OVCAR3, OVCAR5 and CAOV3. Starting substrate in red, downstream, products observed after 24h in black. A4= androstenedione, T = testosterone, An = androsterone, DHT = dihydrotestosterone, 5a-dione = 5a-androstanedione, A'diol/Adiol/3a-diol = androst-5-ene-3β,17β-diol

Analysis of public genomic datasets identified changes in under-expression and over-expression of *SRD5A1, AKR1C2, AKR1C3, HSD3B2, HSD17B3 and HSD17B4* and *CYP17A1* and these became our potential targets of interest to investigate for androgen metabolism in ovarian cancer. We used current knowledge on their enzymatic function from the literature to create these experiments to observe downstream androgen metabolism and this approach was successful.

Androstenedione is metabolised by SRD5A1 to produce 5α-dione in all four cell lines, particularly CAOV3 with almost 33 nmol/L and 20 nmol/L in the other three cell lines.

At each advancing timepoint for all the cell lines, 5α-dione concentration rose with simultataneous decrease in the starting steroid. Androstenedione also activated AKR1C3 to produce testosterone in all the cell lines, mostly in OVCAR3. *SRD5A1* was identified as being upregulated in the TCGA data for serous ovarian cancer and this correlates with this steroid metabolism observation and increased *SRD5A1* gene expression in the ovarian cancer cell lines. Incidentally, increased AKR1C3 expression is observed in both liver and renal cell cancer and is associated with a reduced 5-year survival rate and therefore AKR1C3 has become a therapeutic target (Zheng et al., 2022).

The addition of testosterone as a treatment stimulated downstream synthesis and changes. In these experiments, the common theme observed in the cancer cell lines was to consume testosterone at varying rates and produce androstenedione which was the largest downstream steroid synthesise and then there was further metabolism of androstenedione to 5α-dione. Here, testosterone was almost completely consumed by IGROV1 (mixed endometrioid and clear cell ovarian cancer cell line) after 24h and with simultaneous synthesis of the highest concentrations of androstenedione and 5α-dione compared to the other cell lines. However, DHT synthesis was also observed with addition of testosterone in two cell lines. Here, the enzymes are interacting. First HSD17B4 converts testosterone to androstenedione followed by SRD5A1 metabolising newly synthesised androstenedione to 5α-dione. SRD5A1 also converts testosterone to the potent androgen, DHT, but the preference in these cell lines is towards creating androstenedione and 5α-dione which are weaker androgens. This suggests HSD17B4 has greater affinity for testosterone over SRD5A1 in these ovarian

cancer cell lines but to date there is no literature to support this claim. Furthermore, HSD17B4 expression was highest in OVCAR5 ($p<0.05$), yet conversion of testosterone to androstenedione was higher in IGROV1, suggesting steroid metabolism in Type 1 ovarian cancer is perhaps more active compared to Type 2 ovarian cancers. One study has investigated HSD17B4 protein expression in 6 normal ovarian surface epithelium specimens compared to 60 epithelial ovarian cancer tissue samples. It confirmed that HSD17B4 expression increased in ovarian cancer specimens and suggested this was a protective mechanism by both androgen and estrogen inactivation. HSD17B2 also performs the same role as HSD17B4 and whilst its protein expression was absent in normal ovary, it was expressed in the cancer specimens. However, they could not display a difference in expression frequency for HSD17B4 and HSD17B2 between the different histological types of ovarian cancer, particularly Type 1 cancers, likely due to the limited number of cases (Motohara et al., 2010).

Another alternative reason for not observing all testosterone metabolism was that it could have been converted to alternative steroids in other pathways that we have not detected on our mass spectrometry platform, nor identified in analysis from RNA expression.

When 5α-dione was used as the treatment steroid, androsterone synthesis was notably observed in OVCAR5 and CAOV3. This was surprising as the TCGA dataset had suggested downregulation of *AKR1C2* which encodes the enzyme that performs conversion of 5α-dione to androsterone. Small amounts of DHT synthesis were seen

in response to addition of 5α-dione confirming *AKR1C3* expression. This is important because synthesis of DHT further supports the plausibility of a role for androgens in the aetiology of ovarian cancer, as it has been shown to directly stimulate AR for ovarian cancer cell proliferation (Sheach et al., 2009a).

Overall, the trajectory of androgen metabolism in these experiments appears to direct towards production of 5α-dione and androsterone, which are weak androgens. This fits with a study demonstrating serum androsterone (androsterone glucuronide) significantly elevated in non-serous ovarian cancer (Type 1 tumours) identified by LC-MS/MS (n=102 serous vs n=67 non-serous) (Trabert et al., 2019). The same study found there were notable elevations (non-significant) for DHEA, androstenedione, and testosterone for non-serous tumours. Evidence for 5α-dione being related as a biomarker for epithelial ovarian cancer has not been previously reported. Previous work has focussed on androstenedione, testosterone and DHT as targets of interest and not considered the remaining pool of androgens (Ose et al., 2017). Hence it is possible that a reservoir of 5α-dione and androsterone measured in circulation provide a phenotypic characterization of individual patterns of androgen metabolism that could be a biomarker for epithelial ovarian cancer. These may be better markers of androgenic activity in postmenopausal women than measuring DHEA, testosterone, or androstenedione alone.

A potential role for 5α-dione and androsterone in epithelial ovarian cancer development or progression has not been previously described. In this study, whilst 5α-dione did trigger a trend of increasing cell proliferation in IGROV1, it did not significantly influence cell proliferation in the four cancer cell lines but alternative roles

may exist. Another quantitative method to detect AR activity in response to 5α-dione is androgen reporter gene assays. These assays can measure the transcriptional activity of *AR* in the presence of 5α-dione and the functionality of its binding sites (androgen response elements) in DNA (Makkonen et al., 2011). I did confirm a previous study finding that DHT causes ovarian cancer cell proliferation where *AR* is expressed. It has also been shown to increase oncogene expression related to G protein signalling (Rab25 and Rab35) in ovarian cancer cells (Sheach et al., 2009a). In my study, DHEA and 17-hydroxyprogesterone addition to all the cell lines also did not stimulate any steroid synthesis because of the absence of *HSD3B2*, *CYP17A1* and *CYP21A2* observed in mRNA expression of the four cell lines which would perform metabolism of these steroids.

Whilst androgen metabolism has been observed, analysis of the TCGA dataset showed there was no influence of the multiple genes involved in androgen metabolism on survival. This infers that if androgen metabolism is dysregulated in epithelial ovarian cancer, it may only be a pathological feature of the disease; however, this could be exploited for diagnostic purposes. Hence, similar experiments on ovarian tumour tissue may confirm if similar androgen metabolic events occur.

Limitations: A normal human ovarian surface epithelial (OSE) cell line was not used for comparison but it is uncertain how useful a normal OSE model is given the ovary exists in two states: pre-menopausal and post-menopausal. OSE lines are derived from pre-menopausal patients yet over 80% of ovarian cancer affects post-menopausal women. Cell lines from benign ovarian tumours, borderline ovarian

tumours and mucinous ovarian cancers were not studied either and these may exhibit altered androgen metabolism that could direct towards potential diagnostic biomarkers. A solution to this would be to attempt this same study using organoids. However, this preliminary work was focussed largely on serous ovarian cancer as it is the most prevalent type of ovarian cancer. Finally, the use of genomic data sources that possess small numbers for Type 1 ovarian cancers could be considered as inadequate to make decisions on biological investigations from.

Chapter 4 Androgen metabolism in epithelial ovarian tumours

4.1 Introduction

Whilst epithelial ovarian cancer has been shown to have driver events, such as *TP53* mutation, the disease is still genomically heterogeneous with high genetic divergence.

Monolayer cell lines are an important source for investigation of potential new biological mechanisms in ovarian cancer and they allow control of most experimental variables and permit quantitative analysis. However, given that primary tumours are often diverse from commonly used ovarian cancer cell lines (Domcke et al., 2013), they have limited physiological relevance as they capture very few aspects of the three-dimensional tumour microenvironment.

Ex vivo tumour biopsies can be superior to single cell lines as they maintain the heterogeneity of tumour cell subpopulations and undisrupted supporting stromal tissue cells. It removes many of the *in vivo* experiment complexities and maintains cell-cell interactions. Whilst patient derived samples provide limited ability for comparison of experimental results, they are extremely important in validating the findings from initial cell line investigations.

The synthesis of androgens (androstenedione and testosterone) by epithelial ovarian cancers in post-menopausal women has been demonstrated by ovarian vein sampling, but those early studies were uncertain if malignancy influenced steroid activity, and they were limited by the methodology for steroid analysis of that era (Heinonen, 1991). A study that reported ovarian malignancy associated with serum steroid hormones did so only by testing serum samples for progesterone and androstenedione from women with ovarian cancer before treatment and compared them again with their repeated post-treatment samples. Women that developed recurrences had serum steroid

hormone concentrations that returned to their pre-treatment levels (Mählck et al., 1986). At present there is a paucity of studies examining ovarian intra-tumour steroidogenesis and metabolism.

The effect of peritoneal fluid on steroid production was analysed in a study with 11 ovarian tumours (benign and malignant). It demonstrated that epithelial ovarian tumours incubated in the patient's own peritoneal fluid stimulated the release of progesterone from both benign and malignant tissue (Elattar et al., 2012). This is suggestive that there are components in peritoneal fluid which can stimulate steroid production from ovarian tumours This may be a potential mechanism of disease behaviour whereby steroid metabolism is involved in tumour initiation and/or progression.

In another study, benign and malignant ovarian tumour pieces were incubated in plain media for 3h and then the media was analysed for steroids to detect *ex vivo* biosynthesis. However, the steroid analysis was performed using radioimmunoassay which is inferior to mass spectrometry. This study observed that progesterone and androstenedione release were greater in malignant tumours whilst testosterone release was greater in benign tumours. Upon adding testosterone to postmenopausal control ovaries, there was a 6-fold rise in androstenedione production but no change in estradiol (Ridderheim et al., 1993). However, both these studies did not have results showing exactly how the ovarian tumours metabolised these androgens. Currently, there are no published studies exploring steroid metabolism in human ovarian tumour tissue combined with mass spectrometry for quantitative analysis.

By networking with the regional Gynaecological Cancer Centre, I obtained fresh human ovarian tumour tissue to investigate **my hypothesis that benign and malignant ovarian tumours have distinct androgen metabolism characteristics.**

The aims of this study were to evaluate the metabolites produced by *ex-vivo* ovarian tumour specimens, incubated and treated with androgens, and thereby validate the *in vitro* findings of androgen metabolism in ovarian cancer cell lines (Chapter 3). This would provide information to identify a panel of steroids that could potentially be detected *in vivo* in patients with ovarian tumours.

4.2 Methods

To observe and characterise the steroidogenic activity within ovarian tumour tissue, fresh tissue specimens were obtained from patients undergoing surgery for suspected or confirmed ovarian cancer without neoadjuvant therapy. These specimens were then prepared and treated with selected androgens. Then evaluation of steroid metabolism was performed by steroid profiling of the tumour media using liquid chromatography tandem mass spectrometry (LC-MS/MS) over three timepoints 12h, 24h and 36h. Since the *in vitro* investigations in **Chapter 3** indicated changes in androgen metabolism in the ovarian cancer cell lines, the same steroids were selected as treatments for the tumour tissues with the intention to validate the use of the earlier cell line models.

4.2.1 Patient recruitment

NHS ethical approval was secured to recruit eligible patients for human biomaterial (24-hour urine collections, serum and ovarian tissue) and is described in **Chapter 2**.

Tissues were retrieved from women having surgery for suspected or confirmed ovarian cancer and women with benign ovarian masses. All recruits had no previous treatment. Women undergoing oophorectomy for non-related reasons were assigned as controls, however the amount of tissue retrieved from this group was not sufficient for these experiments. In this investigation, 45 women with ovarian masses were identified as potential tissue donors but only 17 patients had suitable tissue following surgical removal. After using seven tissue specimens for method development, ten patient specimens were analysed for steroid metabolism. Six tumours were from malignant specimens (all Stage III—IV disease), two were borderline serous ovarian tumours (both Stage I) and two tumours were benign serous type (**Figure 4.1**). Nine of the ten tissue donors were post-menopausal, aged between 48-77 years (median age 62 years).

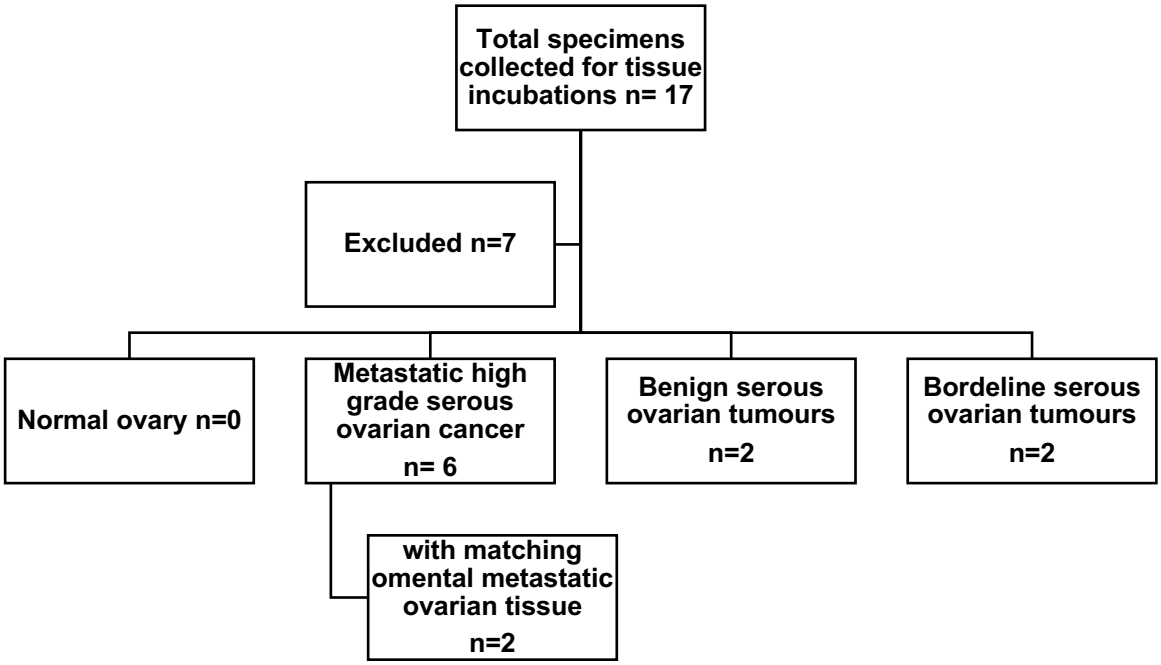

Fig. 4.1: Fresh ovarian tumour tissues obtained for studying androgen metabolism

A total of 45 women were initially selected as suitable candidates for tissue provision but often the tumours were either necrotic, insufficient or did not remain viable for the *ex vivo* experiments. Ovarian tissues (n=17) were used for incubation with androgens, of which 7 specimens were used for method development. Healthy control tissue was insufficient to perform triplicate experiments and were not included in this study. Type 1 ovarian tumour material was not obtained either. Of the 10 tumour specimens used in the study, 9 were from post-menopausal patients. All included ovarian tumour specimens were of serous subtype (metastatic ovarian cancer Stage III/IV n=6, borderline serous n=2 and benign serous n=2).

4.2.2 Method development

This method required a significant amount of time to develop. Initial training with a histopathologist was undertaken to develop skills in ensuring tissues that were correctly sampled. Whilst the intention was to sample several tumours, many specimens were either insufficient to perform in triplicate or were unsuitable due to ischaemia or necrosis. In fluid filled cystic masses, the distortion resulted in surface epithelium that was devoid of stromal tissue. The histopathologists and surgical team

at the Cancer Centre also placed limitations on the tissues extracted to preserve accuracy in their final staging; hence no sampling of the Fallopian tube or tissue adjacent to it was permitted. This restriction often prevented obtaining surface epithelium with viable stromal tissue and it reduced the number of tissue samples suitable for this investigation.

Women undergoing oophorectomy for non-related reasons were assigned as controls, but at surgery insufficient tissue was obtained to perform this investigation in triplicate and no normal ovarian tissue was obtained. As the standard of care is usually neoadjuvant chemotherapy for confirmed ovarian cancer, it was infrequent to find suitable patients having primary debulking surgery.

Initial results using 200 mg tissue pieces with 5 ml of media were unsuccessful as the concentrations of steroid metabolites saturated the mass spectrometer beyond its upper limit of quantification. The use of very small tumour pieces at 10-30 mg in the steroid incubations did not result in any observed steroid metabolism changes that could be detected by LC-MS/MS. Using several iterations to develop the method, the optimal weight was 90-100 mg pieces of tissue in 5 ml of media with charcoal stripped foetal calf serum and the chosen steroid treatment at 100 nmol/L concentration. The selection of time points also required optimisation. Initial selection of chosen time-points were 12h, 24h and 48h on the basis that more downstream steroid metabolic events might be observed with a longer course, however tissue ischaemia occurred by 48h. Eventually the levels of the steroid metabolites became measurable within the limits of quantification on our LC-MS/MS platform.

4.2.3 Method for investigating androgen metabolism in fresh ovarian tumour tissues

Fresh ovarian tumour tissue was transferred to the University within 3h of surgery in room temperature phenol red free RPMI (Gibco). A biopsy of the tumour was also taken for RNA extraction and gene expression analysis, with the intention of comparing the control ovary specimens to the malignant and benign tumours. Another biopsy was sent to the histopathologists to confirm sampling of the epithelium and stroma. The management of timing between the tissue retrieval and the utilisation of the tissue in the laboratory were standardized to decrease the impact of tissue necrosis. Tissues were then washed with warm PBS at 37°C (Gibco) and dissected in aseptic conditions. Viable tissues were cut to 90-100 mg (wet weight) pieces and kept briefly in warm PBS whilst the steroid-media mix was prepared. The steroid-media mix was made of 5ml fresh phenol red free RPMI with 5% charcoal stripped foetal calf-serum, 1% penicillin streptomycin and 100 nmol/L of the selected steroid substrate. Each cut tissue piece was placed in an individual 10 ml centrifuge tube (Corning) and the media mix was then added accordingly.

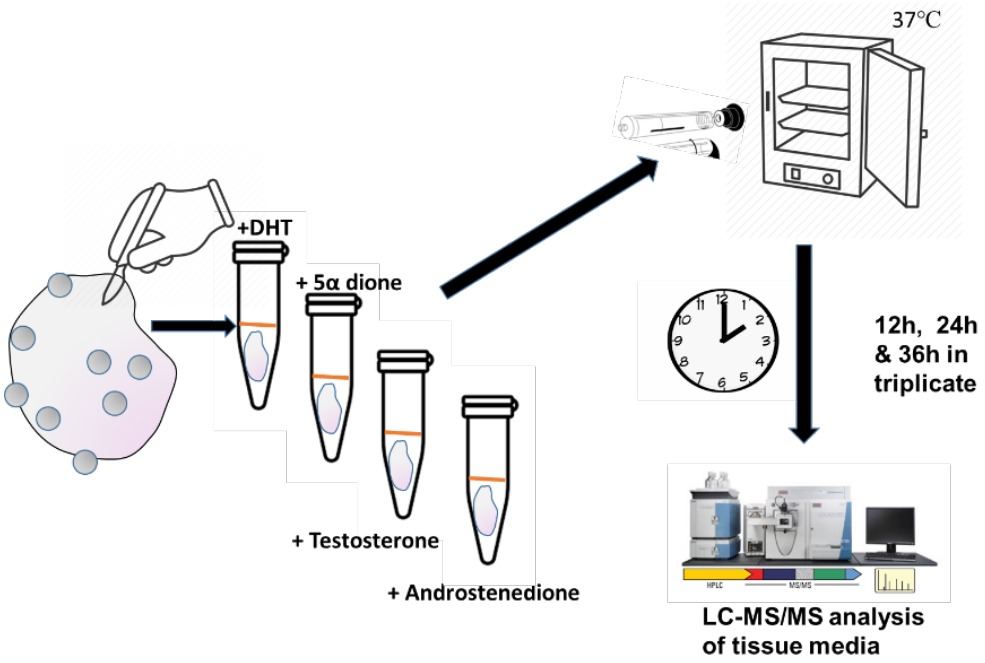

Fig. 4.2: *Ex-vivo* ovarian tumour incubation

Ovarian tumour material was obtained at surgery and transferred to the laboratory within 3h and cut to 100 mg pieces and placed individually with 5 ml of media and 100 nmol/L concentration of androgen and placed in a hybridization incubator that continually rotated the tubes. The specimens were incubated over three time points: 12h, 24h and 36h and this was performed in triplicate. At the end of each time point, the tissue media was extracted and steroid analysis was performed using mass spectrometry (liquid chromatography tandem mass spectrometry, LC-MS/MS).

The selected steroids used were 5α-dione, androstenedione, testosterone and DHT. For each treatment, there were three replicates and one control containing steroid media only. The tubes were placed in a hybridization incubator (HB-1D, Techne), set at 37°C for 12h which continually rotated the tubes with tissues and media. In addition, further tissues of the specimen were prepared as described and incubated for 24h and 36h to create a time course of steroid metabolism in the tumours **(Figure 4.2).**

After each elapsed timepoint, the tubes were removed from the hybridisation incubator and vortexed briefly for 30 seconds. The tissue was removed and the remaining media was stored in silanized tubes at -20°C till ready for steroid extraction by LC-MS/MS.

The final histopathological report along with confirmation that the epithelium and stromal area had been sampled, was later provided from the histopathlogists at the Cancer Centre. This information was used to correlate with the steroid analysis data for each tumour incubation. For two high grade serous ovarian cancer specimens, it was possible to also retrieve matching omental metastatic tissue that remained viable and this was used to perform a steroid analysis; 50 mg of tissue was used and prepared similarly with the media mix and steroid substrates.

4.2.4 Steroid profiling by liquid chromatography tandem mass spectrometry

To identify and quantify the steroids from the incubations, LC-MS/MS was performed on the tissue media samples. The frozen supernatant was thawed, vortexed and 1 ml was used for steroid extraction and subsequently completed as described in **Chapter 2**. The concentrations of androstenedione, DHT, testosterone, androsterone, 5α-dione and androst-5-ene-3β,17β-diol (Adiol) for each timepoint and replicate were recorded. The mean value from the triplicate results was calculated along with the standard deviation and both were graphically plotted using GraphPad Prism v9.3.

4.2.5 Steroidogenic gene expression analysis in fresh ovarian tumour tissue (RNA extraction and real-time PCR)

Fresh tumour tissue with a wet weight of 50 mg was washed with PBS and placed in a 2 ml microcentrifuge tube with a 5 mm autoclaved stainless-steel bead and 600 µL lysis buffer (Buffer RLT, Qiagen). The tissue was disrupted and homogenized using a Tissue Lyser at 30 Hz for 3 minutes. The bead was then removed and the homogenate used for RNA extraction using the RNeasy mini kit (Qiagen) described in **Chapter 2**.

The extracted RNA was used in a reverse transcriptase reaction to generate cDNA. This was in anticipation of quantifying gene expression of selected steroidogenic enzymes by Real-Time polymerase chain reaction (qPCR), using TaqmanTM Gene Expression Assays (Thermo Fisher), described in **Chapter 2**. Unfortunately, this experiment was not completed due to the coronavirus pandemic (COVID-19) which heavily impacted access to the University laboratories.

4.3. Results

4.3.1 Androgen metabolism in benign ovarian tumours

Two benign serous ovarian tumours were analysed for androgen metabolism: an ovarian serous adenofibroma (**Figure 4.3**) and an ovarian serous cystadenoma (**Figure 4.3**).

On addition of 100 nmol/L DHT to the ovarian serous adenofibroma specimen, the results showed continual stepwise loss of the initial DHT concentration from 100 nmol/L to 14 nmol/L after 36h. This was associated with a subsequent production in

5α-dione to a peak of 20 nmol/L by 24 hours and a small production of approximately 2 nmol/L androsterone and 2 nmol/L Adiol. The remainder of the DHT consumed could not be accounted for.

When 100 nmol/L 5α-dione was added to this ovarian serous adenofibroma, it decreased to 21 nmol/L after 36h. Synthesis of small amounts of DHT (2 nmol/L) and androsterone (2 nmol/L) were observed simultaneously but the loss of 5α-dione could not be completely accounted for.

Starting with 100 nmol/L testosterone**,** the concentration decreased to 52 nmol/L by 36h in the ovarian serous adenofibroma specimen. This was associated with a production of 24 nmol/L androstenedione and 2 nmol/L of 5α-dione. No other steroids were detected and the change in concentration of testosterone again could not be completely accounted for.

Finally, 100 nmol/L androstenedione added to the serous ovarian adenofibroma specimen showed a stepwise decrease to 36 nmol/L by 36h. This was associated with a corresponding production of 12 nmol/L testosterone, 9 nmol/L 5α-dione and 1 nmol/L androsterone.

In these incubations and all that followed, where the decrease in starting steroid could not be completely accounted, two reasons may be responsible. Firstly, the steroid metabolites synthesised may be outside the scope of the mass spectrometer and therefore were not identified. The more likely reason is that the tumours may not have released the lipophilic steroid products into the media that was analysed, a known issue with this method.

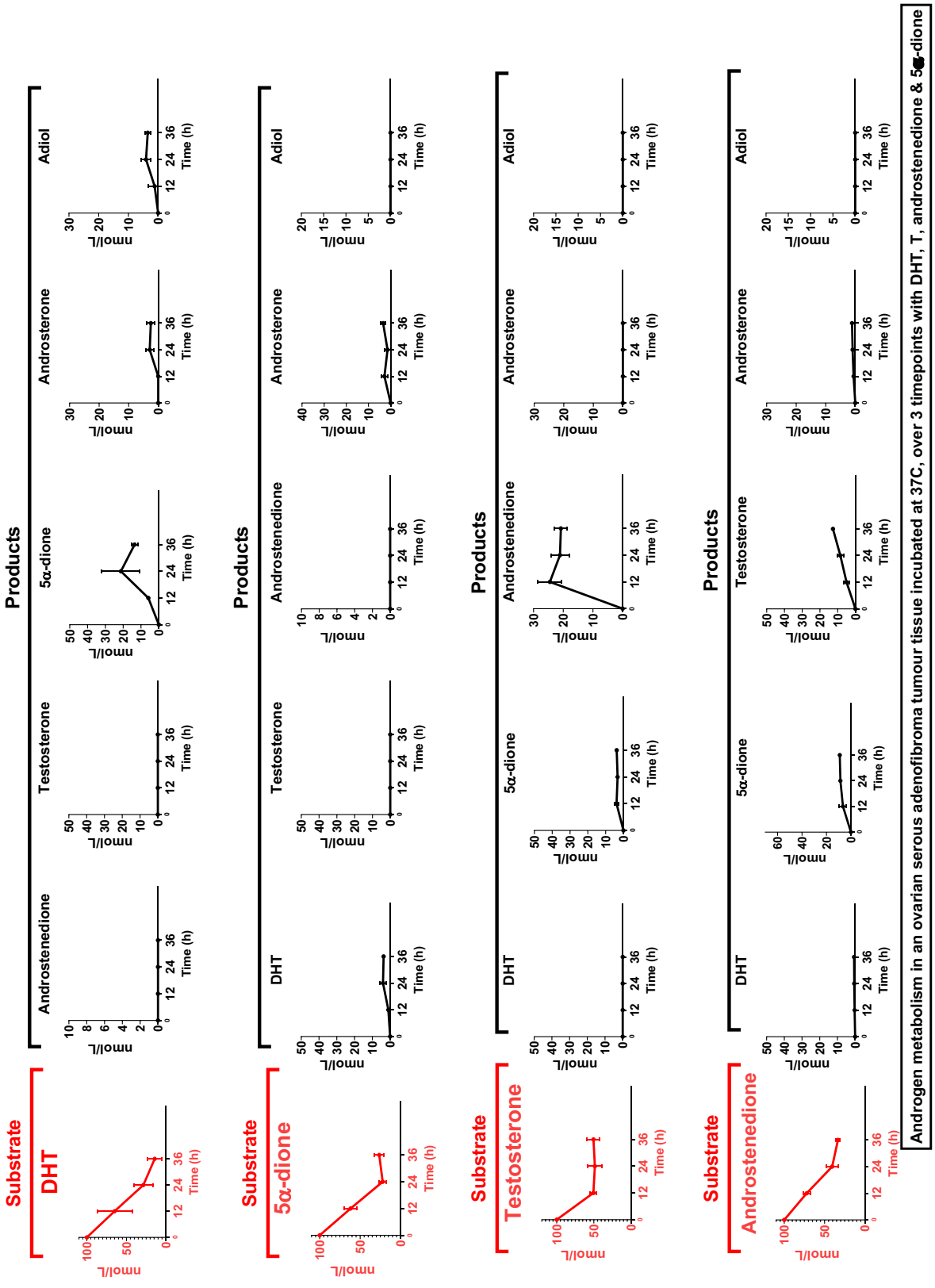

Fig. 4.3: Androgen metabolism in an ovarian serous adenofibroma tumour

The tumour sample was divided into 100 mg pieces and treated with four androgens at 100nmol/L for three separate time points to create a time course (12h, 24h and 36h). All experiments were performed in triplicate with serum-free media. Steroid analysis of the tumour media at each timepoint was performed by mass spectrometry. The decrease in the starting androgen is in red (left panel) is observed alongside simultaneous synthesis of androstenedione, testosterone, dihydrotestosterone (DHT), 5α-androstanedione (5α-dione), androsterone and androst-5-ene-3β,17β-diol (Adiol). Mean + SD values are plotted (n=1).

Androgen metabolism in the ovarian serous cystadenoma tumour was associated with large decreases in all initial androgens but these losses could not be completely accounted for (**Figure 4.4**).

Incubation with 100 nmol/L DHT for the serous cystadenoma specimen showed a fall in the initial concentration of DHT from 100 nmol/L to 78 nmol/L after 24h and remained static by 36hours. The decrease in DHT was associated with a simultaneous production of 5 nmol/l 5α-dione and 17 nmol/l of Adiol which peaked at 24h and then dropped to 12 nmol/l by 36h. The sum of products accounts for the decrease in DHT.

Incubation with 100 nmol/L 5α-dione for the serous cystadenoma specimen showed a rapid fall in the starting androgen to almost 40 nmol/L by 12hours with only a small decrease to 37 nmol/L by 36h. A peak production of 27 nmol/L androsterone was observed by 12h and this fell to 21 nmol/L by 36h. Production of a total of 1 nmol/L DHT was observed by the end of the time course.

The addition of 100nmol/L testosterone to the serous cystadenoma specimen was observed with a decrease to 90 nmol/L by 36h. A corresponding production of 2 nmol/L, 1 nmol/L 5α-dione, and 8 nmol/L androstenedione was observed and this accounts for the change in testosterone.

Incubation with 100 nmol/L androstenedione with the serous cystadenoma sample was observed by a fall to 79 nmol/L after 36h. Approximately 6 nmol/L of 5α-dione and 4 nmol/L testosterone was detected correspondingly but the remainder was unaccounted for.

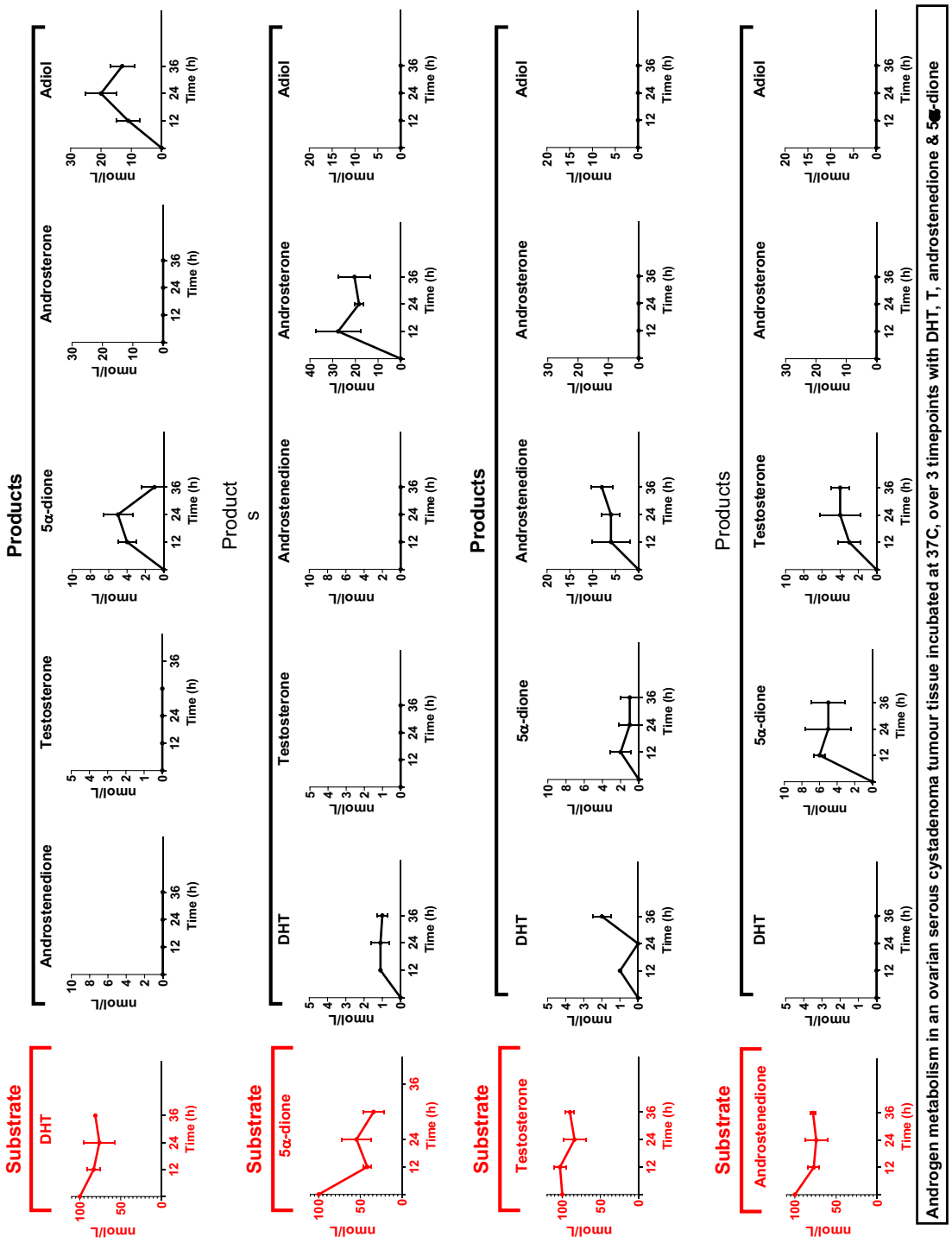

Fig. 4.4 Androgen metabolism in an ovarian serous cystadenoma

The tumour sample was divided into 100 mg pieces and treated with four androgens at 100nmol/L for three separate time points to create a time course (12h, 24h and 36h). All experiments were performed in triplicate with serum-free media. Steroid analysis of the tumour media at each timepoint was performed by mass spectrometry. The decrease in the starting androgen is in red (left panel) is observed alongside simultaneous synthesis of

androstenedione, testosterone, dihydrotestosterone (DHT), 5α-androstanedione (5α-dione), androsterone and androst-5-ene-3β,17β-diol (Adiol). Mean + SD values are plotted (n=1).

4.3.2 Androgen metabolism in borderline ovarian serous tumours

Only two borderline ovarian tumours (BOTs) were obtained for this investigation and both were Stage 1 serous BOTS. The steroid analysis data for these two specimens were combined for interpretation (**Figure 4.5**).

Following the addition of 100 nmol/L DHT to the serous BOTs there was a stepwise decrease to 22 nmol/L of DHT after 36h with a corresponding appearance of 21 nmol/L androsterone and a peak of 14 nmol/L in Adiol. Small amounts of 5α-dione (3 nmol/L) and androstenedione (1 nmol/L) were also observed after 36h. The remaining DHT was unaccounted for.

When the serous BOTs were incubated with 100 nmol/L 5a-dione, the concentration of 5α-dione decreased to 11 nmol/L after 36h with a simultaneous production of 27 nmol/L androsterone. A small amount of Adiol (2 nmol/L) was observed but the majority of 5α-dione loss was unaccounted for.

The addition of 100 nmol/L testosterone to the serous BOTs was observed with the concentration of testosterone falling to 70 nmol/L at the end of the time course with a corresponding appearance of 14 nmol/L androstenedione and very minimal amounts (<1nmol/L) of DHT and 5a-dione. The remaining testosterone loss was unaccounted for.

Finally, incubation of the serous BOTs with 100 nmol/L androstenedione was observed and the concentration of androstenedione decreased to 41 nmol/L after 36 h

with the corresponding appearance of 10 nmol/L testosterone, 8 nmol/L androsterone and approximately 3 nmol/L 5α-dione. The majority of androstenedione loss was again unaccounted for.

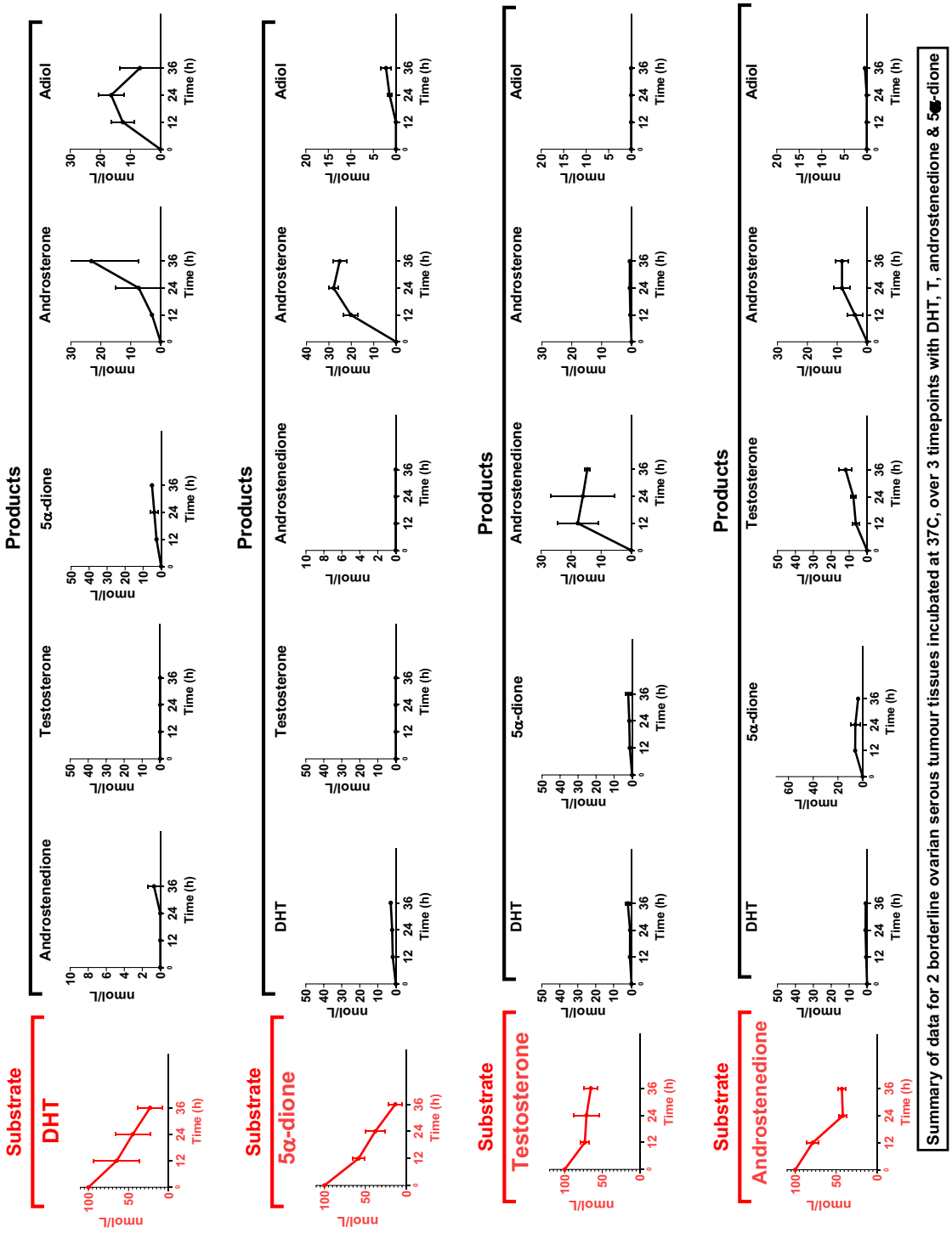

Fig. 4.5: Androgen metabolism in borderline ovarian serous tumours

The tumour samples from 2 patients (both Stage I, serous BOTs) were divided into 100 mg pieces and treated with four androgens at 100nmol/L for three separate time points to create a time course (12h, 24h and 36h). All experiments were performed in triplicate with serum-free media. Steroid analysis of the tumour media at each timepoint was performed by mass spectrometry. The decrease in the starting androgen is in red (left panel) is observed alongside

simultaneous synthesis of androstenedione, testosterone, dihydrotestosterone (DHT), 5α-androstanedione (5α-dione), androsterone and androst-5-ene-3β,17β-diol (Adiol). The mean and standard deviation values for both tumours are plotted.

4.3.3 Androgen metabolism in high grade serous ovarian carcinoma tumours

Six metastatic high grade serous ovarian carcinoma (HGSOC) tumour specimens were obtained for this investigation and treated with the four androgens at 100 nmol/L concentration. The steroid extraction data for these six specimens was combined to provide interpretation (**Figure 4.6**).

The incubation of the six HGSOC samples with 100 nmol/L DHT led to 98% of DHT lost after 36 h with a corresponding rise in 5α-dione, peaking at 28 nmol/L by 12h and then disappearing by 36h. Simultaneously, there was production of 4 nmol/L androsterone and 6 nmol/L of Adiol by the end of the time course.

Incubation of HGSOC with 100 nmol/L 5α-dione was observed with the concentration dropping to 26 nmol/L after 36h. The only metabolite detected was androsterone, measuring at 11 nmol/l by the end of the time course, thus the loss of 5a-dione was unaccounted for.

When the HGSOC samples were treated with 100 nmol/L testosterone, 99% of the testosterone was lost by 36h but there was corresponding synthesis of DHT, peaking at 30 nmol/L by 24h and then dropping to 15 nmol/L after 36h. 5α-dione production was noted at 10 nmol/L by 12h but then disappeared by 36 hours. Androstenedione production was also observed peaking at 4 nmol/L by 24h and then also disappearing at 36h. 6 nmol/L androsterone and 7 nmol/L of Adiol were observed at the end of the time course.

Finally, the addition of 100 nmol/L androstenedione to the HGSOC samples caused all the androstenedione to disappear by 36h but the biggest fall was seen in the first 12h. A corresponding peak rise of 42 nmol/L 5α-dione was observed at 24h and then dropped to 29 nmol/L by 36h. Testosterone appearance peaked at 27 nmol/L and then decreased to 6 nmol/L by the end of the time course. Androsterone production peaked at 12 nmol/L by 36h and 3 nmol/L Adiol was observed at the end of the experiment.

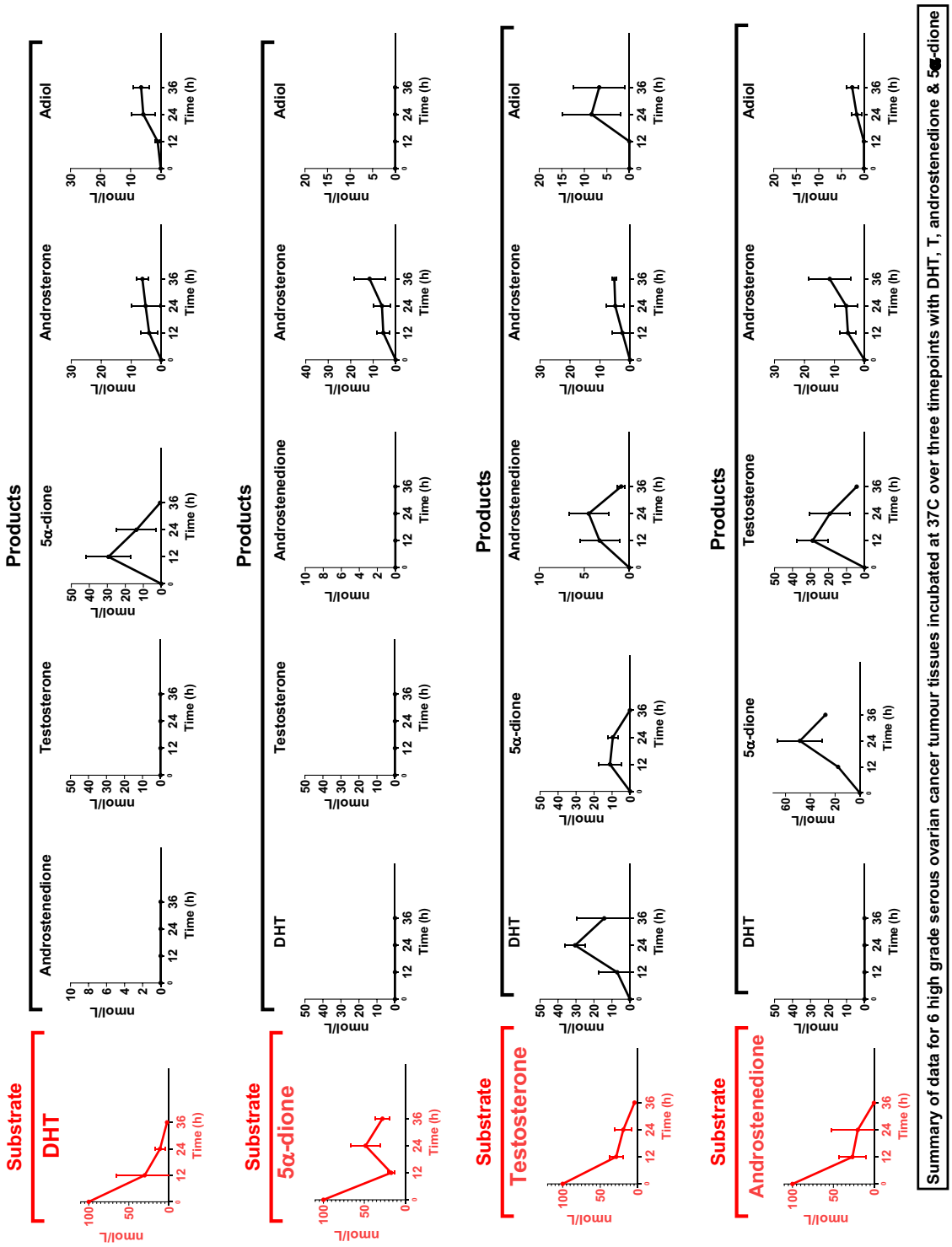

Fig. 4.6: Androgen metabolism in metastatic high grade serous ovarian cancer samples

The tumour samples from 6 patients were divided into 100 mg pieces and treated with four androgens at 100nmol/L for three separate time points to create a time course (12h, 24h and 36h). All experiments were performed in triplicate with serum-free media. Steroid analysis of

the tumour media at each timepoint was performed by mass spectrometry. The decrease in the starting androgen is in red (left panel) is observed alongside simultaneous synthesis of androstenedione, testosterone, dihydrotestosterone (DHT), 5α-androstanedione (5α-dione), androsterone and androst-5-ene-3β,17β-diol (Adiol). The mean and standard deviation values for the six tumours are plotted.

4.4 Discussion

In this study, benign, borderline and malignant serous ovarian tumours have been shown to perform androgen metabolism with generation of new steroid products which are also further metabolised. Benign and borderline serous tumours demonstrated modest androgen metabolism but high grade serous ovarian carcinoma in particular exhibited the most interesting steroidogenic behaviour. The overall picture of androgen metabolism seen in this study is depicted in **Figure 4.7**.

Overall, the small cluster of high grade serous ovarian carcinomas demonstrated avid consumption of the four androgen treatments (DHT, 5α-dione, testosterone and androstenedione) by the end of the 36h time course. The observed androgen metabolism activity would have been conducted by AKR1C2, AKR1C3, HSD17B2, HSD17B2, HSD17B4 and SRD5A1. Androstenedione stimulated very large rises in 5α-dione (42nmol/L) and testosterone (27nmol/L) by 12-24h. These were then subsequently converted to androsterone and Adiol at 36h. This demonstrates the importance of using successive timepoints to follow pathways, giving more detail to the steps in steroidogenic behaviour.

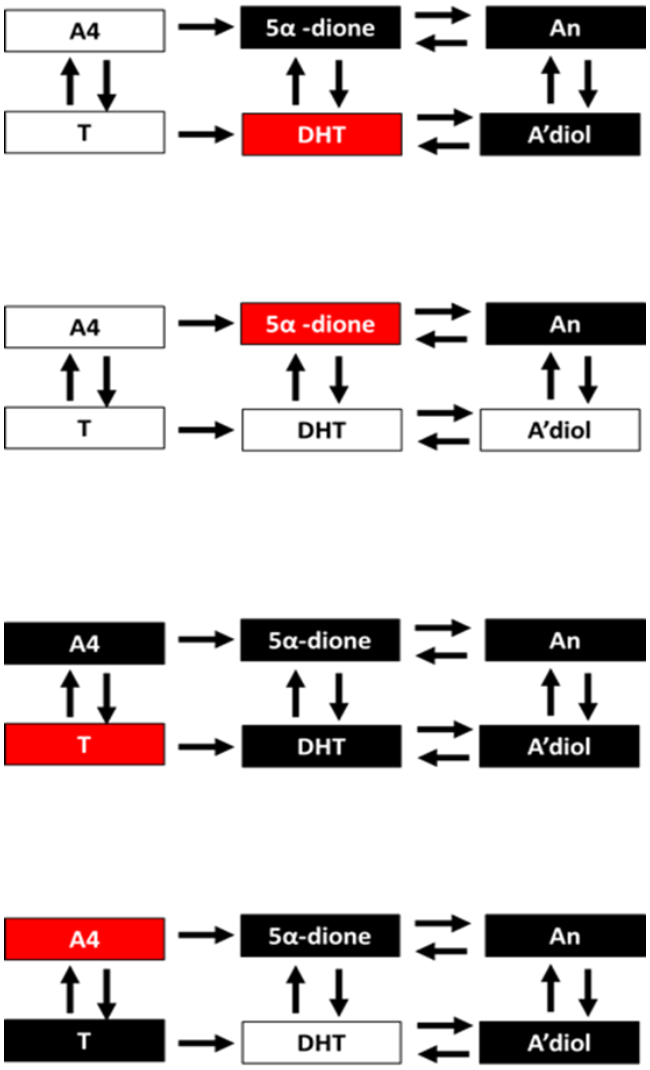

Fig. 4.7: Summary of the androgen metabolites observed after steroid treatment in six high grade serous ovarian cancers (*ex vivo*)

Starting substrate in red, downstream, products observed after 24h in black. A4= androstenedione, T = testosterone, An = androsterone, DHT = dihydrotestosterone, 5a-dione = 5a-androstanedione, A'diol/Adiol/3a-diol = androst-5-ene-3β,17β-diol

The results of the malignant ovarian tumour incubations also correlate with the cell line data described in **Chapter 3**; evidence of 5α-dione and androsterone production in the ovarian cancer cell lines is observed in these malignant tumours. The rise in 5α-dione and androsterone suggests again that the pathway of androgen metabolism is towards production of weaker androgens. If these malignant ovarian tumour tissues are actively

performing the steroidogenic conversions seen in the experiments, the same resulting metabolites may be forming a reservoir in patients, that could be exploited for diagnostic purpose. The production of androsterone by the tumour tissues is particularly encouraging as this metabolite can be confidently detected in urine samples by GC-MS (Arlt et al., 2011).

The results from the ovarian serous cystadenoma (benign) tumour showed consumption of DHT and testosterone but this was reciprocated by downstream steroid metabolism (**Figure 4.4**). Metabolism of DHT to Adiol was observed most likely indicating AKR1C2 activity. In the presence of testosterone, a small concentration of DHT was produced indicating SRD5A1 function, but it appears more testosterone was rapidly converted to 5α-dione and androstenedione which indicates activity of HSD17B2/B4 followed by SRD5A1 again. Upon treatment with androstenedione as the initial steroid, metabolism to 5α-dione was observed again.

Then, when 5α-dione was the selected steroid treatment, a large amount of androsterone production was observed during the time course indicating AKR1C2 activity again and demonstrating the capacity for further downstream steroid metabolism.

The results of the steroid analysis for the incubation of the borderline ovarian serous tumours also show decreases in the initial androgen concentrations and corresponding metabolites. The synthesis of androsterone appeared the most prominent steroid metabolite following treatment with DHT, 5α-dione and androstenedione. This also indicates SRD5A1 and AKR1C2 activity in serous BOTs are a characteristic but the low number of specimens limits any firm conclusion.

These results are novel as there are no publications describing the effects of exposing human ovarian tumours *ex vivo* to steroid treatments and observing the downstream metabolic changes. Only one previous study observed steroid production from ovarian tumours (benign and malignant) and normal ovaries after incubation (Ridderheim et al., 1993). That study commented that more progesterone and androstenedione was released from the tumours compared to the normal control ovaries and it was most marked in the malignant tumours which synthesised the largest amounts of these two hormones. Malignant ovarian tumour tissue released more steroids *per mg* tissue compared to benign tumour tissue and normal ovary. However, that study had several limitations. First, the pieces of tumour tissue were incubated for only 3h. Second, none of the tumours were treated with any steroids to observe if that influenced steroid synthesis. Third, only a few steroids were investigated (progesterone, androstenedione, testosterone and estradiol) and this was analysed by radioimmunoassay, which is very inaccurate for measuring steroids, especially estradiol. Finally, none of the results for the malignant tumours were analsyed according to histological subtype to characterise pathological differences.

In my study, many of these issues were addressed with three timepoints incorporated to allow for a longer period to observe steroid changes and follow downstream biosynthesis to reflect true tumour biology. The addition of steroids to the serum-free media was performed to magnify any characteristic steroidogenic behaviours by the tumours. Most importantly, mass spectrometry was used to search for more many more steroids eliminating the reliability issues of radioimmunoassay.

Limitations: The number of specimens that this investigation intended to possess did not materialise and the low sample numbers inhibit any firm conclusions. There were

several restrictions with tissue procurement described earlier in this chapter and there was also the difficult issue of navigating the proposed and then abandoned migration of the Cancer Centre itself. During this protracted phase of uncertainty, local ethics approval was denied and an application for NHS ethics had to be submitted. This was subsequently granted but a significant amount of time and opportunities to obtain tissues were lost. One criticism of the method that may not be avoidable is the use of plastic for the incubation of the tissues. Silanized glass vials are the preferred choice for holding media with steroids, as steroids tend to adhere to plastics. However, glass vials were not a safe option in the rotating hybridization incubator. It is inevitable that some of the unaccounted steroid losses were due to this method flaw. Tissues are also lipophilic and can retain steroids. The attempts to study the androgen metabolism in the metastatic omental metastases failed for this reason.

Due to limited tissue resources, the methods to release the steroids from the tissues were not explored. This difficulty may explain why few studies use tumour tissue for such experiments. Organoids may be an alternative option that may be more reliable and easier to work with (Hill et al., 2018) but I struggled with this method development. Another criticism is that Type 1 ovarian cancers were not examined in this study. The steroidogenic behaviour in clear cell, endometrioid and mucinous tumours may well be diverse. Finally, RT-qPCR gene expression was not performed in the tumour tissues due to COVID-19 laboratory restrictions and there were no normal ovarian tissues for comparison.

The method development phase was challenging in learning to examine tumour tissue for viability and ensuring the sampling is all from the same area. This was often difficult in the cancerous tissues but persistence led to adapting the method to and

troubleshooting such as avoiding saturation of the mass spectrometer and optimising the limits of quantification to work with tissue media. This study stands on its own as a first attempt at examining steroid production in *ex vivo* ovarian tumours with mass spectrometry. It also provides a method approach and template for future *ex vivo* ovarian tumour tissue incubations to explore steroid metabolism.

Chapter 5 Urinary steroid profiling as a novel diagnostic tool to detect and differentiate ovarian tumours

5.1 Introduction

In **Chapter 3**, androgens stimulated epithelial ovarian cancer cell lines to perform downstream steroid metabolism. In **Chapter 4**, *ex vivo* ovarian tumour tissues also demonstrated steroid metabolism in response to the same androgens. The next step is to explore the *in vivo* steroid metabolic changes in patients with benign, borderline and malignant ovarian tumours. This chapter summarises the evaluation of a novel approach of mass spectrometry-based urinary steroid profiling as a diagnostic tool for the detection of epithelial ovarian cancer.

Urine steroid metabolomics uses mass spectrometry to quantify several distinct steroids and their metabolites, followed by application of a machine learning algorithm to reveal steroid profile patterns that are diagnostic for a given condition. This novel biomarker tool was first described in a proof-of-principle study to differentiate between benign and malignant adrenocortical tumours (Arlt et al., 2011). They performed analysis of urinary steroid metabolite excretion on 24-hour collections with patients with benign and malignant adrenal tumours followed by machine learning analysis of the data, a combined approach they termed urine steroid metabolomics (USM). They found that a distinct subset of nine steroid metabolites indicated adrenal cancer with a sensitivity and specificity of 90% which is superior to the diagnostic value of imaging techniques such as CT, MRI, and PET scans (Arlt et al., 2011). They subsequently prospectively validated this new biomarker test for the differential diagnosis of adrenal tumours in an international multi-centre prospective test validation study, the EURINE-ACT study, which recruited more than 2000 patients with newly diagnosed adrenal tumours (Bancos et al., 2020). The proof-of-principle study 2011 employed gas chromatography-mass spectrometry (GC–MS) profiling, a powerful technique that is widely used for multi-targeted steroid analysis in biological samples (Arlt et al., 2011, Taylor et al., 2015). GC–MS data permits quantitative metabolite profiles to be directly compared between samples and utilized as metabolic biomarkers. It provides good specificity and reproducibility

in a wide range of applications and is coupled to sample pre-treatment and chromatographic separation steps to reduce biological complexity.

I have explained the close embryological relationship between the adrenal glands and the ovaries in **Chapter 1**. Therefore, it made logical sense to see whether benign and malignant ovarian tumours could be differentiated with steroid metabolome profiling, similar to the successful application of this approach to the differential diagnosis of benign and malignant adrenal tumours.

Attempts at utilising urinary steroid metabolites as a biomarker for ovarian cancer have made only twice before. In the first study, 1484 volunteer women provided 24h urine collections. After a median interval of 130 months, 12 of these women developed epithelial ovarian cancer and their pre-diagnosis samples were analysed by GC-MS for only 3 metabolites: DHEA, androsterone and etiocholanolone. While the authors claimed that low androgens might indicate ovarian cancer, the extremely small number of ovarian cancer patients did not allow statistically valid conclusions (Cuzick et al., 1983). In the second study, 15 post-menopausal women with epithelial ovarian cancer and 10 age-matched healthy women had their 24h urines analysed by GC-MS to search for 23 metabolites of progesterone, androgens and glucocorticoids. They found 9 urinary steroid metabolites at significantly higher concentrations compared to the healthy controls. These metabolites (in brackets) were derived from androgen precursors (DHEA, 16α-hydroxy-DHEA, androstenetriol), progesterone (pregnanediol, PD) and 17-hydroxyprogesterone (pregnanetriol, PT), and mineralocorticoid precursors (tetrahydro-11-dehydrocorticosterone (THA) and tetrahydrocorticosterone (THB)) (Bufa et al., 2008). However, no details were supplied regarding the clinical background of the patients, or absence of steroid medications, or the histology or stage of ovarian cancer. Therefore, only very limited conclusions can be drawn from this article.

In studies evaluating the risk of androgens with development of epithelial ovarian cancer, pre-diagnosis serum concentrations (obtained and stored at least 2 years before diagnosis) of testosterone and androstenedione were associated with an increased risk in endometrioid and mucinous tumours (which are Type 1 ovarian cancers), but not serous or clear cell (Ose et al., 2017). An inverse association was observed between androstenedione and high-grade serous cancers (Type 2 ovarian cancers). This suggests there are different associations between androgens and histologic subtypes of epithelial ovarian cancer, and this complements my *in vitro* results (**Chapter 3)**, however, this has not yet been explored adequately by urinary steroid profiling. The differences displayed in androgen metabolism I observed in *ex vivo* specimens from benign serous ovarian tumours, serous BOTs and serous ovarian carcinomas **(Chapter 4)** also directs towards investigation of this pattern in urinary samples to search for diagnostic biomarkers.

In this study, 24h urines were obtained from healthy controls and patients with benign, borderline and malignant epithelial ovarian tumours with **the aim to determine if urinary steroid profiling by GC-MS could define a steroid metabolite panel that could discriminate between them. I set out to test the hypothesis that ovarian cancers exhibit urinary steroid profiles that differ from benign ovarian tumours and may be distinct in Type 1 and Type 2 ovarian cancers and borderline ovarian tumours**.

5.2 Methods

5.2.1 Study population

Urine samples were collected from patients between 2017 and 2020 under HRA ethics (REC reference: 18/NE/0011, IRAS ID 225991) with informed consent. Patients were prospectively asked to provide a 24-hour urine collection before their surgery for suspected or confirmed

ovarian cancer or for benign gynaecological conditions.

The healthy control cohort included patients undergoing bilateral salpingo-oophorectomy as part of a hysterectomy for non-cancerous reasons (e.g., fibroids, pelvic organ prolapse); all of them had normal ovaries confirmed on histology (n=11). It also included healthy female nurses (n=21), who satisfactorily completed a health questionnaire and had a pelvic ultrasound scan that confirmed normal appearance of their ovaries and a normal CA125 test. From the 24h collection, a 20ml aliquot was transferred and stored as samples in a -20°C freezer. Urine samples that had been stored at -20°C from healthy female volunteers (University of Birmingham ethics approval ERN 17_0494) were also included in the study (n=33). These participants had also satisfactorily completed a health questionnaire but had not had a pelvic scan or CA125 test. A total of 65 healthy controls provided 24h urines for this study.

Urine from patients with ovarian tumours identified as either benign, borderline or epithelial cancer by final histological diagnosis were included in the analysis (**Figure 5.1**). Exclusion criteria for all participants were defined as a) used oral contraception / implant within the last 6 months, b) used HRT on GnRH analogues within last 3 months, c) used steroid treatment within last 3 months including inhalers and d) commenced chemotherapy.

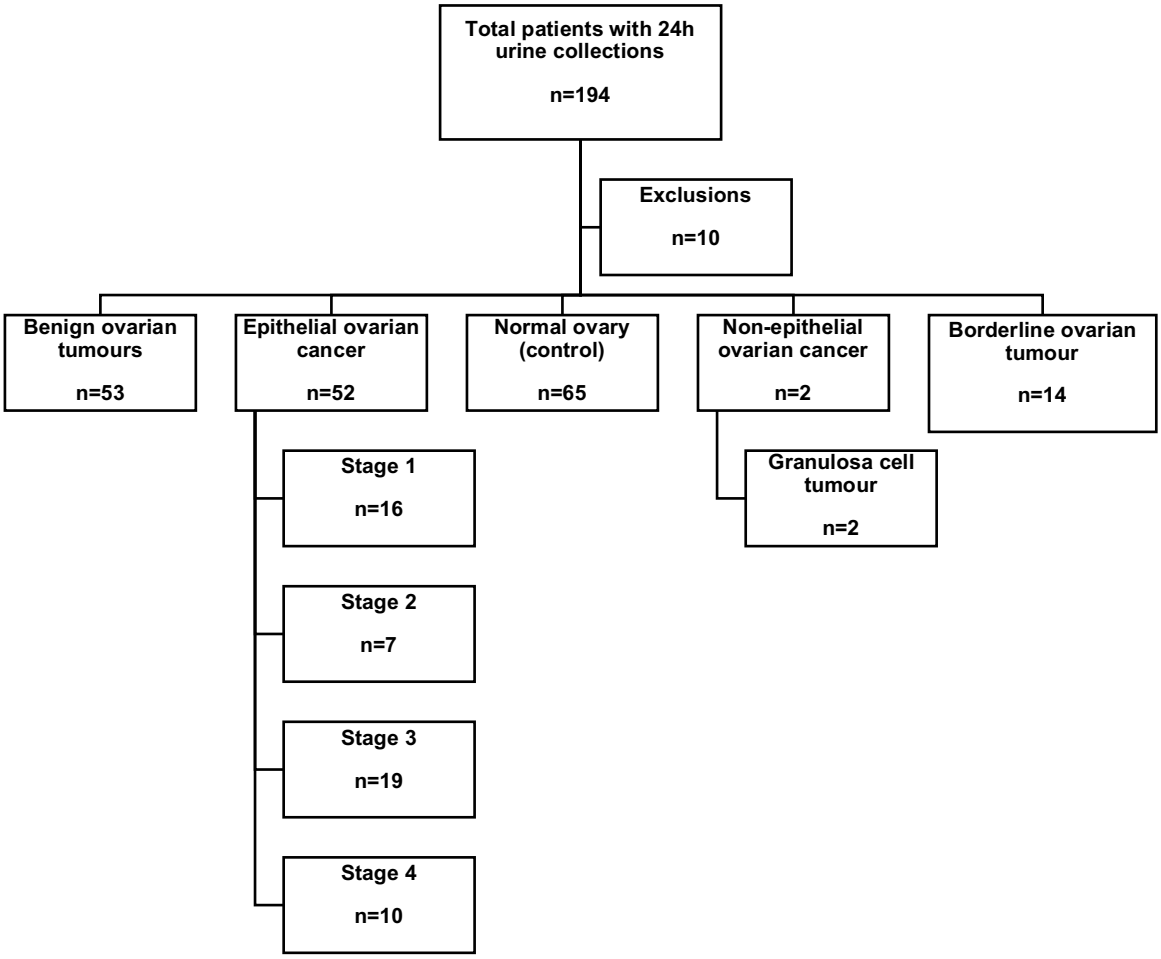

Fig. 5.1: Breakdown of participants providing 24h urine collections and their histological subtypes of ovarian tumours.

Non-epithelial ovarian cancers were excluded in this investigation.

Grouping of borderline ovarian tumours with malignant ovarian tumours

Borderline ovarian tumours (BOTs) are a pathological diagnostic dilemma and whilst they are of low malignant potential, they can form invasive or lethal recurrence. In clinical practice, total hysterectomy and bilateral salpingo-oophorectomy and infra-colic omentectomy with careful exploration of the abdominal cavity is the standard surgical procedure. The only exception is in women who have not fulfilled their reproductive wishes. As the consensus clinically is to manage patients with BOTs as at risk of higher rate of invasive recurrence, it is acceptable to

group the small number of BOTs in this study with the ovarian cancer cohort. **In this study, serous BOTs were grouped together with Type 2 ovarian cancers for analysis. The mucinous BOTs were combined with Type 1 ovarian cancers for analysis.**

5.2.2. Steroid extraction and analysis

Measurement of 24-h urinary steroid metabolite excretion from 184 women (n=52 with ovarian cancers, n=14 with borderline ovarian tumours, n=53 with benign ovarian tumours and n=65 healthy controls) (**Table 5.2**) was carried out by GC-MS, as described in **Chapter 2**.

To prepare samples for GC-MS analysis, free and conjugated steroids were extracted from 1ml urine by solid-phase extraction using SepPak C18 columns (Waters, Milford, Ma, USA). Columns were prepared by washes with 4 ml methanol (Sigma) and 4 ml double distilled water (ddH_2O). After sample loading, the columns were washed with 4 ml ddH_2O and steroids were eluted in 4 ml methanol in a clean boro-silicate tube. Samples were left to evaporate in a heat-block (55°C), aided by N_2 stream. The remaining dry samples (steroids) were incubated for 3 hours at 55°C in a hydrolysis buffer (3 ml 0.1M acetate buffer [pH 4.8-5.0] + 10 mg ascorbate + 200 units Helix pomatia (sulfatase/glucuronidase (all Sigma-Aldrich) to remove glucuronide and sulphate groups (deconjugation). Deconjugated steroids were subsequently reloaded onto SepPak columns and eluted into glass tubes with 4ml methanol. The final stage of sample preparation consisted of chemical derivatisation, to improve thermo-stability and volatility of sensitivity for mass spectrometry. To achieve this, samples were again evaporated and three drops of 2% methoxyamine-pyridine were added. After vortexing, tubes were incubated at 55°C for one hour, then evaporated under N_2. In the next step, 75 µl of N-trimethylsilylimidazole (Sigma-Aldrich) were added; tubes were vortexed again and incubated at 120°C overnight. Subsequently, samples were extracted by liquid-liquid extraction adding 2 ml cyclohexane and

2 ml ddH_2O, each step followed by vortexing. After centrifugation (1,000 x *g* for 5 minutes), the bottom aqueous layer was discarded. Another 2 ml ddH_2O were added, followed by the same sequence of vortexing and centrifugation. The top layer, which contained the extracted steroids in cyclohexane, was evaporated under N2 and reconstituted in 400µl cyclohexane before being transferred to injection vials. The samples were then injected into an Agilent 5975 GC mass-spectrometer operating in selected-ion monitoring (SIM) mode to achieve sensitive and specific detection and quantification of 32 selected steroid metabolites described in **Table 5.1.**

Table 5.1: Urine steroid metabolites as assessed by gas chromatography-mass spectrometry

No.	Abbreviation	Common Name	Chemical name	Metabolite of
Androgen metabolites				
1	An	Androsterone	5α-androstan-3α-ol-17-one	Androstenedione, testosterone, 5α-dihydrotestosterone
2	Etio	Etiocholanolone	5β-androstan-3α-ol-17-one	Androstenedione, testosterone
3	Total androgens	Sum of An + Et		
Androgen precursor metabolites				
4	11β-OH-An	11β-hydroxy-androsterone	5α-androstan-3α,11β-diol-17-one	Androsterone, 11-oxygenated androgens
5	11-oxo-An	11-oxo-androsterone	3α, 5α-3-hydroxyandrostane-11,17-dione	Androsterone, 11-oxygenated androgens
6	DHEA	Dehydroepiandrosterone	5-androsten-3β-ol-17-one	DHEA, DHEAS
7	16α-OH-DHEA	16α-hydroxy-DHEA	5-androstene-3β,16α-diol-17-one	DHEA, DHEAS
8	5-PT	Pregnenetriol	5-pregnene-3β,17-20α-triol	17-hydroxy-pregnenolone
9	5-PD	Pregnenediol	5-pregnen-3β,20α-diol and 5,17(20)-pregnadien-3β-ol	Pregnenolone
10	Total precursor androgens	Sum of: 11β-OH-An, DHEA, 16α-OH-DHEA, 5-PT , Sum 5-PD		

Mineralocorticoid and mineralocorticoid pre-cursor metabolites				
11	THA	Tetrahydro-11-dehydro-corticosterone	5β-pregnane-3α,21-diol-11,20-dione	Corticosterone, 11-dehydro-corticosterone
12	5α-THA	5α-tetrahydro-11-dehydro-corticosterone	5β-pregnane-3α,21-diol-11,20-dione	Corticosterone, 11-dehydro-corticosterone
13	THB	Tetrahydro-corticosterone	5β-pregnane-3α,11β,21-triol-20-one	Corticosterone
14	5α-THB	5α-tetrahydro-corticosterone	5α-pregnane-3α,11β,21-triol-20-one	Corticosterone
15	TH-DOC	Tetrahydro-11-deoxy-corticosterone	5β-pregnane-3α,21-diol-20-one	11-deoxy-corticosterone
16	3α5β-TH-aldo	Tetrahydro-aldosterone	5β-pregnane-3α,11β,21-triol-20-one-18-al	Aldosterone
Glucocorticoid precursor metabolites				
17	PD	Pregnanediol	5β-pregnane-3α,20α-diol	Progesterone
18	3α-5α-17HP	5α-17-hydroxy-pregnanolone	5α-pregnane-3α,17α-diol-20-one	Progesterone, 17-hydroxy-progesterone
19	17-HP	17-hydroxy-pregnanolone	5β-pregnane-3α,17α-diol-20-one	17-hydroxy-progesterone
20	PT	Pregnanetriol	5β-pregnane-3α,17α,20α-triol	17-hydroxy-progesterone
21	PTONE	Pregnanetriolone	5β-pregnane-3α,17α,20α-triol-11-one	21-deoxycortisol
22	THS	Tetrahydro-11-deoxycortisol	5β-pregnane-3α,17α,21-triol-20-one	11-deoxycortisol
Glucocorticoid metabolites				

23	F	Cortisol	4-pregnene-11β,17,21-triol-3,20-dione	Cortisol
24	6β-OH-F	6β-hydroxy-cortisol	4-pregnene-6β,11β,17,21-tetrol-3,20-dione	Cortisol
25	THF	Tetrahydro-cortisol	5β-pregnane-3α,11β,17,21-tetrol-one	Cortisol
26	5α-THF	5α-tetrahydro-cortisol	5α-pregnane-3α,11β,17,21-tetrol-one	Cortisol
27	α-cortol	α-cortol	5β-pregnane-3α,11β,17,20α,21-pentol	Cortisol
28	β-cortol	β-cortol	5β-pregnane-3α,11β,17,20β,21-pentol	Cortisol
29	11β-OH-Et	11β-hydroxy-etiocholanolone	5β-androstan-3α-11β-diol-17-one	Cortisol
30	E	Cortisone	4-pregnene-17α,21-diol-3,11,20-trione	Cortisol
31	THE	Tetrahydro-cortisone	5β-pregnene-3α,17,21-triol-11,20-dione	Cortisone
32	α-cortolone	α-cortolone	5β-pregnane-3α,17,20α,21-tetrol-11-one	Cortisone
33	β-cortolone	β-cortolone	5β-pregnane-3α,17,20β,21-tetrol-11-one	Cortisone
34	11-oxo-Etio	11-oxo-etiocholanolone	5β-androstan-3α-ol-11,17-dione	Cortisol, cortisone
35	Total glucocorticoids	Sum of all cortisol metabolites		Cortisol, cortisone

5.2.3 Statistical Analysis

Data analysis was performed using Stata Statistical Software: Release 16. College Station, TX: StataCorp LLC (2019). Graphical representation was performed using Graphpad Prism Software v9.3. Data are summarized as median (IQR) values unless otherwise stated. Comparisons between groups were made with linear regression models with adjustment for age, BMI and CA-125 value (at diagnosis).

5.3 Results

5.3.1 Patient characteristics

Through local and national recruitment, a total of 184 women provided a 24-hour urine sample (**Figure 5.1**). The healthy control group had a total of 65 women with a median age 52 years, a median BMI 24.9kg/m^2 and the median CA125 was 21 U/ml. All of these completed a health questionnaire satisfactorily and of these, 11 women (17%, all postmenopausal) had their ovaries removed for unrelated reasons as part of a hysterectomy and had normal ovaries confirmed by histology. There were also 21 (32%) women who had normal ovarian appearance on ultrasound scanning and a normal CA125 value. The remaining 33 (51%) female samples were obtained from the Institute of Metabolism & Systems Research, University of Birmingham. These 33 healthy control samples data have been checked by several endocrinologists at the University of Birmingham.

Histological diagnosis for all 119 patients with benign or malignant ovarian tumours were provided. The characteristics of all the study participants are summarized in **Table 5.2**. The benign ovarian tumour group consisted of 53 patients with a median age of 59 years, a median BMI 27kg/m^2 and median CA125 was 48.7 U/ml. There were 14 patients diagnosed with a

borderline ovarian tumour; their median age was 61 years, median BMI 26 kg/m^2 and median CA125 was 82 U/ml. Lastly, 52 patients with epithelial ovarian cancer were included. Their median age was 63.5 years, median BMI 27kg/m^2 and the median CA125 was 154 U/ml.

Table 5.2: Characteristics of included participants who donated a 24h urine sample (n=184)

	Healthy control n=65	**Benign ovarian tumours n=53**	**Borderline ovarian tumours n=14**	**Epithelial ovarian cancer n=52**
Age, years median (range)	52 (30-76)	59 (28-82)	61 (45-80)	63.5 (40-85)
BMI, kg/m2 median [IQR]	24.9 [23, 27.9]	27 [23.3, 32]	25.8 [24, 48]	27 [23, 31.9]
CA125 U/ml median [IQR]	21 [16.8, 44]	48.7 [11.5, 90.5]	82 [65, 278]	154 [51, 1058]
Post-menopausal (n)	41	42	11	45
Pre-menopausal (n)	24	11	3	7
Histological subtypes		Serous n=33 Mucinous n=6	Serous n=6 *Stage 1 n=5* *Stage 3 n=1* Mucinous n=8 *Stage 1 n=8*	High grade serous n=36 *Stage 1 n = 8* *Stage 2 n = 5* *Stage 3 n= 13* *Stage 4 n= 10* Mucinous n=5 *Stage 1 n=4* *Stage 3 n=1* Carcinosarcoma n=2 *Stage 2 n=1* *Stage 3 n=1*

		Endometrioid n= 9 Germ cell tumour n=5		Clear cell n=7 *Stage 1 n=4* *Stage 2 n=1* *Stage 3 n=2* Low grade serous n=2 *Stage 3 n=2*

5.3.2 Histological diagnosis of the ovarian tumours

Table 5.2 shows the histological composition of the included patients with an ovarian tumour. The largest proportion amongst the 53 benign tumours were serous (62%); followed by endometrioid tumours (17%), mucinous (11%) and germ cell tumours (9%, mature teratomas). Of the 14 borderline ovarian tumours, 6 were serous and 8 were mucinous; the majority were stage 1 (n=13, 93%). The greater proportion of the 52 epithelial ovarian cancers were high grade serous (69%) and almost two thirds of this subtype were advanced stage (III/IV). Grouping of the mucinous BOTs with the Type 1 and serous BOTs with Type 2 ovarian cancers for analysis was done and **Table 5.3** shows the baseline characteristics of the final groups for comparison analysis which were healthy control (n=65), benign ovarian tumour (n=53), Type 1 ovarian cancers and BOTs (n=22) and Type 2 ovarian cancers and BOTs (n=44).

Table 5.3: Groups for comparative analysis of urine steroid metabolites

	Healthy control n=65	**Benign ovarian tumour n=53**	**Type 1 ovarian cancers including BOTS n=22**	**Type 2 ovarian cancers including BOTs n=44**
Age, years median (range)	52 (30-36)	59 (28-82)	61 (45-80)	63.5 (40-85)
BMI, kg/m2 median [IQR]	24.9 [23, 27.9]	27 [23.3, 32]	25.8 [24, 48]	27 [23, 31.9]
CA125 U/ml median [IQR]	21 [16.8, 44]	48.7 [11.5, 90.5]	82 [65, 278]	154 [51, 1058]
Histological subtypes included		Serous, Mucinous, Endometrioid, Germ cell	*Clear cell cancer, Low grade serous cancer, Mucinous cancer, Mucinous BOT*	*High grade serous carcinoma, Carcinosarcoma, Serous BOT*

5.3.3 24-h urinary steroid metabolite excretion in women with healthy ovaries, benign ovarian tumours and Type 1 or 2 ovarian cancers including BOTS

Steroid metabolite excretion in 24-hour urine was measured by GC-MS in selected-ion-monitoring mode. Data for all 32 steroid metabolites was obtained and is presented in **Table 5.4.** Significant metabolites identified between the comparison groups is displayed in **Figure 5.3**. A series of quantitative comparisons were performed using a linear regression model with log transformation of the steroid metabolite concentrations and adjustment for age, BMI and CA125 values. All statistically significant results are collated and comparisons are presented.

Table 5.4: Comparison between benign ovarian tumours and ovarian cancers and BOTs with healthy controls

24h urine were analysed from the three groups of women (all-non treated) for 32 steroid metabolites. The metabolites were measured by gas chromatography-mass spectrometry selected ion-monitoring analysis. Median [interquartile range] 24-hour urinary steroid metabolite production (µg/24h) and p-values (significant in bold) are shown. The p-values (significant in bold) are given when comparing each ovarian tumour group (benign or epithelial cancers including BOTs) with the healthy controls using a linear regression model with the log transformed steroid metabolite as the outcome (adjusted for age, BMI and CA125 value). Significant steroid metabolites are coloured (pre-cursor glucocorticoid metabolites, yellow; glucocorticoid metabolites, orange; androgen metabolites, blue).

No.	Steroid metabolite	Healthy controls n=65	Benign ovarian tumours n=53	All cancers (Type 1 & 2 Ovarian cancers & BOTs) n= 66
		Median [IQR]	Median [IQR] p- value (vs controls)	Median [IQR] p-value (vs controls)
1	**An**	707 [312, 1124]	452.5 [230, 917] p=0.749	466 [236, 909] p=0.944
2	**Etio**	806 [437, 1250]	674 [390, 1252] p=0.868	751 [411, 1408] p=0.725
3	**Total androgens**	1451 [739, 2405]	1165 [612, 2151.5] p=0.807	1330 [682, 2368] p=0.761
4	**11β-OH-An**	353 [247,504]	545.5 [324.5, 866] p=0.171	520 [333, 765] p=0.529
5	**11-oxo-An**	20 [17, 27]	24 [16, 44] p=0.948	25 [18, 37] p=0.336
6	**DHEA**	134 [35, 391]	102 [51, 324] p=0.838	87 [36, 162] p=0.774
7	**16α-OH-DHEA**	154.5 [88, 360]	120 [52, 216] p=0.404	65 [33, 113] p=0.816
8	**5-PT**	104 [61, 177]	171 [93, 221.5] p=0.141	**168 [119, 319] p= 0.015**
9	**5-PD**	98 [62, 209]	110 [65, 178] p=0.116	**109 [78, 248] p=0.030**

10	**Total androgen precursors**	1022 [572, 1601]	1235 [638, 1859] p=0.203	1212 [687, 1580] p=0.355
11	**THA**	74 [54, 109]	84 [58, 119] p=0.945	89 [64, 124] p=0.870
12	**5α-THA**	59 [41, 82]	30.5 [21, 47] p=0.755	32.5 [24, 43] p=0.291
13	**THB**	83 [58, 118]	105 [66, 158.5] p=0.424	119 [72, 167] p=0.164
14	**5α-THB**	152 [106, 225]	76.5 [27, 298] 0.607	136 [47, 258] p=0.271
15	**TH-DOC**	11 [7, 17]	17 [9, 30] p=0.160	14 [10, 30] p=0.160
16	**3α5β-TH-aldo**	32 [24 , 41]	45 [27, 111] p=0.038	68.5 [32, 150] p=0.004
17	**PD**	149 [99, 282]	223 [94, 331] p=0.324	257 [126, 424] p=0.102
18	**3α-5α-17HP**	5 [4, 8]	7 [3, 19] p=0.233	**7 [4, 39] p=0.037**
19	**17-HP**	44 [26, 75]	65 [30, 140] p=0.251	**77 [47, 213] p=0.017**
20	**PT**	291 [188, 422]	301 [203, 568] 0.586	353 [244, 762] p=0.179
21	**PTONE**	8 [5, 11]	12 [6, 20] p=0.221	11 [7, 25] p=0.249
22	**THS**	53 [35, 70]	59 [37, 117] p=0.057	**70 [52, 110] p=0.021**
23	**F**	44 [33, 53]	77.5 [39, 122] p=0.442	84 [53, 120] p=0.192
24	**6β-OH-F**	100 [78, 127]	122 [54, 219] p=0.816	162 [102, 303] p=0.205
25	**THF**	1058 [789, 1415]	1437 [815, 2225] p=0.099	**1746 [1160, 2084] p=0.024**
26	**5α-THF**	752 [436, 1057]	808 [480, 1535] p=0.883	925 [498, 1387] p=0.873
27	**α-cortol**	205 [170, 283]	372 [220, 491] p=0.503	402 [263, 530] p=0.288

28	**β-cortol**	310 [245, 486]	448 [325, 592] p=0.894	458 [337, 675] p=0.722
29	**11β-OH-Et**	264 [127, 421]	270 [137, 443] p=0.811	286 [129, 428] p=0.629
30	**E**	72 [56, 85]	94 [58, 135] p=0.345	99 [66, 135] p=0.384
31	**THE**	2100 [1500, 2659]	1864 [1486, 3272] p=0.424	2117 [1571, 2889] p=0.570
32	**α-cortolone**	874 [651, 1146]	1136 [740, 1545] p=0.429	1127 [807, 1516] p=0.664
33	**β-cortolone**	424 [320, 545]	467 [319, 624] p=0.822	426 [282, 565] p=0.450
34	**11-oxo-Etio**	264 [141, 438]	148 [71, 293] p=0.732	158 [94, 281] p=0.440
35	**Total glucocorticoids**	6412 [5070, 8396]	7222 [5466, 11724] p=0.444	8320 [6621, 10506] p=0.433
Steroid metabolites did not differ between healthy controls and benign ovarian tumours. When all epithelial ovarian cancers(including BOTs) were compared to the controls, five steroid metabolites were identified as significantly increased in the affected group: 5-PT, 5-PD, 17-HP, THS and THF. Steroid no. 18 (3α -5α-17HP) was also identified as a significant steroid metabolite (p=0.037) in this analysis but its absolute values were considered too low to be certain of biological value.				

Steroid metabolites did not differ between healthy controls and benign ovarian tumours. Similarly, there were no differences comparing the steroid metabolites from benign ovarian tumours with malignant ovarian tumours only (BOTs excluded) (data not shown).

However, differences in urinary steroid metabolites were observed when comparing the healthy controls (n=65) with all epithelial cancer patients (Type 1,Type 2 ovarian cancers and BOTs (n=66)). Six steroid metabolites were identified as significantly increased in the cancer patients group compared to healthy controls: 5-PT, 5-PD, 3α-5α-17HP, 17-HP, THS and THF (**Table 5.5**). 5-PT and 5-PD are androgen pre-cursor steroid metabolites derived from 17-hydroxy-pregnenolone and pregnenolone respectively. 3α-5α-17HP and 17-HP are both

metabolites of 17-hydroxy-progesterone whilst THS, is a metabolite of 11-deoxycortisol; all are glucocorticoid pre-cursor metabolites. THF is a glucocorticoid metabolite of cortisol (**Figure 5.5**).

In the next analysis, I investigated whether steroid metabolites differed between healthy controls and Type 1 (including serous BOTs) or Type 2 cancers (including mucinous BOTs) separately. Steroid metabolites did not differ between Type 2 ovarian cancer group compared to healthy controls (data not shown) or compared to the benign ovarian tumour group (**Table 5.5**). However, when urinary steroid metabolites for Type 1 ovarian cancer group (n=22) were compared with the patients with benign ovarian tumours (n=53), five steroid metabolites were found to be significantly increased in the Type 1 ovarian cancers group: 5-PT (p=0.015), 5-PD (p=0.009) PD (p=0.008), 17-HP (p=0.005) and PT (p=0.006) (**Table 5.5**).

A non-statistically significant trend was observed. Etiocholanolone (Et) and the total androgen metabolites (Androsterone + Etiocholanolone) were increased in the Type1 ovarian cancers group compared to the benign ovarian tumours group (Et p=0.067, total androgen metabolites p=0.094) (**Figure 5.2**). This non-significant trend was repeated for these androgen metabolites when comparing Type 1 ovarian cancers with the healthy controls group (**Figure 5.2**).

Urinary steroid profiling revealed three significantly increased metabolites in the Type 1 ovarian cancers group compared to Type 2 ovarian cancers group: 5-PT (p=0.048), 5-PD (p=0.006) and 17-HP (p=0.040) **(Table 5.5).** Again, a non-statistically significant trend was observed for etiocholanolone and the total androgen metabolites where Type 1 ovarian cancers possessed the higher absolute values and medians for etiocholanolone (p=0.06) and the total androgen metabolites (p=0.106) compared to Type 2 ovarian cancers .

In addition, Type 2 ovarian cancers had lower medians for all androgen metabolites and androgen pre-cursor metabolites compared to both benign ovarian tumours and the Type 1 ovarian cancers, but this was non-statistically significant (**Table 5.5**).

Table 5.5: Summary of 24h urinary steroid metabolites in patients with benign, Type 1 and Type 2 ovarian cancers

Median [interquartile range] 24-hour urinary steroid metabolite production (µg/24h) and p-values are shown; metabolites measured by gas chromatography-mass spectrometry selected ion-monitoring analysis in 24-h urines collected by women prior to surgery.

The p-values (**significant in bold**) are given when comparing type 1 and 2 ovarian cancers (including BOTs) individually against benign ovarian tumours using a linear regression model with the log transformed steroid metabolite as the outcome (adjusted for age, BMI and CA125 value).

The p-values for the comparison between type 1 cancers including mucinous BOTs against type 2 cancers including serous BOTs is in italic (***significant in bold italic).*** Only three metabolites were significant in this final comparison (glucocorticoid precursors metabolites, yellow , androgen precursor metabolites, blue)

No.	**Abbreviation**	**Benign tumours n=53**	**Type 1 cancers (including mucinous BOTs) n=22**	**Type 2 cancers (including serous BOTs) n=44**
		Median [IQR]	Median [IQR] p-value (vs benign) *p-value (vs Type 2 & serous BOTS*)	Median [IQR] p-value (vs benign)
1	**An**	452.5 [230, 916.5]	675 [262, 1058] p=0.98 *p=0.42*	408 [231, 792] p=0.30
2	**Etio**	674 [390, 1251.5]	1311 [524, 2092] p=0.067 *p=0.06*	570 [375, 1076] p=0.951
3	**Total androgens**	1164.5 [612, 2151.5]	2115 [890, 2675] p=0.094 *p=0.106*	978 [613, 1600] 0.816

4	**11β-OH-An**	545.5 [324.5, 866]	519 [339, 788] p=0.318 *p=0.786*	521 [318, 765] p=0.182
5	**11-oxo-An**	24 [16, 44]	24 [19, 29] p=0.082 *p=0.429*	28 [18, 44] p=0.261
6	**DHEA**	102 [50.5, 323.5]	128 [48, 202] 0.672 *p=0.577*	72 [35, 149] p=0.309
7	**16α-OH-DHEA**	120 [52, 216]	83 [33, 176] p=0.178 *p=0.844*	57 [35, 107] p=0.071
8	**5-PT**	171 [93, 221.5]	294 [122, 504] **p=0.015** ***p=0.048***	150 [106, 233] p=0.461
9	**5-PD**	110 [65, 178]	195 [108, 547] **p=0.009** ***p=0.006***	97 [65, 163] p=0.991
10	**Total precursor androgens**	1235 [638, 1858.5]	1527 [737, 1845] p=0.921 *p=0.229*	950 [668, 1316] p=0.302
11	**THA**	84 [58, 119]	89 [45, 122] *p=0.465* *p=0.162*	88 [65, 131] p=0.349
12	**5α-THA**	30.5 [21, 47]	26 [17, 43] p=0.998 *p=0.144*	37 [26, 46] p=0.076
13	**THB**	105 [66, 158.5]	133 [62, 170]	114 [76, 167]

			p=0.865 *p=0.506*	p=0.231
14	**5α-THB**	76.5 [27, 298]	65 [26, 211] p=0.309 *p=0.05*	137 [59, 293] p=0.049
15	**TH-DOC**	17 [9, 30]	24 [14, 77] p=0.111 *p=0.09*	13 [9, 19] p=0.268
16	**3α5β-TH-aldo**	45 [27, 111]	71 [29, 116] p=0.567 *p=0.526*	68 [36, 174] p=0.136
17	**PD**	223 [94, 330.5]	413 [251, 1150] **p=0.008** ***p=0.002***	207 [105, 323] p=0.850
18	**3α-5α-17HP**	7 [3, 19]	14 [5, 43] P=0.120 *p=0.535*	6 [3, 17] p=0.289
19	**17-HP**	65 [30, 140]	176 [74, 385] **p=0.005** ***p=0.040***	65 [36, 96] p=0.236
20	**PT**	301 [202.5, 568] 0.586	663 [418, 1267] **p=0.006** ***p=0.008***	268 [190, 525] p=0.880
21	**PTONE**	11.5 [6, 20]	10 [5, 20] p=0.370 *p=0.201*	11 [7, 26] p=0.731
22	**THS**	59 [37, 117]	64 [45, 85] p=0.512 *p=0.083*	77 [57, 115] p=0.194

23	**F**	77.5 [39, 122]	79 [45, 120] p=0.718 *p=0.152*	84 [58, 122] p=0.148
24	**6β-OH-F**	122 [54, 218.5]	216 [86, 359] p=0.285 *p=0.653*	150 [102, 241] p=0.076
25	**THF**	1437 [814.5, 2224.5]	1765 [1111, 2024] p=0.609 *p=0.755*	1725 [1160, 2185] p=0.305
26	**5α-THF**	807.5 [479.5, 1535]	781 [401, 1298] p=0.442 *p=0.220*	1042 [498, 1754] p=0.644
27	**α-cortol**	371.5 [219.5, 490.5]	347 [233, 476] p=0.438 *p=0.05*	406 [308, 547] p=0.171
28	**β-cortol**	447.5 [324.5, 592]	487 [367, 675] p=0.288 *p=0.519*	440 [328, 696] p=0.591
29	**11β-OH-Et**	270 [136.5, 442.5]	276 [192, 428] p=0.920 *p=0.837*	323 [122, 493] p=0.739
30	**E**	93.5 [57.5, 135]	92 [55, 125] p=0.273 *p=0.194*	105 [66, 141] p=0.702
31	**THE**	1863.5 [1486, 3271.5]	2126 [1376, 2984] p=0.634 *p=0.912*	2108 [1571, 2740] p=0.741
32	**α-cortolone**	1135.5 [740, 1544.5]	941 [695, 1516]	1193 [837, 1553]

			p=0.210 *p=0.266*	p=0.851
33	**β-cortolone**	465.5 [319, 623.5]	441 [282, 551] p=0.554 *p=0.749*	411 [261, 590] p=0.328
34	**11-oxo-Etio**	148 [70.5, 293]	140 [110, 229] p=0.488 *p=0.914*	170 [93, 307] p=0.545
35	**Total glucocorticoids**	7222 [5465.5, 11723.5]	8934 [5086, 10290] p=0.636 *p=0.506*	8158 [6743, 11105] p=0.796

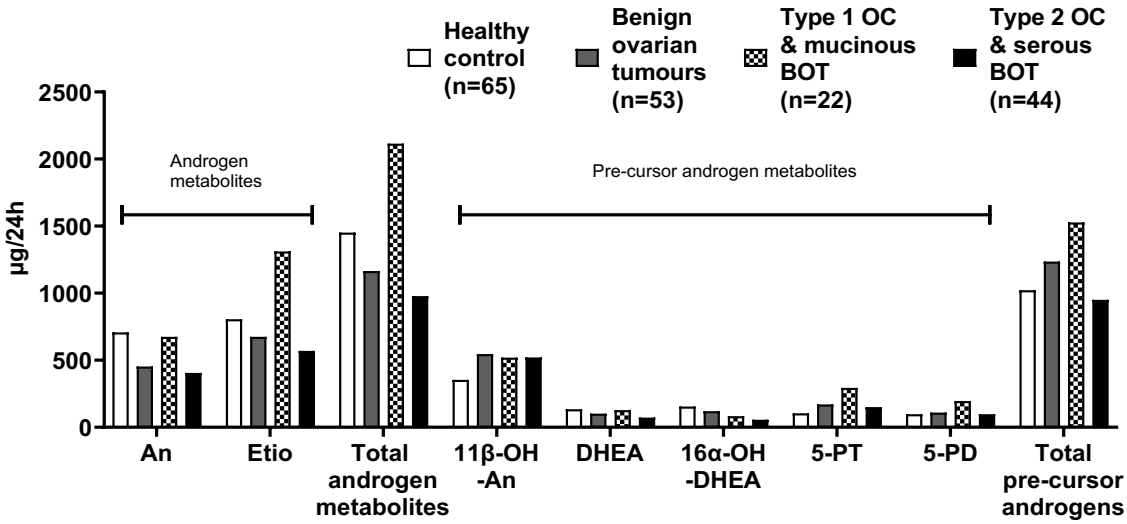

Fig 5.2: 24h urinary androgen metabolites in patients with normal ovary, benign ovarian tumours, and Type 1 and 2 ovarian cancers including BOTs

Median metabolite values (µg/24h) shown; measured by gas chromatography-mass spectrometry in 24-h urines collected by healthy controls and untreated patients. Histology was confirmed after surgery. Type 1 ovarian cancers (chequered bars), Type 2 ovarian cancers (black bars). Total androgen metabolites and total pre-cursor androgens were higher in Type 1 ovarian cancers and mucinous BOTs compared to the other three groups.

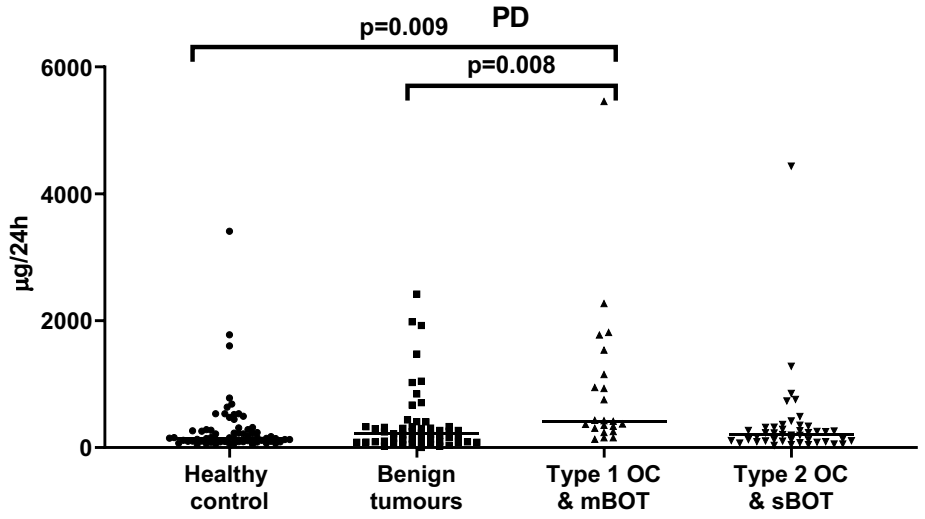
PD
p=0.009
p=0.008
6000
4000
2000
0
µg/24h
Healthy control
Benign tumours
Type 1 OC & mBOT
Type 2 OC & sBOT

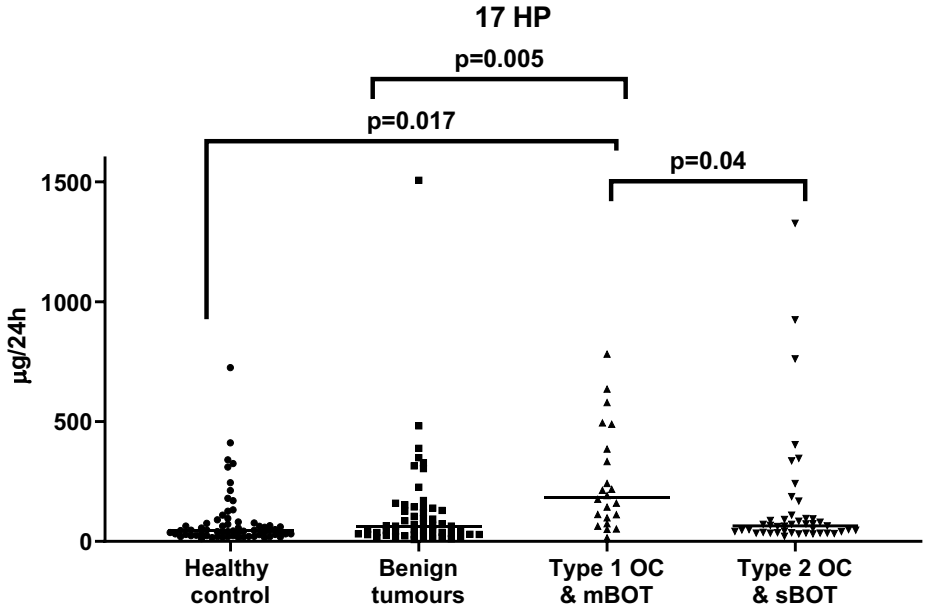
17 HP
p=0.005
p=0.017
p=0.04
1500
1000
500
0
µg/24h
Healthy control
Benign tumours
Type 1 OC & mBOT
Type 2 OC & sBOT

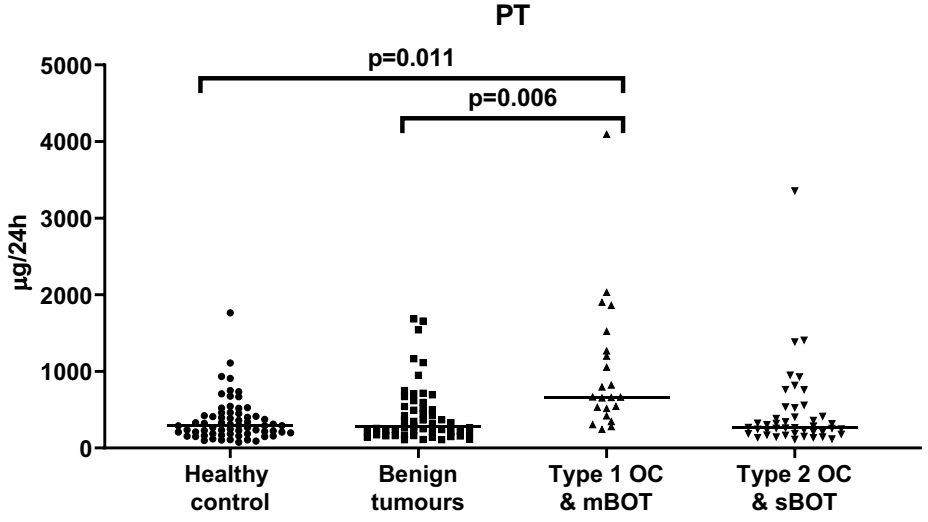
PT
p=0.011
p=0.006
5000
4000
3000
2000
1000
0
µg/24h
Healthy control
Benign tumours
Type 1 OC & mBOT
Type 2 OC & sBOT

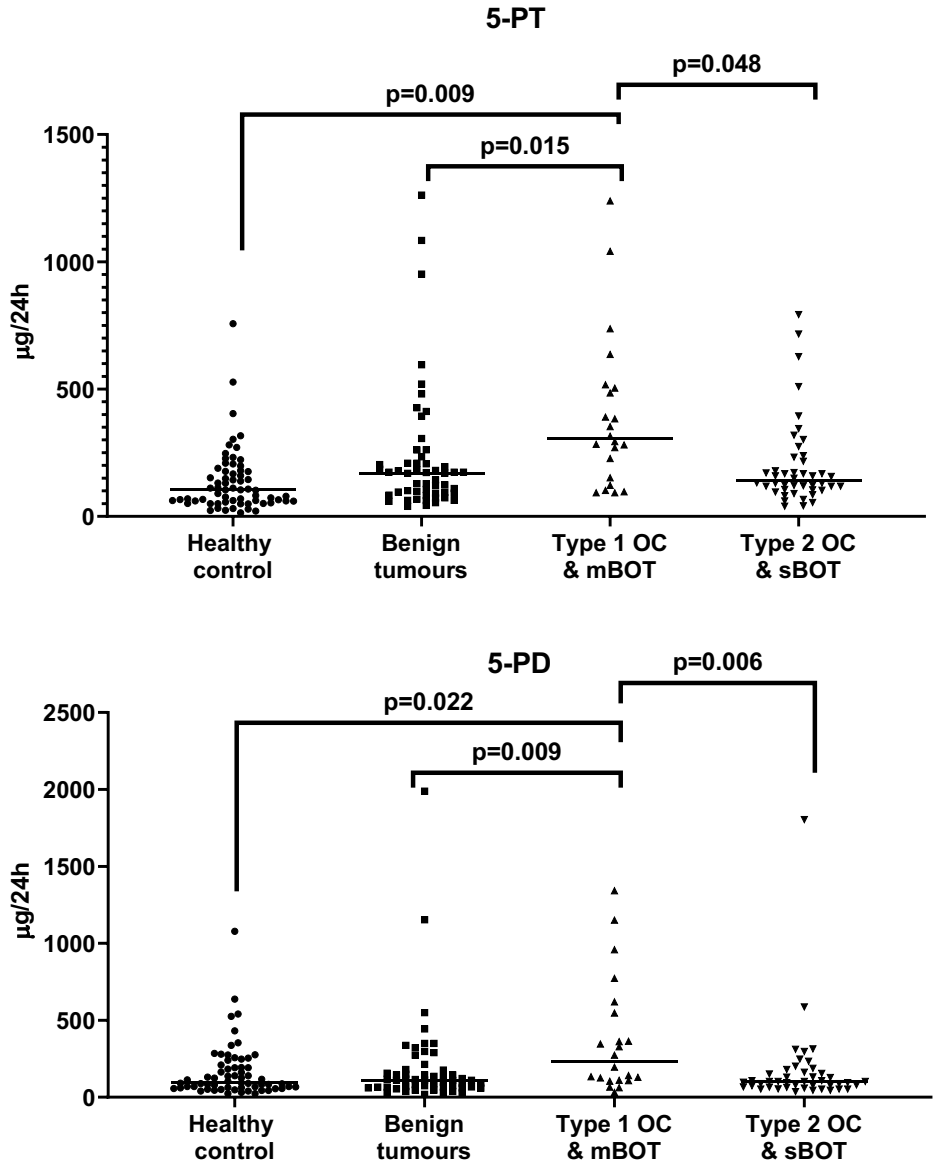

Fig 5.3: Graphical representation of 24-hour urinary steroid metabolite excretion in women with benign, Type 1 and Type 2 ovarian cancers and healthy controls.

24-hour urine collections were obtained from the four groups (pre-treatment) and analysed for 32 steroid metabolites using GC-MS. Type 1 OC group consists of fourteen type 1 ovarian cancers and eight mucinous BOTs. Type 2 OC group consists of thirty-six high grade serous ovarian cancers, two carcinosarcomas and six serous BOTs. Healthy controls n=65, benign ovarian tumours n=53. Five metabolites were found to differentiate Type 1 OC from the other groups (5-PT, 5-PD, PD, 17-HP and PT). The data for these is graphically displayed. For each steroid metabolite, each dot represents the absolute value from an individual patient and the line represents the median. Comparisons between the four groups were made with linear regression models to adjust for age, BMI and CA125 values and the significant p-values are displayed. (PD = pregnanediol, 17-HP = 17-hydroxy-pregnanolone, PT= pregnanetriol, 5-PT = pregenentriol, 5-PD = pregnenediol).

The urinary steroid excretion profile for the patients with Type 1 ovarian cancers differ distinctly from the benign, Type 2 ovarian cancers and healthy control groups. Type 1 ovarian cancer patients had a significantly higher excretion of androgen precursor metabolites (5-PT and 5-PD) when compared to all the other groups. Though the absolute values and medians for etiocholanolone, a metabolite of androstenedione and testosterone, was observed to be consistently the highest in Type 1 ovarian cancer, it was non-statistically significant when compared to the benign tumours ($p=0.06$) and Type 2 cancers groups ($p=0.067$).

Amongst the glucocorticoid precursor metabolites, 17-HP was significantly higher in the urinary steroid profile for Type 1 ovarian cancers when compared to all groups whilst PD and PT were significantly higher in the profile for Type 1 ovarian cancers when compared to the benign tumours.

Tetrahydrocortisone (THF), a glucocorticoid metabolite, was increased significantly in the comparison between Type 1 and Type 2 ovarian cancers including BOTs with the healthy controls (**Table 5.4**) but not compared to the benign tumours. Furthermore, when Type 1 and Type 2 cancers and BOTs were separated, THF did not remain a statistically significant metabolite. There was no statistical difference between the groups for total glucocorticoids, mineralocorticoids and total precursor androgen metabolites.

I further investigated the Type 1 ovarian cancers by correlating the histology and steroid metabolites in patients' levels who were outliers in the dot-plot graphs (**Figure 5.3**). Of the Type 1 ovarian cancers including mucinous BOTs, no steroid metabolite differences were seen in patients with clear cell or low grade serous ovarian cancer (data not shown). However, distinct differences in steroid metabolites were seen in 3 out of 5 mucinous ovarian carcinomas and 4 out of 8 mucinous BOTs.

5.3.4 Mucinous ovarian cancers and BOTs exhibit a distinct steroid profile

I identified all steroid metabolites that were >75th and >95th centiles of the healthy controls and

found that the majority of these were 5-PT, 5-PD, PD, 17-HP and PT and they were consistently elevated in mucinous BOTs and mucinous carcinomas. The group, Type 1, comprised of 22 tumours, of which 13 were mucinous. . The median excretion values for these steroid metabolites were elevated above the 95th centile in either the mucinous BOTs or mucinous carcinomas or both. Next, I investigated the values of the steroid metabolites in all the mucinous ovarian tumours (mucinous benign n=6, mucinous BOT n=8, mucinous cancer n=5). Of the five mucinous cancers, four were infiltrative subtype and one was expansile subtype). The data for the five identified metabolites plus the androgen metabolites androsterone and etiocholanolone were plotted **(Figure 5.4**).

The five significant urinary steroid metabolites show an incremental alteration from benign mucinous ovarian tumour to mucinous BOT and then to mucinous ovarian cancer. Hence, there is a possibility that steroid metabolism is a pathognomic feature of the development of mucinous benign, mucinous BOTs and mucinous ovarian cancer (**Figure 5.4**). Statistical analysis with the student's *t* test confirmed a significant increase for all five urinary metabolites from the healthy controls compared to each mucinous tumour subtype (for benign, BOT and cancer, all $p<0.05$) but the numbers of specimens are small; a limitation of investigating mucinous tumours.

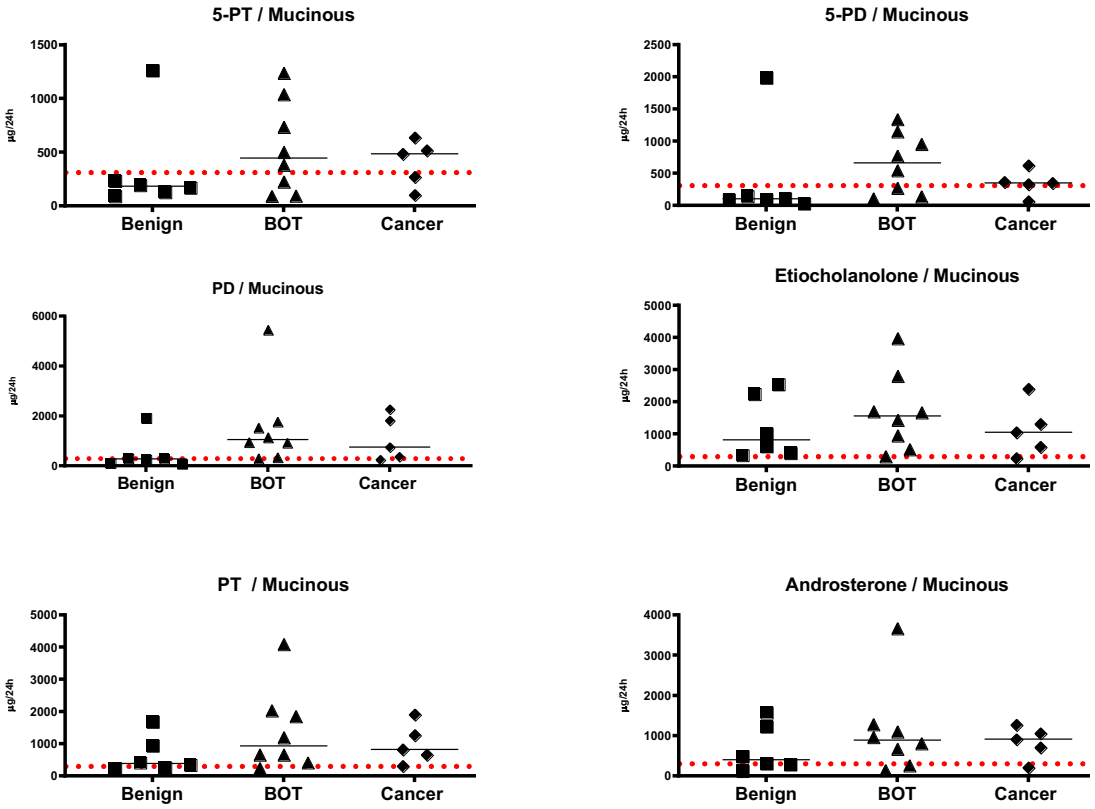

Fig. 5.4: 24h urinary steroid metabolite excretion for androsterone, etiocholanolone, 5-PT, 5-PD, PD, and PT in 19 mucinous ovarian tumours (benign n=6, borderline n=8 and malignant =5) measured by GC-MS.

The 95th centile values (red dotted line) for these metabolites in the healthy controls is shown for reference. The black markers are the individual metabolite values and the black solid line is the median for each tumour status. Here, the concentrations of these metabolites in mucinous ovarian tumours exceed the 95th centile compared to healthy controls and with some demonstrating incremental elevation from benign ovarian tumour to borderline ovarian tumour (BOT) to mucinous cancer. Student's t test performed between each tumour type and healthy controls consistently showed statistical significance ($p<0.05$).

5.4 Discussion

This is the very first comprehensive human study performing urine steroid profiling with mass spectrometry for a variety of subtypes of epithelial ovarian cancer. I examined 32 steroid metabolites in 24h urine collections from patients with epithelial ovarian cancer, borderline ovarian tumours and benign tumours and healthy controls. This study has therefore considered the spectrum of epithelial ovarian neoplasms which is typical of clinical practice, but often

overlooked in many studies.

I found that steroid metabolites were elevated in the group comprising all cancer histology types (including BOTs) compared to healthy controls. Then I identified that when compared to benign tumours, the difference in steroid metabolite profile persisted only in a comparison between benign tumours and Type 1 cancer (including mucinous BOTs) whereas no difference in steroid metabolites were seen between benign tumours and Type 2 group.

Of the 32 steroid metabolites investigated, 5 steroid metabolites, **(**5-PT, 5-PD, PD, 17-HP and PT) show a statistically significant elevation in the Type 1 cancer group compared to benign and healthy controls. I found that the median values of these metabolites in the Type 1 group were above the 95th centile of the median values in the healthy controls. Finally, I investigated the levels of these 5 steroid metabolites across benign mucinous tumours, mucinous BOTs and mucinous cancers and found that three of these are progressively elevated with advancing ovarian neoplastic status. This has parallels with the genetic changes in mucinous cancer pathogenesis suggesting that steroid metabolites maybe involved in the aetiopathogenesis of mucinous cancer.

At the outset, the main aim was to provide proof-of-concept for urine steroid profiling as a novel detection tool for epithelial ovarian cancer that would represent a significant advance in patient screening and stratification. However, I have not found evidence in this study to show that urinary steroid profiling can detect high grade serous ovarian cancer (HGSOC) and serous BOTs. HGSOC is the most common form of the disease and accounts for over 70% of all ovarian cancer cases. In **Figure 5.2,** I did note that there was a trend for Type 2 ovarian cancers including the serous BOTs to have lower median values for the androgen metabolites

compared to all other ovarian tumour types and healthy controls. This non-statistical finding may pair with a study evaluating the risk of androgens with development of epithelial ovarian cancer. In serum samples from women, taken at least 2 years prior to their ovarian cancer diagnosis, their concentrations of androstenedione were shown to have an inverse association with high-grade serous ovarian cancer (Type 2) (Ose et al., 2017). Therefore, in this study, whilst Type 2 ovarian cancers are capable of androgen synthesis (*in vitro* and *ex vivo*) the mechanisms linking androgen concentrations to high grade serous ovarian cancer *in vivo* remains unclear.

However, an unexpected discovery was the potential role for urinary steroid profiling for mucinous ovarian BOTs and mucinous ovarian cancer. The comparison between Type 1 tumours and benign tumours revealed five significant steroid metabolites. Of the 22 included patients in the Type 1 group, 5 had mucinous ovarian cancer and 8 patients had mucinous BOT. All these histology reports have been re-reviewed by a team of specialist gynaecological cancer pathologists at University of Birmingham to confirm the diagnosis. The number of specimens of the mucinous type in this study is small but in our patient recruitment, 5 out of 66 (7.6%%) patients had a mucinous cancer which is higher than the quoted prevalence of 3% (Morice et al., 2019).

The five steroid metabolites, 5-PT, 5-PD, PD, 17-HP and PT were all consistently observed in mucinous BOTs and mucinous carcinomas. No difference in the steroid concentrations were observed according to stage of disease for mucinous ovarian cancer.

Furthermore, the mucinous BOTs appeared to trend with the highest absolute values for these select steroid metabolites. The median excretion values in the mucinous BOTs were elevated above the 95th centile control value for 4 out of 5 of the panel of steroid metabolites. This

suggests that mucinous BOTs exhibit dysregulation in steroidogenesis which could be utilised as a biomarker and that steroidogenic dysregulation may play a role in mucinous carcinogenesis.

Of clinical benefit, these five steroid metabolites may be able to differentiate mucinous carcinomas and BOTs against other ovarian malignant and benign tumour types. At present, clinicians often employ invasive investigations to distinguish a primary mucinous tumour from metastatic disease to the ovary (Krukenberg tumour) (Morice et al., 2019) . This typically involves ruling out a gastrointestinal primary cancer and requires the patient to undergo colonoscopy and upper gastrointestinal endoscopy. The prospect of a non-invasive urinary steroid profiling test as a substitute would be highly beneficial in such cases. Urinary steroid profiling could also be potentially used for post-operative surveillance of patients after surgery for mucinous BOTs and mucinous ovarian cancers.

Currently the treatment options for women with mucinous ovarian cancer are limited. There is a lack of clear evidence from RCTs evaluating adjuvant chemotherapy in early-stage mucinous cancer, hence surgery alone is recommended for stage 1 mucinous ovarian cancer and adjuvant chemotherapy reserved for stage 2 or advanced patients (Morice et al., 2019). The results in this study suggests that there may be a potential utility of drugs that target the early steps in steroid synthesis (**Figure 5.5**) for women with a recurrent mucinous ovarian cancer after surgery as current therapeutic options are extremely limited for those patients. Blocking the early pathway could slow down the progression of a recurrence, while aldosterone and cortisol could be replaced by drugs that already treat adrenal insufficiency.

Whilst the risk of recurrence is lower than in Stage I serous ovarian cancers (6% vs 20%), patients with mucinous ovarian cancer require close surveillance, but a suitable method of imaging and frequency pattern for this surveillance is very unclear. A quarter of mucinous

ovarian cancer patients are under 44 years old, so they may have received a unilateral salpingo-oophorectomy and these too require close monitoring (Morice et al., 2019). For Stage I mucinous BOTs, the understanding of treatment and surveillance patterns is even more uncertain (Hannibal et al., 2020). Hence research into how mucinous tumours develop and progress is needed which may potentially unlock therapeutic options. Meanwhile, there could be potential benefits of urinary steroid metabolite profiling for post-operative surveillance in such patients; it is non-invasive hence it can be performed more frequently.

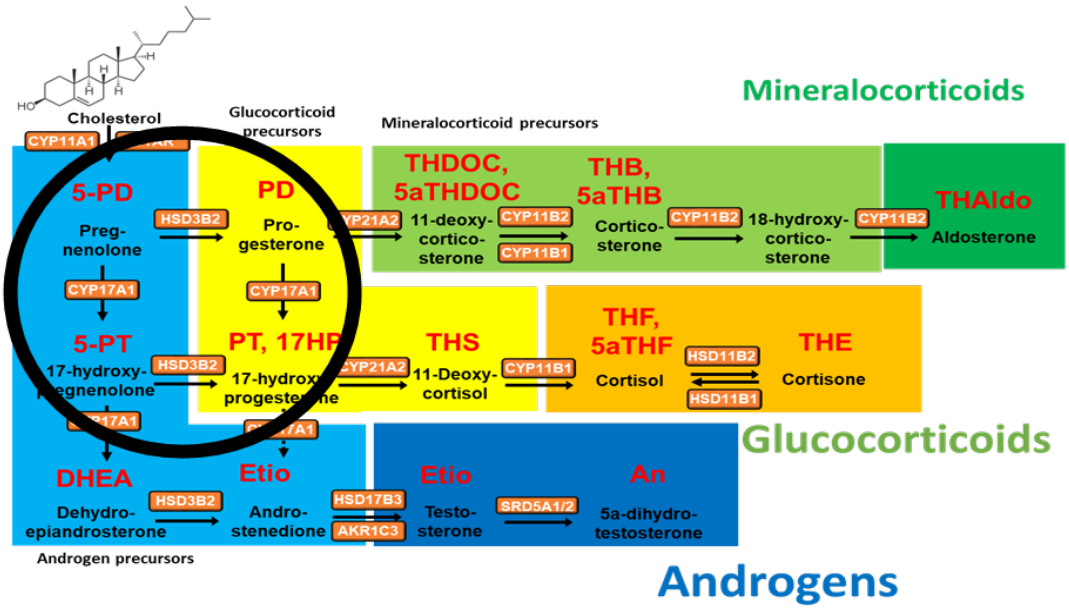

Fig. 5.5: Identification of the five urinary steroid metabolites from in Type 1 ovarian cancers and mucinous BOTs.

Glucocorticoid precursors (PD, PT, 17-HP) and androgen precursors (5-PD, 5-PT) were significant urinary steroid metabolites identified from the Type 1 group (n=5 mucinous ovarian cancers and n=8 mucinous BOTs). This could represent early immature steroidogenesis and it may indicate a key pathological change in early ovarian carcinogenesis. These steroid metabolites are derived from the steroids synthesised by the activity of CYP11A1, CYP17A1 and HSD3B2. The results in this study suggests that there may be a potential utility of drugs that target the early steps / enzymes in steroid synthesis for women with a recurrent mucinous ovarian cancer after surgery as current therapeutic options are extremely limited for those patients. Blocking the early pathway could slow down the progression of a recurrence and the necessity of aldosterone and cortisone could be replaced by drugs that already treat adrenal insufficiency.

Another finding was the observation that glucocorticoid precursors (PD, PT, 17-HP) and androgen precursors (5-PD, 5-PT) were significant urinary steroid metabolites identified from the Type 1 group of which 73% were Stage 1 (**Figure 5.5**). This could represent early immature

steroidogenesis and it may indicate a key pathological change in early ovarian carcinogenesis. Alternatively, the trend for the highest absolute values of steroid metabolites steered towards PT, 17-HP and 5-PT; all three are derived from CYP17A1 activity. CYP17A1, which performs two of the five steroid reactions to produce the five urinary steroid metabolites identified may have a key role and significant increased CYP17 expression has been observed in Type 1 tumours by immunohistochemistry (**Figure 5.6**).

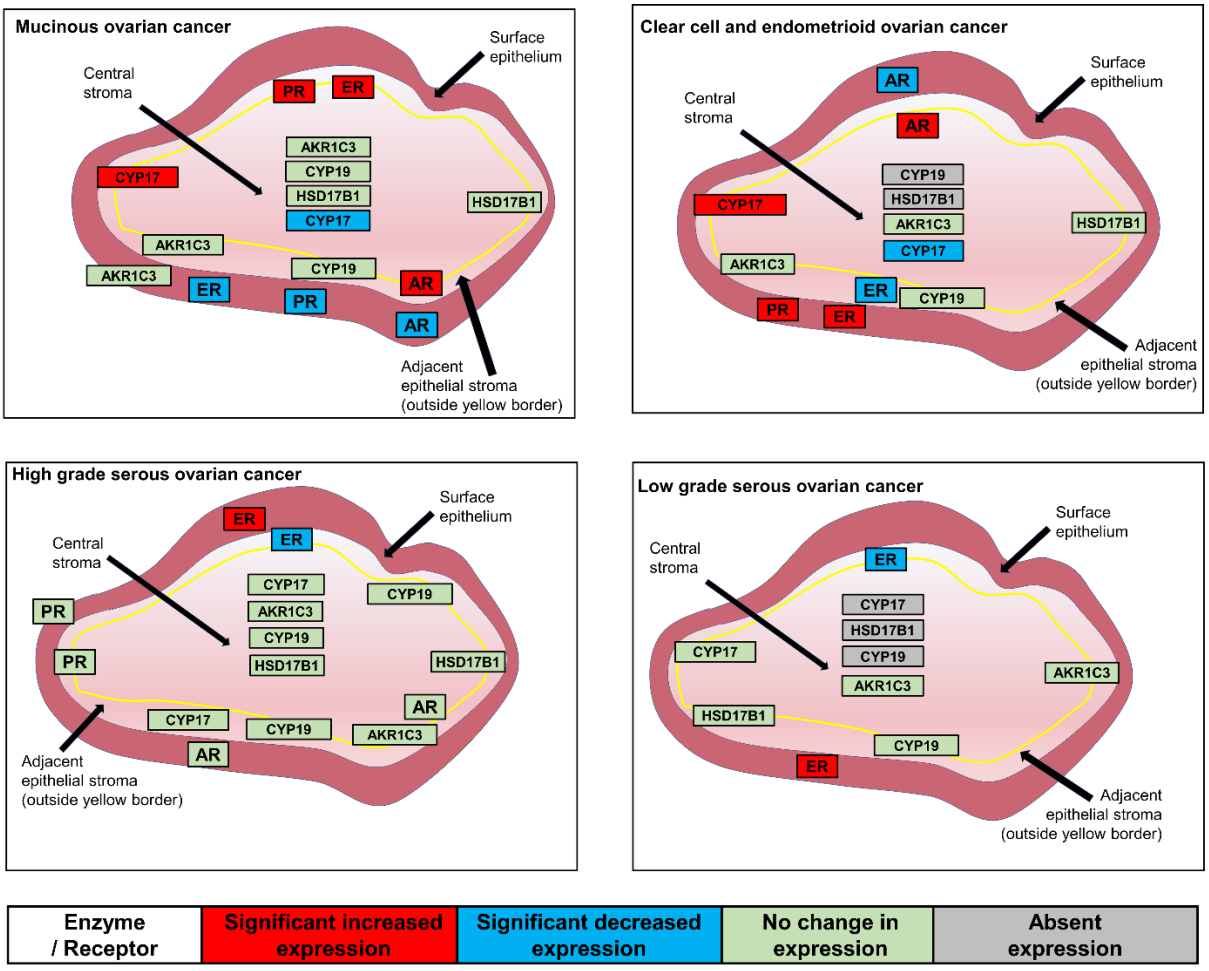

Fig. 5.6: Immunohistochemistry for sex steroid related enzymes and receptors in four subtypes of ovarian cancers including BOTs

(Adapted from the data, (Blanco et al., 2017)). Immunohistochemistry was performed on ovarian cancers including BOTs (mucinous n=15, clear cell/endometrioid n=19, low grade serous ovarian cancer n =25, high grade serous ovarian cancer n =30). The graphic illustrates the ovary with epithelium and stroma for the four tumour subtypes. Expression of selected proteins was compared from three locations: surface epithelium, adjacent stroma to the surface epithelium and the central stroma. Red = increased expression, $p<0.05$ of protein in

that zone, $p<0.05$. Blue = decreased expression of protein, $p<0.05$, in that zone. Green = no significant change in expression in its location. Grey = absent expression*. Higher expression of CYP17, progesterone receptor, estrogen receptor and androgen receptor were observed in the mucinous ovarian cancers and BOTs in the adjacent stromal epithelium.* Similar findings were observed in clear cell/endometrioid tumours. Serous ovarian tumours did not appear to display any similar patterns. Changes in expression of steroid-related proteins in the adjacent stromal epithelium support the hypothesis that this area is activated to elaborate steroid hormones that may stimulate further neoplastic growth.

Conclusion: This study has demonstrated urinary steroid profiling can differentiate Type 1 ovarian cancers including mucinous BOTs from both Type 2 ovarian cancers including serous BOTs and benign ovarian tumours and healthy controls. It has also shown that mucinous ovarian carcinomas and mucinous BOTs display urinary precursor androgen and glucocorticoid metabolites in a unique steroid profile which linked to CYP17 expression and activity. Further investigations in this area with larger specimen numbers is required to enable progress into this research finding. However, given the low prevalence of this disease, this will be very hard to accomplish; hence one possible avenue could be to extend the ethics application to recruit patients with known recurrent mucinous ovarian cancer and patients undergoing surveillance for mucinous BOTs.

Chapter 6 Final conclusions and future directions

I have investigated steroid metabolomics and androgen metabolites in cell lines, tissue and in 24-hour urine to characterise the complex web of steroid interactions and steroid pathways that are active in ovarian cancer. I also investigated the utility of steroid metabolomics as a diagnostic marker in epithelial ovarian cancer.

At the outset, I conducted an *in-silico* analysis, that identified five genes involved in androgen metabolism (*SRD5A1*, *AK1C3*, *HSD17B3*, *HSD17B4* and *HSD17B7*) as being upregulated in epithelial ovarian cancer and this provided initial baseline data to direct a biological study observing androgen metabolism in representative epithelial ovarian cancer cell lines. In a series of steroid treatments with the ovarian cancer cell lines I found that the trajectory of androgen metabolism appeared to direct towards production of 5α-dione and androsterone, which are weak androgens. This finding was repeated in *ex vivo* steroid incubations with tumour tissue from benign, borderline and malignant serous ovarian tumours but they were not identified in urinary steroid profiling of patients. Neither of these two androgens have been identified in the literature as significant in the detection of epithelial ovarian cancer. Then, I identified five urinary steroid metabolites that can discriminate between Type 1 ovarian cancers (including specific histotypes of BOTs) from healthy ovary, benign tumours as well as Type 2 ovarian cancers including serous BOTs. When the results were analysed according to histological sub-type, I realized that many of the Type 1 cancers were mucinous ovarian cancers or mucinous BOTs (13 out of 22). Of exciting interest, I observed an incremental elevation in the concentration rise of these steroid metabolites with progressive increase from benign mucinous tumour to mucinous BOT and mucinous ovarian cancer suggesting steroid dysregulation could be involved as a pathogenic event in the development of mucinous BOTs and mucinous ovarian cancer. I expand on this and provide an interpretation of my results and future directions below.

6.1 Findings for mucinous ovarian borderline tumours and mucinous cancers

These *in vivo* results provide evidence that mucinous borderline ovarian tumours and mucinous ovarian cancers exhibit a distinct urinary steroid profile, and this may be of diagnostic potential. The significant urinary steroid metabolites identified 5-PD, PD, 5-PT, PT and 17-HP are derived from two groups: androgen precursors and glucocorticoid precursors (**Figure 6.1**). Cholesterol is converted to pregnenolone by CYP11A1 yielding the metabolite 5-PD and pregenolone is converted to 17-hydroxy-pregnenolone by CYP17A1 yielding 5-PT; both are androgen pre-cursor metabolites. Pregnenolone is also converted by HSD3B2 to progesterone which yields PD and progesterone is converted by CYP17A1 to 17-hydroxyprogesterone and yield the metabolites PT and 17HP in this final step. Both progesterone and 17-hydroxyprogesterone are glucocorticoid precursors. CYP17A1 is also involved in the metabolism of 17 hydroxyprogesterone to androstenedione, which derives the steroid metabolite, etiocholanolone, and in my urinary profiling study, I found the highest absolute values for etiocholanolone to be attributed to mucinous BOTS and mucinous ovarian cancers.

Increases in these glucocorticoid and androgen precursors suggest that dysregulation occurs early in the steroidogenesis pathway in patients with mucinous tumours. In this study, five out of 13 of our mucinous cancer cases were Stage I suggesting that the steroid dysregulation is an early pathological event in mucinous cancer development. The observed incremental elevation of these precursors from mucinous tumours to mucinous BOTs and to mucinous ovarian cancers is also compatible with this hypothesis. My findings are consistent with evidence from the literature where, immunohistochemistry of mucinous BOTs and mucinous ovarian cancers had significantly higher CYP17 expression compared to Type 2 ovarian cancers and BOTs (Blanco et al., 2017). This would infer that CYP17A1 function may be dysregulated in the steroid pathway in mucinous cancers (**Figure 5.6**). At present, the protein expression of HSD3B2 in mucinous ovarian tumours is unknown.

My findings also correlate with previous studies attempting to find associations between hormone related pathways and epithelial ovarian cancer risk. Higher pre-diagnosis serum concentrations of testosterone and androstenedione were associated with an increased risk of developing in endometrioid and mucinous tumors but not serous or clear cell subtypes (Ose et al., 2017, Trabert et al., 2019).

Of the five significant urinary metabolites identified in my study, three were glucocorticoid precursors and an alternative explanation could be that these glucocorticoid precursors are elevated secondary to the stress response of developing cancer. However, as most of the cancers in the study were Stage I, this seems less likely.

My *in-silico* analysis had also identified upregulated genes *HSD17B4* and *AKR1C3* which are involved with production of other androgens further downstream, and this may represent the inadequacy of this method of interrogating data. There is a large RNA-seq data set for mucinous ovarian neoplasms in the European Genome-Phenome Archive (https://ega-archive.org/studies/EGAS00001003545) and at the time of writing, I am awaiting data access rights. Using that data, I would perform a search for changes in gene expression of all steroidogenic components compared to GTEx normal ovary data, similar to my study for HGSOC in **Chapter 3**. Then I would use those findings of upregulated and down-regulated genes to direct a biological study to characterise steroid synthesis in mucinous ovarian cancer cell lines and fresh mucinous ovarian tumours (benign, BOTs and cancers). This could be performed in parallel to obtaining 24h urine collections from patients with suspected or confirmed mucinous ovarian tumours and performing urinary steroid profiling by GC-MS.

The potential clinical utility of diagnosing mucinous ovarian cancer pre-operatively is that they could have this 24h urinary test in the workup investigations on being referred to a Gynaecological oncologist. As it is non-invasive, it is easy to administer. Furthermore, patients could avoid the additional raft of investigations, such as colonoscopy, that they currently endure to determine if they have a differential diagnosis of primary bowel cancer. In addition,

these patients would be recommended primary debulking surgery at the outset as chemotherapeutic options are very limited. As some Cancer Centres begin to focus on niche disease subtypes, it may be that these patients are referred earlier to tertiary centres that focus on cytoreductive surgery specifically for mucinous ovarian cancer.

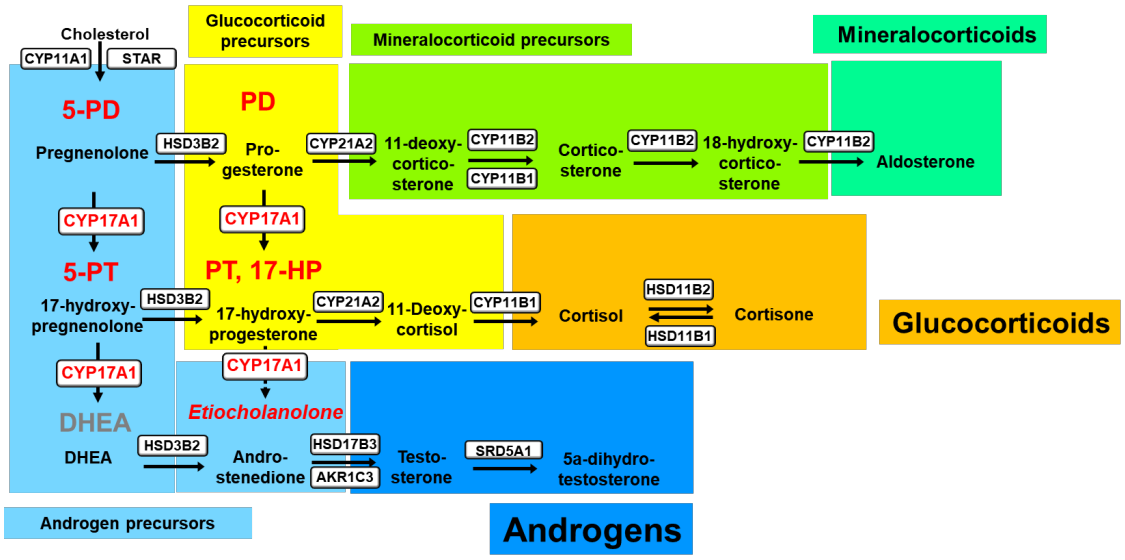

Fig. 6.1: Significantly increased steroid metabolites identified in 24h urines from patients in Type 1 ovarian cancers including mucinous BOTs (n=22).

Here, 5-PD, PD, 5-PT, PT and 17-HP were significantly elevated (red, bold) ($p<0.05$) in three comparisons: with Type 2 ovarian cancers including serous BOTs, with benign tumours and with healthy controls . On further analysis, these metabolites were consistently elevated in mucinous ovarian cancers (n=5) and mucinous BOTs (n=8). Etiocholanolone was also found to have higher concentrations in Type 1 ovarian cancers and mucinous BOTs (non-statistically significant). DHEA concentrations did not differ in the comparisons. The concentration changes in these identified metabolites suggest dysregulation of steroid synthesis of glucocorticoid precursors and androgen precursors could be biomarkers for mucinous ovarian cancers and mucinous BOTs. Four out five mucinous cancers in this study were Stage I. Protein expression of CYP17A1 (white box, red text) has been shown to be significantly increased in mucinous ovarian cancers and mucinous BOTs which may explain this finding. Gene and protein expression of StAR, CYP11A1 and HSD3B2 in Type 1 ovarian cancers and mucinous BOTs is unknown.

6.2 Findings for high grade serous ovarian cancer

Unfortunately, we found no evidence to show that urinary steroid profiling discriminates for high grade serous ovarian cancer (HGSOC) or Type 2 ovarian tumours. The analysis of the TCGA dataset for HGSOC indicated that the genes for several steroidogenic components had reduced expression compared to normal and at first, it did suggest that steroidogenesis was not an avenue worth exploring.

However, there was an increased 2- fold difference in *SRD5A1*, which has an integral role metabolizing testosterone to DHT and androstenedione to 5a-dione. The *in vitro* cell line studies indicated that high grade serous ovarian cancer cells do preferentially create weaker androgens such as 5α-dione. However, the metabolites associated with these androgens were not significantly increased in the 24-h urine collections of patients with HGSOC.This may be due to the downregulation of the steroidogenic genes in this subtype of ovarian cancer, observed in the GEPIA analysis in Chapter 3.

In a serum study, an inverse association was observed between androstenedione and high-grade serous tumours. However, the reported low androstenedione concentration could be attributed to androstenedione conversion to 5α-dione and in that study 5α-dione or its metabolites were not analysed in those samples (Ose et al., 2017).

During the research period, I obtained serum samples from recruited patients, and it is our intention in the future to perform LC-MS/MS to observe whether 5α-dione metabolites are associated with HGSOC. In addition, it would be very interesting to perform experiments to establish the role of 5α-dione. I described that 5α-dione does not activate AR to cause cell proliferation but as discussed earlier, AR independent pathways exist. Previous studies have shown DHT reversing the protective effects of TGF-β1 on healthy ovary and primary ovarian cancer cells (Evangelou et al., 2000, Kohan-Ivani et al., 2016).

In our cell line studies we largely targeted HGSOC as this is the most common histopathological subtype. As a result, I cannot comment confidently on the androgen metabolic activity in Type 1 ovarian cancer cell lines.

The *ex vivo* fresh tumour tissue incubations did show androgen metabolism in keeping with the cell line models but these experiments with tumour tissue sampling is fraught with complexities of viability and reproducibility is a concern. However, a series of steroid incubation experiments using only mucinous BOTs and mucinous ovarian cancers would be highly valuable in validating a urinary steroid profile for this subtype of ovarian tumours.

6.3 Future directions

In this project, five urinary steroid metabolites (two androgen precursors and three glucocorticoid precursors) were significantly increased in Type 1 ovarian cancers and mucinous BOTs compared to Type 2 ovarian cancers, serous BOTs, benign tumours and healthy controls. In addition, there was incremental elevation in the level of 3 of these metabolites with disease progression from benign mucinous tumours to mucinous BOTs and mucinous ovarian cancers. Moreover, we also observed the highest absolute values for androsterone and etiocholanolone in these mucinous BOTs and mucinous cancer subtypes but due to low sample numbers, significance was not achieved. I still maintain a suspicion that these two androgen metabolites are of significance in the mucinous cancer and mucinous BOT subtype.

In the future, I plan to expand our sample set to confirm our findings in the mucinous ovarian tumours. I will continue the collection of 24-hour urines from patients with confirmed and

suspected mucinous ovarian tumours and their specimens will undergo urinary steroid profiling by GC-MS. With NHS ethics in place at almost a dozen sites, recruitment to gather a larger sample set with this subtype is achievable despite a reported low prevalence of 3% for this disease subtype. In this study, one of the reasons I may have had a higher proportion of mucinous ovarian cancers could be that we unknowingly were recruiting more patients who did not have ovarian cancer confirmed in their initial investigations, whilst those patients with an early image guided biopsy diagnosis of ovarian cancer were fast-tracked for neoadjuvant chemotherapy before we could consent them for research and obtain untreated samples. As the number of mucinous cancers in my study was higher than the typical prevalence rate, I obtained a specialist gynaecological pathologist review of all mucinous cancer histology reports, who agree with the original reporting.

In addition, we would integrate tumour genomics with the metabolomic data from urinary steroid profiling. In a study featuring genetic analysis of over 195 cases for mucinous ovarian cancer across all histological grades, including 22 benign and 39 borderline mucinous ovarian tumours, the authors generated a model of progression from benign to mucinous BOT to localized low-grade mucinous ovarian cancer and progressively through to high-grade and/or metastatic mucinous ovarian cancer. Benign tumours were shown to initiate with either a *KRAS* or *CDKN2A* event whilst mucinous BOTs were significantly more likely to have both events and additional copy number alterations. Grade 1 mucinous ovarian cancers had yet more copy number alterations and *TP53* mutations. A pattern was outlined with copy number alterations shown to be the key drivers associated with increasing grade and metastatic progression and are potential prognostic markers (Cheasley et al., 2019). However, at present none of the genes identified are known to affect steroid biosynthesis. With an integrated genomic-metabolomic approach I could observe if progressive copy number alteration and oncogene

mutations are associated with increased biosynthesis of urinary steroid metabolites in mucinous ovarian cancers and mucinous BOTs.

In addition, I will amend the ethics agreement and recruitment plan to include patients undergoing post-operative surveillance for mucinous ovarian disease. I suspect that there may be a urinary steroid profile that not only detects primary mucinous BOTs and mucinous ovarian cancers but also could detect recurrence; this is an area of gynaecological oncology which remains poorly researched. Currently metastatic mucinous ovarian cancer has very limited therapeutic options which are targeted according to the genomic alterations described; but the median overall survival for these patients at 12-33 months which is far worse than advanced HGSOC (OS 35-60 months) (Morice et al., 2019).

This investigation confirms the current literature reports that androgen metabolism does occur in high grade serous ovarian cancer, however, urinary steroid profiling using mass spectrometry does not identify any diagnostic markers for this subtype.

Of exciting interest, this study identifies a novel finding that steroidogenic dysregulation is potentially involved in pathogenesis of Type 1 and mucinous ovarian tumours with incremental rises in a panel of select steroid metabolites with disease progression from benign mucinous ovarian tumour to mucinous BOT and mucinous ovarian cancer.

In conclusion, my research has unearthed a hitherto unknown potential role for steroid metabolomics as a diagnostic marker for mucinous ovarian tumours as well as identifying potential mechanisms of pathogenesis.

References

ABE, Y., TAKEUCHI, T., IMAI, Y., MURASE, R., KAMEI, Y., FUJIBUCHI, T., MATSUMOTO, S., UEDA, N., OGASAWARA, M., SHIGEMOTO, K. & KITO, K. 2006. A Small Ras-like protein Ray/Rab1c modulates the p53-regulating activity of PRPK. *Biochem Biophys Res Commun,* 344**,** 377-85.

ABRAHAM, G. E. 1974. Ovarian and adrenal contribution to peripheral androgens during the menstrual cycle. *J Clin Endocrinol Metab,* 39**,** 340-6.

ACKERMANN, D., GROESSL, M., PRUIJM, M., PONTE, B., ESCHER, G., D'USCIO, C. H., GUESSOUS, I., EHRET, G., PECHÈRE-BERTSCHI, A., MARTIN, P. Y., BURNIER, M., DICK, B., VOGT, B., BOCHUD, M., ROUSSON, V. & DHAYAT, N. A. 2019. Reference intervals for the urinary steroid metabolome: The impact of sex, age, day and night time on human adult steroidogenesis. *PLoS One,* 14**,** e0214549.

ARLT, W. 2004. Dehydroepiandrosterone and ageing. *Best Pract Res Clin Endocrinol Metab,* 18**,** 363-80.

ARLT, W., BIEHL, M., TAYLOR, A. E., HAHNER, S., LIBÉ, R., HUGHES, B. A., SCHNEIDER, P., SMITH, D. J., STIEKEMA, H., KRONE, N., PORFIRI, E., OPOCHER, G., BERTHERAT, J., MANTERO, F., ALLOLIO, B., TERZOLO, M., NIGHTINGALE, P., SHACKLETON, C. H. L., BERTAGNA, X., FASSNACHT, M. & STEWART, P. M. 2011. Urine Steroid Metabolomics as a Biomarker Tool for Detecting Malignancy in Adrenal Tumors. *The Journal of Clinical Endocrinology & Metabolism,* 96**,** 3775-3784.

ARLT, W., CALLIES, F., VAN VLIJMEN, J. C., KOEHLER, I., REINCKE, M., BIDLINGMAIER, M., HUEBLER, D., OETTEL, M., ERNST, M., SCHULTE, H. M. & ALLOLIO, B. 1999. Dehydroepiandrosterone replacement in women with adrenal insufficiency. *N Engl J Med,* 341**,** 1013-20.

ATTARD, G., REID, A. H., AUCHUS, R. J., HUGHES, B. A., CASSIDY, A. M., THOMPSON, E., OOMMEN, N. B., FOLKERD, E., DOWSETT, M., ARLT, W. & DE BONO, J. S. 2012. Clinical and biochemical consequences of CYP17A1 inhibition with abiraterone given with and without exogenous glucocorticoids in castrate men with advanced prostate cancer. *J Clin Endocrinol Metab,* 97**,** 507-16.

AUCHUS, R. J. 2004. The backdoor pathway to dihydrotestosterone. *Trends Endocrinol Metab,* 15**,** 432-8.

AUCHUS, R. J., LEE, T. C. & MILLER, W. L. 1998. Cytochrome b5 augments the 17,20-lyase activity of human P450c17 without direct electron transfer. *J Biol Chem,* 273**,** 3158-65.

AUERSPERG, N. 2013. The origin of ovarian cancers--hypotheses and controversies. *Front Biosci (Schol Ed),* 5**,** 709-19.

AUERSPERG, N., WONG, A. S., CHOI, K. C., KANG, S. K. & LEUNG, P. C. 2001. Ovarian surface epithelium: biology, endocrinology, and pathology. *Endocr Rev,* 22**,** 255-88.

BANCOS, I., TAYLOR, A. E., CHORTIS, V., SITCH, A. J., JENKINSON, C., DAVIDGE-PITTS, C. J., LANG, K., TSAGARAKIS, S., MACECH, M., RIESTER, A., DEUTSCHBEIN, T., PUPOVAC, I. D., KIENITZ, T., PRETE, A., PAPATHOMAS, T. G., GILLIGAN, L. C., BANCOS, C., REIMONDO, G., HAISSAGUERRE, M., MARINA, L., GRYTAAS, M. A., SAJWANI, A., LANGTON, K., IVISON, H. E., SHACKLETON, C. H. L., ERICKSON, D., ASIA, M., PALIMERI, S., KONDRACKA, A., SPYROGLOU, A., RONCHI, C. L., SIMUNOV, B., DELIVANIS, D. A., SUTCLIFFE, R. P., TSIROU, I., BEDNARCZUK, T., REINCKE, M., BURGER-STRITT, S., FEELDERS, R. A., CANU, L., HAAK, H. R., EISENHOFER, G., DENNEDY, M. C., UELAND, G. A., IVOVIC, M., TABARIN, A., TERZOLO, M., QUINKLER, M., KASTELAN, D., FASSNACHT, M., BEUSCHLEIN, F., AMBROZIAK, U., VASSILIADI, D. A., O'REILLY, M. W., YOUNG, W. F., JR., BIEHL, M., DEEKS, J. J. & ARLT, W. 2020. Urine steroid metabolomics for

the differential diagnosis of adrenal incidentalomas in the EURINE-ACT study: a prospective test validation study. *Lancet Diabetes Endocrinol,* 8**,** 773-781.

BANERJEE, S., TOVEY, H., BOWEN, R., FOLKERD, E., KILBURN, L., MCLACHLAN, J., HALL, M., TUNARIU, N., ATTYGALLE, A., LIMA, J., PERRY, S., CHATFIELD, P., HILLS, M., KAYE, S., ATTARD, G., DOWSETT, M. & BLISS, J. M. 2020. Abiraterone in patients with recurrent epithelial ovarian cancer: principal results of the phase II Cancer of the Ovary Abiraterone (CORAL) trial (CRUK - A16037). *Ther Adv Med Oncol,* 12**,** 1758835920975352.

BARNES, J. 1960. Detoxication Mechanisms. The Metabolism and Detoxication of Drugs, Toxic Substances and Other Organic Compounds.

BARWICK, T. D., MALHOTRA, A., WEBB, J. A., SAVAGE, M. O. & REZNEK, R. H. 2005. Embryology of the adrenal glands and its relevance to diagnostic imaging. *Clin Radiol,* 60**,** 953-9.

BENARD, J., DA SILVA, J., DE BLOIS, M. C., BOYER, P., DUVILLARD, P., CHIRIC, E. & RIOU, G. 1985. Characterization of a human ovarian adenocarcinoma line, IGROV1, in tissue culture and in nude mice. *Cancer Res,* 45**,** 4970-9.

BHATLA, N. & DENNY, L. 2018. FIGO Cancer Report 2018. *Int J Gynaecol Obstet,* 143 Suppl 2**,** 2-3.

BLANCO, L. Z., JR., KUHN, E., MORRISON, J. C., BAHADIRLI-TALBOTT, A., SMITH-SEHDEV, A. & KURMAN, R. J. 2017. Steroid hormone synthesis by the ovarian stroma surrounding epithelial ovarian tumors: a potential mechanism in ovarian tumorigenesis. *Mod Pathol*.

BLOBE, G. C., SCHIEMANN, W. P. & LODISH, H. F. 2000. Role of transforming growth factor beta in human disease. *N Engl J Med,* 342**,** 1350-8.

BONADONA, V., BONAÏTI, B., OLSCHWANG, S., GRANDJOUAN, S., HUIART, L., LONGY, M., GUIMBAUD, R., BUECHER, B., BIGNON, Y. J., CARON, O., COLAS, C., NOGUÈS, C., LEJEUNE-DUMOULIN, S., OLIVIER-FAIVRE, L., POLYCARPE-OSAER, F., NGUYEN, T. D., DESSEIGNE, F., SAURIN, J. C., BERTHET, P., LEROUX, D., DUFFOUR, J., MANOUVRIER, S., FRÉBOURG, T., SOBOL, H., LASSET, C. & BONAÏTI-PELLIÉ, C. 2011. Cancer risks associated with germline mutations in MLH1, MSH2, and MSH6 genes in Lynch syndrome. *Jama,* 305**,** 2304-10.

BOWEN, N. J., WALKER, L. D., MATYUNINA, L. V., LOGANI, S., TOTTEN, K. A., BENIGNO, B. B. & MCDONALD, J. F. 2009. Gene expression profiling supports the hypothesis that human ovarian surface epithelia are multipotent and capable of serving as ovarian cancer initiating cells. *BMC Med Genomics,* 2**,** 71.

BUFA, A., POÓR, V., BÁLINT, A., MOLNÁR, S., JEGES, S., PÓTÓ, L., GŐCZE, P. & KILÁR, F. 2008. Endogenous Urinary Steroids in Postmenopausal Women with Epithelial Ovarian Cancer. *Chromatographia,* 68**,** 131-135.

BUICK, R. N., PULLANO, R. & TRENT, J. M. 1985. Comparative properties of five human ovarian adenocarcinoma cell lines. *Cancer Res,* 45**,** 3668-76.

BUTLER, M. S., RICCIARDELLI, C., TILLEY, W. D. & HICKEY, T. E. 2013. Androgen receptor protein levels are significantly reduced in serous ovarian carcinomas compared with benign or borderline disease but are not altered by cancer stage or metastatic progression. *Horm Cancer,* 4**,** 154-64.

CARDILLO, M. R., PETRANGELI, E., ALIOTTA, N., SALVATORI, L., RAVENNA, L., CHANG, C. & CASTAGNA, G. 1998. Androgen receptors in ovarian tumors: correlation with oestrogen and progesterone receptors in an immunohistochemical and semiquantitative image analysis study. *J Exp Clin Cancer Res,* 17**,** 231-7.

CARLSON, K. 1989. IUPAC-IUB Joint Commission on Biochemical Nomenclature (JCBN). The nomenclature of steroids. Recommendations 1989. *Eur J Biochem,* 186**,** 429-58.

CAVALIERI, E. L. & ROGAN, E. G. 2011. Unbalanced metabolism of endogenous estrogens in the etiology and prevention of human cancer. *J Steroid Biochem Mol Biol,* 125**,** 169-80.

CHADHA, S., RAO, B. R., SLOTMAN, B. J., VAN VROONHOVEN, C. C. & VAN DER KWAST, T. H. 1993. An immunohistochemical evaluation of androgen and progesterone receptors in ovarian tumors. *Hum Pathol,* 24**,** 90-5.

CHAN, K. K. L., SIU, M. K. Y., JIANG, Y. X., WANG, J. J., WANG, Y., LEUNG, T. H. Y., LIU, S. S., CHEUNG, A. N. Y. & NGAN, H. Y. S. 2017. Differential expression of estrogen receptor subtypes and variants in ovarian cancer: effects on cell invasion, proliferation and prognosis. *BMC Cancer,* 17**,** 606.

CHAPMAN, K., HOLMES, M. & SECKL, J. 2013. 11beta-hydroxysteroid dehydrogenases: intracellular gate-keepers of tissue glucocorticoid action. *Physiol Rev,* 93**,** 1139-206.

CHEASLEY, D., WAKEFIELD, M. J., RYLAND, G. L., ALLAN, P. E., ALSOP, K., AMARASINGHE, K. C., ANANDA, S., ANGLESIO, M. S., AU-YEUNG, G., BÖHM, M., BOWTELL, D. D. L., BRAND, A., CHENEVIX-TRENCH, G., CHRISTIE, M., CHIEW, Y. E., CHURCHMAN, M., DEFAZIO, A., DEMEO, R., DUDLEY, R., FAIRWEATHER, N., FEDELE, C. G., FEREDAY, S., FOX, S. B., GILKS, C. B., GOURLEY, C., HACKER, N. F., HADLEY, A. M., HENDLEY, J., HO, G. Y., HUGHES, S., HUNSTMAN, D. G., HUNTER, S. M., JOBLING, T. W., KALLI, K. R., KAUFMANN, S. H., KENNEDY, C. J., KÖBEL, M., LE PAGE, C., LI, J., LUPAT, R., MCNALLY, O. M., MCALPINE, J. N., MES-MASSON, A. M., MILESHKIN, L., PROVENCHER, D. M., PYMAN, J., RAHIMI, K., ROWLEY, S. M., SALAZAR, C., SAMIMI, G., SAUNDERS, H., SEMPLE, T., SHARMA, R., SHARPE, A. J., STEPHENS, A. N., THIO, N., TORRES, M. C., TRAFICANTE, N., XING, Z., ZETHOVEN, M., ANTILL, Y. C., SCOTT, C. L., CAMPBELL, I. G. & GORRINGE, K. L. 2019. The molecular origin and taxonomy of mucinous ovarian carcinoma. *Nat Commun,* 10**,** 3935.

CHEN, G., QIU, L., GAO, J., WANG, J., DANG, J., LI, L., JIN, Z. & LIU, X. 2021. Stress Hormones: Emerging Targets in Gynecological Cancers. *Front Cell Dev Biol,* 9**,** 699487.

CHEN, V. W., RUIZ, B., KILLEEN, J. L., COTÉ, T. R., WU, X. C. & CORREA, C. N. 2003. Pathology and classification of ovarian tumors. *Cancer,* 97**,** 2631-42.

CHENE, G., OUELLET, V., RAHIMI, K., BARRES, V., CACERES, K., MEUNIER, L., CYR, L., DE LADURANTAYE, M., PROVENCHER, D. & MES MASSON, A. M. 2015. DNA damage signaling and apoptosis in preinvasive tubal lesions of ovarian carcinoma. *Int J Gynecol Cancer,* 25**,** 761-9.

COHEN, J. D., LI, L., WANG, Y., THOBURN, C., AFSARI, B., DANILOVA, L., DOUVILLE, C., JAVED, A. A., WONG, F., MATTOX, A., HRUBAN, R. H., WOLFGANG, C. L., GOGGINS, M. G., DAL MOLIN, M., WANG, T. L., RODEN, R., KLEIN, A. P., PTAK, J., DOBBYN, L., SCHAEFER, J., SILLIMAN, N., POPOLI, M., VOGELSTEIN, J. T., BROWNE, J. D., SCHOEN, R. E., BRAND, R. E., TIE, J., GIBBS, P., WONG, H. L., MANSFIELD, A. S., JEN, J., HANASH, S. M., FALCONI, M., ALLEN, P. J., ZHOU, S., BETTEGOWDA, C., DIAZ, L. A., JR., TOMASETTI, C., KINZLER, K. W., VOGELSTEIN, B., LENNON, A. M. & PAPADOPOULOS, N. 2018. Detection and localization of surgically resectable cancers with a multi-analyte blood test. *Science,* 359**,** 926-930.

COUZINET, B., MEDURI, G., LECCE, M. G., YOUNG, J., BRAILLY, S., LOOSFELT, H., MILGROM, E. & SCHAISON, G. 2001. The postmenopausal ovary is not a major androgen-producing gland. *J Clin Endocrinol Metab,* 86**,** 5060-6.

CRUM, C. P., DRAPKIN, R., MIRON, A., INCE, T. A., MUTO, M., KINDELBERGER, D. W. & LEE, Y. 2007. The distal fallopian tube: a new model for pelvic serous carcinogenesis. *Curr Opin Obstet Gynecol,* 19**,** 3-9.

CUZICK, J., BULSTRODE, J. C., STRATTON, I., THOMAS, B. S., BULBROOK, R. D. & HAYWARD, J. L. 1983. A prospective study of urinary androgen levels and ovarian cancer. *Int J Cancer,* 32**,** 723-6.

DE TOLEDO, M. C., SARIAN, L. O., SALLUM, L. F., ANDRADE, L. L., VASSALLO, J., DE PAIVA SILVA, G. R., PINTO, G. A., SOARES, F. A., FONSECA, C. D. & DERCHAIN, S. F. 2014. Analysis of the contribution of immunologically-detectable HER2, steroid receptors and of the "triple-negative" tumor status to disease-free and overall survival of women with epithelial ovarian cancer. *Acta Histochem,* 116**,** 440-7.

DENNEFORS, B. L., JANSON, P. O., HAMBERGER, L. & KNUTSSON, F. 1982. Hilus cells from human postmenopausal ovaries: gonadotrophin sensitivity, steroid and cyclic AMP production. *Acta Obstet Gynecol Scand,* 61**,** 413-6.

DIXON-SUEN, S. C., WEBB, P. M., WILSON, L. F., TUESLEY, K., STEWART, L. M. & JORDAN, S. J. 2019. The Association Between Hysterectomy and Ovarian Cancer Risk: A Population-Based Record-Linkage Study. *J Natl Cancer Inst,* 111**,** 1097-1103.

DOMCHEK, S. M., FRIEBEL, T. M., SINGER, C. F., EVANS, D. G., LYNCH, H. T., ISAACS, C., GARBER, J. E., NEUHAUSEN, S. L., MATLOFF, E., EELES, R., PICHERT, G., VAN T'VEER, L., TUNG, N., WEITZEL, J. N., COUCH, F. J., RUBINSTEIN, W. S., GANZ, P. A., DALY, M. B., OLOPADE, O. I., TOMLINSON, G., SCHILDKRAUT, J., BLUM, J. L. & REBBECK, T. R. 2010. Association of risk-reducing surgery in BRCA1 or BRCA2 mutation carriers with cancer risk and mortality. *Jama,* 304**,** 967-75.

DOMCKE, S., SINHA, R., LEVINE, D. A., SANDER, C. & SCHULTZ, N. 2013. Evaluating cell lines as tumour models by comparison of genomic profiles. *Nat Commun,* 4**,** 2126.

DOWNIE, D., MCFADYEN, M. C., ROONEY, P. H., CRUICKSHANK, M. E., PARKIN, D. E., MILLER, I. D., TELFER, C., MELVIN, W. T. & MURRAY, G. I. 2005. Profiling cytochrome P450 expression in ovarian cancer: identification of prognostic markers. *Clin Cancer Res,* 11**,** 7369-75.

DOWSETT, M., CANTWELL, B., LAL, A., JEFFCOATE, S. L. & HARRIS, A. L. 1988. Suppression of postmenopausal ovarian steroidogenesis with the luteinizing hormone-releasing hormone agonist goserelin. *J Clin Endocrinol Metab,* 66**,** 672-7.

EDMONDSON, R. J., MONAGHAN, J. M. & DAVIES, B. R. 2002. The human ovarian surface epithelium is an androgen responsive tissue. *Br J Cancer,* 86**,** 879-885.

ELATTAR, A., WARBURTON, K. G., MUKHOPADHYAY, A., FREER, R. M., SHAHEEN, F., CROSS, P., PLUMMER, E. R., ROBSON, C. N. & EDMONDSON, R. J. 2012. Androgen receptor expression is a biological marker for androgen sensitivity in high grade serous epithelial ovarian cancer. *Gynecol Oncol,* 124**,** 142-7.

EVANGELOU, A., JINDAL, S. K., BROWN, T. J. & LETARTE, M. 2000. Down-regulation of transforming growth factor beta receptors by androgen in ovarian cancer cells. *Cancer Res,* 60**,** 929-35.

EVANGELOU, A., LETARTE, M., JURISICA, I., SULTAN, M., MURPHY, K. J., ROSEN, B. & BROWN, T. J. 2003. Loss of coordinated androgen regulation in nonmalignant ovarian epithelial cells with BRCA1/2 mutations and ovarian cancer cells. *Cancer Res,* 63**,** 2416-24.

FEINGOLD, K. R. 2000. Adrenal Disease and Function. *In:* FEINGOLD, K. R., ANAWALT, B., BOYCE, A., CHROUSOS, G., DE HERDER, W. W., DHATARIYA, K., DUNGAN, K., HERSHMAN, J. M., HOFLAND, J., KALRA, S., KALTSAS, G., KOCH, C., KOPP, P., KORBONITS, M., KOVACS, C. S., KUOHUNG, W., LAFERRÈRE, B., LEVY, M., MCGEE, E. A., MCLACHLAN, R., MORLEY, J. E., NEW, M., PURNELL, J., SAHAY, R., SINGER, F., SPERLING, M. A., STRATAKIS, C. A., TRENCE, D. L. & WILSON, D. P. (eds.) *Endotext.* South Dartmouth (MA): MDText.com, Inc.

FOGLE, R. H., STANCZYK, F. Z., ZHANG, X. & PAULSON, R. J. 2007. Ovarian Androgen Production in Postmenopausal Women. *The Journal of Clinical Endocrinology & Metabolism,* 92**,** 3040-3043.

FOLKINS, A. K., JARBOE, E. A., SALEEMUDDIN, A., LEE, Y., CALLAHAN, M. J., DRAPKIN, R., GARBER, J. E., MUTO, M. G., TWOROGER, S. & CRUM, C. P. 2008. A candidate precursor to pelvic serous cancer (p53 signature) and its prevalence in ovaries and fallopian tubes from women with BRCA mutations. *Gynecol Oncol,* 109**,** 168-73.

FORADORI, C. D., WEISER, M. J. & HANDA, R. J. 2008. Non-genomic actions of androgens. *Front Neuroendocrinol,* 29**,** 169-81.

FOTOPOULOU, C., HALL, M., CRUICKSHANK, D., GABRA, H., GANESAN, R., HUGHES, C., KEHOE, S., LEDERMANN, J., MORRISON, J., NAIK, R., ROLLAND, P. & SUNDAR, S. 2017. British Gynaecological Cancer Society (BGCS) epithelial ovarian/fallopian tube/primary peritoneal cancer guidelines: recommendations for practice. *Eur J Obstet Gynecol Reprod Biol,* 213**,** 123-139.

GILBERT, L., BASSO, O., SAMPALIS, J., KARP, I., MARTINS, C., FENG, J., PIEDIMONTE, S., QUINTAL, L., RAMANAKUMAR, A. V., TAKEFMAN, J., GRIGORIE, M. S., ARTHO, G. & KRISHNAMURTHY, S. 2012. Assessment of symptomatic women for early diagnosis of ovarian cancer: results from the prospective DOvE pilot project. *Lancet Oncol,* 13**,** 285-91.

GOHAGAN, J. K., PROROK, P. C., HAYES, R. B. & KRAMER, B. S. 2000. The Prostate, Lung, Colorectal and Ovarian (PLCO) Cancer Screening Trial of the National Cancer Institute: history, organization, and status. *Control Clin Trials,* 21**,** 251s-272s.

GUI, T. & SHEN, K. 2012. The epidermal growth factor receptor as a therapeutic target in epithelial ovarian cancer. *Cancer Epidemiol,* 36**,** 490-6.

GUPTA, M. K., GURYEV, O. L. & AUCHUS, R. J. 2003. 5alpha-reduced C21 steroids are substrates for human cytochrome P450c17. *Arch Biochem Biophys,* 418**,** 151-60.

HAMILTON, T. C., YOUNG, R. C., MCKOY, W. M., GROTZINGER, K. R., GREEN, J. A., CHU, E. W., WHANG-PENG, J., ROGAN, A. M., GREEN, W. R. & OZOLS, R. F. 1983. Characterization of a human ovarian carcinoma cell line (NIH:OVCAR-3) with androgen and estrogen receptors. *Cancer Res,* 43**,** 5379-89.

HANDELSMAN, D. J. & WARTOFSKY, L. 2013. Requirement for mass spectrometry sex steroid assays in the Journal of Clinical Endocrinology and Metabolism. *J Clin Endocrinol Metab,* 98**,** 3971-3.

HANNIBAL, C. G., FREDERIKSEN, K., VANG, R., KURMAN, R. J. & KJAER, S. K. 2020. Risk of specific types of ovarian cancer after borderline ovarian tumors in Denmark: A nationwide study. *Int J Cancer,* 147**,** 990-995.

HARING, R., WALLASCHOFSKI, H., TEUMER, A., KROEMER, H., TAYLOR, A. E., SHACKLETON, C. H., NAUCK, M., VÖLKER, U., HOMUTH, G. & ARLT, W. 2013. A SULT2A1 genetic variant identified by GWAS as associated with low serum DHEAS does not impact on the actual DHEA/DHEAS ratio. *J Mol Endocrinol,* 50**,** 73-7.

HAVELOCK, J. C., RAINEY, W. E., BRADSHAW, K. D. & CARR, B. R. 2006. The post-menopausal ovary displays a unique pattern of steroidogenic enzyme expression. *Hum Reprod,* 21**,** 309-17.

HAVRILESKY, L. J., HURTEAU, J. A., WHITAKER, R. S., ELBENDARY, A., WU, S., RODRIGUEZ, G. C., BAST, R. C., JR. & BERCHUCK, A. 1995. Regulation of apoptosis in normal and malignant ovarian epithelial cells by transforming growth factor beta. *Cancer Res,* 55**,** 944-8.

HAVRILESKY, L. J., MOORMAN, P. G., LOWERY, W. J., GIERISCH, J. M., COEYTAUX, R. R., URRUTIA, R. P., DINAN, M., MCBROOM, A. J., HASSELBLAD, V., SANDERS, G. D. & MYERS, E. R. 2013. Oral contraceptive pills as primary prevention for ovarian cancer: a systematic review and meta-analysis. *Obstet Gynecol,* 122**,** 139-147.

HAWKER, J. R., JR. 2003. Chemiluminescence-based BrdU ELISA to measure DNA synthesis. *J Immunol Methods,* 274**,** 77-82.

HEEMSKERK-GERRITSEN, B. A., SEYNAEVE, C., VAN ASPEREN, C. J., AUSEMS, M. G., COLLÉE, J. M., VAN DOORN, H. C., GOMEZ GARCIA, E. B., KETS, C. M., VAN LEEUWEN, F. E., MEIJERS-HEIJBOER, H. E., MOURITS, M. J., VAN OS, T. A., VASEN, H. F., VERHOEF, S., ROOKUS, M. A. & HOONING, M. J. 2015. Breast cancer risk after salpingo-oophorectomy in healthy BRCA1/2 mutation carriers: revisiting the evidence for risk reduction. *J Natl Cancer Inst,* 107.

HEINONEN, P. K. 1991. Androgen production by epithelial ovarian tumours in post-menopausal women. *Maturitas,* 13**,** 117-22.

HEINZELMANN-SCHWARZ, V. A., GARDINER-GARDEN, M., HENSHALL, S. M., SCURRY, J. P., SCOLYER, R. A., SMITH, A. N., BALI, A., VANDEN BERGH, P., BARON-HAY, S., SCOTT, C., FINK, D., HACKER, N. F., SUTHERLAND, R. L. & O'BRIEN, P. M. 2006. A distinct molecular profile associated with mucinous epithelial ovarian cancer. *Br J Cancer,* 94**,** 904-13.

HENDRIX, N. D., WU, R., KUICK, R., SCHWARTZ, D. R., FEARON, E. R. & CHO, K. R. 2006. Fibroblast growth factor 9 has oncogenic activity and is a downstream target of Wnt signaling in ovarian endometrioid adenocarcinomas. *Cancer Res,* 66**,** 1354-62.

HERBISON, A. E. 2016. Control of puberty onset and fertility by gonadotropin-releasing hormone neurons. *Nat Rev Endocrinol,* 12**,** 452-66.

HILL, S. J., DECKER, B., ROBERTS, E. A., HOROWITZ, N. S., MUTO, M. G., WORLEY, M. J., FELTMATE, C. M., NUCCI, M. R., SWISHER, E. M., NGUYEN, H., YANG, C., MORIZANE, R., KOCHUPURAKKAL, B. S., DO, K. T., KONSTANTINOPOULOS, P. A., LIU, J. F., BONVENTRE, J. V., MATULONIS, U. A., SHAPIRO, G. I., BERKOWITZ, R. S., CRUM, C. P. & D'ANDREA, A. D. 2018. Prediction of DNA Repair Inhibitor Response in Short Term Patient-Derived Ovarian Cancer Organoids. *Cancer Discovery***,** CD-18-0474.

HÖHN, A. K., BRAMBS, C. E., HILLER, G. G. R., MAY, D., SCHMOECKEL, E. & HORN, L. C. 2021. 2020 WHO Classification of Female Genital Tumors. *Geburtshilfe Frauenheilkd,* 81**,** 1145-1153.

HOLCAKOVA, J., BARTOSIK, M., ANTON, M., MINAR, L., HAUSNEROVA, J., BEDNARIKOVA, M., WEINBERGER, V. & HRSTKA, R. 2021. New Trends in the Detection of Gynecological Precancerous Lesions and Early-Stage Cancers. *Cancers (Basel),* 13.

HURTEAU, J., RODRIGUEZ, G. C., WHITAKER, R. S., SHAH, S., MILLS, G., BAST, R. C. & BERCHUCK, A. 1994. Transforming growth factor-beta inhibits proliferation of human ovarian cancer cells obtained from ascites. *Cancer,* 74**,** 93-9.

JABARA, S., CHRISTENSON, L. K., WANG, C. Y., MCALLISTER, J. M., JAVITT, N. B., DUNAIF, A. & STRAUSS, J. F., 3RD 2003. Stromal cells of the human postmenopausal ovary display a distinctive biochemical and molecular phenotype. *J Clin Endocrinol Metab,* 88**,** 484-92.

JACOBS, I. J., MENON, U., RYAN, A., GENTRY-MAHARAJ, A., BURNELL, M., KALSI, J. K., AMSO, N. N., APOSTOLIDOU, S., BENJAMIN, E., CRUICKSHANK, D., CRUMP, D. N., DAVIES, S. K., DAWNAY, A., DOBBS, S., FLETCHER, G., FORD, J., GODFREY, K., GUNU, R., HABIB, M., HALLETT, R., HEROD, J., JENKINS, H., KARPINSKYJ, C., LEESON, S., LEWIS, S. J., LISTON, W. R., LOPES, A., MOULD, T., MURDOCH, J., ORAM, D., RABIDEAU, D. J., REYNOLDS, K., SCOTT, I., SEIF, M. W., SHARMA, A., SINGH, N., TAYLOR, J., WARBURTON, F., WIDSCHWENDTER, M., WILLIAMSON, K., WOOLAS, R., FALLOWFIELD, L., MCGUIRE, A. J., CAMPBELL, S., PARMAR, M. & SKATES, S. J. 2016. Ovarian cancer screening and mortality in the UK Collaborative Trial of Ovarian Cancer Screening (UKCTOCS): a randomised controlled trial. *Lancet,* 387**,** 945-956.

JÜHLEN, R., IDKOWIAK, J., TAYLOR, A. E., KIND, B., ARLT, W., HUEBNER, A. & KOEHLER, K. 2015. Role of ALADIN in human adrenocortical cells for oxidative stress response and steroidogenesis. *PLoS One,* 10**,** e0124582.

KABAWAT, S. E., BAST, R. C., JR., BHAN, A. K., WELCH, W. R., KNAPP, R. C. & COLVIN, R. B. 1983. Tissue distribution of a coelomic-epithelium-related antigen recognized by the monoclonal antibody OC125. *Int J Gynecol Pathol,* 2**,** 275-85.

KARVONEN, H., ARJAMA, M., KALEVA, L., NIININEN, W., BARKER, H., KOIVISTO-KORANDER, R., TAPPER, J., PAKARINEN, P., LASSUS, H., LOUKOVAARA, M., BÜTZOW, R., KALLIONIEMI, O., MURUMÄGI, A. & UNGUREANU, D. 2020. Glucocorticoids induce differentiation and chemoresistance in ovarian cancer by promoting ROR1-mediated stemness. *Cell Death Dis,* 11**,** 790.

KINDELBERGER, D. W., LEE, Y., MIRON, A., HIRSCH, M. S., FELTMATE, C., MEDEIROS, F., CALLAHAN, M. J., GARNER, E. O., GORDON, R. W., BIRCH, C., BERKOWITZ, R. S., MUTO, M. G. & CRUM, C. P. 2007. Intraepithelial carcinoma of the fimbria and pelvic serous carcinoma: Evidence for a causal relationship. *Am J Surg Pathol,* 31**,** 161-9.

KOHAN-IVANI, K., GABLER, F., SELMAN, A., VEGA, M. & ROMERO, C. 2016. Role of dihydrotestosterone (DHT) on TGF-β1 signaling pathway in epithelial ovarian cancer cells. *J Cancer Res Clin Oncol,* 142**,** 47-58.

KOURANTI, I., SACHSE, M., AROUCHE, N., GOUD, B. & ECHARD, A. 2006. Rab35 regulates an endocytic recycling pathway essential for the terminal steps of cytokinesis. *Curr Biol,* 16**,** 1719-25.

KRONE, N., HUGHES, B. A., LAVERY, G. G., STEWART, P. M., ARLT, W. & SHACKLETON, C. H. 2010. Gas chromatography/mass spectrometry (GC/MS) remains a pre-eminent discovery tool in clinical steroid investigations even in the era of fast liquid chromatography tandem mass spectrometry (LC/MS/MS). *J Steroid Biochem Mol Biol,* 121**,** 496-504.

KUCHENBAECKER, K. B., HOPPER, J. L., BARNES, D. R., PHILLIPS, K. A., MOOIJ, T. M., ROOS-BLOM, M. J., JERVIS, S., VAN LEEUWEN, F. E., MILNE, R. L., ANDRIEU, N., GOLDGAR, D. E., TERRY, M. B., ROOKUS, M. A., EASTON, D. F., ANTONIOU, A. C., MCGUFFOG, L., EVANS, D. G., BARROWDALE, D., FROST, D., ADLARD, J., ONG, K. R., IZATT, L., TISCHKOWITZ, M., EELES, R., DAVIDSON, R., HODGSON, S., ELLIS, S., NOGUES, C., LASSET, C., STOPPA-LYONNET, D., FRICKER, J. P., FAIVRE, L., BERTHET, P., HOONING, M. J., VAN DER KOLK, L. E., KETS, C. M., ADANK, M. A., JOHN, E. M., CHUNG, W. K., ANDRULIS, I. L., SOUTHEY, M., DALY, M. B., BUYS, S. S., OSORIO, A., ENGEL, C., KAST, K., SCHMUTZLER, R. K., CALDES, T., JAKUBOWSKA, A., SIMARD, J., FRIEDLANDER, M. L., MCLACHLAN, S. A., MACHACKOVA, E., FORETOVA, L., TAN, Y. Y., SINGER, C. F., OLAH, E., GERDES, A. M., ARVER, B. & OLSSON, H. 2017. Risks of Breast, Ovarian, and Contralateral Breast Cancer for BRCA1 and BRCA2 Mutation Carriers. *Jama,* 317**,** 2402-2416.

KÜHNEL, R., DELEMARRE, J. F., RAO, B. R. & STOLK, J. G. 1987. Correlation of multiple steroid receptors with histological type and grade in human ovarian cancer. *Int J Gynecol Pathol,* 6**,** 248-56.

KURMAN R, E. L. H., RONNETT B, M. BERLIN. 2011. *Blaustein's Pathology of the female genital Tract. 6th edition.*, Heidelberg: Springer;.

KURMAN, R. J. & SHIH IE, M. 2016. The Dualistic Model of Ovarian Carcinogenesis: Revisited, Revised, and Expanded. *Am J Pathol,* 186**,** 733-47.

LABRIE, F. 2015. All sex steroids are made intracellularly in peripheral tissues by the mechanisms of intracrinology after menopause. *J Steroid Biochem Mol Biol,* 145**,** 133-8.

LABRIE, F., BELANGER, A., BELANGER, P., BERUBE, R., MARTEL, C., CUSAN, L., GOMEZ, J., CANDAS, B., CASTIEL, I., CHAUSSADE, V., DELOCHE, C. & LECLAIRE, J. 2006. Androgen glucuronides, instead of testosterone, as the new markers of androgenic activity in women. *J Steroid Biochem Mol Biol,* 99**,** 182-8.

LABRIE, F., MARTEL, C., BÉLANGER, A. & PELLETIER, G. 2017. Androgens in women are essentially made from DHEA in each peripheral tissue according to intracrinology. *The Journal of Steroid Biochemistry and Molecular Biology,* 168**,** 9-18.

LANE, D., MATTE, I., RANCOURT, C. & PICHÉ, A. 2011. Prognostic significance of IL-6 and IL-8 ascites levels in ovarian cancer patients. *BMC Cancer,* 11**,** 210.

LANGER, R. D., WHITE, E., LEWIS, C. E., KOTCHEN, J. M., HENDRIX, S. L. & TREVISAN, M. 2003. The Women's Health Initiative Observational Study: baseline characteristics of participants and reliability of baseline measures. *Ann Epidemiol,* 13**,** S107-21.

LASLEY, B. L., CRAWFORD, S. L. & MCCONNELL, D. S. 2013. Ovarian adrenal interactions during the menopausal transition. *Minerva Ginecol,* 65**,** 641-51.

LAU, K. M., MOK, S. C. & HO, S. M. 1999. Expression of human estrogen receptor-alpha and -beta, progesterone receptor, and androgen receptor mRNA in normal and malignant ovarian epithelial cells. *Proc Natl Acad Sci U S A,* 96**,** 5722-7.

LEBBE, M., TAYLOR, A. E., VISSER, J. A., KIRKMAN-BROWN, J. C., WOODRUFF, T. K. & ARLT, W. 2017. The Steroid Metabolome in the Isolated Ovarian Follicle and Its Response to Androgen Exposure and Antagonism. *Endocrinology,* 158**,** 1474-1485.

LEE, P., ROSEN, D. G., ZHU, C., SILVA, E. G. & LIU, J. 2005. Expression of progesterone receptor is a favorable prognostic marker in ovarian cancer. *Gynecol Oncol,* 96**,** 671-7.

LEE, T. C., MILLER, W. L. & AUCHUS, R. J. 1999. Medroxyprogesterone acetate and dexamethasone are competitive inhibitors of different human steroidogenic enzymes. *J Clin Endocrinol Metab,* 84**,** 2104-10.

LEVINE, D., PARK, K., JURETZKA, M., ESCH, J., HENSLEY, M., AGHAJANIAN, C., LEWIN, S., KONNER, J., DEROSA, F., SPRIGGS, D., IASONOS, A. & SABBATINI, P. 2007. A phase II evaluation of goserelin and bicalutamide in patients with ovarian cancer in second or higher complete clinical disease remission. *Cancer,* 110**,** 2448-56.

LI, H., LIU, Y., WANG, Y., ZHAO, X. & QI, X. 2021. Hormone therapy for ovarian cancer: Emphasis on mechanisms and applications (Review). *Oncol Rep,* 46.

LINDGREN, P. R., BÄCKSTRÖM, T., CAJANDER, S., DAMBER, M. G., MÄHLCK, C. G., ZHU, D. & OLOFSSON, J. I. 2002. The pattern of estradiol and progesterone differs in serum and tissue of benign and malignant ovarian tumors. *Int J Oncol,* 21**,** 583-9.

LOUIE, M. C. & SEVIGNY, M. B. 2017. Steroid hormone receptors as prognostic markers in breast cancer. *Am J Cancer Res,* 7**,** 1617-1636.

LOVEDAY, C., TURNBULL, C., RUARK, E., XICOLA, R. M., RAMSAY, E., HUGHES, D., WARREN-PERRY, M., SNAPE, K., ECCLES, D., EVANS, D. G., GORE, M., RENWICK, A., SEAL, S., ANTONIOU, A. C. & RAHMAN, N. 2012. Germline RAD51C mutations confer susceptibility to ovarian cancer. *Nat Genet,* 44**,** 475-6; author reply 476.

LU, K. H., PATTERSON, A. P., WANG, L., MARQUEZ, R. T., ATKINSON, E. N., BAGGERLY, K. A., RAMOTH, L. R., ROSEN, D. G., LIU, J., HELLSTROM, I., SMITH, D., HARTMANN, L., FISHMAN, D., BERCHUCK, A., SCHMANDT, R., WHITAKER, R., GERSHENSON, D. M., MILLS, G. B. & BAST, R. C., JR. 2004. Selection of potential markers for epithelial ovarian cancer with gene expression arrays and recursive descent partition analysis. *Clin Cancer Res,* 10**,** 3291-300.

MADSEN, C., BAANDRUP, L., DEHLENDORFF, C. & KJAER, S. K. 2015. Tubal ligation and salpingectomy and the risk of epithelial ovarian cancer and borderline ovarian tumors: a nationwide case-control study. *Acta Obstet Gynecol Scand,* 94**,** 86-94.

MÄHLCK, C. G., BÄCKSTRÖM, T., KJELLGREN, O. & VON SCHOULTZ, B. 1986. Plasma progesterone and androstenedione in relation to changes in tumor volume and recurrence in women with ovarian carcinoma. *Gynecol Obstet Invest,* 22**,** 157-64.

MAKKONEN, H., JÄÄSKELÄINEN, T., RYTINKI, M. M. & PALVIMO, J. J. 2011. Analysis of androgen receptor activity by reporter gene assays. *Methods Mol Biol,* 776**,** 71-80.

MANCHANDA, R., ABDELRAHEIM, A., JOHNSON, M., ROSENTHAL, A. N., BENJAMIN, E., BRUNELL, C., BURNELL, M., SIDE, L., GESSLER, S., SARIDOGAN, E., ORAM, D., JACOBS, I. & MENON, U. 2011. Outcome of risk-reducing salpingo-oophorectomy in BRCA carriers and women of unknown mutation status. *Bjog,* 118**,** 814-24.

MARCOS, J. & POZO, O. J. 2015. Derivatization of steroids in biological samples for GC-MS and LC-MS analyses. *Bioanalysis,* 7**,** 2515-36.

MARTI, N., GALVÁN, J. A., PANDEY, A. V., TRIPPEL, M., TAPIA, C., MÜLLER, M., PERREN, A. & FLÜCK, C. E. 2017. Genes and proteins of the alternative steroid backdoor pathway for dihydrotestosterone synthesis are expressed in the human ovary and seem enhanced in the polycystic ovary syndrome. *Mol Cell Endocrinol,* 441**,** 116-123.

MELHEM, A., YAMADA, S. D., FLEMING, G. F., DELGADO, B., BRICKLEY, D. R., WU, W., KOCHERGINSKY, M. & CONZEN, S. D. 2009. Administration of glucocorticoids to ovarian cancer patients is associated with expression of the anti-apoptotic genes SGK1 and MKP1/DUSP1 in ovarian tissues. *Clin Cancer Res,* 15**,** 3196-204.

MILLER, W. L. & AUCHUS, R. J. 2011. The Molecular Biology, Biochemistry, and Physiology of Human Steroidogenesis and Its Disorders. *Endocrine Reviews,* 32**,** 81-151.

MITRA, A. K., DAVIS, D. A., TOMAR, S., ROY, L., GURLER, H., XIE, J., LANTVIT, D. D., CARDENAS, H., FANG, F., LIU, Y., LOUGHRAN, E., YANG, J., SHARON STACK, M., EMERSON, R. E., COWDEN DAHL, K. D., M, V. B., NEPHEW, K. P., MATEI, D. & BURDETTE, J. E. 2015. In vivo tumor growth of high-grade serous ovarian cancer cell lines. *Gynecol Oncol,* 138**,** 372-7.

MOON, Y. S., TSANG, B. K., SIMPSON, C. & ARMSTRONG, D. T. 1978. 17 beta-Estradiol biosynthesis in cultured granulosa and thecal cells of human ovarian follicles: stimulation by follicle-stimulating hormone. *J Clin Endocrinol Metab,* 47**,** 263-7.

MORICE, P., GOUY, S. & LEARY, A. 2019. Mucinous Ovarian Carcinoma. *N Engl J Med,* 380**,** 1256-1266.

MOTOHARA, K., TASHIRO, H., TAURA, Y., OHBA, T. & KATABUCHI, H. 2010. Immunohistochemical analysis of 17 beta-hydroxysteroid dehydrogenase isozymes in human ovarian surface epithelium and epithelial ovarian carcinoma. *Medical Molecular Morphology,* 43**,** 197-203.

MUNGENAST, F. & THALHAMMER, T. 2014. Estrogen biosynthesis and action in ovarian cancer. *Front Endocrinol (Lausanne),* 5**,** 192.

NAGAMANI, M. & URBAN, R. J. 2003. Expression of messenger ribonucleic acid encoding steroidogenic enzymes in postmenopausal ovaries. *J Soc Gynecol Investig,* 10**,** 37-40.

NAKANO, R., SHIMA, K., YAMOTO, M., KOBAYASHI, M., NISHIMORI, K. & HIRAOKA, J. 1989. Binding sites for gonadotropins in human postmenopausal ovaries. *Obstet Gynecol,* 73**,** 196-200.

NIWA, K., ONOGI, K., WU, Y., MORI, H., HARRIGAN, R. C. & TAMAYA, T. 2008. Clinical implication of medroxyprogesterone acetate against advanced ovarian carcinoma: a pilot study. *Eur J Gynaecol Oncol,* 29**,** 252-5.

O'BRIEN, M. E., DOWSETT, M., FRYATT, I. & WILTSHAW, E. 1994. Steroid hormone profile in postmenopausal women with ovarian cancer. *Eur J Cancer,* 30a**,** 442-5.

OKAMOTO, S., OKAMOTO, A., NIKAIDO, T., SAITO, M., TAKAO, M., YANAIHARA, N., TAKAKURA, S., OCHIAI, K. & TANAKA, T. 2009. Mesenchymal to epithelial transition in the human ovarian surface epithelium focusing on inclusion cysts. *Oncol Rep,* 21**,** 1209-14.

ORENTREICH, N., BRIND, J. L., RIZER, R. L. & VOGELMAN, J. H. 1984. Age changes and sex differences in serum dehydroepiandrosterone sulfate concentrations throughout adulthood. *J Clin Endocrinol Metab,* 59**,** 551-5.

OSE, J., POOLE, E. M., SCHOCK, H., LEHTINEN, M., ARSLAN, A. A., ZELENIUCH-JACQUOTTE, A., VISVANATHAN, K., HELZLSOUER, K., BURING, J. E., LEE, I. M., TJONNELAND, A., DOSSUS, L., TRICHOPOULOU, A., MASALA, G., ONLAND-MORET, N. C., WEIDERPASS, E., DUELL, E. J., IDAHL, A., TRAVIS, R. C., RINALDI, S., MERRITT, M. A., TRABERT, B., WENTZENSEN, N., TWOROGER, S. S., KAAKS, R. & FORTNER, R. T. 2017. Androgens Are Differentially Associated with Ovarian Cancer Subtypes in the Ovarian Cancer Cohort Consortium. *Cancer Res,* 77**,** 3951-3960.

PANDEY, A. V. & MILLER, W. L. 2005. Regulation of 17,20 lyase activity by cytochrome b5 and by serine phosphorylation of P450c17. *J Biol Chem,* 280**,** 13265-71.

PARK, B. Y., GRISHAM, R. N., DEN HOLLANDER, B., THAPI, D., BERMAN, T., DE STANCHINA, E., ZHOU, Q., IYER, G., AGHAJANIAN, C. & SPRIGGS, D. R. 2016. Tumor Inhibition by Enzalutamide in a Xenograft Model of Ovarian Cancer. *Cancer Invest,* 34**,** 517-520.

PATEK, E. 1974. The epithelium of the human Fallopian tube. A surface ultrastructural and cytochemical study. *Acta Obstet Gynecol Scand Suppl,* 31**,** 1-28.

PAYNE, A. H. & HALES, D. B. 2004. Overview of steroidogenic enzymes in the pathway from cholesterol to active steroid hormones. *Endocr Rev,* 25**,** 947-70.

RAMUS, S. J. & GAYTHER, S. A. 2009. The contribution of BRCA1 and BRCA2 to ovarian cancer. *Mol Oncol,* 3**,** 138-50.

RAMUS, S. J., SONG, H., DICKS, E., TYRER, J. P., ROSENTHAL, A. N., INTERMAGGIO, M. P., FRASER, L., GENTRY-MAHARAJ, A., HAYWARD, J., PHILPOTT, S., ANDERSON, C., EDLUND, C. K., CONTI, D., HARRINGTON, P., BARROWDALE, D., BOWTELL, D. D., ALSOP, K., MITCHELL, G., CICEK, M. S., CUNNINGHAM, J. M., FRIDLEY, B. L., ALSOP, J., JIMENEZ-LINAN, M., POBLETE, S., LELE, S., SUCHESTON-CAMPBELL, L., MOYSICH, K. B., SIEH, W., MCGUIRE, V., LESTER, J., BOGDANOVA, N., DÜRST, M., HILLEMANNS, P., ODUNSI, K., WHITTEMORE, A. S., KARLAN, B. Y., DÖRK, T., GOODE, E. L., MENON, U., JACOBS, I. J., ANTONIOU, A. C., PHAROAH, P. D. & GAYTHER, S. A.

2015. Germline Mutations in the BRIP1, BARD1, PALB2, and NBN Genes in Women With Ovarian Cancer. *J Natl Cancer Inst,* 107.

RHODES, D. R., KALYANA-SUNDARAM, S., MAHAVISNO, V., VARAMBALLY, R., YU, J., BRIGGS, B. B., BARRETTE, T. R., ANSTET, M. J., KINCEAD-BEAL, C., KULKARNI, P., VARAMBALLY, S., GHOSH, D. & CHINNAIYAN, A. M. 2007. Oncomine 3.0: genes, pathways, and networks in a collection of 18,000 cancer gene expression profiles. *Neoplasia,* 9**,** 166-80.

RICE, M. S., MURPHY, M. A., VITONIS, A. F., CRAMER, D. W., TITUS, L. J., TWOROGER, S. S. & TERRY, K. L. 2013. Tubal ligation, hysterectomy and epithelial ovarian cancer in the New England Case-Control Study. *Int J Cancer,* 133**,** 2415-21.

RIDDERHEIM, M., MÄHLCK, C. G., SELSTAM, G., STENDAHL, U. & BÄCKSTRÖM, T. 1993. Steroid Production in Different Parts of Malignant and Benign Ovarian Tumors in Vitro</em&gt. *Cancer Research,* 53**,** 2309.

RISCH, H. A. 1998. Hormonal etiology of epithelial ovarian cancer, with a hypothesis concerning the role of androgens and progesterone. *J Natl Cancer Inst,* 90**,** 1774-86.

SAORIN, A., DI GREGORIO, E., MIOLO, G., STEFFAN, A. & CORONA, G. 2020. Emerging Role of Metabolomics in Ovarian Cancer Diagnosis. *Metabolites,* 10.

SCHIFFER, L., BARNARD, L., BARANOWSKI, E. S., GILLIGAN, L. C., TAYLOR, A. E., ARLT, W., SHACKLETON, C. H. L. & STORBECK, K. H. 2019. Human steroid biosynthesis, metabolism and excretion are differentially reflected by serum and urine steroid metabolomes: A comprehensive review. *J Steroid Biochem Mol Biol,* 194**,** 105439.

SCHMITTGEN, T. D. & LIVAK, K. J. 2008. Analyzing real-time PCR data by the comparative C(T) method. *Nat Protoc,* 3**,** 1101-8.

SCHÜLER-TOPRAK, S., WEBER, F., SKRZYPCZAK, M., ORTMANN, O. & TREECK, O. 2018. Estrogen receptor β is associated with expression of cancer associated genes and survival in ovarian cancer. *BMC Cancer,* 18**,** 981.

SCULLY R, S. L. 1999. *Histological typing of ovarian tumours, volume 9. ,* New York, Springer Berlin.

SCULLY, R. E. & COHEN, R. B. 1964. OXIDATIVE-ENZYME ACTIVITY IN NORMAL AND PATHOLOGIC HUMAN OVARIES. *Obstet Gynecol,* 24**,** 667-81.

SEIDMAN, J. D., HORKAYNE-SZAKALY, I., HAIBA, M., BOICE, C. R., KURMAN, R. J. & RONNETT, B. M. 2004. The histologic type and stage distribution of ovarian carcinomas of surface epithelial origin. *Int J Gynecol Pathol,* 23**,** 41-4.

SHACKLETON, C. H. 1986. Profiling steroid hormones and urinary steroids. *J Chromatogr,* 379**,** 91-156.

SHACKLETON, C. H. & SNODGRASS, G. H. 1974. Steroid excretion by an infant with an unusual salt-losing syndrome: a gas chromatographic-mass spectrometric study. *Ann Clin Biochem,* 11**,** 91-9.

SHAHZAD, M. M. K., AREVALO, J. M., ARMAIZ-PENA, G. N., LU, C., STONE, R. L., MORENO-SMITH, M., NISHIMURA, M., LEE, J. W., JENNINGS, N. B., BOTTSFORD-MILLER, J., VIVAS-MEJIA, P., LUTGENDORF, S. K., LOPEZ-BERESTEIN, G., BAR-ELI, M., COLE, S. W. & SOOD, A. K. 2018. Stress effects on FosB and interleukin-8 (IL8)-driven ovarian cancer growth and metastasis. *J Biol Chem,* 293**,** 10041.

SHAW, P. A., RITTENBERG, P. V. & BROWN, T. J. 2001. Activation of androgen receptor-associated protein 70 (ARA70) mRNA expression in ovarian cancer. *Gynecol Oncol,* 80**,** 132-8.

SHAW, R., LUESLEY, D., MONGA, A. 2010. *Gynaecology*, Churchill Livingstone.

SHEACH, L., ADENEY, E., KUCUKMETIN, A., WILKINSON, S., FISHER, A., ELATTAR, A., ROBSON, C., EDMONDSON, R., SHEACH, L., ADENEY, E., KUCUKMETIN, A., WILKINSON, S., FISHER, A., ELATTAR, A., ROBSON, C. & EDMONDSON, R. 2009a. Androgen-related expression of G-proteins in ovarian cancer. *British Journal of Cancer,* 101**,** 498-503.

SHEACH, L. A., ADENEY, E. M., KUCUKMETIN, A., WILKINSON, S. J., FISHER, A. D., ELATTAR, A., ROBSON, C. N. & EDMONDSON, R. J. 2009b. Androgen-related expression of G-proteins in ovarian cancer. *Br J Cancer,* 101**,** 498-503.

SHERMAN-BAUST, C. A., KUHN, E., VALLE, B. L., SHIH IE, M., KURMAN, R. J., WANG, T. L., AMANO, T., KO, M. S., MIYOSHI, I., ARAKI, Y., LEHRMANN, E., ZHANG, Y., BECKER, K. G. & MORIN, P. J. 2014. A genetically engineered ovarian cancer mouse model based on fallopian tube transformation mimics human high-grade serous carcinoma development. *J Pathol,* 233**,** 228-37.

SIEH, W., KÖBEL, M., LONGACRE, T. A., BOWTELL, D. D., DEFAZIO, A., GOODMAN, M. T., HØGDALL, E., DEEN, S., WENTZENSEN, N., MOYSICH, K. B., BRENTON, J. D., CLARKE, B. A., MENON, U., GILKS, C. B., KIM, A., MADORE, J., FEREDAY, S., GEORGE, J., GALLETTA, L., LURIE, G., WILKENS, L. R., CARNEY, M. E., THOMPSON, P. J., MATSUNO, R. K., KJÆR, S. K., JENSEN, A., HØGDALL, C., KALLI, K. R., FRIDLEY, B. L., KEENEY, G. L., VIERKANT, R. A., CUNNINGHAM, J. M., BRINTON, L. A., YANG, H. P., SHERMAN, M. E., GARCÍA-CLOSAS, M., LISSOWSKA, J., ODUNSI, K., MORRISON, C., LELE, S., BSHARA, W., SUCHESTON, L., JIMENEZ-LINAN, M., DRIVER, K., ALSOP, J., MACK, M., MCGUIRE, V., ROTHSTEIN, J. H., ROSEN, B. P., BERNARDINI, M. Q., MACKAY, H., OZA, A., WOZNIAK, E. L., BENJAMIN, E., GENTRY-MAHARAJ, A., GAYTHER, S. A., TINKER, A. V., PRENTICE, L. M., CHOW, C., ANGLESIO, M. S., JOHNATTY, S. E., CHENEVIX-TRENCH, G., WHITTEMORE, A. S., PHAROAH, P. D., GOODE, E. L., HUNTSMAN, D. G. & RAMUS, S. J. 2013. Hormone-receptor expression and ovarian cancer survival: an Ovarian Tumor Tissue Analysis consortium study. *Lancet Oncol,* 14**,** 853-62.

SIMPSON, E., RUBIN, G., CLYNE, C., ROBERTSON, K., O'DONNELL, L., JONES, M. & DAVIS, S. 2000. The role of local estrogen biosynthesis in males and females. *Trends Endocrinol Metab,* 11**,** 184-8.

SIMS, A. H., SMETHURST, G. J., HEY, Y., OKONIEWSKI, M. J., PEPPER, S. D., HOWELL, A., MILLER, C. J. & CLARKE, R. B. 2008. The removal of multiplicative, systematic bias allows integration of breast cancer gene expression datasets - improving meta-analysis and prediction of prognosis. *BMC Med Genomics,* 1**,** 42.

SOONG, T. R., HOWITT, B. E., HOROWITZ, N., NUCCI, M. R. & CRUM, C. P. 2019. The fallopian tube, "precursor escape" and narrowing the knowledge gap to the origins of high-grade serous carcinoma. *Gynecol Oncol,* 152**,** 426-433.

STORBECK, K. H., GILLIGAN, L., JENKINSON, C., BARANOWSKI, E. S., QUANSON, J. L., ARLT, W. & TAYLOR, A. E. 2018. The utility of ultra-high performance supercritical fluid chromatography-tandem mass spectrometry (UHPSFC-MS/MS) for clinically relevant steroid analysis. *J Chromatogr B Analyt Technol Biomed Life Sci,* 1085**,** 36-41.

STORBECK, K. H., SCHIFFER, L., BARANOWSKI, E. S., CHORTIS, V., PRETE, A., BARNARD, L., GILLIGAN, L. C., TAYLOR, A. E., IDKOWIAK, J., ARLT, W. & SHACKLETON, C. H. L. 2019. Steroid Metabolome Analysis in Disorders of Adrenal Steroid Biosynthesis and Metabolism. *Endocr Rev,* 40**,** 1605-1625.

SUZUKI, T., SASANO, H., TAKEYAMA, J., KANEKO, C., FREIJE, W. A., CARR, B. R. & RAINEY, W. E. 2000. Developmental changes in steroidogenic enzymes in human postnatal adrenal cortex: immunohistochemical studies. *Clin Endocrinol (Oxf),* 53**,** 739-47.

SYED, V., ULINSKI, G., MOK, S. C., YIU, G. K. & HO, S. M. 2001. Expression of gonadotropin receptor and growth responses to key reproductive hormones in normal and malignant human ovarian surface epithelial cells. *Cancer Res,* 61**,** 6768-76.

SZOTEK, P. P., CHANG, H. L., BRENNAND, K., FUJINO, A., PIERETTI-VANMARCKE, R., LO CELSO, C., DOMBKOWSKI, D., PREFFER, F., COHEN, K. S., TEIXEIRA, J. & DONAHOE, P. K. 2008. Normal ovarian surface epithelial label-retaining cells exhibit stem/progenitor cell characteristics. *Proc Natl Acad Sci U S A,* 105**,** 12469-73.

TANG, Z., LI, C., KANG, B., GAO, G., LI, C. & ZHANG, Z. 2017. GEPIA: a web server for cancer and normal gene expression profiling and interactive analyses. *Nucleic Acids Res,* 45**,** W98-w102.

TAYLOR, A. E., KEEVIL, B. & HUHTANIEMI, I. T. 2015. Mass spectrometry and immunoassay: how to measure steroid hormones today and tomorrow. *European Journal of Endocrinology,* 173**,** D1-D12.

THE CANCER GENOME ATLAS RESEARCH NETWORK 2011. Integrated genomic analyses of ovarian carcinoma. *Nature,* 474**,** 609-15.

THOMPSON, P., WILSON, P., OSBORNE, R., SLEVIN, M., WILTSHAW, F., BLAKE, P., HARPER, P., COLEMAN, R., WILLIAMS, C., SWEETENHAM, J. & ET AL. 1991. The clinical activity of cyproterone acetate in advanced ovarian carcinoma. A London Gynaecology Oncology Group Study. *Br J Cancer,* 64**,** 973-4.

TONE, A. A. 2017. Taking the Tube: From Normal Fallopian Tube Epithelium to Ovarian High-grade Serous Carcinoma. *Clin Obstet Gynecol,* 60**,** 697-710.

TRABERT, B., MICHELS, K. A., ANDERSON, G. L., BRINTON, L. A., FALK, R. T., GECZIK, A. M., HARRIS, H. R., PAN, K., PFEIFFER, R. M., QI, L., ROHAN, T., WENTZENSEN, N. & XU, X. 2019. Circulating androgens and postmenopausal ovarian cancer risk in the Women's Health Initiative Observational Study. *Int J Cancer,* 145**,** 2051-2060.

TSANG, B. K., ARMSTRONG, D. T. & WHITFIELD, J. F. 1980. Steroid biosynthesis by isolated human ovarian follicular cells in vitro. *J Clin Endocrinol Metab,* 51**,** 1407-11.

TUMOLO, S., RAO, B. R., VAN DER BURG, M. E., GUASTALLA, J. P., RENARD, J. & VERMORKEN, J. B. 1994. Phase II trial of flutamide in advanced ovarian cancer: an EORTC Gynaecological Cancer Cooperative Group study. *Eur J Cancer,* 30a**,** 911-4.

UHLÉN, M., FAGERBERG, L., HALLSTRÖM, B. M., LINDSKOG, C., OKSVOLD, P., MARDINOGLU, A., SIVERTSSON, Å., KAMPF, C., SJÖSTEDT, E., ASPLUND, A., OLSSON, I., EDLUND, K., LUNDBERG, E., NAVANI, S., SZIGYARTO, C. A., ODEBERG, J., DJUREINOVIC, D., TAKANEN, J. O., HOBER, S., ALM, T., EDQVIST, P. H., BERLING, H., TEGEL, H., MULDER, J., ROCKBERG, J., NILSSON, P., SCHWENK, J. M., HAMSTEN, M., VON FEILITZEN, K., FORSBERG, M., PERSSON, L., JOHANSSON, F., ZWAHLEN, M., VON HEIJNE, G., NIELSEN, J. & PONTÉN, F. 2015. Proteomics. Tissue-based map of the human proteome. *Science,* 347**,** 1260419.

VAN KAMMEN, E., THIJSSEN, J. H., DONKER, G. H. & SCHWARZ, F. 1975. The excretion of metabolites of testosterone and of estradiol in male patients with chronic renal failure. *Steroids,* 26**,** 508-15.

VASSILOMANOLAKIS, M., KOUMAKIS, G., BARBOUNIS, V., HAJICHRISTOU, H., TSOUSIS, S. & EFREMIDIS, A. 1997. A phase II study of flutamide in ovarian cancer. *Oncology,* 54**,** 199-202.

VENERIS, J. T., DARCY, K. M., MHAWECH-FAUCEGLIA, P., TIAN, C., LENGYEL, E., LASTRA, R. R., PEJOVIC, T., CONZEN, S. D. & FLEMING, G. F. 2017. High glucocorticoid receptor expression predicts short progression-free survival in ovarian cancer. *Gynecol Oncol,* 146**,** 153-160.

WANG, S., HU, C., WU, F. & HE, S. 2017. Rab25 GTPase: Functional roles in cancer. *Oncotarget,* 8**,** 64591-64599.

WANG, Y., YANG, J., GAO, Y., DONG, L. J., LIU, S. & YAO, Z. 2007. Reciprocal regulation of 5alpha-dihydrotestosterone, interleukin-6 and interleukin-8 during proliferation of epithelial ovarian carcinoma. *Cancer Biol Ther,* 6**,** 864-71.

WEIDNER N., C. R., SUSTER S., WEISS LM 2009. Modern Surgical Pathology. *In:* NOEL WEIDNER, R. J. C., SAUL SUSTER, LAWRENCE M. WEISS (ed.) *Modern Surgical Pathology, 2nd Edition.* 2nd Edition ed.: Elsevier.

WESTWOOD, M., RAMAEKERS, B., LANG, S., GRIMM, S., DESHPANDE, S., DE KOCK, S., ARMSTRONG, N., JOORE, M. & KLEIJNEN, J. 2018. Risk scores to guide referral decisions for people with suspected ovarian cancer in secondary care: a systematic review and cost-effectiveness analysis. *Health Technol Assess,* 22**,** 1-264.

WIDSCHWENDTER, M., ROSENTHAL, A. N., PHILPOTT, S., RIZZUTO, I., FRASER, L., HAYWARD, J., INTERMAGGIO, M. P., EDLUND, C. K., RAMUS, S. J., GAYTHER, S. A., DUBEAU, L., FOURKALA, E. O., ZAIKIN, A., MENON, U. & JACOBS, I. J. 2013. The sex hormone system in carriers of BRCA1/2 mutations: a case-control study. *Lancet Oncol,* 14**,** 1226-32.

WILSON, J. D., AUCHUS, R. J., LEIHY, M. W., GURYEV, O. L., ESTABROOK, R. W., OSBORN, S. M., SHAW, G. & RENFREE, M. B. 2003. 5alpha-androstane-3alpha,17beta-diol is formed in tammar

wallaby pouch young testes by a pathway involving 5alpha-pregnane-3alpha,17alpha-diol-20-one as a key intermediate. *Endocrinology,* 144**,** 575-80.

YAGER, J. D. 2015. Mechanisms of estrogen carcinogenesis: The role of E2/E1-quinone metabolites suggests new approaches to preventive intervention--A review. *Steroids,* 99**,** 56-60.

YAMAMOTO, Y., YAMADA, R., OGURI, H., MAEDA, N. & FUKAYA, T. 2009. Comparison of four malignancy risk indices in the preoperative evaluation of patients with pelvic masses. *Eur J Obstet Gynecol Reprod Biol,* 144**,** 163-7.

ZHENG, J., YANG, Z., LI, Y., YANG, L. & YAO, R. 2022. Knockdown of AKR1C3 Promoted Sorafenib Sensitivity Through Inhibiting the Phosphorylation of AKT in Hepatocellular Carcinoma. *Front Oncol,* 12**,** 823491.